SELF-EVALUATION TECHNIQUE FOR SPECTRUM SHARING IN MIMO COGNITIVE RADIO SYSTEMS

Rattasat Laikanok

A Thesis Submitted in Partial Fulfillment of the Requirements for the Degree of Doctor of Philosophy in Telecommunication Engineering

Suranaree University of Technology

Academic Year 2017

เทคนิคการประเมินตนเองสำหรับการแบ่งปันสเปกตรัมในระบบวิทยุรู้คิดแบบไมโม

นายรัฐศาสตร์ ลายกนก

วิทยานิพนธ์นี้เป็นส่วนหนึ่งของการศึกษาตามหลักสูตรปริญญาวิศวกรรมศาสตรดุษฎีบัณฑิต

สาขาวิชาวิศวกรรมโทรคมนาคม

มหาวิทยาลัยเทคโนโลยีสุรนารี

ปีการศึกษา 2560

SELF-EVALUATION TECHNIQUE FOR SPECTRUM SHARING IN MIMO COGNITIVE RADIO SYSTEMS

Suranaree University of Technology has approved this thesis submitted in partial fulfillment of the requirements for the Degree of Doctor of Philosophy.

Thesis Examining Committee

(Asst. Prof. Dr. Wipawee Hattagam)

Chairperson

(Assoc. Prof. Dr. Peerapong Uthansakul)

Member (Thesis Advisor)

(Assoc. Prof. Dr. Monthippa Uthansakul)

Member

(Asst. Prof. Dr. Chanchai Thaijiam)

Member

(Dr. Dheerasak Anantakul)

Member

(Prof. Dr. Santi Maensiri)

Vice Rector for Academic Affairs and Internationalization

(Assoc. Prof. Flt. Lt. Dr. Konton Chamniprasart)

Dean of Institute of Engineering

รัฐศาสตร์ ลายกนก : เทคนิคการประเมินตนเองสำหรับการแบ่งปันสเปกตรัมในระบบวิทยุรู้คิดแบบไมโม (SELF-EVALUATION TECHNIQUE FOR SPECTRUM SHARING IN MIMO COGNITIVE RADIO SYSTEMS) อาจารย์ที่ปรึกษา : รองศาสตราจารย์ ดร.พีระพงษ์ อุฑารสกุล, 174 หน้า.

ปัจจุบันระบบการสื่อสารไร้สายได้ถูกคิดค้นและพัฒนามาอย่างต่อเนื่อง เนื่องจากความต้องการของผู้ใช้บริการที่มากขึ้นเรื่อยๆ รวมไปถึงการพัฒนาแอพลิเคชั่นใหม่อีกมาก ทำให้ทรัพยากรความถี่ที่มีน้อยอยู่แล้ว กลับน้อยลงไปอีก ไม่เพียงพอต่อการใช้งาน ส่วนหนึ่งเป็นเพราะการจับจองสเปกตรัมของผู้ใช้ที่ประมูลมาถูกต้องตามกฎหมาย แต่การใช้ยังไม่คุ้มค่าพอ จึงเกิดเทคโนโลยีวิทยุรู้คิดขึ้นมาเพื่ออนุญาตให้ผู้ใช้รองเข้ามาใช้ความถี่เดียวกับผู้ใช้หลักในบริเวณเดียวกัน โดยหนึ่งในหัวใจหลักของเทคโนโลยีวิทยุรู้คิดคือการตรวจจับสเปกตรัม ที่จะทำการตรวจหาแถบความถี่ที่ว่างจากการใช้งานของผู้ใช้หลัก แล้วอนุญาตให้ผู้ใช้รองเข้าใช้แถบความถี่นั้นได้ แต่ทว่าวิธีดังกล่าวยังไม่เพียงพอสำหรับรองรับผู้ใช้จำนวนมากที่เพิ่มขึ้นอีกในอนาคต จึงถูกพัฒนาต่อเป็นการเข้าใช้สเปกตรัมร่วมกันระหว่างผู้ใช้หลักและผู้ใช้รองในเวลาเดียวกัน และบริเวณเดียวกัน และระบบวิทยุรู้คิดต้องมีวิธีการจำกัดสัญญาณแทรกสอดไม่ให้มากจนส่งผลต่อการสื่อสารของผู้ใช้หลัก จึงมีการนำเทคโนโลยีหลายสายอากาศตัวส่งหลายสายอากาศตัวรับเข้ามาช่วยในการพัฒนาการลดสัญญาณแทรกสอด ซึ่งสามารถช่วยให้ระบบมีประสิทธิภาพดีขึ้นในระดับหนึ่ง อีกทั้งยังรองรับเทคโนโลยีแอลทีอีอันซึ่งจะเปิดทางไปสู่ระบบสื่อสารเคลื่อนที่ยุคที่ห้า แต่ในงานวิจัยนี้พบว่า ถ้าหากโหนดสมาชิกของเครือข่ายวิทยุรู้คิดอยู่ผิดที่ผิดตำแหน่ง ถึงแม้จะมีความสามารถในการจำกัดสัญญาณแทรกสอดดีแค่ไหน ก็จะเกิดอัตราบิตผิดพลาดขึ้นมากกว่าที่ระบบจะทนได้ ดังนั้นงานวิจัยนี้จึงมีแนวคิดที่จะหาวิธีการที่เครือข่ายวิทยุรู้คิดจะสามารถรับรู้ตำแหน่งของแต่ละโหนดในระบบแล้วใช้ข้อมูลนี้ประเมินตนเองเพื่อการตัดสินใจอย่างเหมาะสมในการทำการสื่อสารเพื่อให้ได้มาซึ่งการใช้สเปกตรัมได้อย่างมีประสิทธิภาพ และคุ้มค่ามากที่สุด

สาขาวิชา วิศวกรรมโทรคมนาคม

ปีการศึกษา 2560

ลายมือชื่อนักศึกษา รัฐศาสตร์ ลายกนก

ลายมือชื่ออาจารย์ที่ปรึกษา

RATTASAT LAIKANOK : SELF-EVALUATION TECHNIQUE FOR SPECTRUM SHARING IN MIMO COGNITIVE RADIO SYSTEMS. THESIS ADVISOR : ASSOC. PROF. PEERAPONG UTHANSAKUL, Ph.D., 174 PP.

COGNITIVE RADIO/MULTIPLE-INPUT-MULTIPLE-OUTPUT/SPECTRUM SHARING/LTE

Recently, the wireless communication system has been developed and continuously improved due to the need of user services including the development of many new applications. This results in higher consumption of frequency resource until it will not be enough to be used in the future. One problem is that the spectrum possession of licensed users is inefficiently utilized. The spectrum sharing in cognitive radio technology can solve the mentioned problems by allowing secondary user to access the same frequency as primary user in the same area, which is divided into two patterns using spectrum sensing. If the system detects an idle channel, it will perform a non-overlapping spectrum sharing. On the other hand, if the system detects an occupied channel, it will continue to perform an overlapping spectrum sharing. To support the recent development of modern technology, the proposed cognitive radio technology in this research can get along with the Long-Term Evolution (LTE) towards fifth-generation mobile systems. In this research, the guidelines for self-evaluation of the cognitive radio network are proposed to judge whether each secondary user is in the appropriate range of communication or not, in terms of frequency, time and position, without causing any damage to the communication of the primary user. Hence, the proposed concept is designed to minimize the interference effect of secondary networks on the communication of primary network as much as possible. The simulation results indicate the specific areas for cognitive radio that can be successfully implemented. The proposed research work is very helpful for service providers to obtain higher benefit from their limited resources.

School of Telecommunication Engineering Student's Signature ____________

Academic Year 2017 Advisor's Signature ____________

ACKNOWLEDGEMENTS

The author wishes to acknowledge the funding support from Suranaree University of Technology (SUT).

The grateful thanks and appreciation are given to the thesis advisor, Assoc. Prof. Dr. Peerapong Uthansakul for his consistent supervision and thoughtful comments on several drafts and advice towards the completion of this study.

My thanks go to Asst. Prof. Dr. Wipawee Hattagam, Assoc. Prof. Dr. Monthippa Uthansakul, Asst. Prof. Dr. Chutima Prommak, Asst. Prof. Dr. Chanchai Thaijiam and Dr. Dheerasak Anantakul for their valuable suggestion and guidance given as examination committees.

The author is also grateful to all faculty and staff members of the School of Telecommunication Engineering and colleagues for their help and assistance throughout the period of this work.

Finally, I would also like to express my deep sense of gratitude to the The OROG Scholarship Program and my parents for their support and encouragement me throughout the course of this study at the Suranaree University of Technology.

Rattasat Laikanok

TABLE OF CONTENTS

Page

TABLE OF CONTENTS (Continued)

Page

TABLE OF CONTENTS (Continued)

Page

TABLE OF CONTENTS (Continued)

Page

TABLE OF CONTENTS (Continued)

Page

LIST OF TABLES

Table **Page**

LIST OF FIGURES

Figure **Page**

LIST OF FIGURES (Continued)

LIST OF FIGURES (Continued)

Figure **Page**

LIST OF FIGURES (Continued)

Figure **Page**

LIST OF FIGURES (Continued)

Figure **Page**

SYMBOLS AND ABBREVIATIONS

CR	=	Cognitive Radio
LTE	=	Long-Term Evolution Standard
PU	=	Primary User
SU	=	Secondary User
MIMO	=	Multiple-Input Multiple-Output Technology
TAS	=	Transmit Antenna Selection Technique
MRC	=	Maximum Ratio Combining Technique
BER	=	Bit Error Rate
RF	=	Radio Frequency
P_D	=	Probability of Detection
P_{FA}	=	Probability of False Alarm
P_{MD}	=	Probability of Missed Detection
ED	=	Energy Detection Method
ROC	=	Receiver Operating Characteristic Curve
FFT	=	Fast Fourier Transform
SNR	=	Signal to Noise Ratio
WRAN	=	Wireless Regional Area Network
AWGN	=	Additive White Gaussian Noise
EGC	=	Equal Gain Combining Technique
OR	=	OR Rule

SYMBOLS AND ABBREVIATIONS (Continued)

AND	=	AND Rule
MJ	=	MAJORITY Rule
CCS	=	Cognitive Compressive Sensing
FRI	=	Finite Rate of Innovation
CSS	=	Cooperative Spectrum Sensing
SSDF	=	Spectrum Sensing Data Falsification attack problem
MAC	=	Media Access Control Protocol
UWB	=	Ultra-Wideband
DSA	=	Dynamic Spectrum Access
QoS	=	Quality of Service
AIP	=	Average Interference Power
PIP	=	Peak Interference Power
LTE-A	=	Long-Term Evolution Advanced Standard
SISO	=	Single-Input Single-Output
SIMO	=	Single-Input Multiple-Output
MISO	=	Multiple-Input Single-Output
WiMAX	=	Worldwide Interoperability for Microwave Access
TD-SCDMA	=	Time Division Synchronous Code Division Multiple Access
BTS	=	Base Transceiver Station
SM	=	Spatial Multiplexing
ML	=	Maximum Likelihood Criterion
STBC	=	Space-Time Block Coding

SYMBOLS AND ABBREVIATIONS (Continued)

FDD	=	Frequency Division Duplex
TDD	=	Time Division Duplex
MJ++	=	MAJORITY++ Rule
MJS++	=	MAJORITY++ Rule with Soft Decision
3GPP	=	Third Generation Partnership Project Group
FCC	=	Federal Communication Commission
CEPT	=	Conference European of Post and Telecommunication Group
FDMA	=	Frequency Division Multiple Access
TDMA	=	Time Division Multiple Access
CDMA	=	Code Division Multiple Access
SDMA	=	Space Division Multiple Access
W-CDMA	=	Wideband Code Division Multiple Access
RDBMS	=	Relational Database Management Systems
GSI	=	Geographic Information System
PT	=	Primary Transmitter
PR	=	Primary Receiver
ST	=	Secondary Transmitter
SR	=	Secondary Receiver
BS	=	Base Station
FC	=	Fusion Center
CDF	=	Cumulative Distribution Function
CEP	=	Condition Error Probability

SYMBOLS AND ABBREVIATIONS (Continued)

BPSK	=	Binary Phase Shift Keying
BFSK	=	Binary Frequency Shift Keying
PAM	=	Pulse Amplitude Modulation
QAM	=	Quadrature Amplitude Modulation
SINR	=	Signal to Interference plus Noise Ratio
PDF	=	Probability Density Function
5G	=	Fifth-Generation Mobile Systems

CHAPTER I

INTRODUCTION

1.1 Background of problem

So far, the wireless communications technology has played a huge role in our daily lives and has been highly developed. So, the frequency resources are plentifully employed and tend to be not enough for usage in the future. Nevertheless, the frequency resources have not been effectively utilized as it should be. Because of the above reason, the idea of sharing frequency channel between the licensed Primary User (PU) and Secondary Users (SUs) staying in the same location has been considered. Most importantly, the spectrum sharing process should not damage the primary communication.

From the above idea, Cognitive Radio (CR) technology was initiated and applied to the standard of IEEE 802.22 (IEEE Standards Association, 2011). According to its advantages, CR system is able to allow SU or unlicensed user to access the same spectrum with PU in which the system has the way to avoid making the interference to PU.

Spectrum sensing is the topic of CR system development to develop the primary signal detection. When PU does not use its frequency channel, CR system will allow SU to change the former frequency channel into the new frequency channel, which is also called non-overlapping spectrum sharing. However, when PU uses this frequency channel, SU is necessary to revoke an access for that frequency channel in order to avoid interference to PU. But when PU occupies the spectrum at all times, SU is unable to increase the available frequency channels. Hence, the spectrum sharing scheme has been developed to be the overlapping spectrum sharing, which allows PU and SU to access the same spectrum at the same time in the same location. Especially, there is a condition that the interference from SU has to be limited to the acceptable level to avoid making the abnormal operation of PU.

From the literatures, the existing works have improved spectrum sensing using only one antenna on both transmitter and receiver. One of the research works has employed the cooperation of nodes to share information with each other as a network. Later, all the data is collected through a central node as a hierarchy. Finally, it has employed the statistical technique for data analysis (C. Hunifang, X. Lei and N. Xiong, 2014). For the spectrum sharing development, the works presented in (S. Puranachaikeeree and R. Suleesathira, 2010) has employed the transmitted beam forming method from the secondary base station to reduce the interference to PU, and the effective SU selection method to reduce the interference between SUs. Especially, the transmitted beam forming method has been applied to the Multiple-Input Multiple-Output (MIMO) technology using Gram-Schmidt Orthogonalization method. Next, the works in (F. A. Khan, K. Tourki, M-S. Alouini and K. A. Qaraqe, 2014) has employed Transmit Antenna Selection (TAS) technique along with the power control method at a transmitter, and Maximum Ratio Combining (MRC) technique at a receiver. Then, the performance analysis is described in terms of the symbol error rate and channel capacity. So far in literatures, there has not been any work that focuses on the self-evaluation guidelines to consider whether the position of SU is suitable to provide a good communication under the acceptable interference level in overlapping spectrum sharing scheme or not. The Ph.D. candidate realizes the need to initiate research on the impact of node positions in CR system and develop self-evaluation technique for secondary network in the system with the aforesaid position information in order to enable CR system for practical operation.

1.2 Research objectives

The objectives of this research are as follows:

1.2.1 To analyze the suitability of SU's location based on bit error rate (BER) for the CR system.

1.2.2 To develop self-evaluation technique for spectrum sharing in MIMO CR system.

1.3 Scope and limitation of the study

1.3.1 According to the current MIMO systems, each transmitter and receiver employ not higher than 4 antenna elements.

1.3.2 This research only considers the physical layer. It experiments on the differences in the number of antenna elements, power consumption, and user positions.

1.3.3 Computer programming is employed to process the spectrum sharing between PU and SU in a form of BER inside the coverage area to illustrate the position that SU utilizes the spectrum together with PU effectively under the acceptable interference level.

1.3.4 In the performance analysis, the experimental results are only shown in a form of BER of each member node.

1.3.5 This research aims to establish the self-evaluation method for spectrum sharing of the secondary networks in order to achieve the efficient utilization of frequency resources. Moreover, this research work focuses on controlling a detrimental effect on the primary network.

1.3.6 Current CR concept cannot satisfy the multimedia applications because the system has to suddenly cut the SU's communication during handoff process. Primary network is the main priority in the system. Hence, this research is suitable for data transferring applications which can wait for the appropriate position of SU in communication.

1.4 Contributions

1.4.1 To precisely specify the status of each spectrum employing MAJORITY++ rule with soft decision technique.

1.4.2 To obtain knowledge to analyze the appropriate positions based on BER condition of the multi-user MIMO CR network.

1.4.3 To enable the CR technology based on SU's locations for LTE technology in practice by employing the spectrum allocation scheme.

1.5 Thesis organization

The remainder of this thesis is organized as follows. The literature reviews are discussed in Chapter II. This chapter presents the detection methods for spectrum sensing and describes the difference between non-overlapping spectrum sharing and overlapping spectrum sharing.

Chapter III describes the background theory of CR systems including MIMO technology and spectrum sensing algorithm. The Ph.D. candidate employs this important knowledge to operate the spectrum sharing in MIMO CR systems.

Chapter IV presents the proposed performance analysis for spectrum sharing in single user, multi-user one-cell, and multi-user multi-cell MIMO CR systems. In addition, it also presents the spectrum allocation scheme to thoroughly allocate the frequency channels to all users.

Chapter V presents the simulation results to show the comparison of spectrum sensing techniques, performance analysis for spectrum sharing, and the working format of the spectrum allocation scheme. The results are very useful for multi-user MIMO CR implementation to make a decision whether the current positions of SUs are suitable to establish the communication or not.

Chapter VI provides the conclusions of the research work and suggestion for further study.

CHAPTER II

LITERATURE REVIEW

2.1 Introduction

This chapter presents a literature review for spectrum sharing, which begins with a brief concept of CR technology. Then it describes the various types of the signal detection methods for spectrum sensing. Moreover, multi-node cooperation technique is applied to spectrum sensing improvement. Next, this chapter presents the difference between non-overlapping spectrum sharing and overlapping spectrum sharing, then the last section concludes the related research of both spectrum sharing patterns.

2.2 Cognitive radio systems

Currently, wireless communication network has the policy in the invariable spectrum allocation in which the governments in most countries allocate spectrum for a concessionaire in long-term usage. Incidentally, the number of subscribers is increasing every year. Hence, the frequency scarcity is the major current problem due to the greater spectrum utilization along with the limited frequency resources. In fact, most of the spectrums are only utilized as a time slot or the signals are inaccessible in some locations, as shown in Fig. 2.1. Thus, the current spectrum utilization is inefficient. The CR system is a system intended to solve the tightness of unequal spectrum utilization and enables the higher efficient spectrum utilization (I. F. Akyildiz, W.-Y. Lee, M. C. Vuran, and S. Mohanty, 2006).

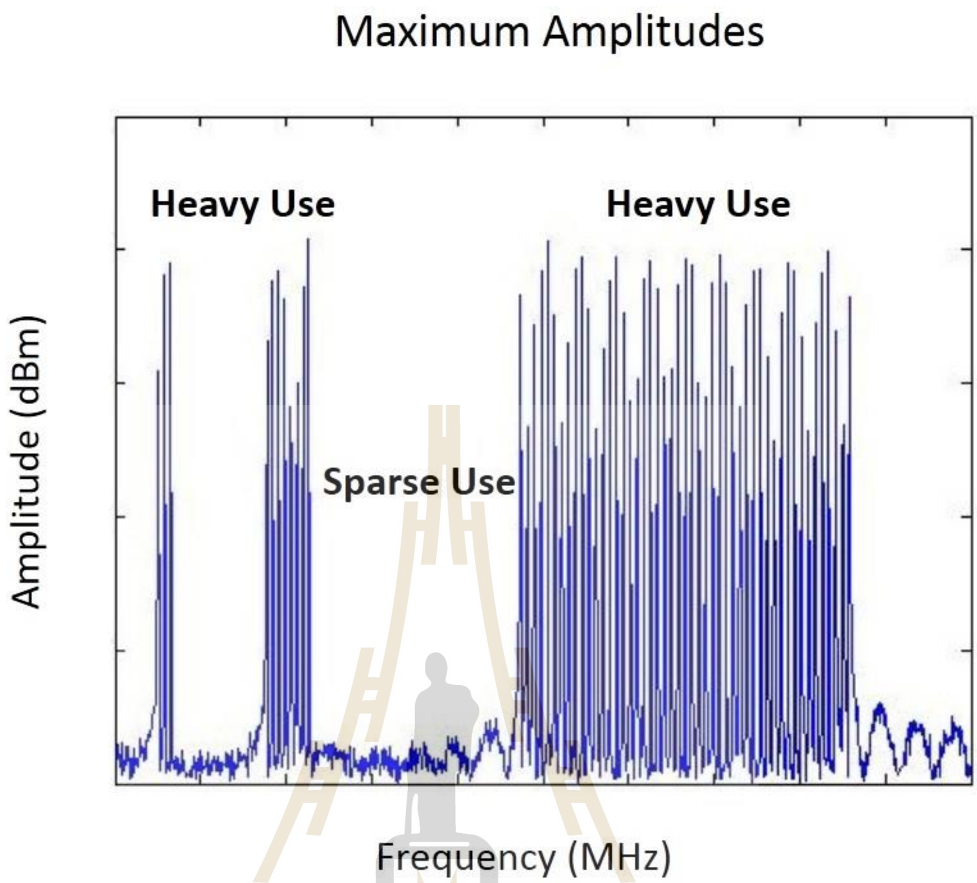

Figure 2.1 Appearance of unequal spectrum utilization.

CR system allows the unlicensed SU to share frequency channel with PU which is licensed by the government. This property enables the users to utilize the higher width of the spectrum by the frequency switching technique. But CR system may be problematic because the spectrum access is changed over time, including the demand for Quality of Service (QoS) of various applications in order to get the best channel. Hence, CR system has to consist of the characteristics, as follow:

1. The system can detect whether PU is active or inactive.

2. The system can provide the communication of SU operating at the same spectrum with PU at the same time on condition that PU can tolerate the interference in the tolerable level.

3. The system can choose the proper SU for the shared spectrum utilization in order to efficiently minimize the interference.

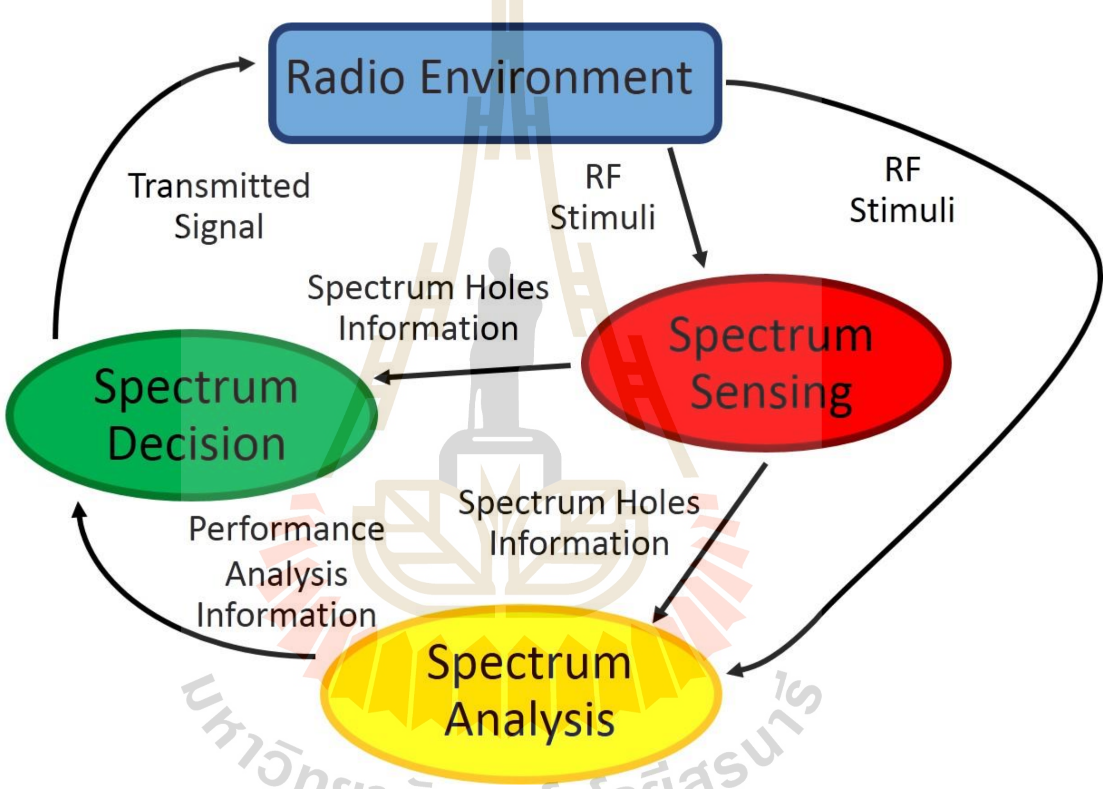

Figure 2.2 Description of cognitive cycle.

2.2.1 Definition of cognitive radio

CR is the system which adapts itself or changes the signal transmission method when the environment changes (B. Fette, 2009). The CR system has two capabilities as follows.

2.2.1.1 Cognitive capability

The process of CR system is the communication and parameter adjustments to suit the changed environment. The necessary steps to adjust the CR system are shown in Fig. 2.2 and called cognitive cycle (S. Heykin, 2005), which consists of three steps:

1. Spectrum sensing: CR system checks the proper spectrum, collects data, and finds the available spectrum which is also called spectrum hole, as shown in Fig. 2.3.

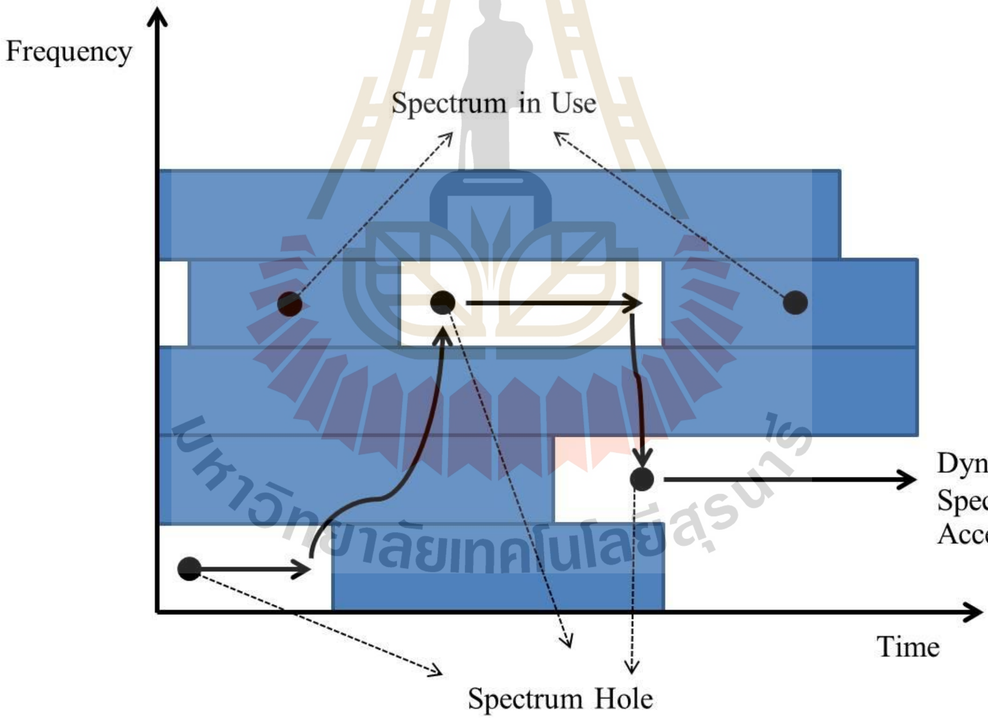

Figure 2.3 Appearance of spectrum hole.

2. Spectrum analysis: CR system analyzes the information to know whether the available spectrum is suitable to communicate or not.

3. Spectrum decision: CR system defines the bit rate, transmission pattern, and bandwidth. Then, a suitable spectrum will be selected according to the characteristics and the demand of user.

2.2.1.2 Reconfigurability

CR system can adjust the parameters to suit transmitting and receiving the signal at various frequencies. Both hardware and software have to be adjusted to suit a utilization in each spectrum. The intelligent system reconfiguration for the transmission without additional hardware consists of the adjustable functions as follows.

1. Operating frequency: CR system can change the frequency of operation depending on the environment. Therefore the communication can be performed dynamically in the appropriate spectrum.

2. Modulation: CR system can adjust the signal modulation to suit the user and channel due to the various communication standards. Especially, the proper modulation adjustment affects the performance of communication systems.

3. Transmitted power: CR system can adjust transmitted power to be appropriate in spectrum sharing. The power in transmission is modified under the defined conditions. If the system transmits signal by the over power, it will cause an unnecessary loss and interference.

4. Communication technology: CR system can configure the user patterns for usage in various communication systems.

2.2.2 Cognitive network architecture

The components of the architecture in CR system are shown in Fig. 2.4 (I. F. Akyildiz, W.-Y. Lee, M. C. Vuran, and S. Mohanty, 2006), in which users in the system can be divided into two groups, including primary network, and CR network which is the secondary network. There are three spectrum types which can be utilized by SU, including an unlicensed band and the other two licensed bands. PU utilizes only the licensed bands. The cognitive network architecture contains the following details.

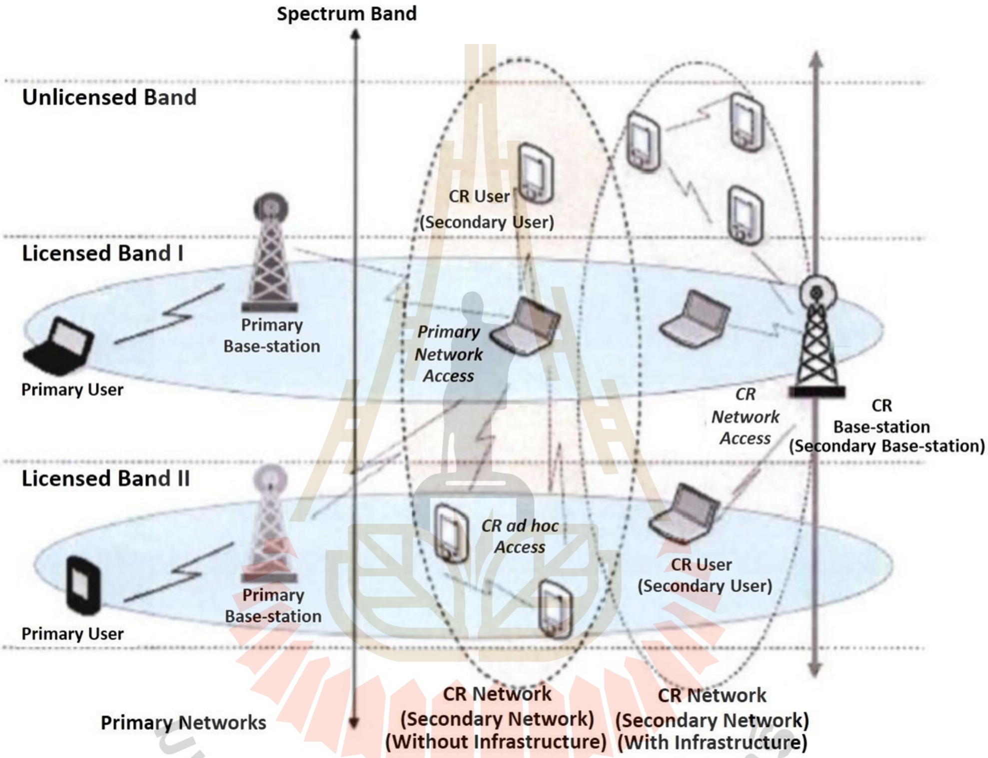

Figure 2.4 Description of cognitive network architecture.

2.2.2.1 Primary network

Primary network is the network which has the right to perfectly utilize the spectrum, which consists of:

1. PU is the user who has the right to utilize the licensed spectrum by the management from only the primary base station. Additionally, PU

should not be affected by the interference from other users. In addition, PU does not require any modifications in the CR system.

2. Primary base station is the basic component of the primary network which has the permission to fully utilize the spectrum. Usually, the primary base station cannot allow the secondary network to operate spectrum sharing.

2.2.2.2 Secondary network

Secondary network is the network which does not have the license to perform at the spectrum of PU. Therefore, in order to access the primary spectrum, it requires an adaptation technique of the network. The secondary network can perform in the infrastructure network and the Ad-hoc network, as shown in Fig. 2.4. The secondary network consists of:

1. SU is the user who needs to access the licensed spectrum occupied by PU.

2. Secondary base station is the basic component of the secondary network. It provides connectivity to SU utilizing the spectrum shared with PU. Sometimes, it is also called Fusion Center (FC).

Fig. 2.4 shows that CR system incorporates the various networks such as primary network, secondary network, and Ad-hoc network of SUs. In the case of secondary network, it accesses the mixed spectrum in which the mixed spectrum access consists of the spectrum access of their own and the spectrum sharing together with the primary network. The secondary network has three patterns to access the spectrum as follows.

1. CR network access: SU can connect to the secondary base station through the spectrum which is licensed and unlicensed.

2. Cognitive Ad-hoc network access: SU can communicate with the other SUs through the Ad-hoc channel.

3. Primary network access: SU can access the primary spectrum through the licensed spectrum.

2.2.3 Spectrum utilization formats of secondary network

From the above network access of SU, there are the occupied spectrum access and available spectrum access. Therefore, the secondary networks vary according to the types of spectrum, which are described as follows.

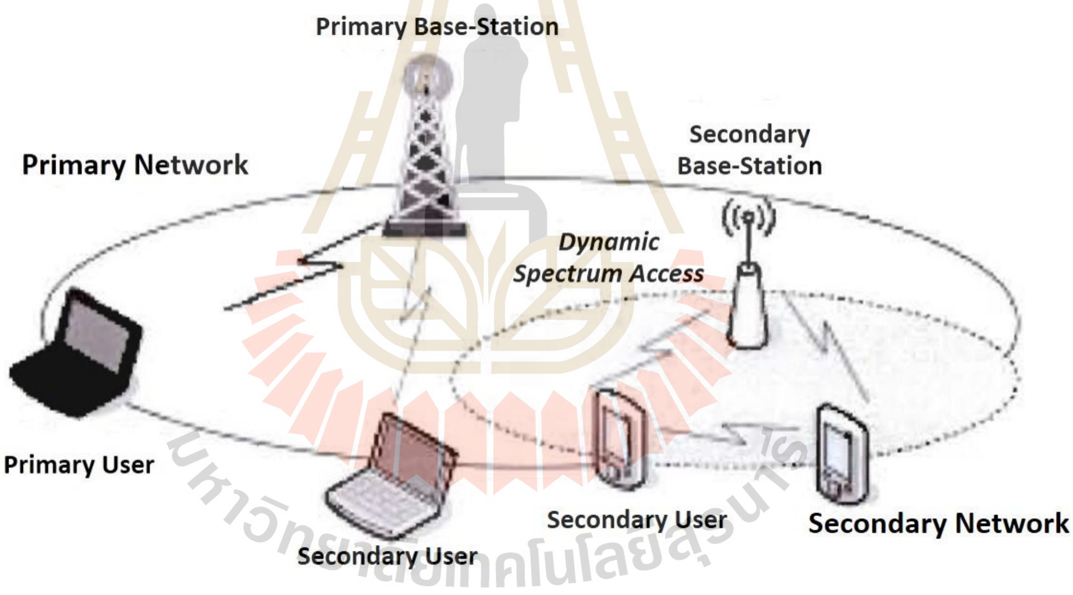

Figure 2.5 Characteristic of secondary network that utilizes spectrum together with the primary network.

2.2.3.1 Spectrum sharing operation on primary spectrum

In Fig. 2.3, the spectrum hole occurs whenever PU does not occupy the spectrum. For this reason, the secondary network can access this spectrum hole through CR system. This form of communication is shown in Fig. 2.5 in which secondary network involves the primary network through the same spectrum in the same area.

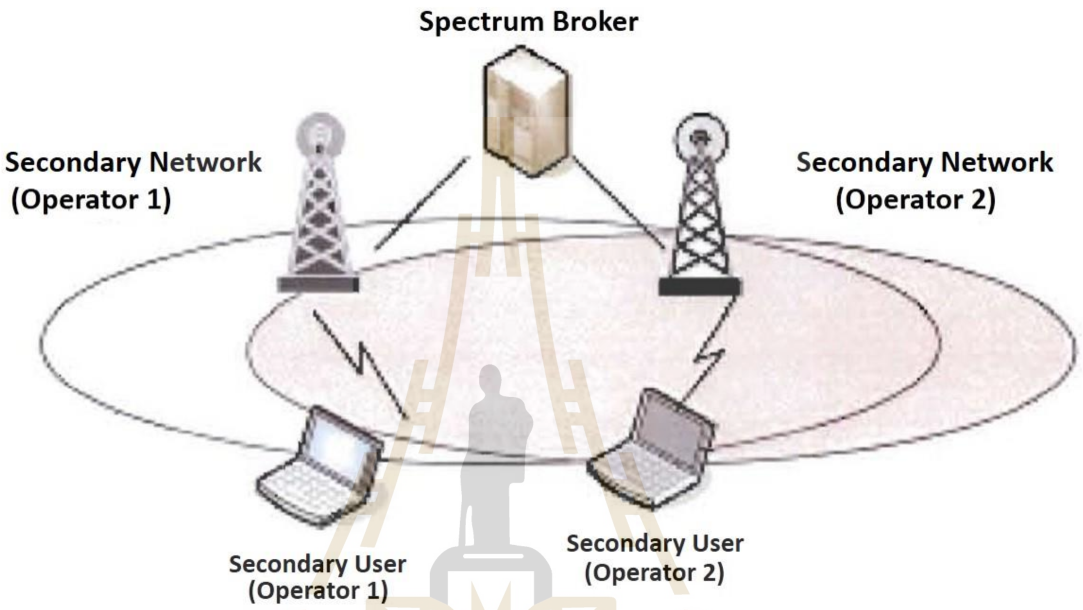

Figure 2.6 Characteristic of secondary networks that utilize unoccupied spectrum.

2.2.3.2 Spectrum sharing operation on available spectrum

Communications systems at the same spectrum cause the interference problems between users. However, the CR system can perform at the same spectrum, which is shown in Fig. 2.6. There is no any primary user occupying the spectrum of the system. Hence, the users have equal rights in spectrum access. Secondary networks need the algorithm to reduce the interference for sharing the same spectrum in the same area. For the above system, SU has to learn the status of itself and other users in order to find the way to fairly share the spectrum.

2.3 Spectrum sensing

The basic principles of spectrum sensing are not complicated (A. M. Wyglinski, M. Nekovee and T. Hou, 2009) because of only two hypotheses that must be interested, including H_0 (idle) and H_1 (busy). The status is idle when PU signal is not detected. The received signal is just ambient noise in the Radio Frequency (RF) environment. On the other hand, the status is busy when the received signal has consisted of the PU signal and the ambient noise. Then, those two hypotheses can be described by

$$\begin{aligned} &H_0 : y(k) = w(k) \\ &H_1 : y(k) = s(k) + w(k), \end{aligned} \tag{2.1}$$

where $y(k)$ represents the received signal, $w(k)$ represents the ambient noise, and $s(k)$ represents the PU signal, for $k = 1,\ldots,n$ and n is the number of received samples.

The operative assessment of spectrum sensing techniques can be significantly viewed from two probabilities, including the probability of detection P_D and probability of false alarm P_{FA}.

P_D is the probability of detecting a signal at the considered frequency when it truly appears. Additionally, P_D can be described in another form which is the probability of remaining apart from the probability of missed detection P_{MD}. This can be written in the form of

$$P_D = 1 - P_{MD}, \tag{2.2}$$

where P_{MD} is the probability of detecting a signal when the busy channel is detected as the idle channel. On the other hand, P_{FA} is the probability of detecting a signal when the idle channel is detected as the busy channel. The P_{MD} and P_{FA} can be defined as

$$P_{MD} = Prob\{Decide\, H_0|H_1\}, \tag{2.3}$$

$$P_{FA} = Prob\{Decide\, H_1|H_0\}. \tag{2.4}$$

It can be seen that P_{FA} is associated with P_D in such a way that P_{FA} is one of the forms of P_D. This is because, within the total number of all detected signals, there are some amount of noise which is misunderstood as the normal signals.

In practice, there are various spectrum sensing methods as follows.

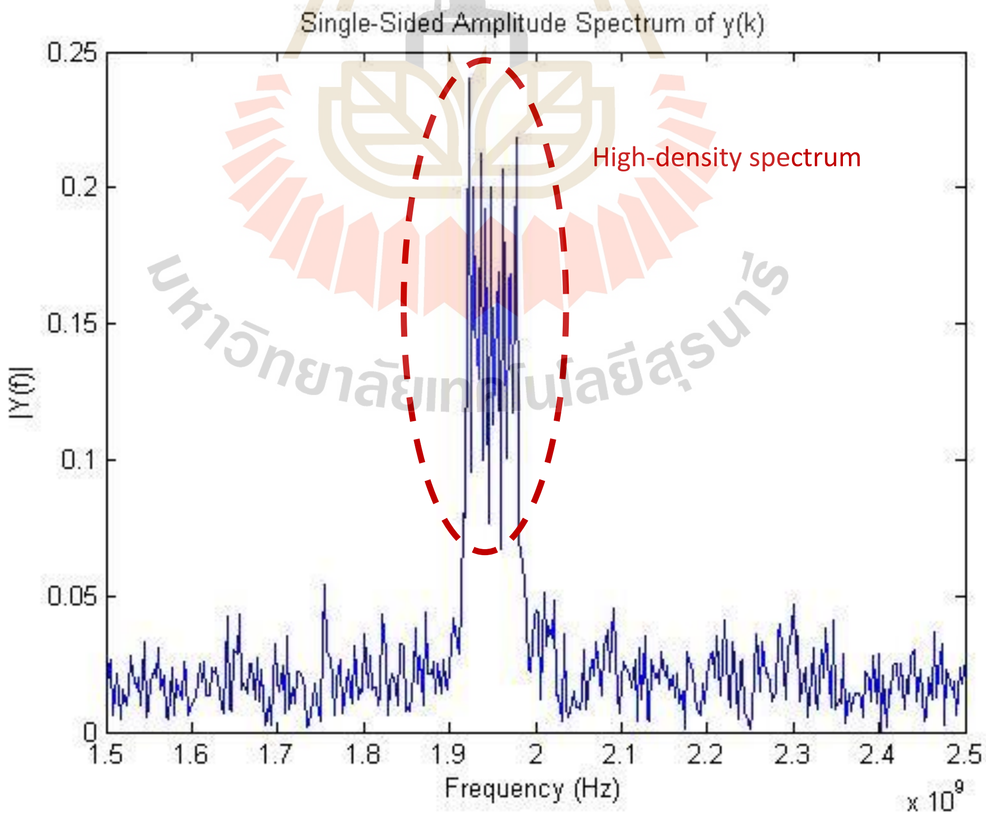

Figure 2.7 Appearance of the detected spectrum when all channels are busy.

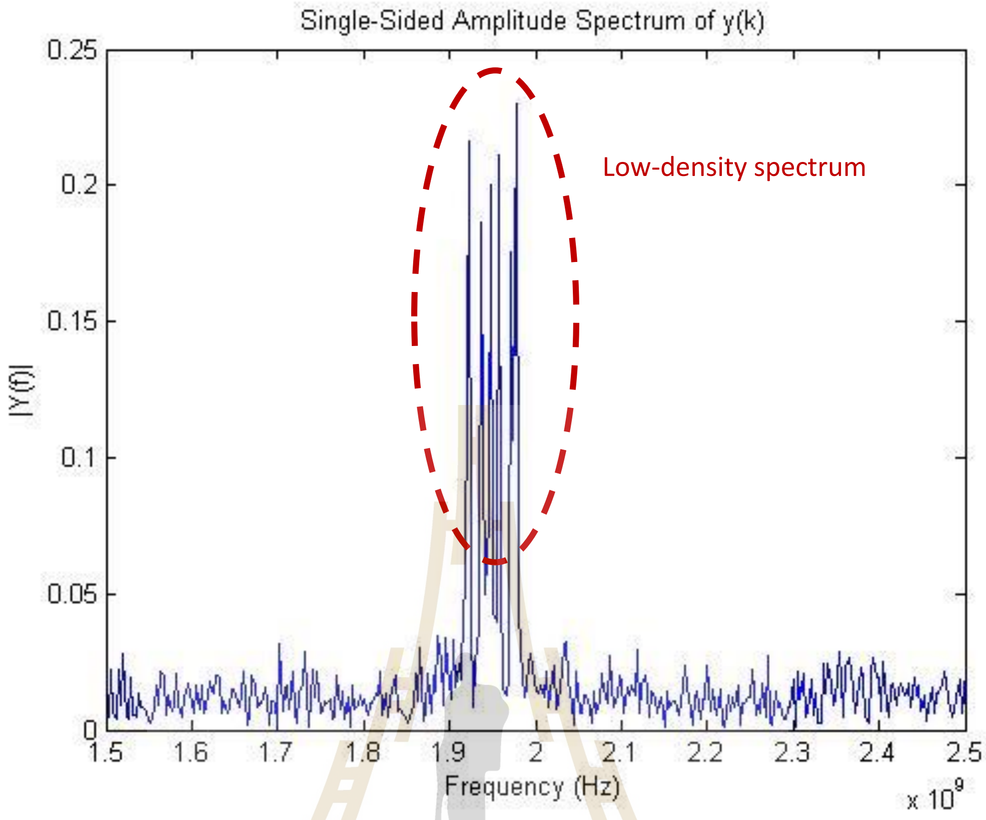

Figure 2.8 Appearance of the detected spectrum when some channels are idle.

2.3.1 Energy detection

The Energy Detection method (ED) is very popular because it can be implemented conveniently. In this research, the Ph.D. candidate has developed the spectrum sensing technique based on ED because this method is not complicated and can be modified in various ways. Moreover, this method has the advantage in which it is easy to discriminate the status of the spectrum energy in quite straightforward appearance. This can be seen in the simulations based on the channel from LTE standard which provides the uplink operating band from 1920 MHz to 1980 MHz. Then, the received spectrum when all of the channel status are busy is presented in Fig. 2.7. The Ph.D. candidate randomly defines some channels to be available in order to investigate the performance of sensing method. Then in Fig. 2.8, it shows the example of received spectrum when some channel statuses are idle.

The probabilities P_{FA} and P_{MD} that the signals are modeled as a zero-mean stationary white Gaussian process, independent of the observation noise, can be described in forms of a simple analysis as follows.

$$P_{FA} = \Gamma\left(n\tau, n\right), \tag{2.5}$$

$$P_{MD} = \Gamma\left(\frac{n\tau}{1+SNR}, n\right), \tag{2.6}$$

where τ is the detection threshold, and $\Gamma(.\,,.)$ is the upper incomplete gamma function.

In practice, the system can separate the various frequencies of each channel from the received signal in (2.1) as follows.

$$y(k) = \sum_{ch=1}^{CH} u_{ch}(k), \tag{2.7}$$

where CH is the number of considered channels.

Then, the signal considered in each channel is brought into the one-bit decision equation as

$$U_d(ch) = \begin{cases} 0, avg\left(\left|\mathbf{u}_{ch}\right|^2\right) < \tau \\ 1, avg\left(\left|\mathbf{u}_{ch}\right|^2\right) \geq \tau \end{cases}. \tag{2.8}$$

In order to indicate the concept of ED, the preliminary simulation has been taken action. When the Ph.D. candidate defines $n = 2000$ samples and $SNR = -30$ dB, the comparison result between the closed form solution appeared in (2.5) and simulated method is shown in Fig. 2.9. In this figure, the evaluation of the probabilities P_D and P_{FA} is presented and this type of graph is well known as the Receiver Operating Characteristic (ROC) curve. The ROC shows the sensitivity in the terms of P_D and the specificity in the terms of P_{FA}. Therefore, the ROC curve that comes near 1 for P_D and 0 for P_{FA} is the ideal case. More importantly, this figure also demonstrates that a result of the spectrum sensing simulation using ED method is similar to the theoretical analysis.

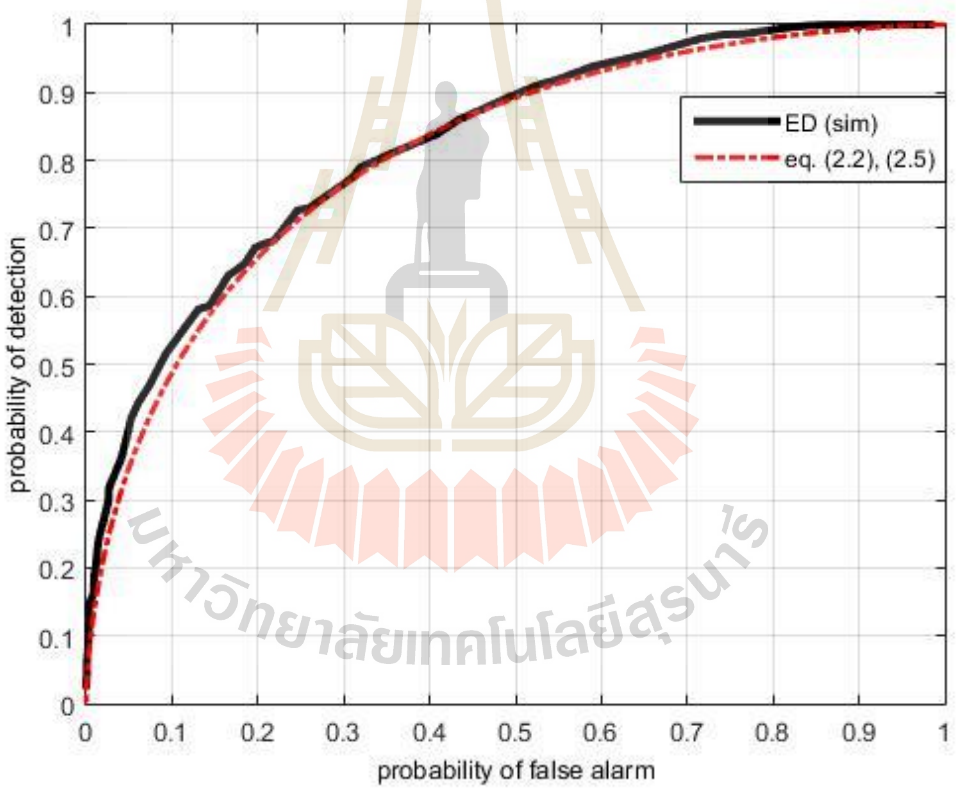

Figure 2.9 ROC curves of the normal ED where $SNR = -30$ dB, and $n = 2000$.

Moreover, the system can define the appropriate threshold from the 90% P_D referred to spectrum sensing standard in CR technology.

2.3.2 Cyclostationary feature detection

Frequently, quite a bit of the detail about the primary signal structure is known. For example, the bit rates, the modulation type, the carrier frequency, and the width of guard bands may be known. Digitally modulated signals have periodic features that may be implicit or explicit. The carrier frequency and symbol rate can be estimated via the square-law devices. For some standards, the primary network utilizes a pilot tone frequency which can be taken advantage by SU. The cyclic prefix usage also leads to the periodic signal structures. The means and correlation sequences of such signals show periodicity. Therefore, such signals are called the cyclostationary signals (W. A. Gardner, 1991 and E. Serpedin, F. Panduru, I. Sari, and G. B. Giannakis, 2005). Then, the test statistic in a cyclic detection is

$$S(f;\zeta)=\frac{1}{n}\sum_{k=1}^{n}y(k)y(k+\zeta)e^{-j2\pi fk}, \tag{2.9}$$

where f is the sampling frequency, and ζ is the delay. Then, the received signal $y(k)$ can be described as

$$y(k)=\sum_{u}s_u(k)e^{j2\pi f_u k}+w(k), \tag{2.10}$$

where $s_u(k)$ is mutually independent zero-mean wide-stationary processes and independent of the circularly symmetric white noise sequence $w(k)$. Then for a large amount of n,

$$S(f;\zeta)\approx\sum_{u}R_u(\zeta)e^{j2\pi f_u\zeta}\delta(f-2f_u), \tag{2.11}$$

where f_u is the operating frequency of u^{th} SU, and

$$R_u(\zeta)=E\{s_u(t)s_u(t+\zeta)\}, \tag{2.12}$$

where $E\{.\}$ is the moment-generating function. This method is easily implemented via Fast Fourier Transforms (FFTs). The information of noise variance is not required for setting up the detection threshold. Therefore, the detection does not suffer from the Signal to Noise Ratio (SNR) wall problem of ED method. However, the performance of the detection degrades in the appearance of timing and frequency jitters which smear out the spectral lines, and RF nonlinearities which induce the spurious peaks. The representative works that consider this scheme are (D. Cabric, S. M. Mishra, and R. W. Brodersen, 2004, K. Kim, I. Akbar, K. Bae, J. S. Um, C. Spooner, and J. Reed, 2007 and P. Sutton, K. Nolan, and L. Doyle, 2008).

2.3.3 Matched filter detection

Frequently, the pilot or sync sequences utilized in the primary network are known to SU. For example, the Wireless Regional Area Network (WRAN) 802.22 standard specifies these sequences. Let $s(k)$, $k = 1, ..., n$, denote the known pilot sequence. By assuming as perfect synchronization, the received signal at SU can be described as

$$y(k) = hs(k) + w(k), \tag{2.13}$$

where $w(k)$ is Additive White Gaussian Noise (AWGN) and h represent an unknown channel gain. For this AWGN setting, the optimal detection is the matched filter (S. M. Kay, 1998). Then, the test statistic is

$$z = \frac{1}{n}\sum_{k=1}^{n} y(k)s^{*}(k). \tag{2.14}$$

Therefore, the performance of the detection can be given by

$$Q^{-1}(P_{FA}) - Q^{-1}(P_D) = \sqrt{n \times SNR}, \tag{2.15}$$

where SNR is defined as

$$SNR = |h|^2 \sum_{k=1}^{n} \frac{|s(k)|^2}{n}. \tag{2.16}$$

At low SNR, the number of required samples is $1/SNR$ instead of the $1/SNR^2$ samples required by ED method. This is a significant advantage. However, performance is degraded in the appearance of frequency and timing offsets, as well as fading in which the gain $|h|^2$ is now random, and delay spread which requires equalization. The matched filter approach has been explored in (T. Li, W. Mow, V. Lau, M. Siu, R. Cheng, and R. Murch, 2007, N. Kundargi, and A. H. Tewfik, 2008 and H. Yu, Y. Sung, and Y. H. Lee, 2008).

2.4 Cooperative techniques based on energy detection

The difference between normal CR and MIMO CR is the number of receive antennas. Hence, the way to take an advantage of multiple antennas is extremely important for MIMO CR system. The utilization of multiple antennas for the spectrum sensing is called cooperative techniques (C. Hunifang, X. Lei and N. Xiong, 2014). In this section, it presents the foundations of techniques which are developed to support the CR system applied to MIMO technology.

2.4.1 Equal gain combining

Equal Gain Combining (EGC) technique fuses all the received signals from each antenna to obtain the following combining result:

$$y_{EGC}(k) = \left(\frac{1}{M}\right) \sum_{m=1}^{M} y_m(k), \tag{2.17}$$

where M is the number of antenna elements.

The use of EGC is to bring the received EGC signal $y_{EGC}(k)$ of (2.17) into (2.7) instead of $y(k)$. Then, the EGC signal considered in each channel is brought into the one-bit decision in (2.8).

2.4.2 Cooperative decision rule

The cooperative decision rule mentions three different styles including OR rule, AND rule and MAJORITY (MJ) rule. After the signals are received, a received signal of each antenna $y_m(k)$ is separately brought into (2.7) sorting by a receive antenna number from $m=1$ to M in which this process is unlike the EGC that combine all signal in (2.17). Then, all signals considered in each channel are brought into the one-bit decision in (2.8). Finally, the system will obtain the data points U_d of all channels of each antenna, and get the total points U_m of the corresponding channel to perform the final decision according to the following logic rule.

$$U_{total}(ch) = \sum_{m=1}^{M} U_m(ch) \begin{cases} < \kappa, & H_0 \\ \geq \kappa, & H_1 \end{cases}, \tag{2.18}$$

where κ is the decision factor in which the OR rule corresponds to the case of $\kappa = 1$, the AND rule corresponds to the case of $\kappa = M$, and the MAJORITY rule corresponds to the case of $\kappa = M/2$.

2.5 Summary of literature

From the study of the related theories and principles, the literature and research related to the spectrum sharing can be divided into two groups, including the non-overlapping spectrum sharing and overlapping spectrum sharing, as shown in Fig. 2.10.

Moreover, both cases of spectrum sharing are described by the simplified structures as shown in Fig. 2.11 and Fig. 2.12, respectively.

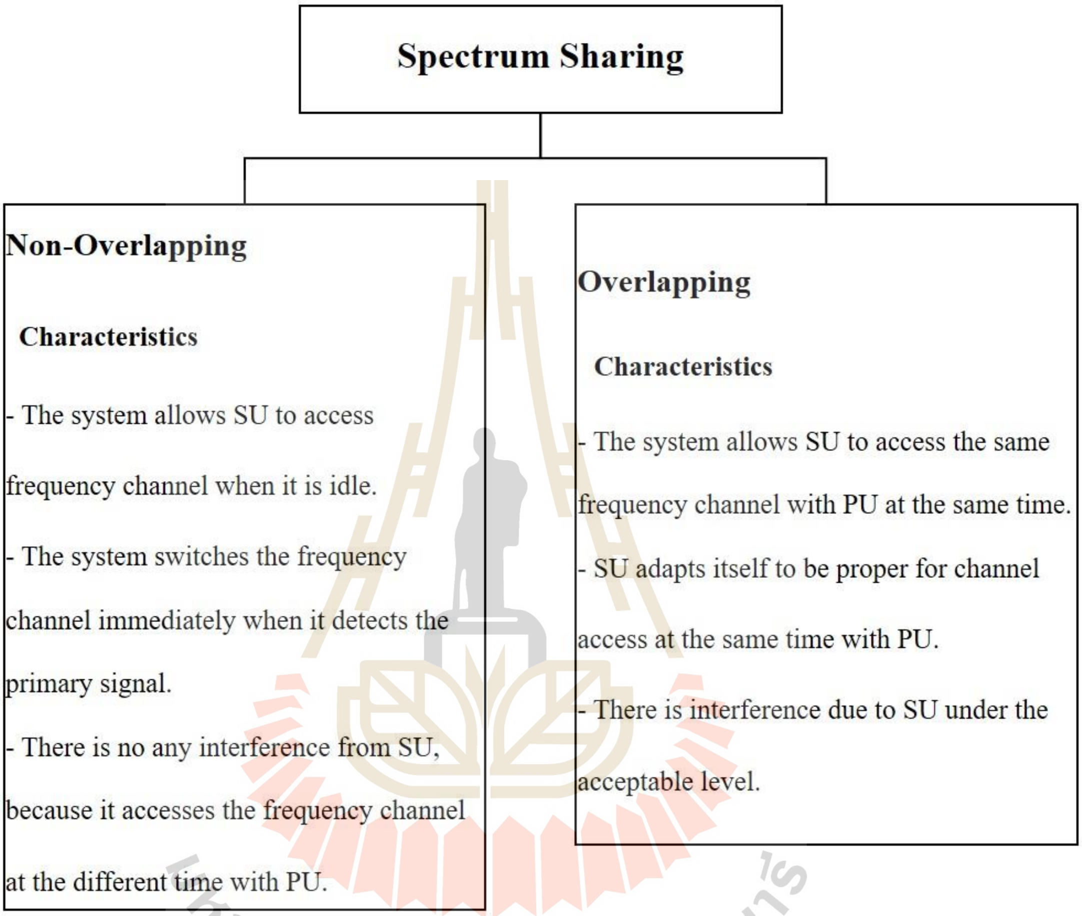

Figure 2.10 Types of spectrum sharing.

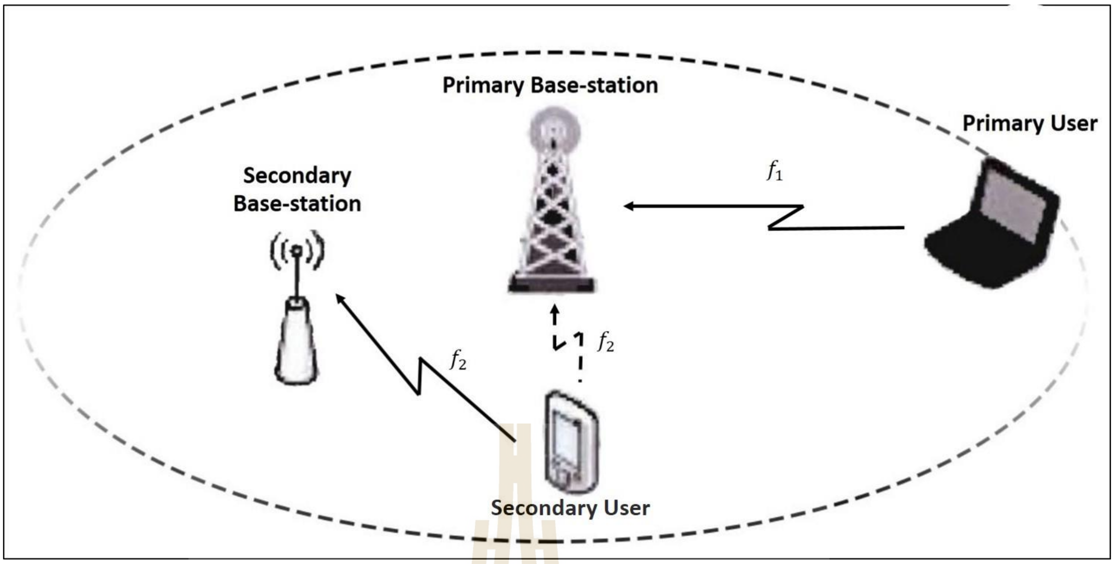

Figure 2.11 System model of non-overlapping spectrum sharing.

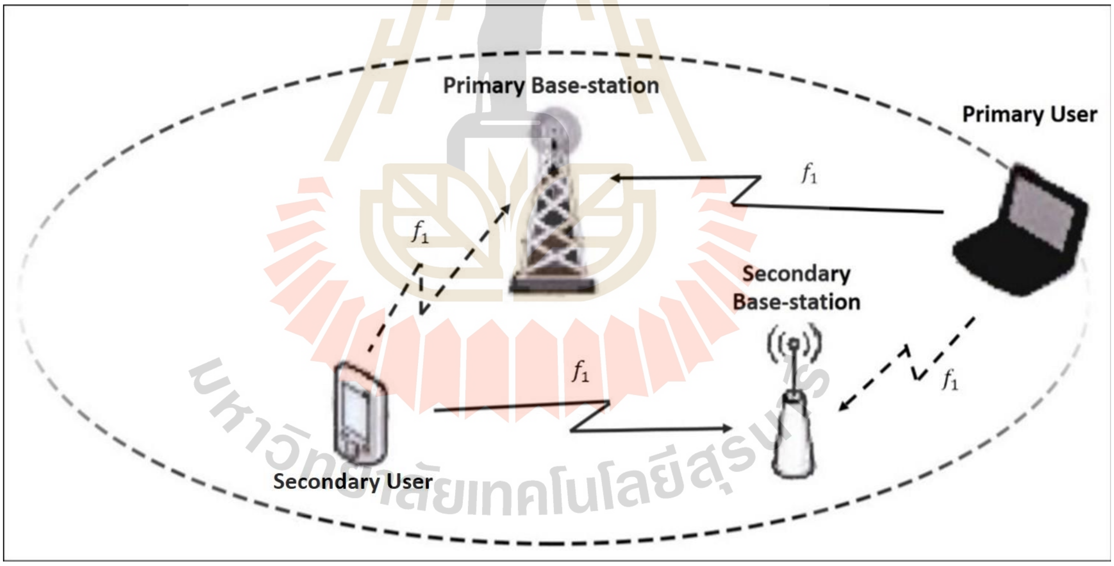

Figure 2.12 System model of overlapping spectrum sharing.

2.5.1 The works related to non-overlapping spectrum sharing

(C. Huifang, X. Lei, and N. Xiong, 2014) has presented the optimization techniques for spectrum sensing using cooperation of node clusters in which each node has only one antenna. The data processing is separated into hierarchies. On the first level, all of the member nodes use the EGC technique. Then on the second level, the data from each group are brought into the processor which operates the statistical decision using MAJORITY rule.

(I. Hwang, and J. W. Lee, 2016) has improved the cooperative decision technique to support an imperfect feedback channel. The work has employed local sensor nodes to generate decision symbols regarding the existence of PU signal by the multi-level detection. Then, the decision symbols are sent over feedback channels to the FC in which the demodulated symbols are combined to draw the cooperative decision. Next, the work has optimally determined the operating parameters of the fusion rule with quantization combining under Neyman–Pearson criterion using a differential evolution algorithm. This work achieves the sensing performance improvement and the wrong identifying reduction on the channel statuses.

(S. Haykin, 2005) has described three basic operations in CR system, including the radio-scene analysis, the channel state estimation and the creation of channel state prediction model, and the transmitted power control and dynamic spectrum management. The knowledge in this work is a very useful guideline for the CR improvement.

(S. Bagheri, and A. Scaglione, 2015) has formulated and studied the Cognitive Compressive Sensing (CCS) problem as a restless multi-armed bandit problem. The work has proposed a novel adaptive Finite Rate of Innovation (FRI) sampling method based on the CCS approach. This work has designed the detection method to support the above problem. This proposed detection method increases an opportunity to detect the sparse signals.

(M. Kitsunezuka, and K. S. J. Pister, 2015) has described a highly sensitive spectrum sensing system based on a cross-correlation technique that employed the low-cost software-defined radio receivers. The duplicated receivers multiplies two data streams and averaged the outputs. This work has used cross-correlation system to suppress uncorrelated noise at the cost of measurement time. Especially, the phase-domain signal detection has been employed due to it is able to tolerate noise than ED.

(M. Grissa, A. A. Yavuz, and B. Hamdaoui, 2016) has proposed the privacy-preserving protocols making the use of various cryptographic mechanisms to protect the location privacy of SUs with the reliable performance and efficient spectrum sensing. The work has presented the cost-performance tradeoffs. Hence, The CR system allows SU to communicate whenever the system detects the idle channel and such SU can pass the conditions of defined parameters.

(L. Zhang, G. Ding, Q. Wu, Y. Zou, Z. Han, and J. Wang, 2015) has provided a comprehensive survey and tutorial on the recent advances in the Byzantine attack and defense for the Cooperative Spectrum Sensing (CSS) in CR networks. This work has classified the existing defense algorithms and provided an in-depth tutorial on the state-of-the-art Byzantine defense schemes in order to solve the Spectrum Sensing Data Falsification (SSDF) attack problem.

(S. Pandit, and G. Singh, 2015) has introduced the control channel on Media Access Control (MAC) protocol applied to be the place for SUs to share the sensing results with other users. Additionally, this work has presented the new self-scheduled multi-channel CR MAC protocol to achieve the better throughput.

(R. Hussain, and M. S. Sharawi, 2015) has designed the novel compact multi-mode multi-band frequency reconfigurable MIMO antenna system equipped with the Ultra-Wideband (UWB) sensing antennas. This work supports the various wireless system standards and the UWB MIMO CR which can cover various frequency bands from 755 to 3450 MHz.

(D.B. Rawat, S. Shetty, and C. Xin, 2016) has investigated a two-stage Stackelberg game for Dynamic Spectrum Access (DSA) in cognitive radio networks employing a spectrum provider (SP) and SU. The work has presented the concept in which the licensed PUs liken the brokers. These PUs open the opportunity for SUs to access idle channel by exchanging the formal payment. Then, they evaluate the cost QoS under the various statuses of user's systems. The proposed concept reaches the unique Stackelberg equilibrium.

2.5.2 The works related to overlapping spectrum sharing

(S. Puranachaikeeree, and R. Suleesathira, 2010) has employed the transmitted beam forming method from the secondary base station to reduce the interference to PU, and the effective SU selection method to reduce the interference between SUs. Especially, the transmitted beam forming method has been applied to the MIMO technology using Gram-Schmidt Orthogonalization method.

(R. Zhang, 2009) has presented the power constraint techniques to limit the interference signals which affect PU in spectrum sharing. This work has compared between two patterns depended on the power of interference, including the Average Interference Power (AIP) and the Peak Interference Power (PIP).

(G. Yang, B. Li, X. Tan, and X. Wang, 2015) has investigated the problem of power control in CR systems based on game theory subject. This work has constrained the interference power at PU and the Signal to Interference plus Noise Ratio

(SINR) of each SU. Moreover, the work has designed the power control scheme to reduce lavish power utilization in order to support the multi-user CR system.

(T. K. Kim, H. M. Kim, M. G. Song, and G. H. Im, 2015) has improved spectrum-sharing protocol for multi-user cooperation in CR. During cooperative transmission, SU transmits its own signal at the same time with a network-coded signal from the PUs. However, the detection errors of the SU cause an error propagation which degrades the performance of the PU and SU. This work has developed a cooperative MRC scheme which mitigates the error propagation and achieves diversity gain. Moreover, the work has applied the constrained BER optimization problem to the adaptive modulation system.

(S. Vassaki, M. I. Poulakis, and A.D. Panagopoulos, 2016) has focused on multi-user single-relay cooperative network. The work has investigated the problem of relay power allocating to individual users in order to optimize the long-term network performance. The power allocation problem has been formulated as a state-based potential game. Finally, this work has used a gradient learning mechanism to achieve the stationary state equilibrium of the game.

(B. Khalfi, M. B. Ghorbel, B. Hamdaoui, and M. Guizani, 2015) has introduced a distributed and fair resource allocation scheme for large-scale wireless dynamic spectrum access networks based on particle ltering theory. This work has made the fair spectrum assignment and covered in the large dynamic spectrum access network to achieve the better throughput.

(M. B. Çelebi, and H. Arslan, 2015) has shown that the long-term evolution advanced (LTE-A) has divided the user groups into small cell and macrocell which need the co-existence between the diverse signals. Additionally, this work has introduced three different power control schemes proposed for heterogeneous networks to improve the gain further and observe the performance in the system-level. The proposed combination methods effectively works in the dense mobile communication environments.

(F. A. Khan, K. Tourki, M-S. Alouini and K. A. Qaraqe, 2014) has employed Transmit Antenna Selection (TAS) technique along with the power control method at a transmitter, and Maximum Ratio Combining (MRC) technique at a receiver. Then, the performance analysis is described in terms of the symbol error rate and channel capacity. Especially, both techniques improves the spectrum sharing performance in MIMO CR system.

(K. Tourki, K. A. Qaraqe, H-C. Yang and M-S. Alouini, 2014) has presented the performance analysis of spectrum sharing in MIMO CR system using a TAS technique. The performance analysis is in forms of the outage probability, BER and the channel capacity under two power constraint methods, including the mean value-based power allocation scheme and the channel state information-based power allocation scheme.

From the literature reviews, there has not been any work that focuses on the self-evaluation guidelines to consider whether the position of SU is suitable to provide a good communication under the acceptable interference level in overlapping spectrum sharing scheme or not. The Ph.D. candidate realizes the need to initiate research on the impact of node positions in CR system and develop self-evaluation technique for the secondary network in the system with the above position information in order to enable CR system for practical operation.

CHAPTER III

BACKGROUND THEORY

3.1 Introduction

The details of this chapter are the explanation of background theories and related contents employed to enable the spectrum sharing operation in CR system for implementation. Then, the details consist of MIMO technology, the overview of LTE standard, GPS system, as well as the spectrum sensing improvement techniques based on the existing techniques. Finally, the last section concludes the chapter.

3.2 MIMO technology

Multiple-Input Multiple-Output (MIMO) is a promising technology for achieving the high-speed data rate needed in the future wireless communication systems. The multiple streams can be transmitted using MIMO, thereby increasing system throughput. Especially, the MIMO technology can be employed to improve the spectrum sensing performance and reduce the effect of interference for spectrum sharing in the CR system. The Single-Input Single-Output (SISO), Single-Input Multiple-Output (SIMO), Multiple-Input Single-Output (MISO), and MIMO antenna configurations are shown in Fig. 3.1. Currently, MIMO technology is applied to most 3G and 4G wireless standards such as Worldwide Interoperability for Microwave Access (WiMAX), Time Division Synchronous Code Division Multiple Access (TD-SCDMA), Long-Term Evolution (LTE), etc.

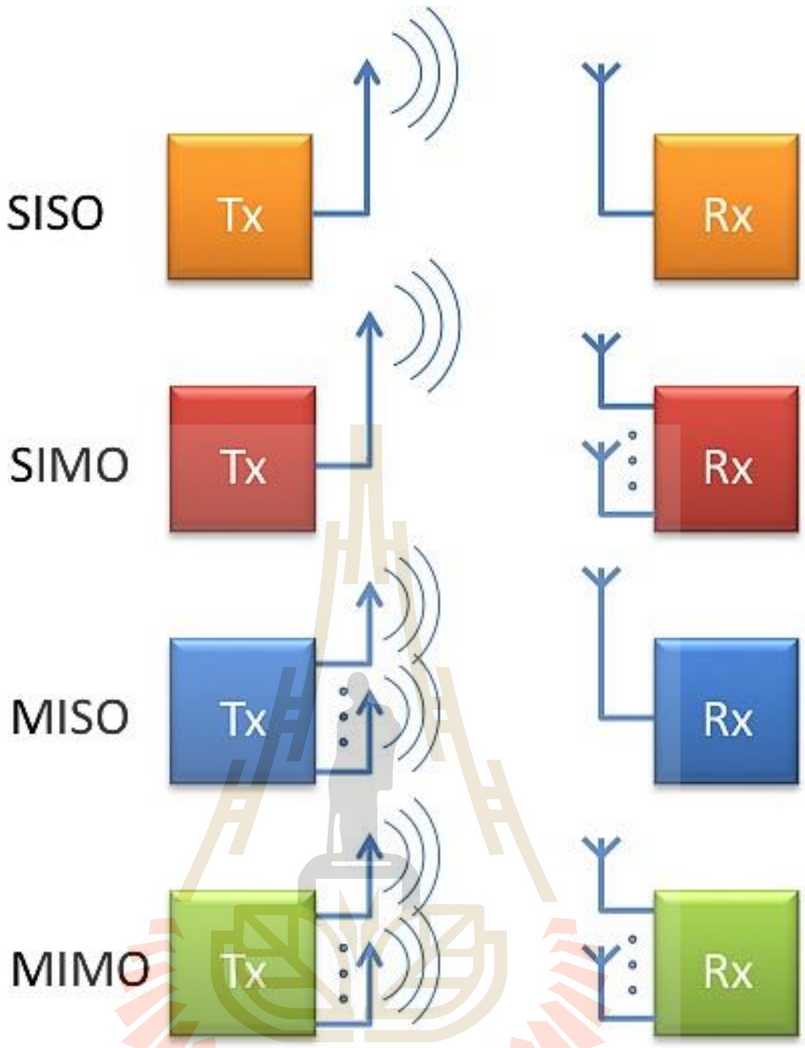

Figure 3.1 Antenna configurations of SISO, SIMO, MISO, and MIMO in wireless data transmission.

In a traditional wireless system, the receiver and transmitter do not back and forth communicate at the same time. The receiver figures out the channel information and decodes the streams by oneself. From above reason, a heavy complex burden on preventing the system from the fully utilization of channel diversity and capacity is thrown into the receiver. These systems are called open-loop systems.

Most current wireless standards allocate a limited feedback channel for a link between the handset and Base Transceiver Station (BTS). This channel can be utilized for many objectives, especially for sending a vital information about the channel back to the BTS. The information enables the simple spatial diversity and multiplexing techniques which increases SNR of the system and potentially simplifies the receiver architecture. These systems are called closed-loop systems.

3.2.1 Open-loop MIMO

For SIMO system, the receiver combines data streams from multiple transmit antennas using MRC method to achieve diversity gain. For multiple transmit antennas in MISO, the channel becomes more complicated and causes an interference between the different transmitted streams. If the transmitter has no any channel information, the receiver has to exploit the MIMO capacity by oneself which means the complicated algorithm is especially required.

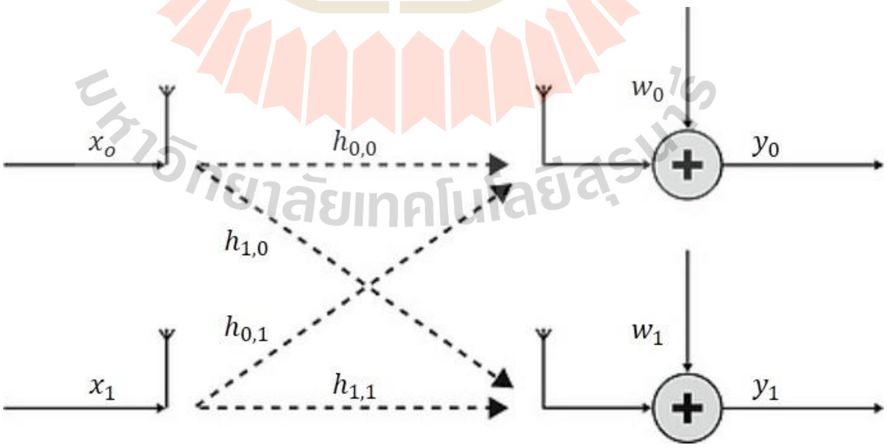

Figure 3.2 Configuration of 2×2 spatial multiplexing system transmitting different data streams via each transmit antenna.

3.2.1.1 Spatial multiplexing

Spatial Multiplexing (SM) is a well-known open-loop MIMO technique widely used in wireless systems. The different data streams are sent through each transmit antenna. The principle 2×2 spatial multiplexing system is depicted in Fig. 3.2. In addition, the optimal detection can be achieved by Maximum Likelihood (ML) criterion.

Unfortunately, the computational complexity of ML criterion is an exponential of the number of transmit antennas and possible constellation points, which makes it unsuitable for practical operation due to a complicated detection algorithm at receiver.

A popular ML algorithm used to detect signals coming from MIMO digital communication systems is the sphere decoding. The principle of the sphere decoding algorithm is to search the closest lattice point to the received signal within a sphere radius. Each code word is represented by a lattice point in a lattice field. Sphere decoding significantly reduces the detection complexity, whereby its performance is comparable to a basic ML detection. Although the sphere decoding is able to reduce complexity, it is not suitable for implementing a large number of antennas and high modulation rates such as 64-QAM.

3.2.1.2 Space-time block coding

Another widely used open-loop MIMO technique is Space-Time Block Coding (STBC). Regarding STBC, a single data stream is transmitted from multiple transmit antennas in which the signal is coded to employ the independent fading in multiple antennas in order to achieve space diversity.

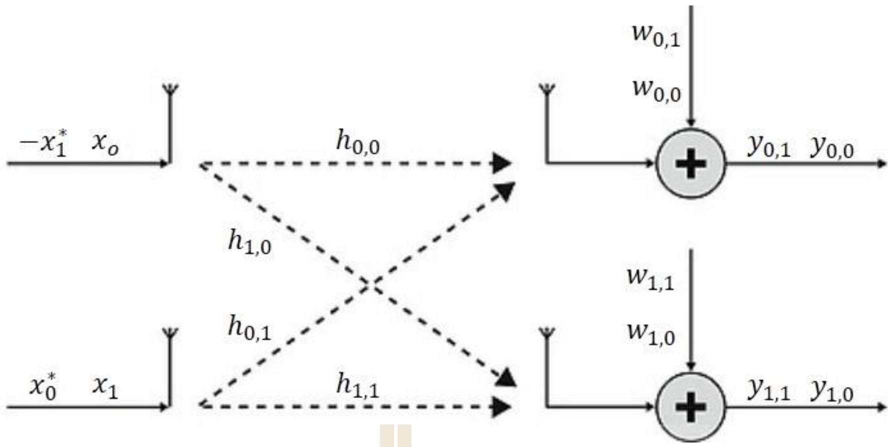

Figure 3.3 Configuration of typical Alamouti coding system transmitting a single stream from multiple transmit antennas.

The most popular STBC is Alamouti coding, as seen in Fig 3.3. It is applied to the various wireless standards. Compared to SM, Alamouti code usage provides the higher diversity gain and does not require the complicated receiver detection. However, Alamouti coding transmits only a single stream instead of multiple streams. A diversity gain is targeted by STBC while a spatial multiplexing gain is targeted by SM. Both SM and STBC usages are chosen according to the channel condition. SM scheme is superior to another only in a specified channel condition. However, many wireless standards adopt both schemes.

Because of this information, there is the work design to switch between the two schemes to achieve optimal performance. (R.W. Heath, Jr. and A.J. Paulraj, 2005) has proposed a criterion for choosing between diversity gain or multiplexing gain, which selected the scheme with the minimum Euclidean distance at the receiver. This method requires an exhaustive search and is not suitable for practical implementation. To solve this problem, the work has suggested using the Demmel condition number to make the selection. For a large Demmel condition number, the channel tends to be singular, thus STBC should be chosen.

3.2.2 Closed-loop MIMO

Closed-loop MIMO becomes a very important technique in modern wireless communications. The BTS transmitter utilizes channel information to enable the simple spatial diversity and beam forming techniques which increase SNR of the system and potentially simplify the receiver architecture.

However, the way to obtain channel information at the transmitter is the main issue in this approach. Currently, most wireless standards allocate a feedback channel to transmit a channel information to the BTS. This feedback solution can be operated in Frequency Division Duplex (FDD) and Time Division Duplex (TDD) systems. A channel information is usually quantized to reduce a heavy overhead problem on the uplink due to a large feedback message size of redundant channel information. Hence, the quantized information feedback is also called limited feedback.

For WiMAX and LTE standards, the system provides a codebook which consists of precoding matrices corresponding to the possible channels. According to the estimated channel information, a corresponding precoding matrix is selected and transmitted back to the BTS. For channel information quantization, it cannot avoid introducing a quantization error which leads to the performance loss and has been discussed in (P. Xia, and G.B. Giannakis, 2006).

In the slow-fading scenario, the channel condition keeps constant in multiple frames. However in the fast-fading scenario, the main issue is a feedback delay. If the delay is longer than the coherence time of the channel, a closed-loop MIMO system will suffer the significant performance loss.

3.2.3 Comparing the advantages and disadvantage

Among open-loop MIMO techniques, spatial multiplexing focuses on the maximum multiplexing gain. However, this technique requires a complicated detection algorithm at receiver even though it can transmit multiple data streams from multiple transmit antennas. Unlike above technique, Alamouti coding technique provides a simple optimal detection and achieves the maximum diversity gain. However, it transmits only one stream from multiple transmit antennas. Therefore, between the spatial multiplexing and Alamouti coding which one should be chosen according to the channel condition.

According to their advantages, closed-loop MIMO techniques utilize a channel information to improve SNR, capacity and simplifier receiver design. However, the closed-loop MIMO techniques have to face the performance loss due to the incomplete channel information in limited feedback.

Each MIMO technique has the advantages and disadvantages of itself. Hence, the appropriate MIMO technique should be chosen for creating the effective wireless system by considering through its service type, channel condition, complexity, and delay.

3.3 Spectrum sensing improvement developed from the existing cooperative techniques

3.3.1 MAJORITY++ rule

From both cooperative spectrum sensing techniques in chapter II, the Ph.D. candidate merges them to improve the performance of spectrum sensing to be more accurate than the existing techniques. The Ph.D. candidate has named this proposed technique as MAJORITY++ (MJ++). The proposed MAJORITY++ rule technique is created by adding the assistant signal which can be written as

$$y_{M+1}(k)=\left(\frac{1}{M}\right)\sum_{m=1}^{M}\varpi_m y_m(k). \tag{3.1}$$

The assistant signal $y_{M+1}(k)$ is obtained using the EGC technique, where ϖ_m is weighting coefficients. The reason of adding ϖ is that the received signal of each antenna element has a phase shift according to the principle of an array antenna (J. Foutz, A. Spanias and M. K. Banavar, 2008).

Then, the signal from (3.1) and the received signal of each antenna element are taken into the process of spectrum decision at (2.7) and (2.8) respectively. After that, the MJ rule is employed to process the signals according to (2.18) in which a decision factor of this technique is given by

$$\kappa_{MJ++}=\left(\frac{M+1}{2}\right). \tag{3.2}$$

The result in (3.2) is used for the final decision in (2.18) instead of κ.

3.3.2 MAJORITY++ rule with soft decision

According to a one-bit decision shown in (2.8), the defect is that there are only two-status results. The aforesaid status result is either an idle or a busy channel to be the final output. In some cases, the idle channel can be the final decision even the signal is slightly below the threshold. This is because the two-status system categorically decides the result comparing between a received signal and threshold level no matter how much the difference between signal and threshold is. For this reason, the Ph. D. candidate has proposed the new idea to increase the opportunity for those weak signals which is slightly lower than the threshold in order to give them the greater scores for cooperative decision. By dividing the threshold into multiple levels, it is also called the multi-status threshold that consists of various sub-thresholds. Moreover, the proper decision scores are given to them causing the leveled decision. Hence, this technique is called the soft decision as shown in (3.3).

$$U_{L,m}(ch) = \begin{cases} 0, & avg\left(\left|\mathbf{u}_{m,ch}\right|^2\right) < \frac{l}{L}\tau \\ 1, & avg\left(\left|\mathbf{u}_{m,ch}\right|^2\right) \geq \tau \end{cases}, \tag{3.3}$$

where l is a constant increasing from 1 up to the number of levels L. The value of $U_{L,m}(ch)$ is between 0 and 1 as same as $U_d(ch)$ in (2.8). The Ph. D. candidate has named this proposed technique as MJS++ for its abbreviation.

3.4 LTE technology

Long-Term Evolution (LTE) technology is a part of international standard from the Third Generation Partnership Project (3GPP) group which are the systems developed next to 3G systems. The main goal of LTE is to achieve the maximum transmission rate and reduce the latency. Moreover, it is the technology which achieves the higher effective utilization of limited frequency resources. Additionally, it can solve the early existing problem in the former era, which is the user identification problem employing the user's location in order to enable each user to transmit signal at the same time, same frequency, and same code. Herein, the multiple access techniques in mobile communication systems are discussed (P. Uthansakul, 2011).

The multiple access technique is the important part of mobile communication systems increasing the higher number of users alongside the limited resources. Because of the different natures between wireless communication and cable or fiber optic communication, the most limited resource in wireless communication is the spectrum. Federal Communication Commission (FCC) and Conference European of Post and Telecommunication (CEPT) are the influential groups on efficient spectrum determination. Until now, the worldwide research has kept trying to develop various techniques based on the physical signal characteristic to perform the simultaneous multi-user communications. Especially, the techniques have become popular and been commercially utilized, including Frequency Division Multiple Access (FDMA), Time Division Multiple Access (TDMA), Code Division Multiple Access (CDMA), and Space Division Multiple Access (SDMA), in which the details are as follows.

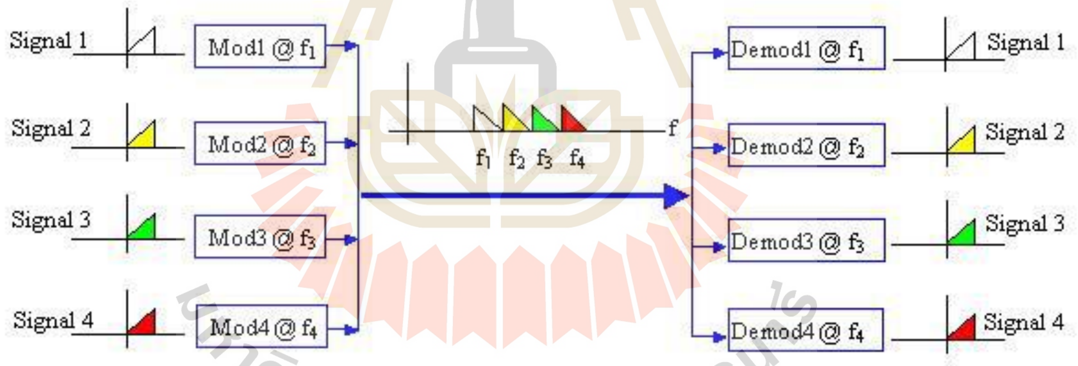

Figure 3.4 Procedure of frequency division multiple access technique.

3.4.1 Frequency division multiple access

FDMA technique is the oldest method enabling each user to perform the communications simultaneously by separating spectrum into various sub-bands, in which a sub-band is allocated to each user. By this sub-band determination, a sub-band has to be the feasible narrowest band that can support the system transmission rate. Hence, the highest number of users is equal to the number of sub-bands as seen in Fig.

3.4. This multiple access technique is suitable for the transmission of the continuous signal. However, it must beware of the interference from beside channel, in which the necessary device is the excellent filter that can sieve only the user sub-band.

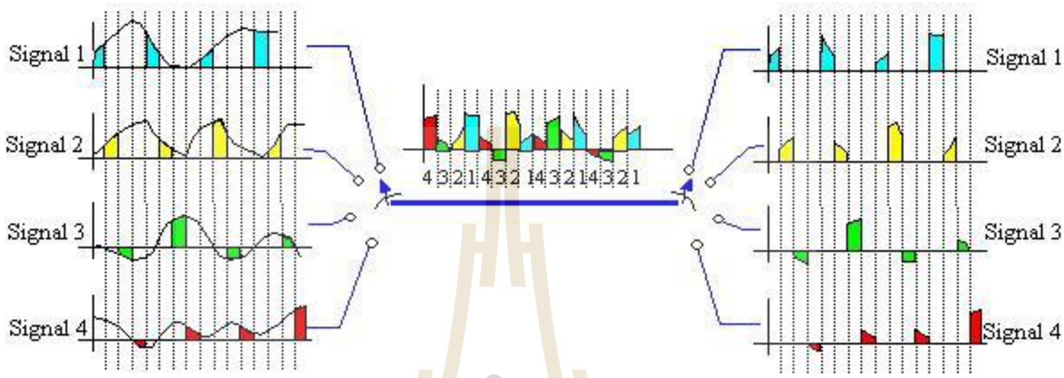

Figure 3.5 Procedure of time division multiple access technique.

3.4.2 Time division multiple access

TDMA technique is the higher efficient spectrum utilization method because it allows each user to utilize the whole spectrum at a different time. The basic time unit is called frame. Each frame is divided into the time slots in order to enable each user for performing the communication only at its time within one frame as seen in Fig. 3.5. Each frame should be properly defined to avoid the time delay or acquirement of the less number of compatible users. This multiple access technique is suitable for the transmission of the discrete signal. In practice, mobile communication systems popularly coordinate FDMA and TDMA for effectively utilizing both frequency and time resources.

3.4.3 Code division multiple access

CDMA technique relies on the signal coding method. Because its code length is very large, it is like the spectrum spread which can be employed by users to perform the communications at the same time and same spectrum. Especially, each user has a unique code. Although there are many constraints in the utilization of CDMA technique in mobile communication systems that affect the practical efficiency being greatly down from the theory, this technique is considered to be the main technique in the third generation mobile communication systems standards such as W-CDMA and CDMA200.

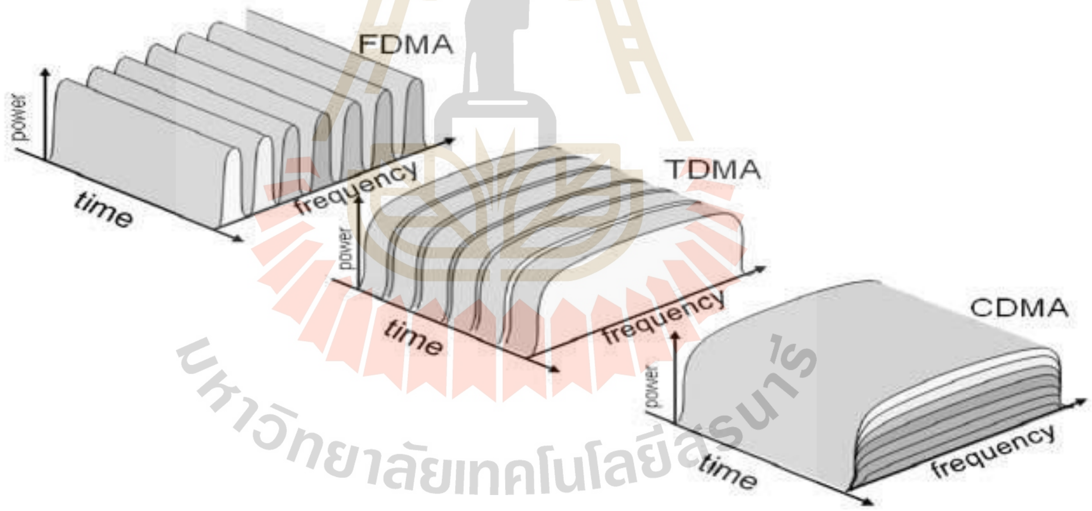

Figure 3.6 Characteristics of FDMA, TDMA, and CDMA.

3.4.4 Space division multiple access

SDMA technique is getting a lot of attention in the latter because it can increase the number of users without the spectrum wastage. In addition, it can also be utilized in combination with FDMA, TDMA, and CDMA providing an additional capability to the system that employs the existing multiple access techniques. This technique relies on the use of array antennas to identify the user using user's location in which users can transmit signal at the same time, same spectrum and same code. Hence, there are two main technologies that can accommodate this technique, including smart antenna and MIMO technologies.

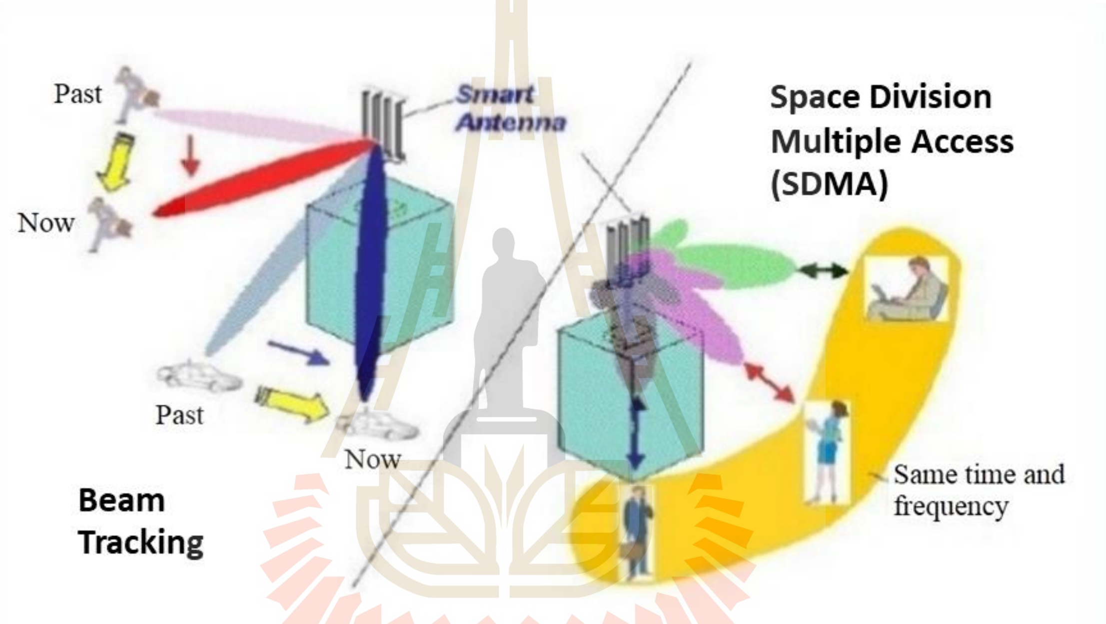

Figure 3.7 Characteristic of SDMA technique.

3.5 GPS Technology

Global Positioning System (GPS) is the technology that navigates and finds the coordinates on the earth by the satellite in order to manage feature information, which is called Relational Database Management Systems (RDBMS). This information is applied for preparing the database of Geographic Information System (GSI) in order to support the country defense plan-based mission, internal security mission, domestic peace maintaining plan, and other practices. For the first time, GPS is limited utilized for the specific groups. Later, apart from military and police organizations, the GPS technology has also played a huge role in our daily lives.

Figure 3.8 Appearance of GPS technology.

This technology enables for knowing the desired position with the high accuracy and has the error just a meter unit. The principle of GPS is to compute the distance between the satellites and a GPS device, which requires at least 3 satellites to achieve the accurate position. The GPS system is a collaboration between three key elements as follows.

1. Space segment: The GPS system is the operation of 24 satellites that orbit around the world at heights of 20000 km from earth, in which those satellites are the transmitters indicating the coordinate of the required position. The above signals are sent from at least 3 satellites in order to send the accurate coordinates to the device on earth.

2. Control segment: This segment is set on earth consisting of 1 main station and 5 sub-stations that cover various positions. It officiates controlling and communicating with the satellites. And it computes the results from each satellite and

sends the information back to the satellites causing the information to be updated all the time.

3. User segment: This segment views the coordinates obtained from the satellites through the processing of the receiver device in order to get the coordinates of the required position on the earth's surface.

3.6 Chapter summary

This research has improved spectrum sharing performance using MIMO technology, which is currently popular. MIMO technology can increase the efficacy of communication by reducing the fading problem. Because MIMO system consists of several antenna elements, it can be employed to develop spectrum sensing in CR technology. From above reason, MIMO technology is applied to ED method in chapter II which is straightforward to identify the channel and easy to implement. The information of the received signal from each antenna is brought to be jointly analyzed causing the higher accurate decision. In addition, the Ph.D. candidate has developed the spectrum sensing techniques based on the existing techniques in order to achieve the higher accurate spectrum sensing in MIMO CR system. Incidentally, this research aims to perform on LTE standard that stands on 4G communication systems. For LTE, the system can transmit the higher amount of information along with the higher speed. Moreover, the GPS technology has been employed to find the positions of the whole users in CR system in order to support the spectrum sharing, which is described in the next chapter.

CHAPTER IV

SPECTRUM SHARING PERFORMANCE ANALYSIS FOR MIMO SYSTEMS

4.1 Introduction

From the investigation of spectrum sensing method in the previous chapters, the CR system is able to know the channel status whether there is the spectrum utilization of PU or not. By the way, spectrum sharing can be divided into two main patterns. The first is non-overlapping spectrum sharing scheme, which allows SU to access spectrum only when the system does not detect any primary signal in order to avoid the interference to primary link. Nevertheless, the Ph.D. candidate pays attention to the higher possibility from another one pattern that is the overlapping spectrum sharing scheme. This spectrum sharing scheme allows SU to access the spectrum together with PU just in case if the occurred interference is on the acceptable level. Overlapping spectrum sharing scheme has been employed to make the cost-effective utilization of frequency resource due to the spectrum scarcity problem. This chapter explains the spectrum sharing system model and the performance analysis for spectrum sharing in CR systems. Especially, the performance analysis for spectrum sharing scheme is based on 3 system types including single user system, multi-user one cell system, and multi-user multi-cell system. In addition, it also presents the spectrum allocation scheme to thoroughly allocate the frequency channels to all users.

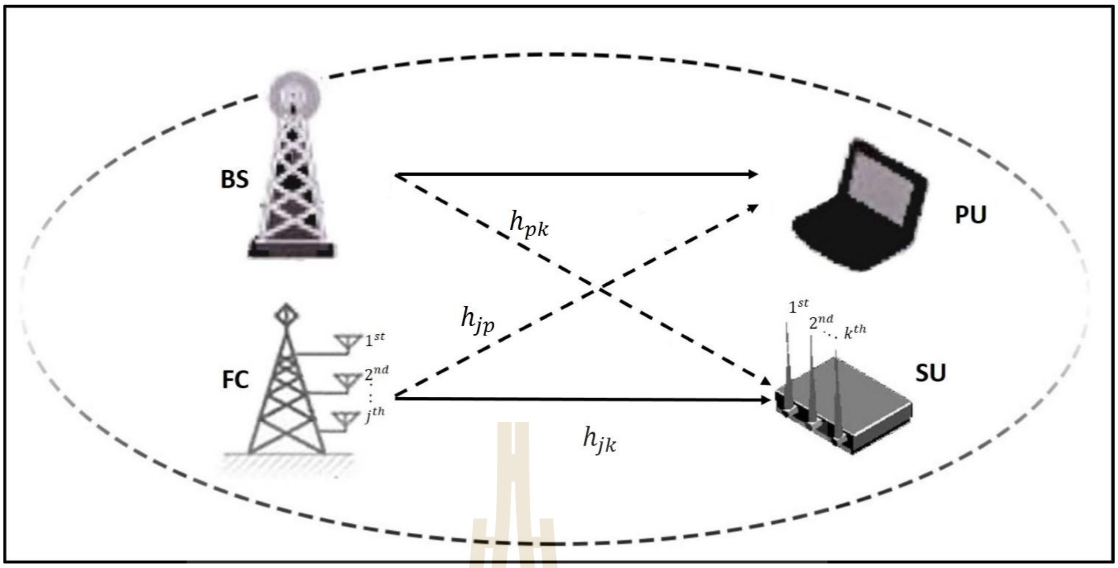

Figure 4.1 Downlink system model for MIMO CR systems.

4.2 System model

For downlink, this research considers the overlapping cognitive network in which the secondary link composes of Secondary Transmitter (ST) and Secondary Receiver (SR) equipping with N and M antennas, respectively. The primary link composed of only one antenna for both Primary Transmitter (PT) and Primary Receiver (PR). Incidentally, h_{jk}, h_{jp} and h_{pk} are the channel coefficients between j^{th} antenna of ST and k^{th} antenna of SR, between j^{th} antenna of ST and an antenna of PR, and between an antenna of PT and k^{th} antenna of SR, respectively, as depicted in Fig. 4.1. From above, the channels are modeled as Rayleigh fading distributed with the channel gains g_{jk}, g_{jp}, and g_{pk}, respectively.

The uplink system model for MIMO CR system is depicted in Fig. 4.2. In turn, h_{kj}, h_{kp}, and h_{pj} are the channel coefficients between k^{th} antenna of ST and j^{th}

antenna of SR, between k^{th} antenna of ST and an antenna of PR, and between an antenna of PT and j^{th} antenna of SR, respectively. The channels are modeled as same as the channels of downlink with the channel gains g_{kj}, g_{kp}, and g_{pj}, respectively.

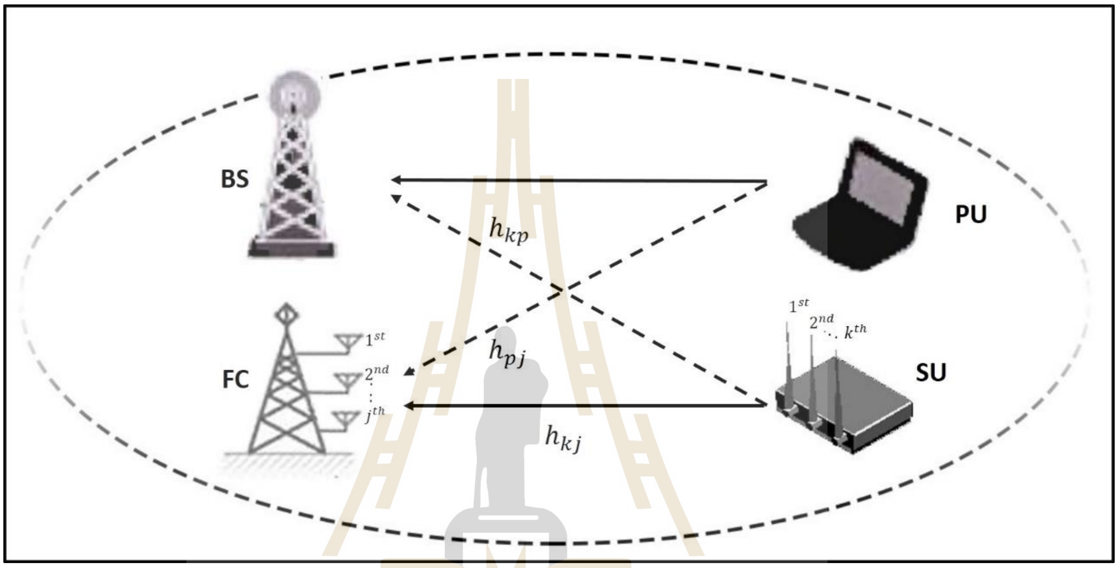

Figure 4.2 Uplink system model for MIMO CR systems.

Accordingly, Base Station (BS) is defined as PT for downlink operation and becomes PR for uplink operation. In addition, Fusion Center (FC) is defined as ST for downlink operation and becomes SR for uplink operation. Analogously, PU is defined as PR for downlink operation and becomes PT on uplink operation while SU is defined as SR for downlink operation and becomes ST for uplink operation. Furthermore, among the transmission slots of ST, one of N antennas is chosen through the ratio selection criterion (K. Tourki, K. A. Qaraqe, H-C. Yang and M-S. Alouini, 2014, Eq. 1), as follows.

$$s = \arg\max_{j} \left(\frac{g_{js}}{g_{jp}} \right) \tag{4.1}$$

and

$$s = \arg\max_{k} \left(\frac{g_{ks}}{g_{kp}} \right), \tag{4.2}$$

for downlink and uplink, respectively. For downlink $g_{js} = \sum_{k=1}^{M} \left| h_{jk} \right|^2$, and $g_{jp} = \left| h_{jp} \right|^2$.

For uplink $g_{ks} = \sum_{j=1}^{M} \left| h_{kj} \right|^2$, and $g_{kp} = \left| h_{kp} \right|^2$.

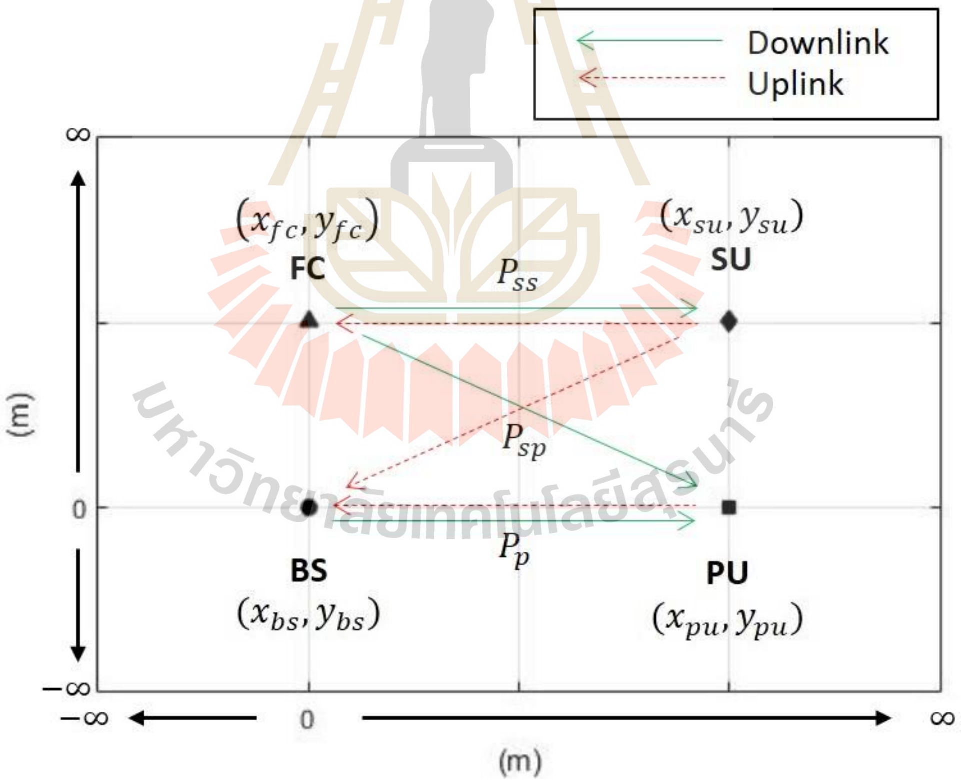

Figure 4.3 Position allocations of all members in MIMO CR systems.

The outgrowth of this research is all positions setting as general spatial parameters that can be employed for any arrangements. As seen in Fig. 4.3, it shows the position allocation of all members in MIMO CR system. Then, the distance between PT to PR can be written as

$$R_p = \left(\left(y_{pu} - y_{bs}\right)^2 + \left(x_{pu} - x_{bs}\right)^2\right)^{\frac{1}{2}}. \tag{4.3}$$

For downlink, the distances from PT to SR and from ST to SR, respectively, are given by

$$D_{ps\_d} = \left(\left(y_{su} - y_{bs}\right)^2 + \left(x_{su} - x_{bs}\right)^2\right)^{\frac{1}{2}}, \tag{4.4}$$

$$D_{ss\_d} = \left(\left(y_{su} - y_{fc}\right)^2 + \left(x_{su} - x_{fc}\right)^2\right)^{\frac{1}{2}}. \tag{4.5}$$

For uplink, yields

$$D_{ps\_u} = \left(\left(y_{fc} - y_{pu}\right)^2 + \left(x_{fc} - x_{pu}\right)^2\right)^{\frac{1}{2}}, \tag{4.6}$$

$$D_{ss\_u} = \left(\left(y_{fc} - y_{su}\right)^2 + \left(x_{fc} - x_{su}\right)^2\right)^{\frac{1}{2}}. \tag{4.7}$$

Hence, the received power of primary link for both downlink and uplink are given by

$$P_p = P_{max}\left(\frac{\lambda}{4\pi R_p}\right)^2 G_t G_r, \tag{4.8}$$

where P_{max} is maximum primary output power, λ is wavelength, G_t and G_r are transmitter gain and receiver gain, respectively. Then, the received power from PT to SR for downlink is expressed as

$$P_{ps\_d} = P_{max}\left(\frac{\lambda}{4\pi D_{ps\_d}}\right)^2 G_t G_r. \tag{4.9}$$

The received power from PT to SR for uplink is expressed as

$$P_{ps\_u} = P_{max}\left(\frac{\lambda}{4\pi D_{ps\_u}}\right)^2 G_t G_r. \tag{4.10}$$

The received power from ST to SR for downlink is expressed as

$$P_{ss\_d} = P_{smax}\left(\frac{\lambda}{4\pi D_{ss\_d}}\right)^2 G_t G_r. \tag{4.11}$$

where P_{smax} is maximum secondary output power. Then, the received power from ST to SR for uplink is expressed as

$$P_{ss\_u} = P_{smax}\left(\frac{\lambda}{4\pi D_{ss\_u}}\right)^2 G_t G_r. \tag{4.12}$$

4.3 Initial statistical equations

In this research, the $m-$ QAM modulation is employed, where m is constellation size. Note that other modulation types can also be analyzed only if their closed-form formulas of BER are known. Then, the approximated BER of the primary network is shown as following.

$$BER_p \approx 0.2e^{-1.5\left(\frac{\gamma_{sp} G_c}{m-1}\right)}, \tag{4.13}$$

where G_c is the coding gain (A. Goldsmith, 2005, Eq. 9.38).

Then, the Signal to Noise Ratio (SNR) from ST to PR is given by

$$\gamma_{sp} = \left(\frac{P_p}{P_{sp} g_{sp} + N_o} \right), \tag{4.14}$$

where N_o is the power spectral density of the noise assumed to be constant for all states, and $g_{sp} = |h_{sp}|^2$. Putting (4.14) into (4.13), then the received power from ST to PR is

$$P_{sp} = \left(\frac{-1.5 P_p G_c}{(m-1)\ln(5BER_p)} - N_o \right) \frac{1}{g_{sp}}. \tag{4.15}$$

When considering the power from (4.15), the BER region of the primary network can be defined according to the interference from ST in the same location as

$$D_{sp} = \frac{\lambda}{4\pi} \left(\frac{P_{smax} G_t G_r}{P_{sp}} \right)^{\frac{1}{2}}. \tag{4.16}$$

By using PR as a reference point, the distance from ST to PR D_{sp} from (4.16) can show the possible position of ST being available to communicate with FC around PR. Hence, the positions of ST affecting PR performance can be predicted.

The Cumulative Distribution Function (CDF) of channel gain from ST to SR attaching with a subscript g_{ss}, in which $g_{ss} = \sum_{k=1}^{M} |h_{sk}|^2$ for downlink and $g_{ss} = \sum_{j=1}^{M} |h_{sj}|^2$ for uplink (K. Tourki, K. A. Qaraqe, H-C. Yang and M-S. Alouini, 2014, Eq. 5), is given by

$$F_{g_{ss}}(x) = \frac{1}{\Gamma(M+1)} \left[\left(\frac{x}{g_{ss}} \right)^{MN} \Gamma\left(1 - M(N-1), \frac{x}{g_{ss}} \right) + \gamma\left(M+1, \frac{x}{g_{ss}} \right) \right], \tag{4.17}$$

where $\Gamma(.\,,.)$ and $\gamma(.,.)$ are the upper incomplete gamma function and the lower incomplete gamma function, respectively.

By the way, performance analysis can be divided into two cases based on the concentration of interference followed by distance, which is described in the next section.

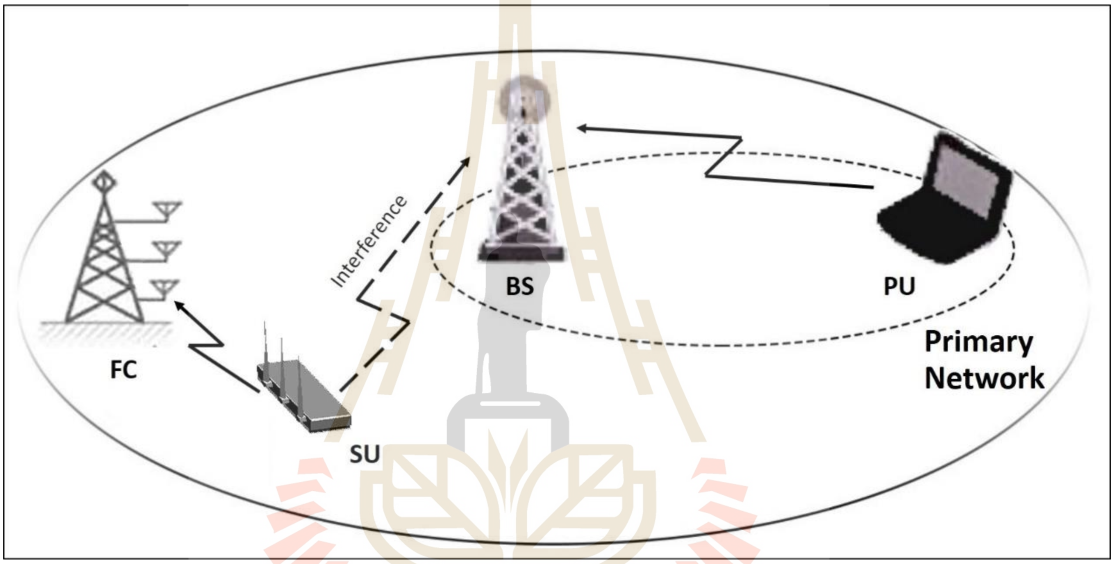

Figure 4.4 The system model when PT is very far from SR.

4.4 Performance analysis without interference from PT-SR

In the first case, the analysis is performed when interference from PT-SR is ignored. Fig. 4.4 illustrates the system model when PT is far overboard from SR. It means that there is almost no interference from PT, which the outage probability can be defined as

$$P_{out} = \Pr\left[\gamma_{ss} < x\right] = F_{g_{ss}}\left(\frac{x}{\frac{P_{ss}}{N_0}}\right), \tag{4.18}$$

where

$$F_{g_{ss}}\left(\frac{x}{\frac{P_{ss}}{N_0}}\right)=\frac{1}{\Gamma(M+1)}\left[\left(\frac{x}{\gamma_{ss}}\right)^{MN}\times\right.$$
$$\left.\Gamma\left(1-M(N-1),\frac{x}{\gamma_{ss}}\right)+\gamma\left(M+1,\frac{x}{\gamma_{ss}}\right)\right]. \tag{4.19}$$

Equation (4.19) is proved in Appendix A.1. This equation also provides the combined SNR from ST-SR link as

$$\gamma_{ss}=g_{ss}\left(\frac{P_{ss}}{N_0}\right). \tag{4.20}$$

P_{ss} also depends on whether it is downlink from (4.11) or uplink from (4.12).

The typical results (Y. Chen and C. Tellambura, 2004, Eq. 32) for obtaining the end-to-end BER in terms of SNR is expressed as

$$BER_{s,sys}=-\int_0^{\infty}\left\{\frac{d}{dx}P_e(x)\right\}F_{\gamma}(x)\,dx, \tag{4.21}$$

where $F_{\gamma}(.)$ is the CDF in terms of SNR for any cases, and $P_e(.)$ is the Condition Error Probability (CEP) that is based on the employed modulation scheme.

$$P_e(x)=a\mathrm{Q}\left(\sqrt{bx}\right), \tag{4.22}$$

where a and b are the modulation-specific constants, such as $(a,b)=(1,2)$ for BPSK, $(a,b)=(1,1)$ for BFSK, and $(a,b)=\left(\frac{2(m-1)}{m},\frac{6\log_2(m)}{(m^2-1)}\right)$ for m - PAM. And $\mathrm{Q}(.)$ is the Gaussian Q-function.

Consider the CDF of g_{ss} in (4.19), the BER of this case is expressed as follows.

$$BER_s(a,b) = \frac{a}{2}\sqrt{\frac{b}{2\pi}} \int_0^\infty \frac{e^{-\frac{b}{2}x}}{\sqrt{x}} F_{g_{ss}}\left(\frac{x}{\frac{P_{ss}}{N_0}}\right) dx. \tag{4.23}$$

So, the closed form of BER in (4.23) can be rewritten as

$$BER_s(a,b) = \frac{\Gamma\left(M+\frac{3}{2}\right)}{\Gamma(M+1)} \frac{\frac{a}{2}\sqrt{\frac{b}{2\pi}}\left(\frac{1}{\gamma_{ss}}\right)^{1+M}}{\left(\frac{1}{\gamma_{ss}}+\frac{b}{2}\right)^{M+\frac{3}{2}}} \left[\left(\frac{1}{MN+\frac{1}{2}}\right) \times\right.$$

$$\left. {}_2F_1\left(1, M+\frac{3}{2}; MN+\frac{3}{2}; \frac{b\gamma_{ss}}{2+b\gamma_{ss}}\right) + \left(\frac{1}{1+M}\right) {}_2F_1\left(1, M+\frac{3}{2}; M+2; \frac{2}{2+b\gamma_{ss}}\right)\right]. \tag{4.24}$$

Equation (4.24) is proved in Appendix A.1, where ${}_2F_1(.,.;.;.)$ is the hypergeometric function (A. Jeffrey and D. Zwillinger, 2007, Eq. 9.14.2).

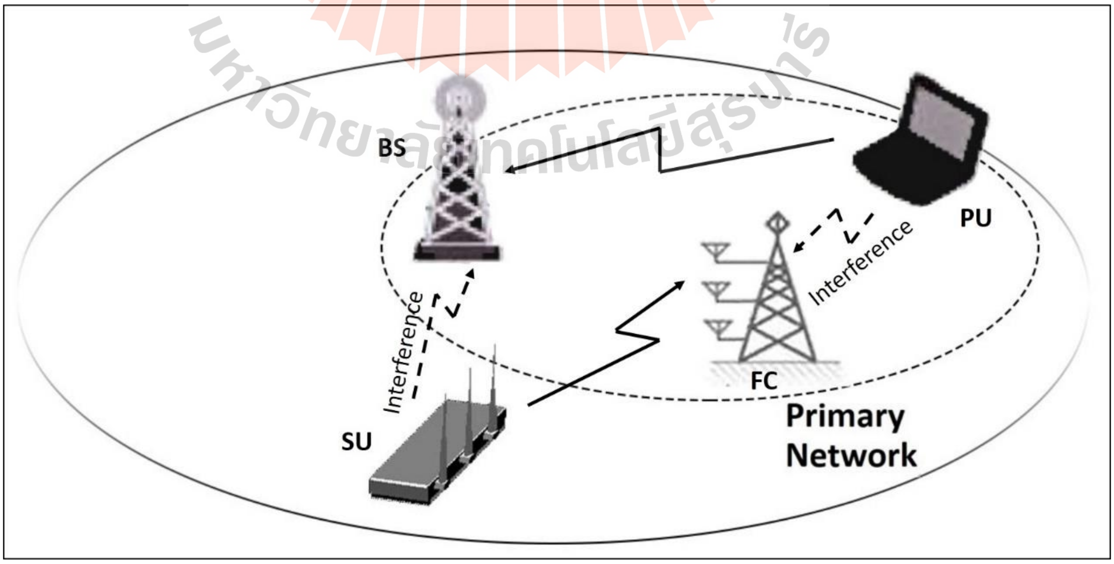

Figure 4.5 The system model when PT is close to SR.

4.5 Performance analysis with interference from PT-SR

For the second case, in the appearing of interference from PU as illustrated in Fig. 4.5, the combined Signal to Interference plus Noise Ratio (SINR) at SR is given by

$$\gamma_{int} = \frac{\frac{P_{ss}}{N_o} g_{ss}}{\frac{P_{ps}}{N_0} g_{ps} + 1} = \frac{\gamma_{ss}}{\gamma_{ps} + 1}, \tag{4.25}$$

where $g_{ps} = \frac{\left|\sum_{k=1}^{M} h_{sk}^{*} h_{pk}\right|^2}{g_{ss}}$ for downlink and $g_{ps} = \frac{\left|\sum_{j=1}^{M} h_{sj}^{*} h_{pj}\right|^2}{g_{ss}}$ for uplink are the channel gains from PT-SR (A. Shah and A. M. Haimovich, 2000 and M. Kang and M. S. Alouini, 2004). The Probability Density Function (PDF) of this channel gain is modeled as

$$p_{g_{ps}}(y) = \frac{1}{g_{ps}} e^{-\frac{y}{g_{ps}}}, \tag{4.26}$$

So the CDF of γ_{int} can be written as

$$F_{\gamma_{int}}(x) = \Pr[\gamma_{int} < x] = F_1(x) + F_2(x), \tag{4.27}$$

where $F_1(.)$ and $F_2(.)$ can be defined from (4.19) at SNR from PT-SR on both downlink and uplink operations. Then,

$$\gamma_{ps} = g_{ps} \frac{P_{ps}}{N_0}, \tag{4.28}$$

where P_{ps} also depends on whether it would be on downlink operation from (4.9) or uplink operation from (4.10). The CDF of γ_{int} can be written as

$$\Pr\left[\gamma_{int} < x\right] = \mathbb{E}_{\gamma_{ps}}\left[F_{g_{ss}}\left(\frac{x\left(y+1\right)}{\frac{P_{ss}}{N_0}}\right) \mid \gamma_{ps} = y\right]. \tag{4.29}$$

Hence,

$$F_{g_{ss}}\left(\frac{x\left(y+1\right)}{\frac{P_{ss}}{N_0}}\right) = \frac{1}{\Gamma\left(M+1\right)}\left[\left(\frac{x}{\gamma_{ss}}\right)^{MN}\left(y+1\right)^{MN} \times \Gamma\left(1-M\left(N-1\right), \frac{x\left(y+1\right)}{\gamma_{ss}}\right) + \gamma\left(M+1, \frac{x\left(y+1\right)}{\gamma_{ss}}\right)\right]. \tag{4.30}$$

Equation (4.30) can be proved in Appendix A.2. Then $F_1(.)$ is defined as

$$F_1\left(x\right) = \int_0^{\infty} \frac{\left(\frac{x\left(y+1\right)}{\gamma_{ss}}\right)^{MN}}{\Gamma\left(M+1\right)} \frac{e^{-\frac{y}{\gamma_{ps}}}}{\gamma_{ps}} \Gamma\left(1-M\left(N-1\right), \frac{x\left(y+1\right)}{\gamma_{ss}}\right) dy, \tag{4.31}$$

$F_1(x)$ is derived to be (4.32) as shown in Appendix A.2, where $\mathrm{Ei}(.)$ is the exponential integral function.

$$\begin{aligned} F_1\left(x\right) = {} & \frac{\left(-1\right)^{M\left(N-1\right)} e^{\frac{1}{\gamma_{ps}}} \left(\frac{\gamma_{ps}}{\gamma_{ss}}\right)^{MN}}{\Gamma\left(M+1\right)\left(M\left(N-1\right)-1\right)!}\left[\Gamma\left(MN+1, \frac{1}{\gamma_{ps}}\right) x^{MN} \mathrm{Ei}\left(\frac{-x}{\gamma_{ss}}\right) + \right. \\ & \left. \left(MN\right)! \sum_{k=0}^{MN} \frac{\left(\frac{1}{\gamma_{ps}}\right)^k}{k!} x^{MN} \left(\frac{1}{\gamma_{ps}} + \frac{x}{\gamma_{ss}}\right)^{-k} \Gamma\left(k, \frac{1}{\gamma_{ps}} + \frac{x}{\gamma_{ss}}\right)\right] + \\ & \frac{\left(\frac{1}{\gamma_{ps}}\right) e^{\frac{1}{\gamma_{ps}}}}{\Gamma\left(M+1\right)\left(M\left(N-1\right)-1\right)!} \sum_{k=0}^{M\left(N-1\right)+k} \left(-1\right)^{M\left(N-1\right)+k} k! \left(\frac{x}{\gamma_{ss}}\right)^{MN-k-1} \times \\ & \left(\frac{1}{\gamma_{ps}} + \frac{x}{\gamma_{ss}}\right)^{k-MN} \Gamma\left(MN-k, \frac{1}{\gamma_{ps}} + \frac{x}{\gamma_{ss}}\right). \end{aligned} \tag{4.32}$$

Next,

$$F_2(x)=\int_0^\infty \frac{\gamma\left(M+1,\frac{x(y+1)}{\gamma_{ss}}\right)}{\Gamma(M+1)}\frac{e^{-\frac{y}{\gamma_{ps}}}}{\gamma_{ps}}dy, \tag{4.33}$$

$F_2(x)$ is derived to be (4.34) as shown in Appendix A.2.

$$F_2(x)=\frac{\left(\frac{1}{\gamma_{ps}}\right)e^{\frac{1}{\gamma_{ps}}}M!}{\Gamma(M+1)}\gamma_{ps}e^{-\frac{1}{\gamma_{ps}}}-\sum_{k=0}^{M}\frac{\left(\frac{x}{\gamma_{ss}}\right)^k}{k!}\left(\frac{1}{\gamma_{ps}}+\frac{x}{\gamma_{ss}}\right)^{-k-1}\times$$
$$\Gamma\left(k+1,\frac{1}{\gamma_{ps}}+\frac{x}{\gamma_{ss}}\right). \tag{4.34}$$

Finally, the BER is obtained by replacing (4.27) into (4.23) expressed as follows.

$$BER_{Int}(a,b)=\frac{a}{2}\sqrt{\frac{b}{2\pi}}\int_0^\infty \frac{e^{-\frac{b}{2}x}}{\sqrt{x}}F_{\gamma_{int}}(x)dx. \tag{4.35}$$

As a result,

$$BER_{Int}(a,b)=\frac{a}{2}\sqrt{\frac{b}{2\pi}}\frac{1}{\Gamma(M+1)}\left[I_1+I_2+I_3+I_4\right], \tag{4.36}$$

where I_1, I_2, I_3 and I_4 are the sub-function that have the closed forms in (4.37), (4.38), (4.39) and (4.40), respectively.

$$I_1=\frac{(-1)^{M(N-1)+1}}{(M(N-1)-1)!}e^{\frac{1}{\gamma_{ps}}}\left(\frac{\gamma_{ps}}{\gamma_{ss}}\right)^{MN}\frac{\Gamma\left(MN+1,\frac{1}{\gamma_{ps}}\right)\Gamma\left(MN+\frac{1}{2}\right)}{\left(MN+\frac{1}{2}\right)\left(\frac{1}{\gamma_{ss}}+\frac{b}{2}\right)^{MN+\frac{1}{2}}}\times$$
$${}_2F_1\left(1,MN+\frac{1}{2};MN+\frac{3}{2};\frac{b\gamma_{ss}}{2+b\gamma_{ss}}\right). \tag{4.37}$$

Next,

$$I_2 = (-1)^{M(N-1)} (MN)!\Gamma\left(MN+\frac{1}{2}\right) e^{\frac{b\gamma_{ss}+2}{4\gamma_{ps}}} \times$$
$$\sum_{k=1}^{MN} \frac{(k-1)!}{k!} \sum_{m=0}^{k-1} \frac{\left(\frac{1}{\gamma_{ps}}\right)^m}{m!} \times \tag{4.38}$$
$$\left(\frac{1}{\gamma_{ss}}+\frac{b}{2}\right)^{-\frac{1}{2}\left(MN+m-k+\frac{3}{2}\right)} \left(\frac{\gamma_{ss}}{\gamma_{ps}}\right)^{\frac{1}{4}(2k+2m-2MN-1)} \times$$
$$\mathrm{W}_{\frac{1}{2}\left(m-k-MN-\frac{1}{2}\right), -\frac{1}{2}\left(MN+m-k+\frac{1}{2}\right)} \left(\frac{b\gamma_{ss}+2}{2\gamma_{ps}}\right),$$

where $W_{\varepsilon,\mu}(.)$ is the Whittaker W-function.

$$I_3 = \left(\frac{1}{\gamma_{ps}}\right) e^{\frac{b\gamma_{ss}+2}{4\gamma_{ps}}} \sum_{k=0}^{M(N-1)-2} (-1)^{M(N-1)+k} k!(MN-k-1)! \times$$
$$\Gamma\left(MN-k-\frac{1}{2}\right) \sum_{m=0}^{MN-k-1} \frac{\gamma_{ss}^{1-m}}{m!} \left(\frac{1}{\gamma_{ss}}+\frac{b}{2}\right)^{-\frac{1}{2}\left(m+\frac{1}{2}\right)} \left(\frac{\gamma_{ss}}{\gamma_{ps}}\right)^{\frac{1}{2}\left(m-\frac{3}{2}\right)} \times \tag{4.39}$$
$$\mathrm{W}_{\frac{1}{2}\left(2k-2MN+m+\frac{3}{2}\right), \frac{1}{2}\left(-m+\frac{1}{2}\right)} \left(\frac{b\gamma_{ss}+2}{2\gamma_{ps}}\right).$$

Finally,

$$I_4 = M!\left[\sqrt{\frac{2\pi}{b}} - \left(\frac{1}{\gamma_{ps}}\right) e^{\frac{b\gamma_{ss}+2}{4\gamma_{ps}}} \sum_{k=0}^{M} \Gamma\left(k+\frac{1}{2}\right) \sum_{m=0}^{k} \frac{\gamma_{ss}^{-m+1}}{m!} \times \right.$$
$$\left. \left(\frac{1}{\gamma_{ss}}+\frac{b}{2}\right)^{-\frac{1}{2}\left(m+\frac{1}{2}\right)} \left(\frac{\gamma_{ss}}{\gamma_{ps}}\right)^{\frac{1}{2}\left(m-\frac{3}{2}\right)} \mathrm{W}_{\frac{1}{2}\left(m-2k-\frac{1}{2}\right), \frac{1}{2}\left(-m+\frac{1}{2}\right)} \left(\frac{b\gamma_{ss}+2}{2\gamma_{ps}}\right)\right], \tag{4.40}$$

All of them are proved in Appendix A.3.

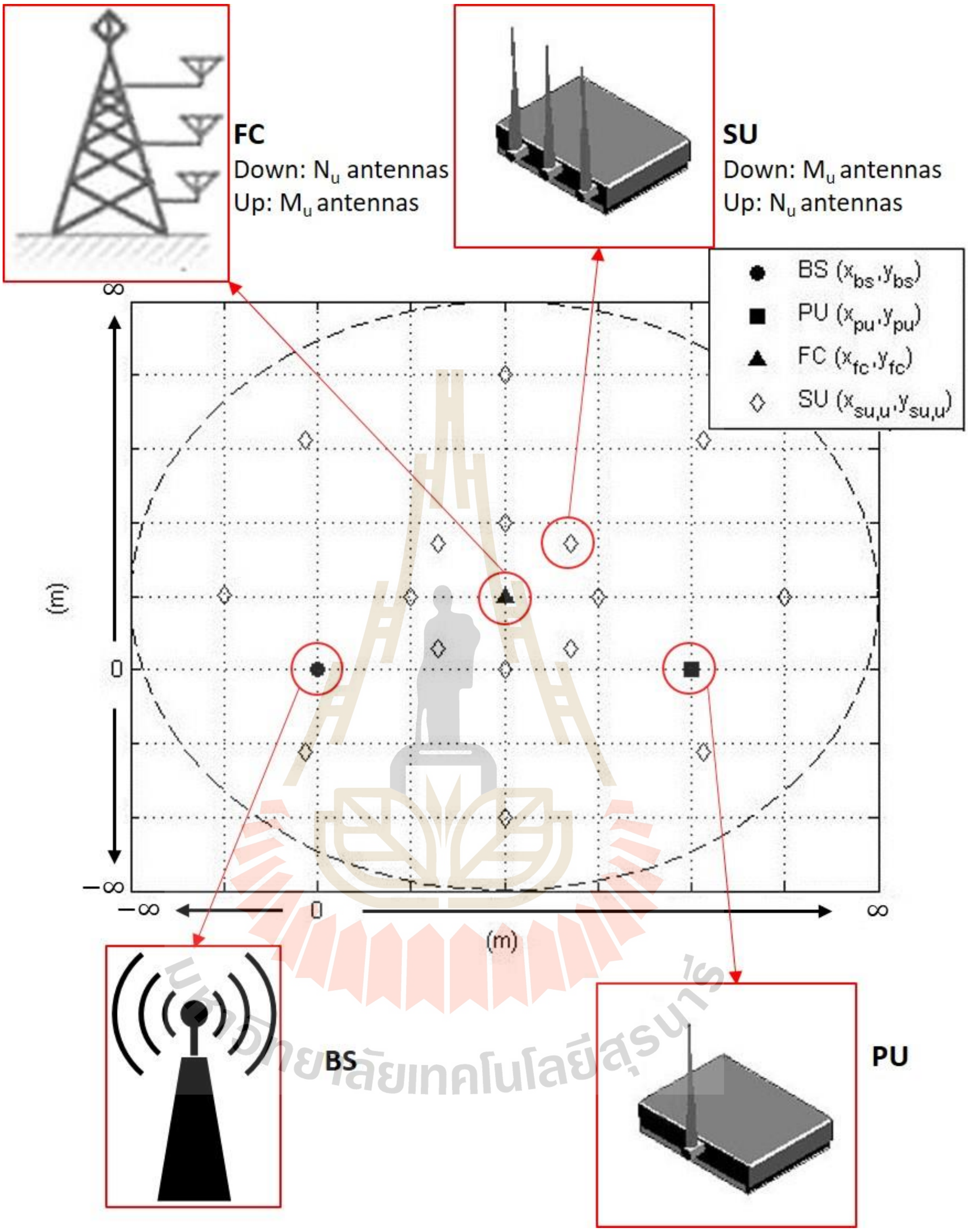

Figure 4.6 System model for multi-user one-cell spectrum sharing in MIMO CR system.

4.6 Multi-user systems

In practice, a cognitive network consists of many SUs, which can be divided into two cases based on the number of picocells in a macrocell as follows.

4.6.1 Multi-user one-cell spectrum sharing

In this case, there is only one FC in the coverage area of the macrocell, and there are SUs scattering inside a coverage area. The primary link is composed of only one antenna for both PT and PR. Whereas, each secondary link is composed of ST and SR that are equipped with N_u and M_u antennas, respectively, that belong to each SU from overall U number of SUs in the coverage area of FC, for $u = 1, 2, \ldots, U$, as seen in Fig. 4.6. As can be seen that the number of antennas of each SU is not necessary to be the same as each other. Nevertheless, the number of antennas have to be not less than 2 antennas to support the MIMO systems.

For downlink, BS is defined as PT while FC is defined as ST, and PU is defined as PR while SUs are defined as SRs. The channel between the selected antenna of FC and the k^{th} antenna of the u^{th} SU has a channel coefficient $h_{sk,u}$. The channel between the selected antenna of FC and an antenna of PU has a channel coefficient h_{sp}. The channel between an antenna of BS and the k^{th} antenna of the u^{th} SU has a channel coefficient $h_{pk,u}$.

For uplink, BS is defined as PR while FC is defined as SR, and PU is defined as PT while SUs are defined as STs. The channel between the selected antenna of the u^{th} SU and the j^{th} antenna of FC has a channel coefficient $h_{sj,u}$. The channel between the selected antenna of the u^{th} SU and an antenna of BS has a channel coefficient $h_{sp,u}$. The channel between an antenna of PU and the j^{th} antenna of FC has a channel coefficient h_{pj}. The channel between the selected antennas of other SUs in the same coverage area and the j^{th} antenna of FC has an average channel coefficient $\bar{h}_{ij,u}$.

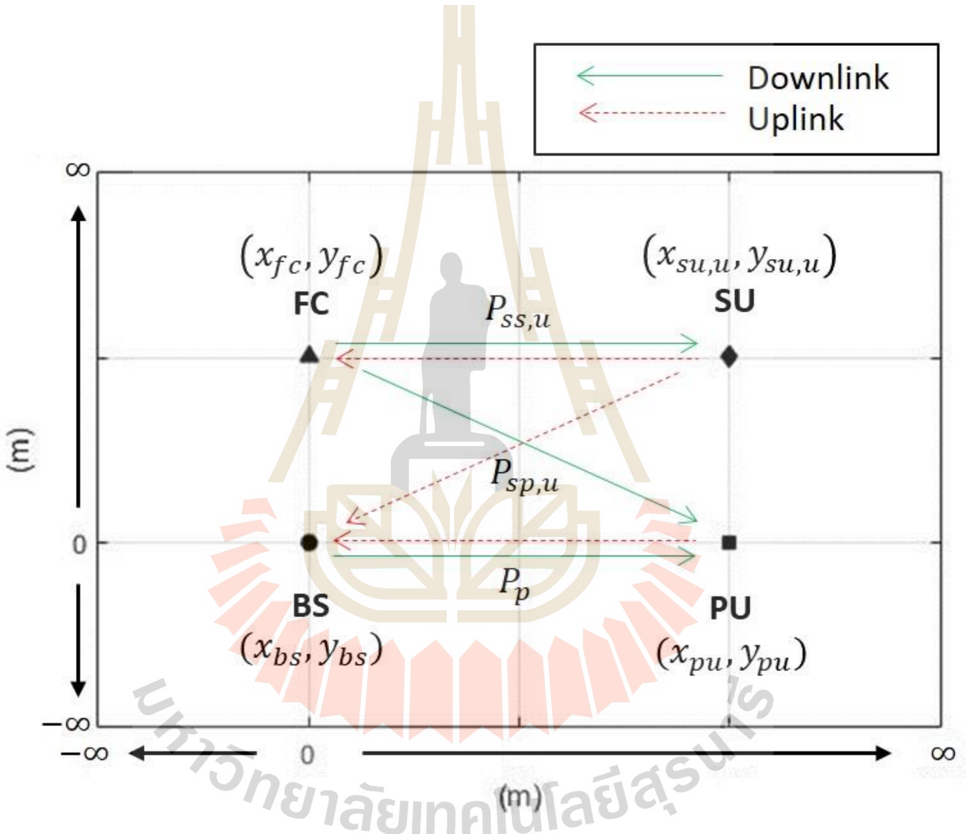

Figure 4.7 Position allocations of each member in multi-user one-cell MIMO CR systems.

For more clarity as shown in Fig. 4.7, the distance equations and power equations are as follows.

For downlink, the distances from PT to SR and from ST to SR are given by

$$D_{ps,u\_d} = \left(\left(y_{su,u} - y_{bs}\right)^2 + \left(x_{su,u} - x_{bs}\right)^2\right)^{\frac{1}{2}}, \tag{4.41}$$

$$D_{ss,u\_d} = \left(\left(y_{su,u} - y_{fc}\right)^2 + \left(x_{su,u} - x_{fc}\right)^2\right)^{\frac{1}{2}}. \tag{4.42}$$

Then, the received power from PT to SR for downlink is expressed as

$$P_{ps,u\_d} = P_{max}\left(\frac{\lambda}{4\pi D_{ps,u\_d}}\right)^2 G_t G_r. \tag{4.43}$$

The received power from ST to SR for downlink is expressed as

$$P_{ss,u\_d} = P_{smax}\left(\frac{\lambda}{4\pi D_{ss,u\_d}}\right)^2 G_t G_r. \tag{4.44}$$

Likewise, for uplink, the distances from PT to SR and from ST to SR are given by

$$D_{ps\_u} = \left(\left(y_{fc} - y_{pu}\right)^2 + \left(x_{fc} - x_{pu}\right)^2\right)^{\frac{1}{2}}, \tag{4.45}$$

$$D_{ss,u\_u} = \left(\left(y_{fc} - y_{su,u}\right)^2 + \left(x_{fc} - x_{su,u}\right)^2\right)^{\frac{1}{2}}. \tag{4.46}$$

The received power from PT to SR for uplink is expressed as

$$P_{ps\_u} = P_{max}\left(\frac{\lambda}{4\pi D_{ps\_u}}\right)^2 G_t G_r. \tag{4.47}$$

Next, the received power from ST to SR for uplink is expressed as

$$P_{ss,u\_u} = P_{smax}\left(\frac{\lambda}{4\pi D_{ss,u\_u}}\right)^2 G_t G_r. \tag{4.48}$$

However, only for uplink, it has the interference power vector due to other SUs in the same coverage area, which can be defined as

$$\mathbf{P}'_{ssI\_u} = \mathbf{P}'_{ss\_u} - \begin{bmatrix} 0 & \cdots & P_{ss,u\_u} & 0 & \cdots & 0 \end{bmatrix}, \tag{4.49}$$

where $P_{ss,u\_u} \in \mathbf{P}_{ss\_u}$.

In order to evaluate BER, the $m-$QAM modulation is employed, where m is constellation size. Then the received power from ST to PR for downlink and uplink are given by

$$P_{sp\_d} = \left(\frac{-1.5 P_p G_c}{(m-1)\ln\left(5BER_p\right)} - N_o \right) \frac{1}{g_{sp}}, \tag{4.50}$$

$$P_{sp\_u} = \left(\frac{-1.5 P_p G_c}{(m-1)\ln\left(5BER_p\right)} - N_o \right) \frac{1}{\bar{g}_{sp}}, \tag{4.51}$$

where $\bar{g}_{sp} = avg\left(\left|\mathbf{h}_{sp}\right|^2\right)$ is an average channel gain from ST-PR. After that, by considering the power from (4.50) and (4.51) for downlink and uplink, respectively, the BER region of primary network due to interference from ST in the same location can be defined by replacing it in (4.16). By using PR as a reference point, the distance from ST to PR D_{sp} can show the possible position of ST being available to communicate with FC around PR. Hence, the positions of ST affecting PR performance can be predicted.

The CDF of $g_{ss,u} = \sum_{k=1}^{M_u} \left|h_{sk,u}\right|^2$ for downlink and $g_{ss,u} = \sum_{j=1}^{M_u} \left|h_{sj,u}\right|^2$ for uplink is given by

$$F_{g_{ss,u}}(x)=\frac{1}{\Gamma(M_u+1)}\times$$
$$\left[\left(\frac{x}{g_{ss,u}}\right)^{M_uN_u}\Gamma\left(1-M_u(N_u-1),\frac{x}{g_{ss,u}}\right)+\gamma\left(M_u+1,\frac{x}{g_{ss,u}}\right)\right]. \tag{4.52}$$

Only in the non-overlapping spectrum sharing case, when interference from PT-SR is ignored ($P_{ps,u}=0$), BER of this case on downlink can be expressed as

$$BER_{s,u}(a,b)=\frac{a}{2}\sqrt{\frac{b}{2\pi}}\int_0^{\infty}\frac{e^{-\frac{b}{2}x}}{\sqrt{x}}F_{g_{ss,u}}\left(\frac{x}{\frac{P_{ss,u}}{N_0}}\right)dx. \tag{4.53}$$

By using (Gradshteyn I. S., 2007, Eq. 6.455.1 and Eq. 6.455.2), the BER in (8) can be written in the closed form as

$$BER_{s,u}(a,b)=\frac{\Gamma\left(M_u+\frac{3}{2}\right)\frac{a}{2}\sqrt{\frac{b}{2\pi}}\left(\frac{1}{\gamma_{ss,u}}\right)^{1+M_u}}{\Gamma(M_u+1)\left(\frac{1}{\gamma_{ss,u}}+\frac{b}{2}\right)^{M_u+\frac{3}{2}}}\left[\left(\frac{1}{M_uN_u+\frac{1}{2}}\right)\times\right.$$
$${}_2F_1\left(1,M_u+\frac{3}{2};M_uN_u+\frac{3}{2};\frac{b\gamma_{ss,u}}{2+b\gamma_{ss,u}}\right)+ \tag{4.54}$$
$$\left.\left(\frac{1}{1+M_u}\right){}_2F_1\left(1,M_u+\frac{3}{2};M_u+2;\frac{2}{2+b\gamma_{ss,u}}\right)\right],$$

Then, SNR from ST-SR link for both downlink and uplink are defined as

$$\gamma_{ss,u}=g_{ss,u}\frac{P_{ss,u}}{N_0}. \tag{4.55}$$

For overlapping spectrum sharing case, when interference from PT-SR is considered ($P_{ps,u}\neq 0$), SNR from PT-SR on downlink is expressed as

$$\gamma_{is,u\_d} = g_{ps,u} \frac{P_{ps,u\_d}}{N_0}, \tag{4.56}$$

where $g_{ps,u} = \frac{\left| \sum_{k=1}^{M_u} h_{sk}^{*} h_{pk,u} \right|^2}{g_{ss,u}}$ is the channel gain from PT-SR for downlink. For uplink of both spectrum sharing cases, SNR is defined as

$$\gamma_{is,u\_u} = g_{ps} \frac{P_{ps,u\_u}}{N_0} + \bar{g}_{is,u} \sum_{u=1}^{U} \frac{P_{ssI,u\_u}}{N_0}, \tag{4.57}$$

where $g_{ps,u} = \frac{\left| \sum_{j=1}^{M_u} h_{sj,u}^{*} h_{pj} \right|^2}{g_{ss,u}}$ and $\bar{g}_{is,u} = \sum_{j=1}^{M_u} \left| \bar{h}_{ij,u} \right|^2$ for uplink. Note that $P_{ps,u} = 0$ in (4.57) only for uplink of non-overlapping case. Then, the BER of overlapping cases for downlink and uplink is

$$BER_{Int,u}(a,b) = \frac{a}{2}\sqrt{\frac{b}{2\pi}} \int_0^{\infty} \frac{e^{-\frac{b}{2}x}}{\sqrt{x}} \int_0^{\infty} \frac{e^{-\frac{y}{\gamma_{is,u}}}}{\gamma_{is,u}} F_{g_{ss,u}}\left(\frac{x(y+1)}{\frac{P_{ss,u}}{N_0}} \right) dydx. \tag{4.58}$$

By using (Gradshteyn I. S., 2007, Eq. 8.352.5, Eq. 8.352.4, Eq. 3.352.1, Eq. 6.228.2, Eq. 3.383.5, and Eq. 3.352.2) as the same way of (4.36) in Appendix A.3, The BER of this case can be written as

$$BER_{Int,u}(a,b) = \frac{a}{2}\sqrt{\frac{b}{2\pi}} \frac{1}{\Gamma(M_u+1)} \left[I_{1,u} + I_{2,u} + I_{3,u} + I_{4,u} \right], \tag{4.59}$$

which is the same as non-overlapping case for uplink, where

$$I_{1,u}=\frac{(-1)^{M_u(N_u-1)+1}}{(M_u(N_u-1)-1)!}e^{\frac{1}{\gamma_{is,u}}}\left(\frac{\gamma_{is,u}}{\gamma_{ss,u}}\right)^{M_uN_u}\frac{\Gamma\left(M_uN_u+1,\frac{1}{\gamma_{is,u}}\right)}{\left(M_uN_u+\frac{1}{2}\right)}\times$$
$$\frac{\Gamma\left(M_uN_u+\frac{1}{2}\right)}{\left(\frac{1}{\gamma_{ss,u}}+\frac{b}{2}\right)^{M_uN_u+\frac{1}{2}}}\,{}_2F_1\left(1,M_uN_u+\frac{1}{2};M_uN_u+\frac{3}{2};\frac{b\gamma_{ss,u}}{2+b\gamma_{ss,u}}\right), \tag{4.60}$$

$$I_{2,u}=(-1)^{M_u(N_u-1)}(M_uN_u)!\Gamma\left(M_uN_u+\frac{1}{2}\right)e^{\frac{b\gamma_{ss,u}+2}{4\gamma_{is,u}}}\sum_{k=1}^{M_uN_u}\frac{(k-1)!}{k!}\times$$
$$\sum_{m=0}^{k-1}\frac{\left(\frac{1}{\gamma_{is,u}}\right)^m}{m!}\left(\frac{1}{\gamma_{ss,u}}+\frac{b}{2}\right)^{-\frac{1}{2}\left(M_uN_u+m-k+\frac{3}{2}\right)}\left(\frac{\gamma_{ss,u}}{\gamma_{is,u}}\right)^{\frac{1}{4}(2k+2m-2M_uN_u-1)}\times \tag{4.61}$$
$$\mathrm{W}_{\frac{1}{2}\left(m-k-M_uN_u-\frac{1}{2}\right),-\frac{1}{2}\left(M_uN_u+m-k+\frac{1}{2}\right)}\left(\frac{b\gamma_{ss,u}+2}{2\gamma_{is,u}}\right),$$

$$I_{3,u}=\left(\frac{1}{\gamma_{is,u}}\right)e^{\frac{b\gamma_{ss,u}+2}{4\gamma_{is,u}}}\sum_{k=0}^{M_u(N_u-1)-2}(-1)^{M_u(N_u-1)+k}k!(M_uN_u-k-1)!\times$$
$$\Gamma\left(M_uN_u-k-\frac{1}{2}\right)\sum_{m=0}^{M_uN_u-k-1}\frac{\gamma_{ss,u}^{1-m}}{m!}\left(\frac{1}{\gamma_{ss,u}}+\frac{b}{2}\right)^{-\frac{1}{2}\left(m+\frac{1}{2}\right)}\times \tag{4.62}$$
$$\left(\frac{\gamma_{ss,u}}{\gamma_{is,u}}\right)^{\frac{1}{2}\left(m-\frac{3}{2}\right)}\mathrm{W}_{\frac{1}{2}\left(2k-2M_uN_u+m+\frac{3}{2}\right),\frac{1}{2}\left(-m+\frac{1}{2}\right)}\left(\frac{b\gamma_{ss,u}+2}{2\gamma_{is,u}}\right),$$

and

$$I_{4,u}=M_u!\left[\sqrt{\frac{2\pi}{b}}-\left(\frac{1}{\gamma_{is,u}}\right)e^{\frac{b\gamma_{ss,u}+2}{4\gamma_{is,u}}}\sum_{k=0}^{M_u}\Gamma\left(k+\frac{1}{2}\right)\sum_{m=0}^{k}\frac{\gamma_{ss,u}^{-m+1}}{m!}\times\right.$$
$$\left.\left(\frac{1}{\gamma_{ss,u}}+\frac{b}{2}\right)^{-\frac{1}{2}\left(m+\frac{1}{2}\right)}\left(\frac{\gamma_{ss,u}}{\gamma_{is,u}}\right)^{\frac{1}{2}\left(m-\frac{3}{2}\right)}\mathrm{W}_{\frac{1}{2}\left(m-2k-\frac{1}{2}\right),\frac{1}{2}\left(-m+\frac{1}{2}\right)}\left(\frac{b\gamma_{ss,u}+2}{2\gamma_{is,u}}\right)\right]. \tag{4.63}$$

However, this section supports only spectrum sharing for multi-user one-cell CR systems, but it does not support multi-user multi-cell CR systems.

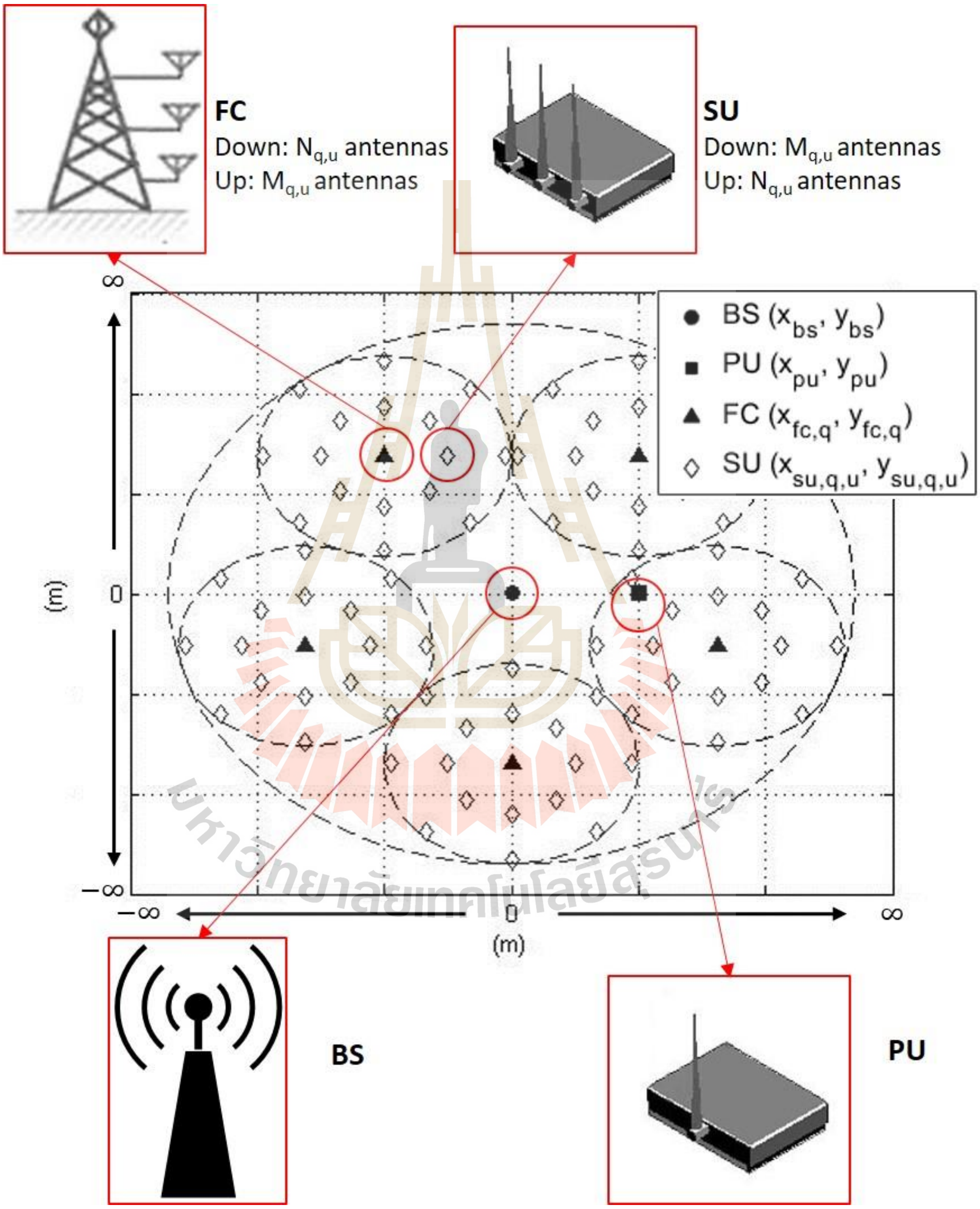

Figure 4.8 System model for multi-user multi-cell spectrum sharing in MIMO CR system.

4.6.2 Multi-user multi-cell spectrum sharing

In this case, there are FCs in a coverage area of the macrocell, and there are SUs scattering inside a coverage area of each FC. The primary link is composed of only one antenna for both PT and PR. Whereas, each secondary link is composed of ST and SR, which is equipped with $N_{q,u}$ and $M_{q,u}$ antennas, respectively, according to each SU from the overall U_q number of SUs in each coverage area of q^{th} FC, as seen in Fig. 4.8. The channel is modeled as Rayleigh fading distribution. Like a multi-user one-cell system, the number of antennas of each SU is not necessary to be the same as each other, there are at least 2 antennas to support the MIMO systems.

For downlink, BS is defined as PT while FC is defined as ST, and PU is defined as PR while SUs are defined as SRs. The channel between the selected antenna of the q^{th} FC and the k^{th} antenna of the u^{th} SU in its coverage area has a channel coefficient $h_{sk,q,u}$. The channel between the selected antenna of the q^{th} FC and an antenna of PU has a channel coefficient $h_{sp,q}$. The channel between an antenna of BS and the k^{th} antenna of the u^{th} SU in the coverage area of the q^{th} FC has a channel coefficient $h_{pk,q,u}$. Finally, the channel between the selected antennas of FCs in other coverage area and the k^{th} antenna of the u^{th} SU in the coverage area of the q^{th} FC has an average channel coefficient $\bar{h}_{ik,q,u}$, which is the average channel between the interference FCs and the considered SU.

For uplink, BS is defined as PR while FC is defined as SR, and PU is defined as PT while SUs are defined as STs. The channel between the selected antenna of the u^{th} SU and the j^{th} antenna of its q^{th} FC has a channel coefficient $h_{sj,q,u}$. The channel between the selected antenna of the u^{th} SU in the coverage area of the q^{th} FC and an antenna of BS has a channel coefficient $h_{sp,q,u}$. The channel between an antenna of PU and the j^{th} antenna of the q^{th} FC has a channel coefficient $h_{pj,q}$. Finally, the channel between the selected antennas of other SUs in the system and the j^{th} antenna of the q^{th} FC has an average channel coefficient $\bar{h}_{ij,q,u}$.

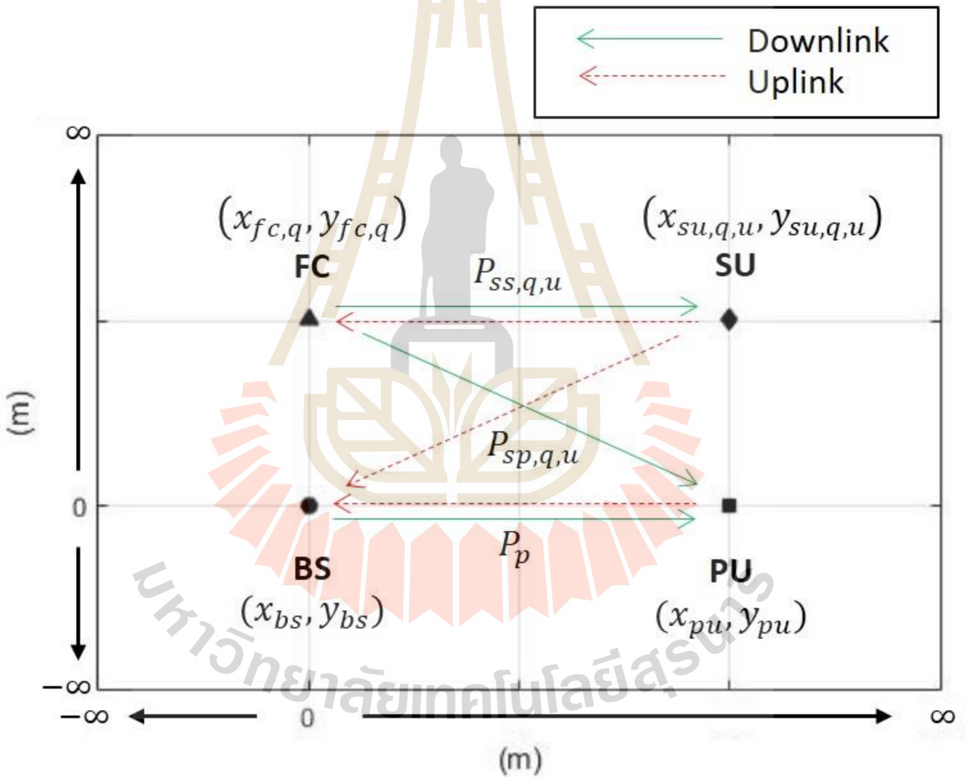

Figure 4.9 Position allocations of each member in multi-user multi-cell MIMO CR systems.

In order to see it clearer, Fig. 4.9 has focused on the considering node positions to create the distance equations and power equations, as follows.

For downlink, the distances from PT to SR and from ST to SR, respectively, are given by

$$D_{ps,q,u\_d} = \left(\left(y_{su,q,u} - y_{bs} \right)^2 + \left(x_{su,q,u} - x_{bs} \right)^2 \right)^{\frac{1}{2}}, \tag{4.64}$$

$$D_{ss,q,u\_d} = \left(\left(y_{su,q,u} - y_{fc,q} \right)^2 + \left(x_{su,q,u} - x_{fc,q} \right)^2 \right)^{\frac{1}{2}}, \tag{4.65}$$

where $q = 1, 2, \cdots, Q$ is the number of FC. Then, the received power from PT to SR for downlink is expressed as

$$P_{ps,q,u\_d} = P_{max} \left(\frac{\lambda}{4\pi D_{ps,q,u\_d}} \right)^2 G_t G_r . \tag{4.66}$$

The received power from ST to SR for downlink is expressed as

$$P_{ss,q,u\_d} = P_{smax} \left(\frac{\lambda}{4\pi D_{ss,q,u\_d}} \right)^2 G_t G_r , \tag{4.67}$$

For downlink, all FCs are the transmitters, hence they also interfere with each other. When considering one of them, the interference power matrix due to the nearby FCs can be found from

$$D_{ssI,q,\mathrm{v},u\_d} = \left(\left(y_{su,q,u} - y_{fc,\mathrm{v}} \right)^2 + \left(x_{su,q,u} - x_{fc,\mathrm{v}} \right)^2 \right)^{\frac{1}{2}}, \tag{4.68}$$

where $v = 1, 2, \cdots, V$, and $V = Q$ that the Ph.D. candidate has defined to be the index to find the interference power from all FC-SU links. Then the downlink interference distance matrix can be obtained as

$$\mathbf{D}_{ssI,q\_d} = \begin{bmatrix} \left[\mathbf{D}_{ssI,q,1\_d}\right]_{1\times U_q} \\ \left[\mathbf{D}_{ssI,q,2\_d}\right]_{1\times U_q} \\ \vdots \\ \left[\mathbf{D}_{ssI,q,q\_d}\right]_{1\times U_q} = \left[\infty\right]_{1\times U_q} \text{; at } v = q \\ \vdots \\ \left[\mathbf{D}_{ssI,q,V\_d}\right]_{1\times U_q} \end{bmatrix}, \tag{4.69}$$

where $D_{ssI,q,\text{v},u\_d} \in \mathbf{D}_{ssI,q,\text{v}\_d}$. At $v = q$ that means the links between the considered FC and all SUs in its coverage area are being considered. At this point, the interference distances can be assumed to be extremely large causing almost no any interference power. Hence, the interference power matrix is

$$\mathbf{P}_{ssI,q\_d} = P_{smax}\left(\frac{\lambda}{4\pi\mathbf{D}_{ssI,q\_d}}\right)^2 G_t G_r = \begin{bmatrix} \mathbf{P}_{ssI,q,1\_d} \\ \mathbf{P}_{ssI,q,2\_d} \\ \vdots \\ \left[0\right]_{1\times U_q} \text{; at } v = q \\ \vdots \\ \mathbf{P}_{ssI,q,V\_d} \end{bmatrix}, \tag{4.70}$$

where $P_{ssI,q,v,u\_d} \in \mathbf{P}_{ssI,q,v\_d}$.

For uplink, the distances from PT to SR and from ST to SR, respectively, are given by

$$D_{ps,q\_u} = \left(\left(y_{fc,q} - y_{pu}\right)^2 + \left(x_{fc,q} - x_{pu}\right)^2\right)^{\frac{1}{2}}, \tag{4.71}$$

and

$$D_{ss,q,u\_u} = \left(\left(y_{fc,q} - y_{su,q,u}\right)^2 + \left(x_{fc,q} - x_{su,q,u}\right)^2\right)^{\frac{1}{2}}. \tag{4.72}$$

The received power from PT to SR for uplink is expressed as

$$P_{ps,q\_u} = P_{max}\left(\frac{\lambda}{4\pi D_{ps,q\_u}}\right)^2 G_t G_r. \tag{4.73}$$

Then, the received power from ST to SR for uplink is expressed as

$$P_{ss,q,u\_u} = P_{smax}\left(\frac{\lambda}{4\pi D_{ss,q,u\_u}}\right)^2 G_t G_r. \tag{4.74}$$

For uplink, all SUs are the transmitters, hence they also interfere with each other both in the difference and same coverage areas of picocells. When considering one of them, the interference power matrix due to SUs in the coverage area of the other nearby FCs can be found from

$$D_{ssI,q,\mathrm{v},u\_u} = \left(\left(y_{fc,\mathrm{v}} - y_{su,q,u}\right)^2 + \left(x_{fc,\mathrm{v}} - x_{su,q,u}\right)^2\right)^{\frac{1}{2}}. \tag{4.75}$$

Hence, the uplink interference distance matrix is

$$\mathbf{D}_{ssI,q\_u} = \begin{bmatrix} \left[\mathbf{D}_{ssI,q,1\_u}\right]_{1\times U_q} \\ \left[\mathbf{D}_{ssI,q,2\_u}\right]_{1\times U_q} \\ \vdots \\ \left[\mathbf{D}_{ssI,q,q\_u}\right]_{1\times U_q} = \left[\infty\right]_{1\times U_q}\ ;\ \text{at } v = q \\ \vdots \\ \left[\mathbf{D}_{ssI,q,V\_u}\right]_{1\times U_q} \end{bmatrix}. \tag{4.76}$$

At $v = q$, the Ph.D. candidate has defined the interference distances as infinity to find the interference power only from the other SUs outside the considered coverage area. Hence, the interference power matrix is

$$\mathbf{P}_{ssI,q\_u} = P_{smax}\left(\frac{\lambda}{4\pi\mathbf{D}_{ssI,q\_u}}\right)^2 G_t G_r = \begin{bmatrix} \mathbf{P}_{ssI,q,1\_u} \\ \mathbf{P}_{ssI,q,2\_u} \\ \vdots \\ [0]_{1\times U_q}\text{; at } v=q \\ \vdots \\ \mathbf{P}_{ssI,q,V\_u} \end{bmatrix}, \tag{4.77}$$

where $P_{ssI,q,v,u\_u} \in \mathbf{P}_{ssI,q,v\_u}$. Then, the interference power matrix due to other SUs in the same coverage area can be defined as

$$\mathbf{P}'_{ssII,q\_u} = \mathbf{P}'_{ss,q\_u} - \begin{bmatrix} 0 & \cdots & P_{ss,q,u\_u} & 0 & \cdots & 0 \end{bmatrix}, \tag{4.78}$$

where $P_{ss,q,u\_u} \in \mathbf{P}_{ss,q\_u}$. In order to find the interference power, the power value of the considered SU has to be removed out from the normally received power matrix which is calculated from (4.74). Hence, the rest values in the matrix are the interference due to each ST-SR link in the same coverage area with considered SU.

In order to evaluate BER, the $m-$QAM modulation is employed, where m is constellation size. Then the received power from ST to PR is given by

$$P_{sp} = \left(\frac{-1.5P_p G_c}{(m-1)\ln(5BER_p)} - N_o\right)\frac{1}{\overline{g}_{sp}}, \tag{4.79}$$

After that, by considering the power from (4.79), the BER region of primary network due to interference from ST in the same location can be defined by replacing it in (4.16). By using PR as a reference point, the distance from ST to PR D_{sp} can show the possible position of ST being available to communicate with FC around PR. Hence, the positions of ST affecting PR performance can be predicted.

Referring to the power equations in this section, the SNR from ST-SR for both downlink and uplink are defined as

$$\gamma_{ss,q,u} = g_{ss,q,u} \frac{P_{ss,q,u}}{N_0}, \tag{4.80}$$

where $g_{ss,q,u} = \sum_{k=1}^{M_{q,u}} \left|h_{sk,q,u}\right|^2$ for downlink and $g_{ss,q,u} = \sum_{j=1}^{M_{q,u}} \left|h_{sj,q,u}\right|^2$ for uplink. Hence, $P_{ss,q,u}$ also depends on whether it is downlink from (4.67) or uplink from (4.74). In addition, the SNR from whole interferences to the considered SR for the downlink is

$$\gamma_{is,q,u\_d} = g_{ps,q,u} \frac{P_{ps,q,u\_d}}{N_0} + \bar{g}_{is,q,u} \sum_{v=1}^{V} \frac{P_{ssI,q,v,u\_d}}{N_0}, \tag{4.81}$$

where $g_{ps,q,u} = \frac{\left|\sum_{k=1}^{M_{q,u}} h^*_{sk,q,u} h_{ps,q,u}\right|^2}{g_{ss,q,u}}$ is the channel gain from PT-SR on the downlink, and $\bar{g}_{is,q,u} = \sum_{k=1}^{M_{q,u}} \left|\bar{h}_{ik,q,u}\right|^2$ is an average channel gain from the interference FC to considered SU. For the uplink, yields

$$\gamma_{is,q,u\_u} = g_{ps,q} \frac{P_{ps,q\_u}}{N_0} + \bar{g}_{is,q,u} \left(\sum_{v=1}^{V} \sum_{u=1}^{U} \frac{P_{ssI,q,v,u\_u}}{N_0} + \sum_{u=1}^{U} \frac{P_{ssII,q,u\_u}}{N_0} \right), \tag{4.82}$$

where $g_{ps,q} = \frac{\left|\sum_{j=1}^{M_{q,u}} h^*_{sj,q,u} h_{pj,q}\right|^2}{g_{ss,q,u}}$ is the channel gain from PT-SR on the uplink, and $\bar{g}_{is,q,u} = \sum_{j=1}^{M_{q,u}} \left|\bar{h}_{ij,q,u}\right|^2$ is an average channel gain from other SUs in the system to the considered FC.

The CDF of $g_{ss,q,u}$ is given by

$$F_{g_{ss},q,u}(x)=\frac{1}{\Gamma\left(M_{q,u}+1\right)}\left[\left(\frac{x}{g_{ss,q,u}}\right)^{M_{q,u}N_{q,u}}\times\right.$$
$$\left.\Gamma\left(1-M_{q,u}\left(N_{q,u}-1\right),\frac{x}{g_{ss,q,u}}\right)+\gamma\left(M_{q,u}+1,\frac{x}{g_{ss,q,u}}\right)\right]. \tag{4.83}$$

Eventually, the BER of overlapping spectrum sharing for downlink and uplink can be expressed as

$$BER_{Int,q,u}(a,b)=\frac{a}{2}\sqrt{\frac{b}{2\pi}}\int_0^\infty\frac{e^{-\frac{b}{2}x}}{\sqrt{x}}\int_0^\infty\frac{e^{-\frac{y}{\gamma_{is,q,u}}}}{\gamma_{is,q,u}}F_{g_{ss},q,u}\left(\frac{x(y+1)}{\frac{P_{ss,q,u}}{N_0}}\right)dydx, \tag{4.84}$$

By using (Gradshteyn I. S., 2007, Eq. 8.352.5, Eq. 8.352.4, Eq. 3.352.1, Eq. 6.228.2, Eq. 3.383.5, and Eq. 3.352.2) as the same way of (4.36) in Appendix A.3, The BER of this case can be written as

$$BER_{Int,q,u}(a,b)=\frac{a}{2}\sqrt{\frac{b}{2\pi}}\frac{1}{\Gamma\left(M_{q,u}+1\right)}\times$$
$$\left[I_{1,q,u}+I_{2,q,u}+I_{3,q,u}+I_{4,q,u}\right], \tag{4.85}$$

by using (4.80), and (4.81) for downlink or (4.82) for uplink. Hence, the sub-functions of (4.85) have to be changed, as follows.

$$I_{1,q,u}=\frac{(-1)^{M(N-1)+1}}{\left(M(N-1)-1\right)!}e^{\frac{1}{\gamma_{is,q,u}}}\left(\frac{\gamma_{is,q,u}}{\gamma_{ss,q,u}}\right)^{MN}\frac{\Gamma\left(MN+1,\frac{1}{\gamma_{is,q,u}}\right)}{\left(MN+\frac{1}{2}\right)}\times$$
$$\frac{\Gamma\left(MN+\frac{1}{2}\right)}{\left(\frac{1}{\gamma_{ss,q,u}}+\frac{b}{2}\right)^{MN+\frac{1}{2}}}{}_2F_1\left(1,MN+\frac{1}{2};MN+\frac{3}{2};\frac{b\gamma_{ss,q,u}}{2+b\gamma_{ss,q,u}}\right), \tag{4.86}$$

$$I_{2,q,u}=(-1)^{M(N-1)}(MN)!\Gamma\left(MN+\frac{1}{2}\right)e^{\frac{b\gamma_{ss,q,u}+2}{4\gamma_{is,q,u}}}\sum_{k=1}^{MN}\frac{(k-1)!}{k!}\times$$
$$\sum_{m=0}^{k-1}\frac{\left(\frac{1}{\gamma_{is,q,u}}\right)^{m}}{m!}\left(\frac{1}{\gamma_{ss,q,u}}+\frac{b}{2}\right)^{-\frac{1}{2}\left(MN+m-k+\frac{3}{2}\right)}\left(\frac{\gamma_{ss,q,u}}{\gamma_{is,q,u}}\right)^{\frac{1}{4}(2k+2m-2MN-1)}\times \tag{4.87}$$
$$\mathrm{W}_{\frac{1}{2}\left(m-k-MN-\frac{1}{2}\right),-\frac{1}{2}\left(MN+m-k+\frac{1}{2}\right)}\left(\frac{b\gamma_{ss,q,u}+2}{2\gamma_{is,q,u}}\right),$$

$$I_{3,q,u}=\left(\frac{1}{\gamma_{is,q,u}}\right)e^{\frac{b\gamma_{ss,q,u}+2}{4\gamma_{is,q,u}}}\sum_{k=0}^{M(N-1)-2}(-1)^{M(N-1)+k}k!(MN-k-1)!\times$$
$$\Gamma\left(MN-k-\frac{1}{2}\right)\sum_{m=0}^{MN-k-1}\frac{\gamma_{ss,q,u}^{1-m}}{m!}\left(\frac{1}{\gamma_{ss,q,u}}+\frac{b}{2}\right)^{-\frac{1}{2}\left(m+\frac{1}{2}\right)}\times \tag{4.88}$$
$$\left(\frac{\gamma_{ss,q,u}}{\gamma_{is,q,u}}\right)^{\frac{1}{2}\left(m-\frac{3}{2}\right)}\mathrm{W}_{\frac{1}{2}\left(2k-2MN+m+\frac{3}{2}\right),\frac{1}{2}\left(-m+\frac{1}{2}\right)}\left(\frac{b\gamma_{ss,q,u}+2}{2\gamma_{is,q,u}}\right),$$

$$I_{4,q,u}=M!\left[\sqrt{\frac{2\pi}{b}}-\left(\frac{1}{\gamma_{is,q,u}}\right)e^{\frac{b\gamma_{ss,q,u}+2}{4\gamma_{is,q,u}}}\sum_{k=0}^{M}\Gamma\left(k+\frac{1}{2}\right)\times\right.$$
$$\sum_{m=0}^{k}\frac{\gamma_{ss,q,u}^{-m+1}}{m!}\left(\frac{1}{\gamma_{ss,q,u}}+\frac{b}{2}\right)^{-\frac{1}{2}\left(m+\frac{1}{2}\right)}\left(\frac{\gamma_{ss,q,u}}{\gamma_{is,q,u}}\right)^{\frac{1}{2}\left(m-\frac{3}{2}\right)}\times \tag{4.89}$$
$$\left.\mathrm{W}_{\frac{1}{2}\left(m-2k-\frac{1}{2}\right),\frac{1}{2}\left(-m+\frac{1}{2}\right)}\left(\frac{b\gamma_{ss,q,u}+2}{2\gamma_{is,q,u}}\right)\right].$$

4.7 GPS error

Although the GPS devices have been developed for knowing the desired position with the high accuracy at the present, there are still some errors that cannot be ignored for the practical spectrum sharing process. All wrongly identified positions obviously affect the SUs' decision. Hence, the GPS error can be added into the performance analysis using

$$\hat{\mathbf{x}}_{su} = \mathbf{x}_{su} \pm \mathbf{rand}\left[0, error_{GPS}\right]_{U \times Q} \cos\left(\tan^{-1}\left(\frac{\mathbf{y}_{su}}{\mathbf{x}_{su}}\right)\right), \tag{4.90}$$

$$\hat{\mathbf{y}}_{su} = \mathbf{y}_{su} \pm \mathbf{rand}\left[0, error_{GPS}\right]_{U \times Q} \sin\left(\tan^{-1}\left(\frac{\mathbf{y}_{su}}{\mathbf{x}_{su}}\right)\right), \tag{4.91}$$

to replace in the distance equations of the above sections. The GPS error is in meters which has the value between 0 and $error_{GPS}$, where $error_{GPS}$ is the highest GPS error according to the accuracy of each GPS device.

4.8 Spectrum allocation scheme

The final process of CR system is the spectrum decision choosing the proper frequency channel for the demand of users. This spectrum allocation scheme arranges the proper frequency channel for each SU in the entire system. Incidentally, a diagram of this concept is shown in Fig. 4.10 along with the steps as follows.

Step 1: After the spectrum sensing process, spectrum allocation process starts with analyzing the first frequency channel, where the number of considered channels is equal to bandwidth value divided by sub-bandwidth value. Hence, the considered frequency channel $F_{sub} = 1, 2, ..., BW / BW_{sub}$, in which BW and BW_{sub} values are defined based on each communication standard. Incidentally, F_{sub} is called the sub-band number.

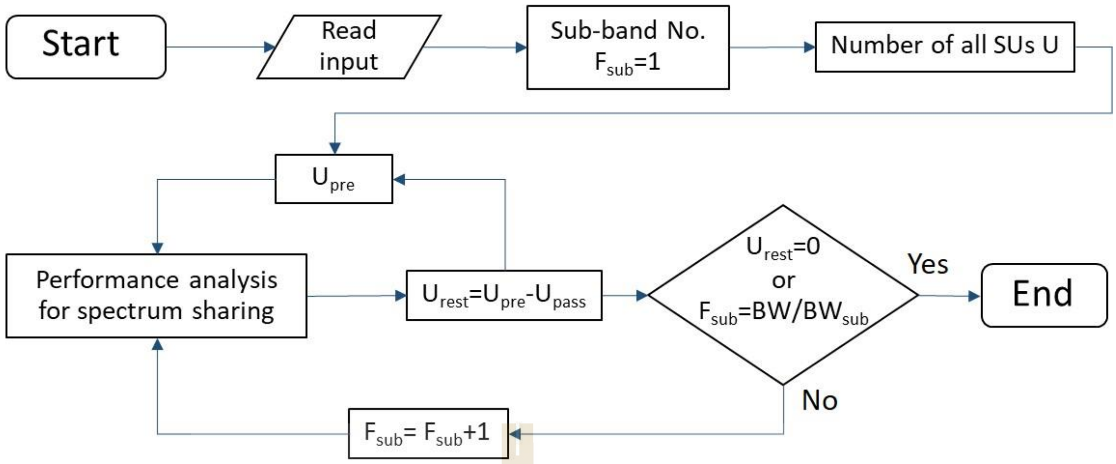

Figure 4.10 Block diagram of spectrum allocation scheme for overlapping spectrum sharing.

Step 2: The number of all SUs and each position of them are brought into the performance analysis process. The proper SU is SU that passes the BER condition on both downlink and uplink in the considered round. Hence, the result of this process is the number of SUs that are appropriate for communication.

Step 3: In order to know whether the spectrum allocation process has already finished or not, the rest number of SUs has to be known. The rest number of SUs represented by U_{rest} in which these SUs still are not passing a BER condition on both downlink and uplink in the considered round can be calculated from

$$U_{rest} = U_{pre} - U_{pass}, \tag{4.92}$$

where U_{pre} is the rest number of SUs from a previous round, and U_{pass} is the number of SUs that pass the BER condition on both downlink and uplink in the considered round and are ready to perform the communication. Note that U_{pre} is equal to a number of all SUs in the first round. Incidentally, U_{pre} and U_{rest} are the same but are in different rounds. For easier explanation, U_{pre} in the considered round is U_{rest} from a previous round.

Then, the steps 2 and 3 will be repeated until the overall SUs is ready to perform the communication or the process comes to the last round in which $F_{sub} = BW / BW_{sub}$. If the process comes to the last round but $U_{rest} \neq 0$, those rest SUs cannot operate at that time.

Step 4: The new term of spectrum sharing has to wait for the next observation time of spectrum sensing process.

4.9 Chapter summary

Early in this chapter, it describes the basic elements of single user CR system model consisting of a single antenna primary link and only one MIMO secondary link. Then, the Ph.D. candidate has provided the performance analysis with the BER equations based on the positions of node members which can support both of downlink and uplink in overlapping spectrum sharing. In order to accord with the reality, the performance analysis of single user CR system has been developed to support the multi-user CR system. The advance on multi-user system model is the picocell of FC inside a macrocell of BS. FC can communicate with multiple SUs at the same time. Incidentally, the difference in the initial equations between downlink and uplink operations can be clearly seen. Moreover, the GPS error issue has been considered together with the multi-user performance analysis in order to support the practical CR system implementation. Finally, the spectrum allocation scheme has been introduced to thoroughly allocate the frequency channels to all users in CR system.

CHAPTER V

SIMULATION RESULTS AND DISCUSSION

5.1 Introduction

This chapter presents the simulation results related to two spectrum sharing patterns from the previous chapters. The simulation results of the spectrum sensing show the efficacy comparison between the various spectrum sensing methods. In the part of the performance analysis of spectrum sharing, the simulation results show the parameter adjustment and the BER regions of both primary and secondary networks on both downlink and uplink operations. Moreover, the working format of the spectrum allocation scheme has been introduced for multi-user CR system.

Table 5.1 System parameters for Long-Term Evolution (LTE)

Uplink (UL) operating band BS receive UE transmit	1920 MHz – 1980 MHz
$F_{UL\_low} - F_{UL\_high}$	
Downlink (DL) operating band BS transmit UE receive	2110 MHz – 2170 MHz
$F_{DL\_low} - F_{DL\_high}$	
Maximum output power	23 dBm
Minimum received power	-103.535 dBm
Maximum number of antennas	4
Tolerated bit error rate (BER)	2×10^{-4}

In addition, all of the simulations are based on the channel model from LTE standard (LTE ETSI, 2011) and the minimum received power (S. P. Thiagarajah, A. Ting, D. Chieng, M. Y. Alias, and T. S. Wei, 2013) that define system parameters as shown in Table 5.1.

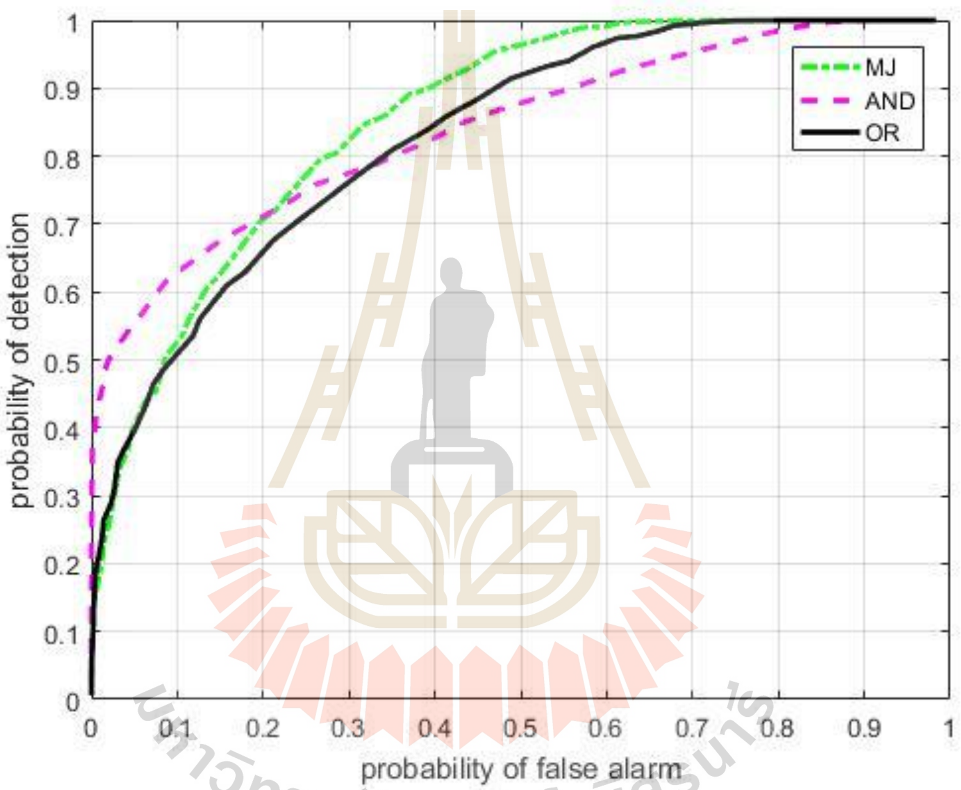

Figure 5.1 Comparison of ROC curves for OR rule, AND rule and MJ rule, where $M = 4$.

5.2 Spectrum sensing simulation results

The simulation starts with randomizing the signaling according to the information in Table 5.1. The signals are detected by employing ED method. Then, the probabilities P_D and P_{FA} are processed by various spectrum sensing techniques. Fig.

5.1 shows the ROC comparison of all three cooperative decision rule techniques where $M = 4$, $SNR = -30$ dB, and $n = 2000$. By considering each technique at 90% P_D, MJ rule reaches the highest P_D at the lowest P_{FA} among three decision rule techniques. The result can be concluded that MJ rule is the most effective technique among those three cooperative decision rule techniques. Thus, this research has selected the MJ rule for the integration of EGC with soft decision to achieve the new higher effective technique as seen in chapter III.

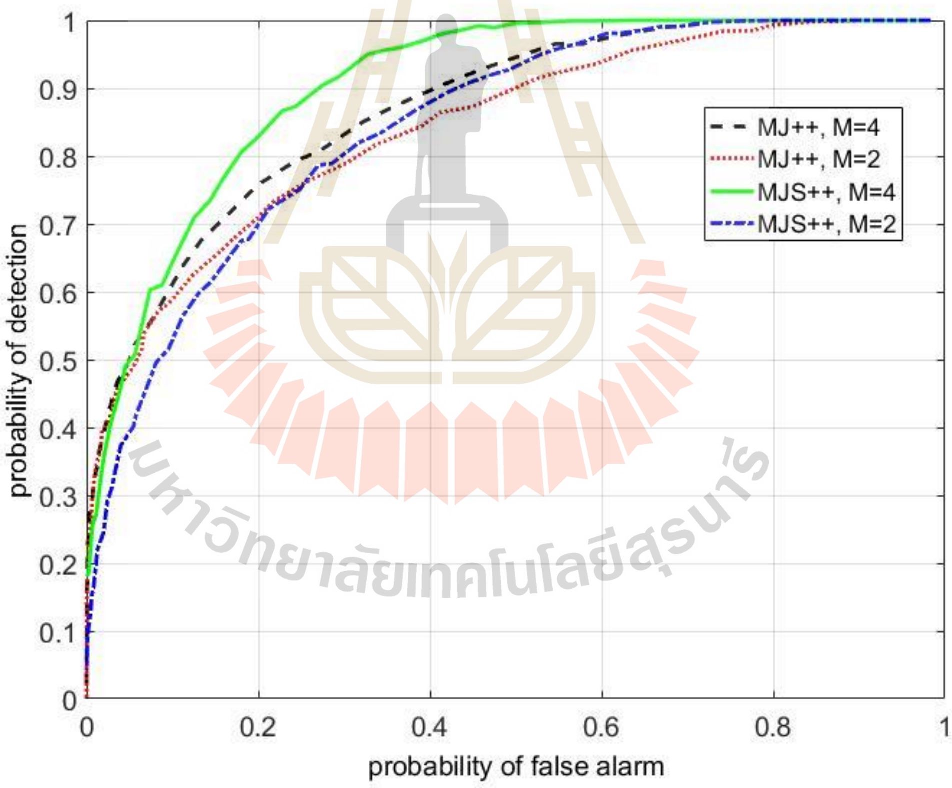

Figure 5.2 Comparison of ROC curves for MJ++ and MJS++, where $M = 2$ and 4.

Fig. 5.2 shows the ROC comparison between MJ++ and MJS++, where $SNR = -30$ dB, and $n = 2000$. The presence of the signal in each channel has randomly occurred. For the MIMO systems, M is the number of receive antennas which is limited to 2 and 4 antennas related to the practical uses. Incidentally, the result can be analyzed as the same way in Fig. 5.1. As expected, MJS++ provides the higher performance than MJ++ for both cases of the number of antennas. The results reveal the benefit of soft decision for spectrum sensing.

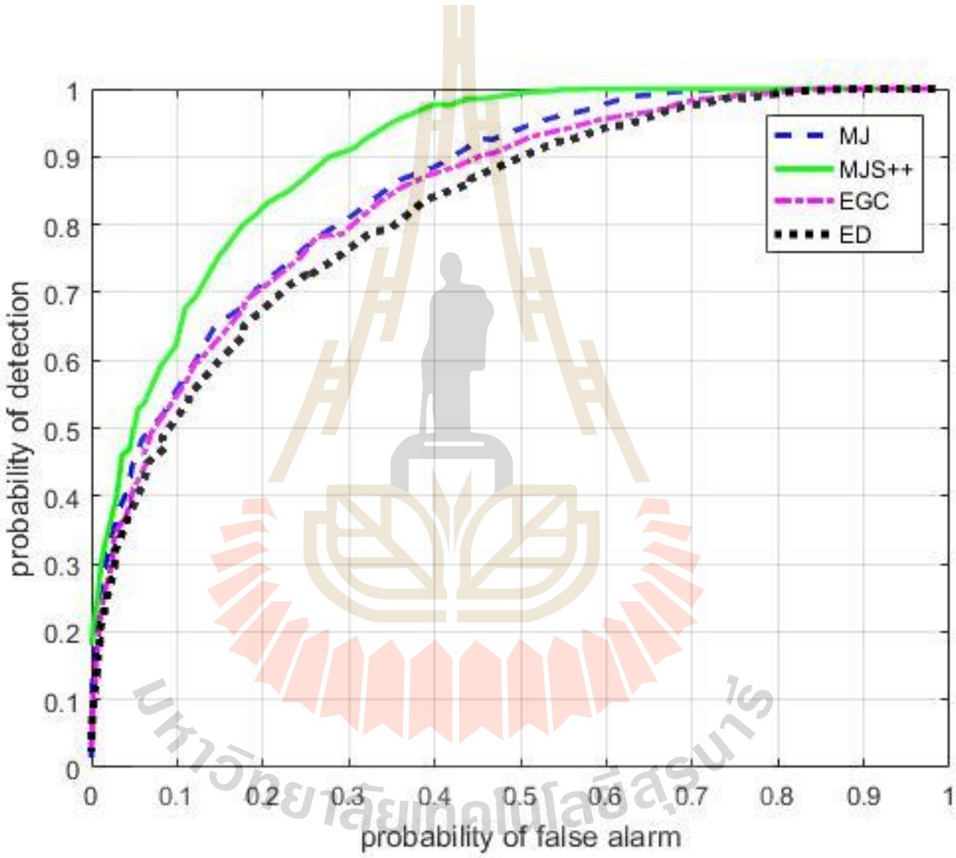

Figure 5.3 Comparison of ROC curves for normal ED at $M = 1$, and EGC, MJ, MJS++ at $M = 4$.

Fig. 5.3 shows the comparison of a proposed technique and the existing techniques in literature, where $M = 4$, $SNR = -30$ dB, and $n = 2000$. For the normal ED method, the antenna is set to 1 because there is no any cooperation in traditional systems. As expected, the proposed techniques outperform the others. At the 90% P_D, the MJS++ technique can reduce the chance of false alarm from 50% of ED technique to 26%. This 24% improvement can indicate the success of proposed technique for practical use.

5.3 Performance analysis simulation results

In practice, CR operator cannot meddle with the parameters of the primary network. Hence, only parameters of SU can be properly adjusted. In this experiment, the Ph.D. candidate defines $(a,b)=(1,2)$, $G_t=0$ dB, and $G_r=6$ dB.

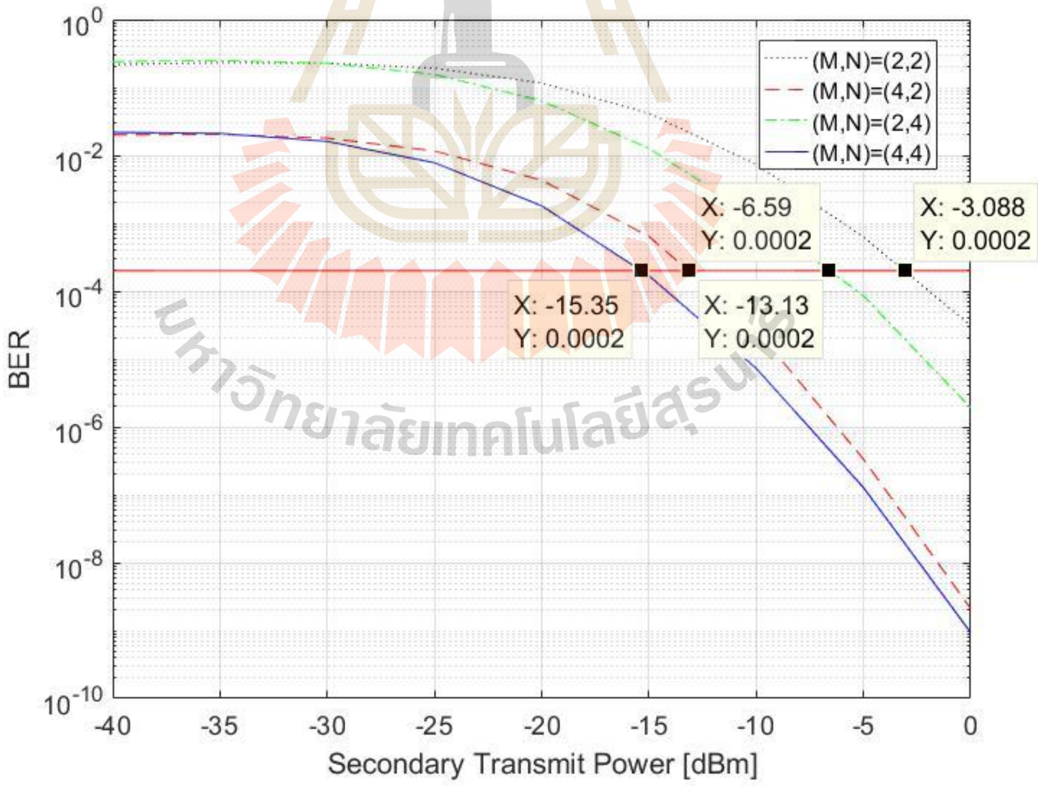

Figure 5.4 The comparison of BER versus P_{smax} for the different number of antennas.

Fig. 5.4 shows the BER versus transmitting power of SU in which the employed powers are cropped to consider only in the range between steady state and the level that BER is less than 2×10^{-4} of each case. The distance between PT and SR is 50 m and the distance between ST and SR is 5 m. It can be seen that increasing the number of antennas can conserve power. As shown in the result, the case of $(M,\ N)=(4,\ 4)$ is enough to support the interference limitation in LTE standard and can save power utilization 94% from conventional MIMO system.

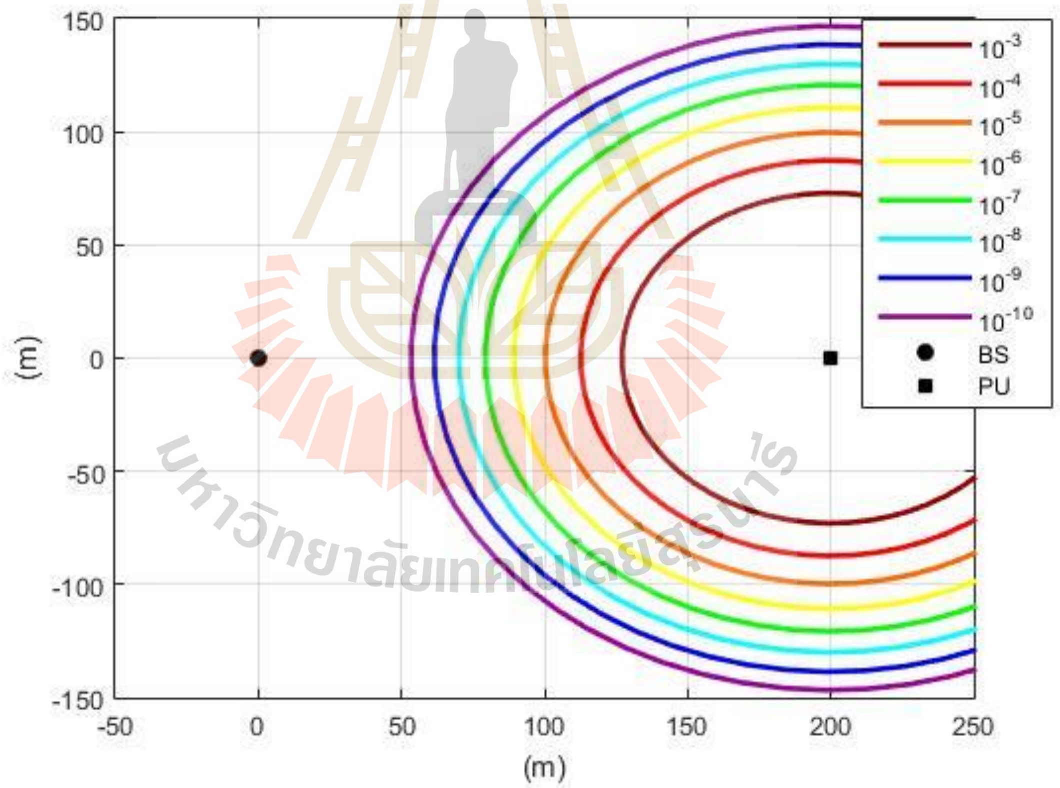

Figure 5.5 BER region of primary network for downlink due to interference from FC in the same location.

Fig. 5.5 and Fig. 5.6 show the BER radiuses of the primary network obtained from (4.16) due to the interference from nearby STs on downlink and uplink, respectively. The considered spectrum has the carrier frequency $f_c = 2.1$ GHz. PU is far from BS with $R_p = 200$ m, and $G_c = 6$ dB. In practice, the system cannot control how close PUs are and when they are near the FC. Therefore, the creation of the BER region in several values on the downlink is presented in Fig. 5.5. By assuming FCs stay around PU, the BER radiuses at various levels are created to predict the dangerous zone on the downlink.

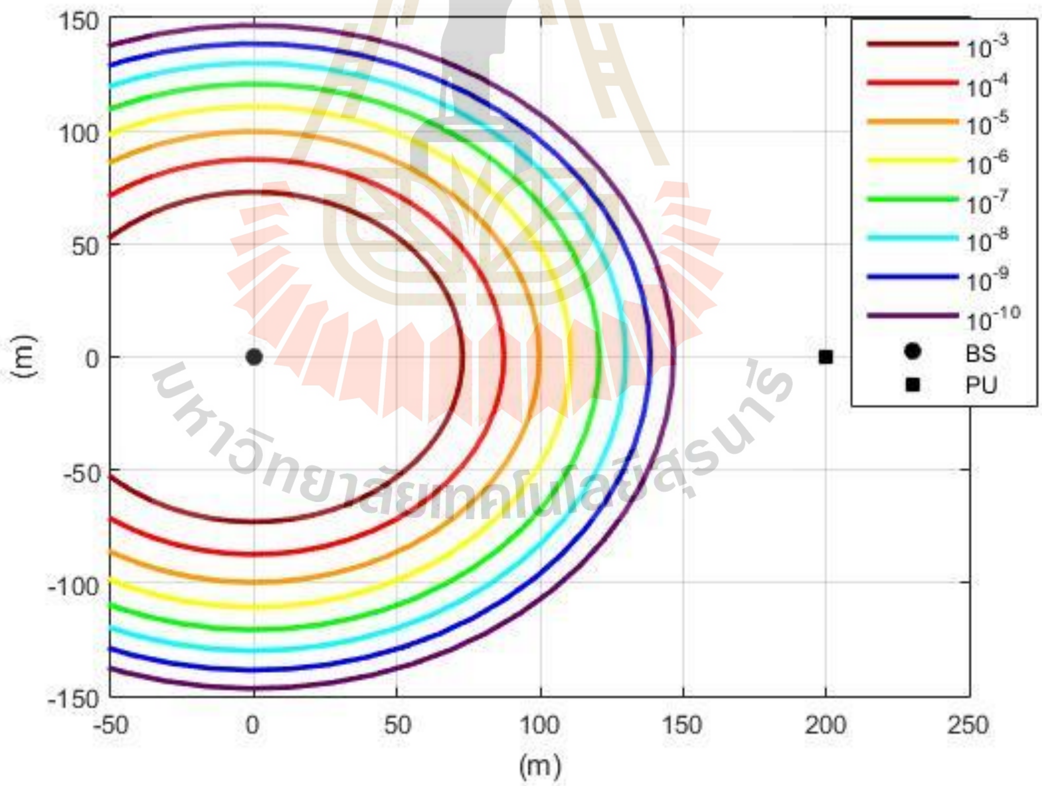

Figure 5.6 BER region of primary network for uplink due to interference from SU in the same location.

For the uplink, the BER radiuses can be created by assuming SUs come near BS in various distances. As seen in Fig. 5.6, there is the available zone for SUs to transmit signals by lightly interfering to the primary network if SU stays outside the circle in which $BER_p = 2 \times 10^{-4}$.

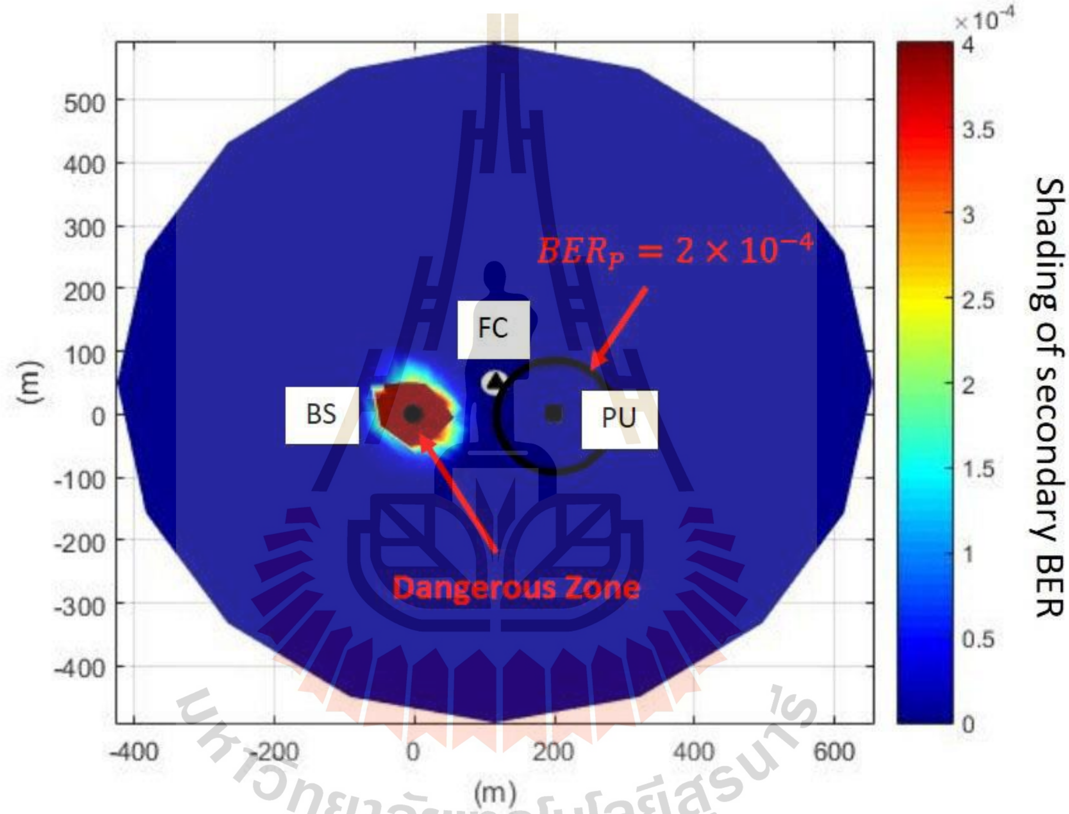

Figure 5.7 BER regions of primary network and secondary network for downlink.

Fig. 5.7 shows the BER regions of primary network and secondary network for downlink. There is the circle around PU in which $BER_p = 2 \times 10^{-4}$ in order to make the preventing condition for PU that comes into the coverage area of FC. When PU approaches FC in which FC is inside the BER radius of PU, FC has to change frequency channel for access in order to avoid the terrible interference to the primary link. The reason is that FC cannot move out by itself. Moreover, there is the dangerous zone in which the BER of the secondary network is more than 2×10^{-4}. Apart from these areas, there is also an available area for SU to pass the BER condition on the downlink.

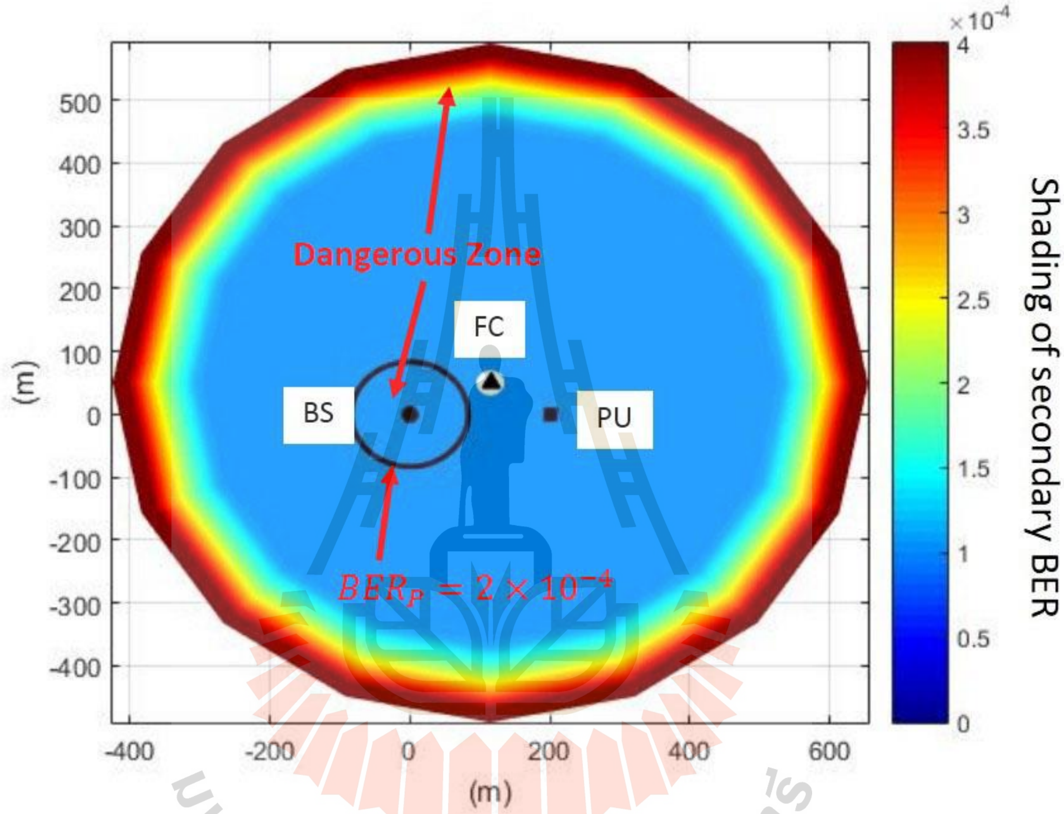

Figure 5.8 BER regions of primary network and secondary network for uplink.

Fig. 5.8 shows the BER regions of primary network and secondary network for uplink. Like the downlink, there are two zone types. The dangerous zone is the area in which the BERs of both primary and secondary networks are more than 2×10^{-4}. Especially, there is BER radius around BS in which the system can also predict that if SU appears inside BER radius, BER of primary link is must more than 2×10^{-4}. Then, the available area is the rest area in which the BERs of both primary and secondary networks are less than 2×10^{-4}.

When combining the results of both figures, the consequence can be a good guideline to make a decision whether to perform the overlapping spectrum sharing or not. If the location of ST is in the available area, the overlapping spectrum sharing scheme can be performed. In turn, if the SU is in the dangerous region, only the non-overlapping spectrum sharing scheme is performed.

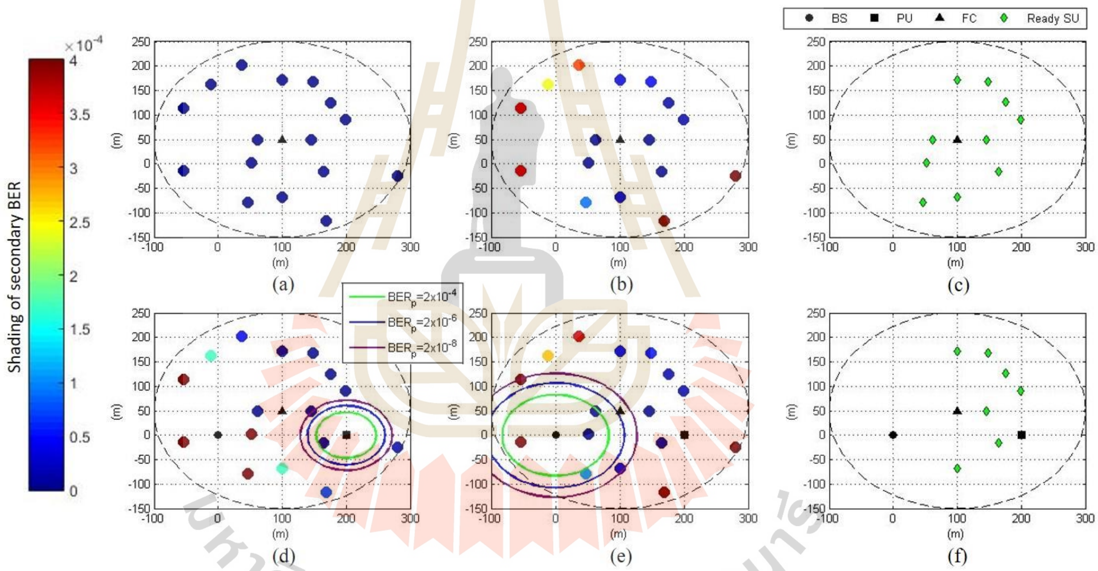

Figure 5.9 Spectrum sharing in multi-user CR systems for non-overlapping operation, (a) downlink, (b) uplink, and (c) their intersection and for overlapping operation, (d) downlink, (e) uplink, and (f) their intersection.

Spectrum sharing schemes in multi-user one-cell MIMO CR systems are shown in Fig. 5.9. The BER of SUs in case of non-overlapping spectrum sharing is presented in Fig. 5.9(a) and Fig. 5.9(b) for downlink and uplink, respectively. This non-overlapping case operates only when the system does not sense any power of PU in spectrum sensing process. Therefore, this case does not consider a primary link in calculation because there is no any interference to secondary links on the downlink.

In turn, each SU makes the interference to each other on the uplink. This caused some SUs to have BERs more than 2×10^{-4}. Then, the intersection result of available SUs between downlink in Fig. 5.9(a) and uplink in Fig. 5.9(b) is shown in Fig. 5.9(c). It is obvious that only some SUs are ready to perform the communication under the case of non-overlapping spectrum sharing.

Next, the case of overlapping spectrum sharing is investigated by assuming $m=16$ for $m-$QAM modulation used by the primary link communication, $G_c=6$ dB, and 0 dBm for transmitted power of BS. Fig. 5.9(d) and Fig. 5.9(e) show the BER results of SUs for downlink and uplink, respectively. Unlike the previous case, there is PU, which is active in the system, influencing the secondary links. In the same way, the primary link also obtains the effect of secondary links due to the interferences from them. For downlink in Fig. 5.9(d), there are the circles around PU to indicate that $BER_p = 2\times10^{-4}$, 2×10^{-6}, and 2×10^{-8}. As same as the single user CR system, If PU appears close to FC that makes FC being inside BER radius of 2*10^-4, FC has to access other frequency channels in order to avoid the unacceptable interference to primary link. In addition, there are some SUs having BERs more than 2×10^{-4} due to the interference from BS which cannot establish the communication at this frequency channel. Apart from these SUs, the other SUs in different positions can pass a BER condition on the downlink. For uplink in Fig. 5.9(e), if any SU stays inside the circle in which $BER_p=2\times10^{-4}$, it causes the harmful interference to the primary link.

Therefore, that SU cannot operate the spectrum sharing at this frequency channel. Additionally, there are some SUs having BER more than 2×10^{-4} due to the interferences from PU and the other nearby SUs. Apart from these SUs, the other SUs can pass the BER condition on the uplink. Finally, the intersection result of available SUs between Fig. 5.9(d) and Fig. 5.9(e) is shown in Fig. 5.9(f). It is observed that some SUs can perform overlapping spectrum sharing under the successful operation on both downlink and uplink. This is based on each SU position under the condition that BERs of primary link and secondary link have to be less than 2×10^{-4}.

The results in Fig. 5.9(c) and Fig. 5.9(f) can reveal that some SUs passing a BER condition in the non-overlapping case does not pass in the overlapping case because of two main causes, including the impact of interference from PT which makes the BER of secondary links to be more than 2×10^{-4}, and the bad positions of those STs staying inside the prediction line in which $BER_p = 2\times10^{-4}$. However, both figures can be the good guideline to perform spectrum sharing in multi-user one-cell MIMO CR systems.

Note that, the expressed results are in a different style with the single user systems in order to easily identify each SU's status.

In this experiments of spectrum sharing in multi-user multi-cell MIMO CR system, the Ph.D. candidate defines $(a,b)=(1,2)$, $G_t = 6$ dBi, $G_r = 6$ dBi, $G_c = 6$ dB, $m = 16$, 0 dBm for the transmitted power of BS. There is a PU per one frequency channel that randomly appear inside the macrocell. There are 5 FCs (5 picocells) and 16 SUs per one coverage area of FC that are randomly placed inside.

For Fig. 5.10, Fig. 5.11 and Fig. 5.12, the Ph.D. candidate defines all of SUs and FCs are composed of 4 antennas.

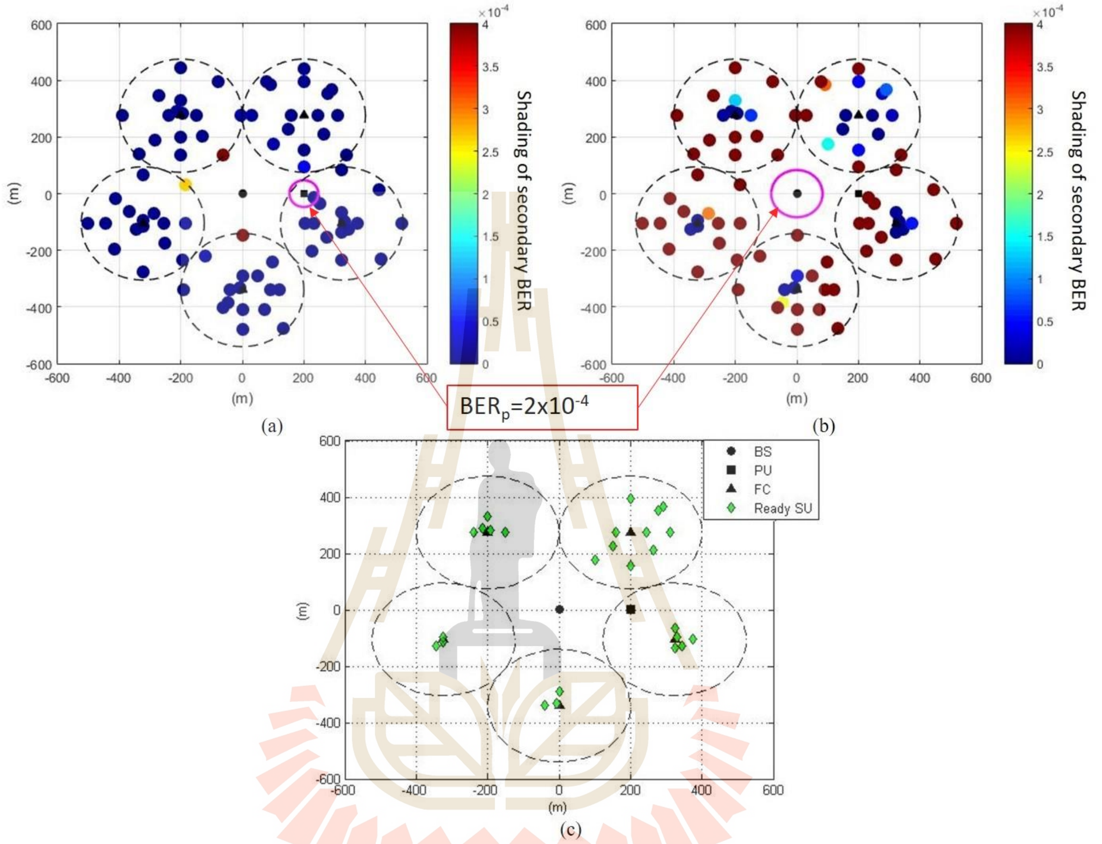

Figure 5.10 Overlapping spectrum sharing in multi-user CR system by ignoring GPS error on (a) downlink and (b) uplink. And (c) the intersection result between downlink and uplink.

Fig. 5.10 is the reference case that ignores the GPS error. Fig. 5.10(a) and Fig. 5.10(b) show the BER results of SUs for downlink and uplink, respectively. For downlink in Fig. 5.10(a), there is the circle around PU to indicate that $BER_p = 2 \times 10^{-4}$. Because FCs cannot move by themselves if PU approaches any FC that makes FC staying inside the BER radius of PU, this FC has to access other frequency channels in order to avoid the unacceptable interference affecting primary link. Moreover, there are some SUs having BER more than 2×10^{-4} due to the interferences from BS and the nearby FCs. Hence, these SUs cannot pass a BER condition on the downlink. Apart from these SUs, the other SUs in different positions can pass the BER condition at this frequency channel on the downlink. For uplink in Fig. 5.10(b), if any SU stays inside the BER radius in which $BER_p = 2\times10^{-4}$, that SU cannot operate the spectrum sharing in this frequency channel. Additionally, there are some SUs having BER more than 2×10^{-4} due to the interferences from PU and the other nearby SUs in which these SUs cannot pass a BER condition at this frequency channel on the uplink. Apart from these SUs, the other SUs in different positions can pass the BER condition on the uplink. Finally, the intersection result of available SUs between Fig. 5.10(a) and Fig. 5.10(b) is shown in Fig. 5.10(c). As the same way in multi-user one-cell system, there are some SUs can perform overlapping spectrum sharing under the successful operation on both downlink and uplink. This is based on each SU position under the condition that BER of primary link and secondary link have to be less than 2×10^{-4}. However, there are two obvious differences from the multi-user one-cell system. First, Apart from BS, there is the higher risk from the interferences of FCs on the downlink. Second, the system can support a larger number of users along with the higher number of interferences on the uplink.

Currently, the GPS devices have the GPS error around 0-10 m (N. Davari, and A. Gholami, 2017 and P. A. Zandbergen, and S. J. Barbeau, 2011) affecting the systems as seen in Fig. 5.11 and Fig. 5.12.

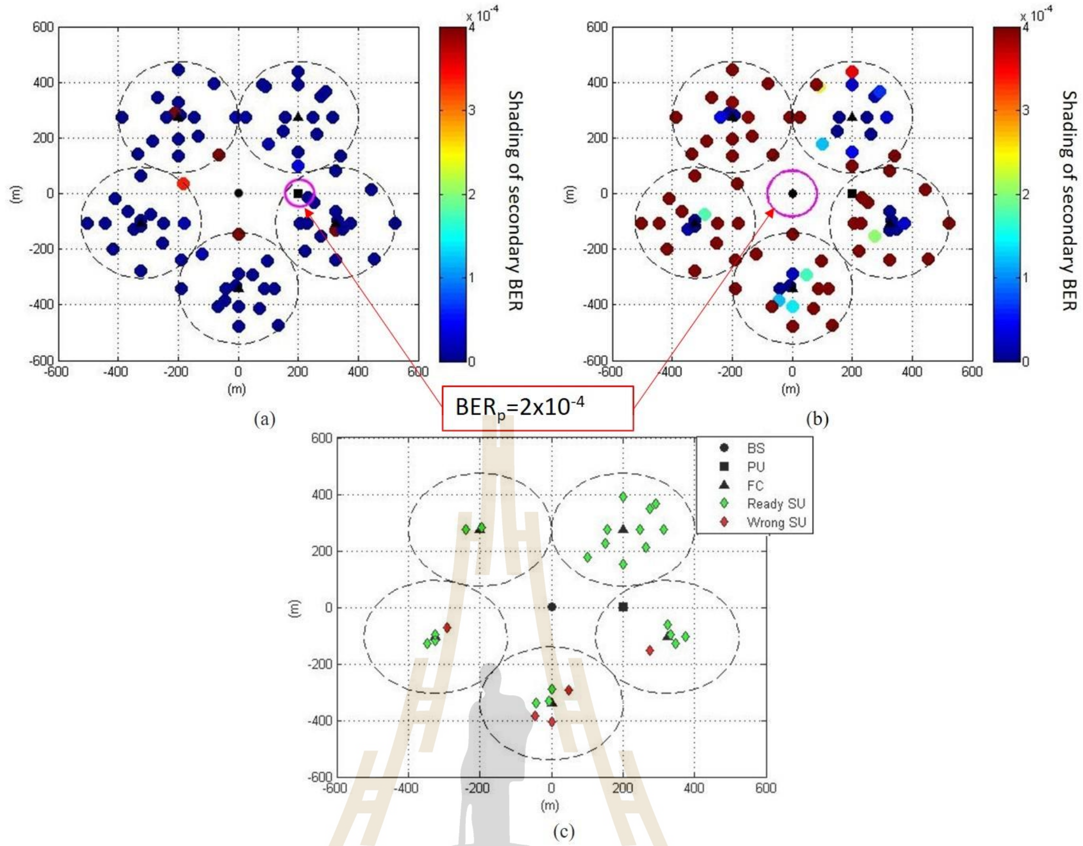

Figure 5.11 Overlapping spectrum sharing in multi-user multi-cell CR system by adding 5 m GPS error on (a) downlink and (b) uplink. And (c) the intersection result between downlink and uplink.

With the same node positions and the same number of antenna elements for each node member as Fig. 5.10, the Ph.D. candidate enhances the GPS error around 0-5 m into the experiment as seen in Fig. 5.11. Fig. 5.11(a) and Fig. 5.11(b) show the BER results of SUs for downlink and uplink respectively, if the GPS errors affecting the most node positions sufficiently increase the distances between interference nodes and SRs, these increased distances may cause the wrong result. These SUs are indicated that they pass the BER condition although they should not pass because the calculated BERs are less than they should be. On the other hand, if the GPS errors affecting the most node positions sufficiently decrease the distances between interference nodes and SRs, these decreased distances may cause the false alarm results that cut the pass occasion of the considered SUs because the calculated BERs are more than they should be. From the same operation as Fig. 5.10, the intersection result of available SUs between Fig. 5.11 (a) and Fig. 5.11(b) is shown in Fig. 5.11(c). Compared to Fig. 5.10(c), it clearly shows that some SUs should not pass in Fig. 5.10(c) but they appear in this figure, the Ph.D. candidate defines them to be the wrong SUs as shown in the form of red mark. Moreover, some SUs that should pass disappear.

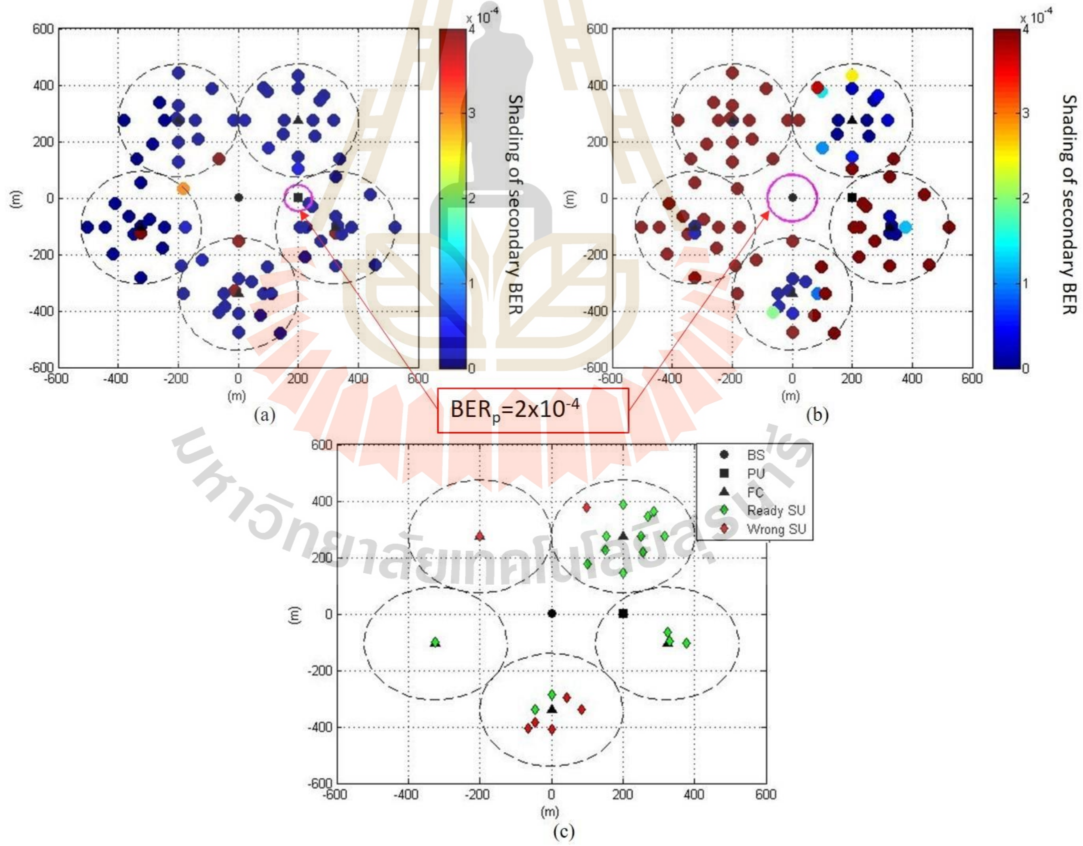

Figure 5.12 Overlapping spectrum sharing in multi-user multi-cell CR system by adding 10 m GPS error on (a) downlink and (b) uplink. And (c) the intersection result between downlink and uplink.

As expected, when we extend the GPS error to 0-10 m in Fig. 5.12, some SUs that should pass disappear and some SUs that should not pass appear more than in Fig. 5.11.

For Fig. 5.10, Fig. 5.11 and Fig. 5.12, the Ph.D. candidate defines $N_{q,u}$ and $M_{q,u}$ are random from 2 up to 4 antennas to see the appeared effect.

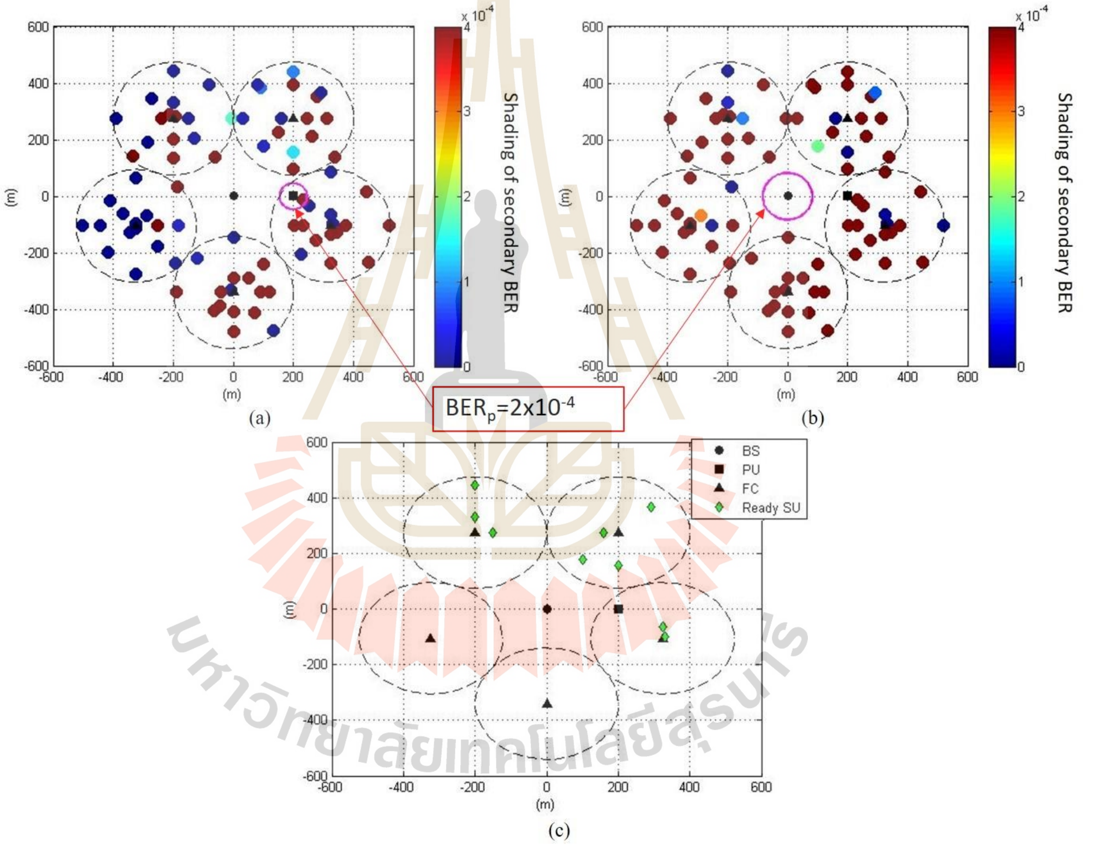

Figure 5.13 Overlapping spectrum sharing in multi-user multi-cell CR system by ignoring GPS error and setting the random number of antennas of SUs on (a) downlink and (b) uplink. And (c) the intersection result between downlink and uplink.

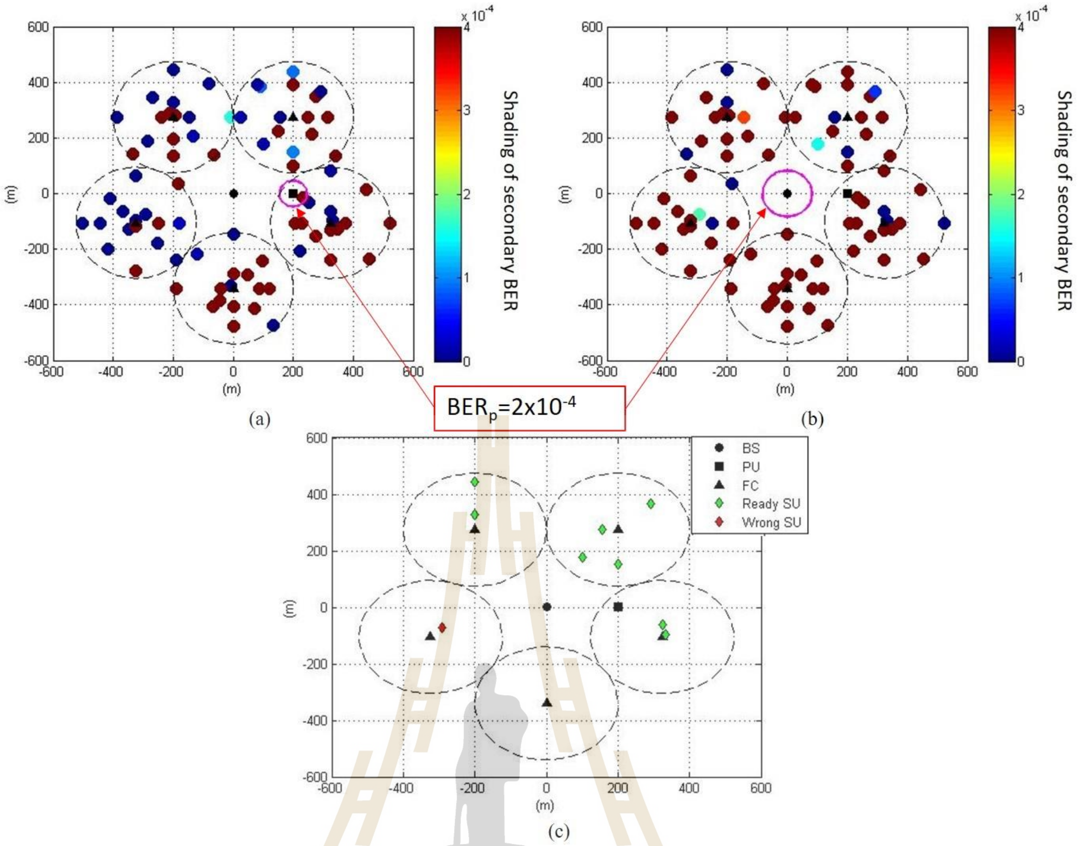

Figure 5.14 Overlapping spectrum sharing in multi-user multi-cell CR system by adding 5 m GPS error and setting the random number of antennas of SUs on (a) downlink and (b) uplink. And (c) the intersection result between downlink and uplink.

When Fig. 5.10, Fig. 5.11 and Fig. 5.12 compared to Fig. 5.13, Fig. 5.14 and Fig. 5.15, respectively, it clearly shows that the results are worse than when the number of antennas of all of SUs and FCs are set as 4 antennas. Referred to Fig. 5.4, the system performance is increased according to the number of antennas of the receiver. When the signals are sent from a source at each antenna, the detail of each signal is not much different because it still is not distorted by noises or interferences. Hence, if the receiver employs the combining technique, the quality of the received signal will be better according to the number of antennas. Moreover, $(M, N) = (4, 4)$ is the best because the transmitter has more choices sending the signal to the best antenna of the receiver.

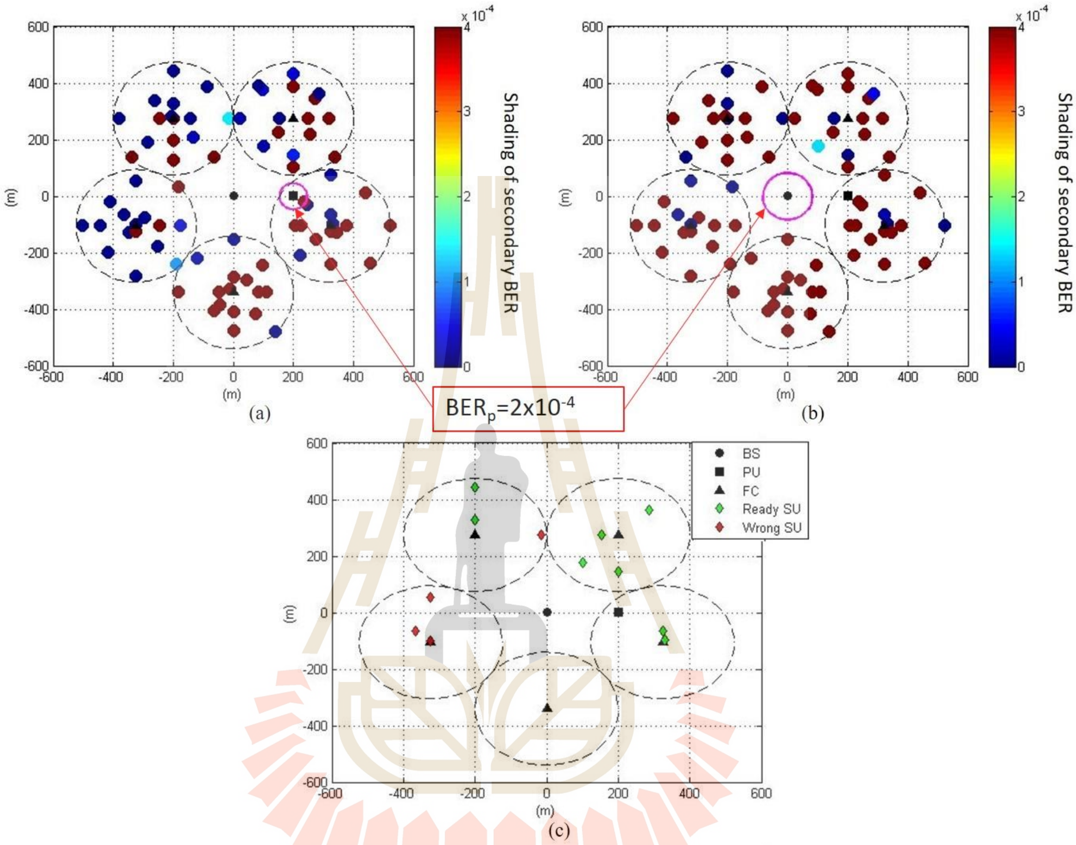

Figure 5.15 Overlapping spectrum sharing in multi-user multi-cell CR system by adding 10 m GPS error and setting the random number of antennas of SUs on (a) downlink and (b) uplink. And (c) the intersection result between downlink and uplink.

5.4 Spectrum allocation scheme simulation results

To achieve the goal of spectrum sharing operation, all processes in Fig. 4.10 are performed in which the results are shown in Fig. 5.16. The Ph.D. candidate defines the system consists of 5 picocells in which each picocell has 16 SUs randomly stayed inside, and PUs at all frequency channels have the random positions. Additionally, the

GPS error is 0-10 m, and $BW_{sub} = 5$ MHz. Hence the number of sub-bandwidths is 12 referring to the bandwidth in Table 5.1.

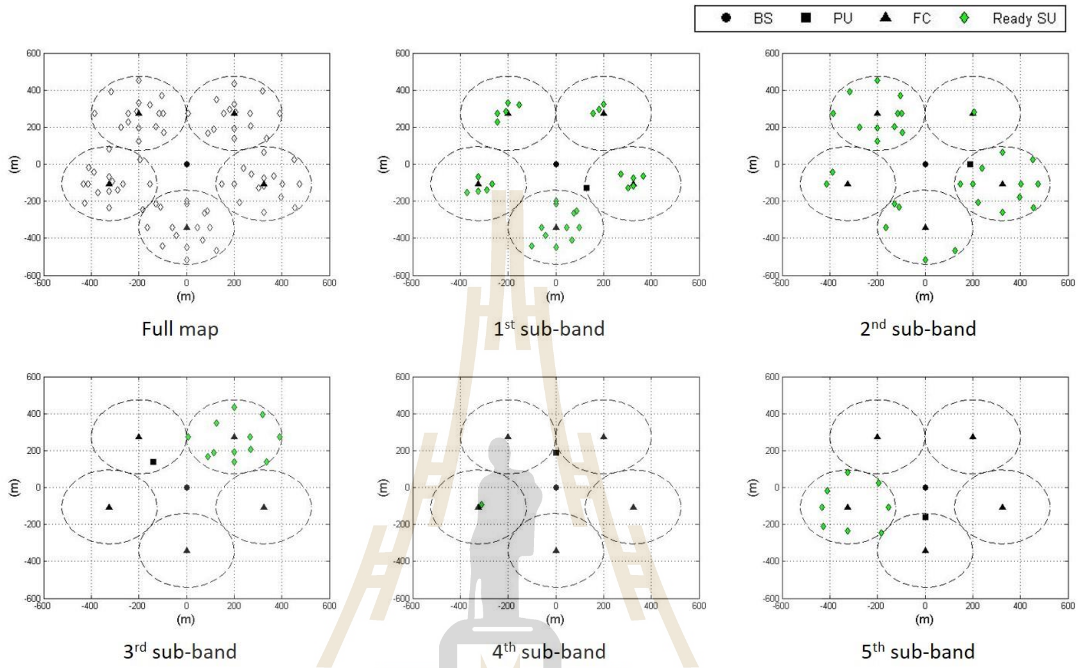

Figure 5.16 Full-system overlapping spectrum sharing with 16 users per picocell.

Starting with the top left figure, it shows the full map of CR system which represents all of node member positions except PU due to their different positions for each frequency channel. Then, PU appears in the next figure. Likewise for Fig. 5.12, after the performance analysis process of 1st sub-bandwidth, the result is shown in the top center figure. The appropriate SUs achieves the permission first reducing the interference factor at the next sub-bandwidth. As seen in the bottom center figure, there is only one SU passing because it was a big factor that affected other SUs made them do not pass. Hence, at the next sub-bandwidth, several remaining SUs achieves the goal. Normally in this experiment, the operation has to be finished within 12 sub-bandwidths.

However this time, all SUs can achieve the goal within 5 sub-bandwidths. Note that the effect of GPS error of this result is existed but not shown and not focused due to the fact that the system does not know how much impact it has in the reality.

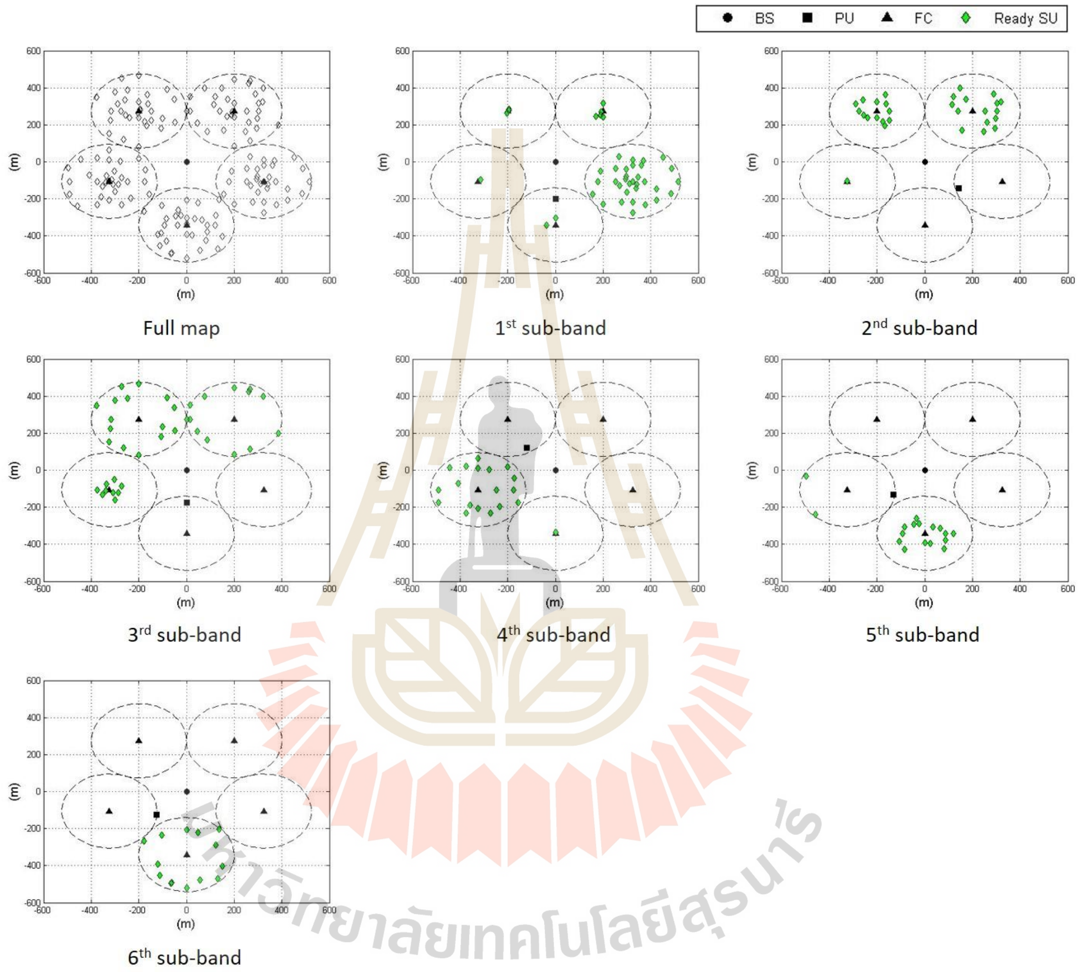

Figure 5.17 Full-system overlapping spectrum sharing with 32 users per picocell.

Referred to (R. Q. Hu, and Y. Qian, 2013), the system provides services for 16–32 users in coverage area of a picocell. For this reason, the Ph.D. candidate enhances the number of SUs to 32 users per picocell into the experiment as seen in Fig. 5.17. In the same way as Fig. 5.16, the system gradually allocates frequency channels to the appropriate SUs. Surely, when the system composes of higher number of SUs, it has to utilize more number of sub-bandwidths than in Fig. 5.16 in order to thoroughly allocate the spectrum to all users.

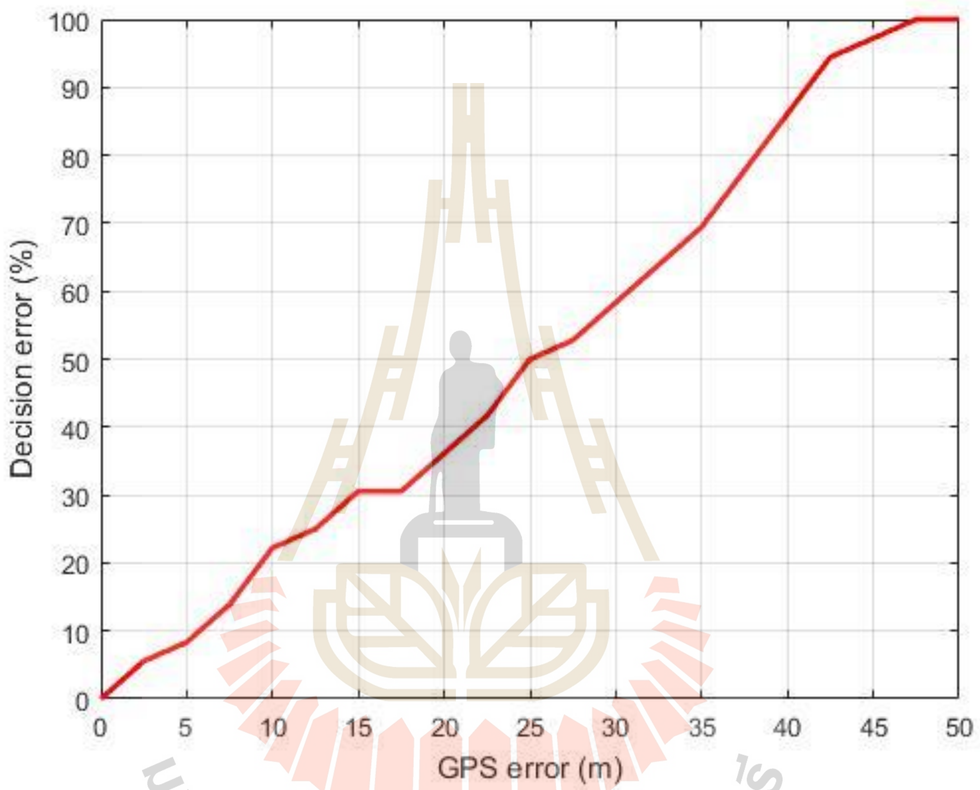

Figure 5.18 The relationship between decision error and GPS error for spectrum sharing in CR MIMO system.

5.5 Limitation of proposed algorithm

Although the proposed algorithm can obviously present the benefits on CR MIMO system, but some assumptions have been predefined in the simulations. These can be the limitation of this research which is worth to address as the followings.

5.5.1 In fact, the moving of each user during the time of the performance analysis process affects the accuracy of the spectrum decision process. Incidentally, in this research, all of the user positions are assumed to be static until the end of the spectrum sharing process. Hence, the method to acquire all updated locations is still a challenge problem in practice. Moreover, the system has to suddenly cut the SU's communication during the handoff process if SU moves into the dangerous area.

5.5.2 The PU's location is assumed to be known by the CR system. This can be happened by employing the option of Assisted GPS in LTE system. However, the policy to force all users to share their locations might be sensitive.

5.5.3 All node members in the CR system are assumed to employ the same LTE technology. Even the CR system concerns only the frequency allocation, but the realization of technology can truly evaluate the performance of CR system.

5.5.4 When the GPS error approaches 47 m, the decision error is 100% as shown in Fig. 5.18. However, the decision error should not more than 50%. Hence, the GPS error of the CR device should less than 25 m.

5.5.5 For this research, the overall process of self-evaluation technique spent around 1 minute deemed which is a significant delays in practice. Nevertheless, the higher effective processing system in the future will definitely solve this problem.

5.5.6 Primary network is the main priority in the system. Hence, this research is suitable for data transferring applications which can wait for the appropriate position of SU in communication. Therefore, the proposed CR concept cannot satisfy the real-time multimedia applications. The possible application of proposed concept would be a non-real-time messaging services.

5.6 Chapter summary

The simulation results can describe the impact on a position of each node in CR system related to a thorough performance analysis in term of BER that support both of downlink and uplink operations. The overlapping spectrum sharing performance is presented by the coverage area which consists of the BER regions of primary and secondary networks. In the dangerous zone, SU cannot perform the overlapping spectrum sharing, but the secondary link can establish in an available area. In term of multi-user systems, the depicted results are in a different style with the single user systems in order to easier identify each SU's status, in which these results clearly show that all SUs affect each other. The number of MIMO antenna elements and the GPS error significantly affect the systems. In addition, the system can thoroughly allocate the frequency channels to all users by employing the spectrum allocation scheme. The results are very useful for multi-user MIMO CR implementation to make a decision whether to establish a communication in each position of SU or not.

CHAPTER VI

THESIS CONCLUSION

6.1 Conclusion

The never-ending demand for mobile data and widespread connectivity in today's wireless world impels the service provider to improve network for spectral efficiencies as well as significant investments in the new technology resources to create their denser networks. Anywise, just those advancements alone are not sufficient to meet the challenges posed by future mobile data traffic when the only limited spectrum is available. Regulatory communication technology research is needed to determine the optimal utilization of frequency resources. Cognitive Radio (CR) is one of the technologies coming to solve spectrum scarcity problem. CR will allow Secondary User (SU) to access the same spectrum with the Primary User (PU) in the same location without excessively distorting the primary communication.

This research has been conducted to study the functioning of CR in term of spectrum sharing between PU and SU. The thesis content starts with understanding the fundamentals of CR to know what the background of problems is, how important CR is, and how the operating characteristic is. Then, the Ph.D. candidate has focused on spectrum sharing which can be divided into 2 types, including non-overlapping spectrum sharing and overlapping spectrum sharing. For non-overlapping spectrum sharing, CR system performs the spectrum detection at the considered frequency channels. If the system does not detect any primary signal, it allows SU to access that spectrum. The fundamental process of spectrum sharing is the spectrum sensing which is focused on the energy detection (ED) method in this thesis. Furthermore, the Ph.D. candidate has developed spectrum sensing efficacy employing Multiple-Input Multiple-Output (MIMO) technology. However, when considering the today's scenario, most communication application programs regularly utilize spectrum in which SU cannot avoid access the idle channel in the different time with PU. Hence, the Ph.D. candidate has focused on the overlapping spectrum sharing in which the system allows SU to access the same frequency channel with PU at the same time. This spectrum sharing scheme comes with the condition that the interference has to be limited to an acceptable level. MIMO technology is applied to reduce interference, well to a certain extent. Whereas, if any member node stays in the bad position, the appeared interference is still high although the system performance has been already improved. So, the Ph.D. candidate has an idea bringing the position information of each node in CR system to create the method in which secondary network can self-evaluate for the appropriate decision in communication in order to obtain the efficient spectrum sharing causing the cost-effective spectrum utilization.

Hereby, the performance analysis with the Bit Error Rate (BER) equations based on the positions of node members has been proposed which can support both of downlink and uplink. In order to advance to the next level, the performance analysis of single user CR system has been developed to support the multi-user CR system. Then, the intersection result from the performance analysis on downlink and uplink enables the system to avoid the terrible damage in multi-user communication. Especially, this result has been developed into the spectrum allocation scheme which can allocate the proper frequency for each SU in an entire system.

In summary, the contributions of proposed self-evaluation technique for spectrum sharing in MIMO CR system can be categorized into three major issues. Firstly, in order not to miss a small chance that might happen, the spectrum sensing technique has been improved employing the physical characteristic of popular MIMO technology. Hence, this new technique can precisely identify the status of each spectrum. Secondly, in order to comply with the form of the actual operation in the Long-Term Evolution (LTE) towards fifth-generation (5G) mobile systems, the single user performance analysis has been expanded into the multi-user performance analysis. This causes a knowledge for analyzing the appropriate positions of the multi-user MIMO CR network. Finally, in order to obtain the complete self-evaluation guideline for spectrum sharing in multi-user CR system, the spectrum allocation scheme has been proposed. This scheme will be the important factor to enable the CR technology to be accepted and brought into practical usage.

For the future work, the performance analysis in term of throughput will be considered because there is a relationship between throughput and BER. Especially, throughput is one of the main parameters which can show the system performance. Incidentally, it will be a great thing if the CR system knows about PU's location by ignoring the information shared from the primary network because the system should not interfere with the primary network. Moreover, it is very interesting to consider the way how to control the transmit power after each SU has already known its BER to adapt itself to utilize power as much as necessary. If this power control scheme can be done successfully, it will make at least two benefits. Firstly, CR system will make the cost-effective power utilization avoiding wasted power consumption. Secondly, it will provide an opportunity to add more other SUs to access the same channel at the same time.

REFERENCES

IEEE Standards Association. (2011). 802.22-2011-IEEE Standard for Information technology–Local and metropolitan area networks–Specific requirements–Part 22: Cognitive Wireless RAN Medium Access Control (MAC) and Physical Layer (PHY) specifications: Policies and procedures for operation in the TV Bands, **IEEE.**

Huifang, C., Lei, X., and Xiong, N. (2014). Reputation-based hierarchically cooperative spectrum sensing scheme in cognitive radio networks. **China Communications, 11(1), 12-25.**

Puranachaikeeree, S., and Suleesathira, R. (2010). Transmitting and Receiving Beamforming for Interference Cancellation in the Downlink of Cognitive Radio System. **Thesis.**

Khan, F. A., Tourki, K., Alouini, M. S., and Qaraqe, K. A. (2014). Performance analysis of a power limited spectrum sharing system with TAS/MRC. **IEEE Transactions on Signal Processing, 62(4), 954-967.**

Akyildiz, I. F., Lee, W. Y., Vuran, M. C., and Mohanty, S. (2006). NeXt generation/dynamic spectrum access/cognitive radio wireless networks: A survey. **Computer networks, 50(13), 2127-2159.**

Fette, B. A. (Ed.). (2009). Cognitive radio technology. **Academic Press.**

Haykin, S. (2005). Cognitive radio: brain-empowered wireless communications. **IEEE journal on selected areas in communications, 23(2), 201-220.**

Wyglinski, A. M., Nekovee, M., and Hou, T. (Eds.). (2009). Cognitive radio communications and networks: principles and practice. **Academic Press.**

Gardner, W. A. (1991). Exploitation of spectral redundancy in cyclostationary signals. **IEEE Signal processing magazine, 8(2), 14-36.**

Serpedin, E., Panduru, F., Sarı, I., and Giannakis, G. B. (2005). Bibliography on cyclostationarity. **Signal Processing, 85(12), 2233-2303.**

Cabric, D., Mishra, S. M., and Brodersen, R. W. (2004, November). Implementation issues in spectrum sensing for cognitive radios. **In Signals, systems and computers, 2004. Conference record of the thirty-eighth Asilomar conference on (Vol. 1, pp. 772-776). IEEE.**

Kim, K., Akbar, I. A., Bae, K. K., Um, J. S., Spooner, C. M., and Reed, J. H. (2007, April). Cyclostationary approaches to signal detection and classification in cognitive radio. **In New frontiers in dynamic spectrum access networks, 2007. DySPAN 2007. 2nd IEEE international symposium on (pp. 212-215). IEEE**.

Sutton, P. D., Nolan, K. E., and Doyle, L. E. (2008). Cyclostationary signatures in practical cognitive radio applications. **IEEE Journal on selected areas in Communications, 26(1).**

Kay, S. M. (1998). Fundamentals of statistical signal processing: Detection theory, **vol. 2.**

Li, T., Mow, W. H., Lau, V. K., Siu, M., Cheng, R. S., and Murch, R. D. (2007). Robust joint interference detection and decoding for OFDM-based cognitive radio systems with unknown interference. **IEEE Journal on Selected Areas in Communications, 25(3).**

Kundargi, N., and Tewfik, A. (2008, March). Sequential pilot sensing of ATSC signals in IEEE 802.22 cognitive radio networks. **In Acoustics, Speech and Signal Processing, 2008. ICASSP 2008. IEEE International Conference on (pp. 2789-2792). IEEE.**

Yu, H., Sung, Y., and Lee, Y. H. (2008, March). On optimal operating characteristics of sensing and training for cognitive radios. **In Acoustics, Speech and Signal Processing, 2008. ICASSP 2008. IEEE International Conference on (pp. 2785-2788). IEEE.**

Huifang, C., Lei, X., and Xiong, N. (2014). Reputation-based hierarchically cooperative spectrum sensing scheme in cognitive radio networks. **China Communications, 11(1), 12-25.**

Hwang, I., and Lee, J. W. (2017). Cooperative Spectrum Sensing With Quantization Combining Over Imperfect Feedback Channels. **IEEE Transactions on Signal Processing, 65(3), 721-732.**

Haykin, S. (2005). Cognitive radio: brain-empowered wireless communications. **IEEE journal on selected areas in communications, 23(2), 201-220.**

Bagheri, S., and Scaglione, A. (2015). The restless multi-armed bandit formulation of the cognitive compressive sensing problem. **IEEE Transactions on Signal Processing, 63(5), 1183-1198.**

Kitsunezuka, M., and Pister, K. S. (2015). Cross-Correlation-Based, Phase-Domain Spectrum Sensing With Low-Cost Software-Defined Radio Receivers. **IEEE Trans. Signal Processing, 63(8), 2033-2048.**

Grissa, M., Yavuz, A. A., and Hamdaoui, B. (2017). Preserving the Location Privacy of Secondary Users in Cooperative Spectrum Sensing. **IEEE Transactions on Information Forensics and Security, 12(2), 418-431.**

Zhang, L., Ding, G., Wu, Q., Zou, Y., Han, Z., and Wang, J. (2015). Byzantine attack and defense in cognitive radio networks: A survey. **IEEE Communications Surveys & Tutorials, 17(3), 1342-1363.**

Pandit, S., and Singh, G. (2015). Backoff algorithm in cognitive radio MAC protocol for throughput enhancement. **IEEE Transactions on Vehicular Technology, 64(5), 1991-2000.**

Hussain, R., and Sharawi, M. S. (2015). Integrated reconfigurable multiple-input–multiple-output antenna system with an ultra-wideband sensing antenna for cognitive radio platforms. **IET Microwaves, Antennas & Propagation, 9(9), 940-947.**

Rawat, D. B., Shetty, S., and Xin, C. (2016). Stackelberg-game-based dynamic spectrum access in heterogeneous wireless systems. **IEEE Systems Journal, 10(4), 1494-1504.**

Zhang, R. (2009). On peak versus average interference power constraints for protecting primary users in cognitive radio networks. **IEEE Transactions on Wireless Communications, 8(4).**

Yang, G., Li, B., Tan, X., and Wang, X. (2015). Adaptive power control algorithm in cognitive radio based on game theory. **IET Communications, 9(15), 1807-1811.**

Kim, T. K., Kim, H. M., Song, M. G., and Im, G. H. (2015). Improved Spectrum-Sharing Protocol for Cognitive Radio Networks With Multiuser Cooperation. **IEEE Transactions on Communications, 63(4), 1121-1135.**

Vassaki, S., Poulakis, M. I., and Panagopoulos, A. D. (2016). State-based potential power allocation game in a cooperative multiuser network. **IET Communications, 10(11), 1320-1328.**

Khalfi, B., Ghorbel, M. B., Hamdaoui, B., and Guizani, M. (2015, April). Distributed fair spectrum assignment for large-scale wireless DSA networks. **In International Conference on Cognitive Radio Oriented Wireless Networks (pp. 631-642). Springer International Publishing.**

Çelebi, M. B., and Arslan, H. (2015). Theoretical Analysis of the Co-Existence of LTE-A Signals and Design of an ML-SIC Receiver. **IEEE Transactions on Wireless Communications, 14(8), 4626-4639.**

Tourki, K., Khan, F. A., Qaraqe, K. A., Yang, H. C., and Alouini, M. S. (2014). Exact performance analysis of MIMO cognitive radio systems using transmit antenna selection. **IEEE Journal on Selected areas in communications, 32(3), 425-438.**

Heath, R. W., and Paulraj, A. J. (2005). Switching between diversity and multiplexing in MIMO systems. **IEEE Transactions on Communications, 53(6), 962-968.**

Uthansakul, P. (Ed.). (2011). Mobile communication systems. **Suranaree University of technology.**

Foutz, J., Spanias, A., and Banavar, M. K. (2008). Narrowband direction of arrival estimation for antenna arrays. **Synthesis Lectures on Antennas, 3(1), 1-76.**

Goldsmith, A. (2005). Wireless communications. **Cambridge university press.**

Chen, Y., and Tellambura, C. (2004). Distribution functions of selection combiner output in equally correlated Rayleigh, Rician, and Nakagami-m fading channels. **IEEE Transactions on Communications, 52(11), 1948-1956.**

Jeffrey, A., and Zwillinger, D. (Eds.). (2007). Table of integrals, series, and products. **Academic Press.**

Shah, A., and Haimovich, A. M. (2000). Performance analysis of maximal ratio combining and comparison with optimum combining for mobile radio communications with cochannel interference. **IEEE Transactions on Vehicular Technology, 49(4), 1454-1463.**

Kang, M., and Alouini, M. S. (2003, May). A comparative study on the performance of MIMO MRC systems with and without co-channel interference. In Communications, 2003. ICC'03. **IEEE International Conference on (Vol. 3, pp. 2154-2158). IEEE.**

ETSI, LTE (2011). Evolved universal terrestrial radio access (e-utra). **User Equipment (UE) radio access capabilities (3GPP TS 36.101 version 10.3.0 Release 10).**

Davari, N., and Gholami, A. (2017). An asynchronous adaptive direct Kalman filter algorithm to improve underwater navigation system performance. **IEEE Sensors Journal, 17(4), 1061-1068.**

Zandbergen, P. A., and Barbeau, S. J. (2011). Positional accuracy of assisted GPS data from high-sensitivity GPS-enabled mobile phones. **The Journal of Navigation, 64(3), 381-399.**

Hu, R. Q., and Qian, Y. (Eds.). (2013). Heterogeneous cellular networks. **John Wiley & Sons.**

Thiagarajah, S. P., Ting, A., Chieng, D., Alias, M. Y., and Wei, T. S. (2013). User data rate enhancement using heterogeneous LTE-802.11 n offloading in urban area. **In Wireless Technology and Applications (ISWTA), 2013 IEEE Symposium on (pp. 11-16). IEEE.**

APPENDIX

APPENDIX A

EQUATION DERIVATION

A.1 Derivation of equations (4.19) and (4.24)

When x in (4.17) is represented with $\frac{x}{\left(\frac{P_{ss}}{N_0}\right)}$, (4.17) becomes

$$F_{g_{ss}}\left(\frac{x}{\left(\frac{P_{ss}}{N_0}\right)}\right)=\frac{1}{\Gamma(M+1)}\times \left[\left(\frac{x}{g_{ss}\left(\frac{P_{ss}}{N_0}\right)}\right)^{MN}\Gamma\left(1-M(N-1),\frac{x}{g_{ss}\left(\frac{P_{ss}}{N_0}\right)}\right)+\gamma\left(M+1,\frac{x}{g_{ss}\left(\frac{P_{ss}}{N_0}\right)}\right)\right], \tag{A.1}$$

when referring to (4.20), (A.1) becomes (4.19). Then, (4.19) is taken into (4.23) as follows.

$$BER_s(a,b)=\frac{a}{2}\sqrt{\frac{b}{2\pi}}\int_0^\infty\frac{e^{-\frac{b}{2}x}}{\sqrt{x}}\frac{1}{\Gamma(M+1)}\times \left[\left(\frac{x}{\gamma_{ss}}\right)^{MN}\times\Gamma\left(1-M(N-1),\frac{x}{\gamma_{ss}}\right)+\gamma\left(M+1,\frac{x}{\gamma_{ss}}\right)\right]dx. \tag{A.2}$$

The Ph.D. candidate defines $A=\frac{a}{2}\sqrt{\frac{b}{2\pi}}\frac{1}{\Gamma(M+1)}$, and employs the distributive law to separate the integration in (A.2) into two parts as follows.

$$P_{s1}=\left(\frac{1}{\gamma_{ss}}\right)^{MN}\int_0^\infty x^{MN-\frac{1}{2}}e^{-\frac{b}{2}x}\Gamma\left(1-M(N-1),\frac{x}{\gamma_{ss}}\right)dx. \tag{A.3}$$

(A. Jeffrey and D. Zwillinger, 2007, Eq. 6.455.1) is employed to obtain

$$P_{s1}=\left(\frac{1}{\gamma_{ss}}\right)^{MN}\frac{\left(\frac{1}{\gamma_{ss}}\right)^{1-M(N-1)}\Gamma\left(M+\frac{3}{2}\right)}{\left(MN+\frac{1}{2}\right)\left(\frac{1}{\gamma_{ss}}+\frac{b}{2}\right)^{M+\frac{3}{2}}}\times$$
$${}_2F_1\left(1,M+\frac{3}{2};MN+\frac{3}{2};\frac{b\gamma_{ss}}{2+b\gamma_{ss}}\right). \tag{A.4}$$

And the next part is

$$P_{s2}=\int_0^{\infty}x^{-\frac{1}{2}}e^{-\frac{b}{2}x}\gamma\left(M+1,\frac{x}{\gamma_{ss}}\right)dx. \tag{A.5}$$

(A. Jeffrey and D. Zwillinger, 2007, Eq. 6.455.2) is employed to obtain

$$P_{s2}=\left(\frac{1}{\gamma_{ss}}\right)^{M+1}\frac{\Gamma\left(M+\frac{3}{2}\right)}{(M+1)\left(\frac{1}{\gamma_{ss}}+\frac{b}{2}\right)^{M+\frac{3}{2}}}\times$$
$${}_2F_1\left(1,M+\frac{3}{2};M+2;\frac{2}{2+b\gamma_{ss}}\right). \tag{A.6}$$

When combining both parts together, the result is

$$BER_s(a,b)=\frac{a}{2}\sqrt{\frac{b}{2\pi}}\frac{1}{\Gamma(M+1)}\left[\frac{\left(\frac{1}{\gamma_{ss}}\right)^{M+1}\Gamma\left(M+\frac{3}{2}\right)}{\left(MN+\frac{1}{2}\right)\left(\frac{1}{\gamma_{ss}}+\frac{b}{2}\right)^{M+\frac{3}{2}}}\times\right.$$
$${}_2F_1\left(1,M+\frac{3}{2};MN+\frac{3}{2};\frac{b\gamma_{ss}}{2+b\gamma_{ss}}\right)+ \tag{A.7}$$
$$\left.\frac{\left(\frac{1}{\gamma_{ss}}\right)^{M+1}\Gamma\left(M+\frac{3}{2}\right)}{(M+1)\left(\frac{1}{\gamma_{ss}}+\frac{b}{2}\right)^{M+\frac{3}{2}}}{}_2F_1\left(1,M+\frac{3}{2};M+2;\frac{2}{2+b\gamma_{ss}}\right)\right].$$

By formatting (A.7), (A.7) becomes (4.24).

A.2 Derivation of equations (4.30), (4.32) and (4.34)

By replacing x in (4.17) with $\frac{x(y+1)}{\left(\frac{P_{ss}}{N_0}\right)}$,

$$F_{g_{ss}}\left(\frac{x(y+1)}{\left(\frac{P_{ss}}{N_0}\right)}\right)=\frac{1}{\Gamma(M+1)}\times \left[\left(\frac{x(y+1)}{g_{ss}\left(\frac{P_{ss}}{N_0}\right)}\right)^{MN}\Gamma\left(1-M(N-1),\frac{x(y+1)}{g_{ss}\left(\frac{P_{ss}}{N_0}\right)}\right)+\gamma\left(M+1,\frac{x(y+1)}{g_{ss}\left(\frac{P_{ss}}{N_0}\right)}\right)\right], \tag{A.8}$$

By referring to (4.20), (A.8) becomes (4.30). Then, (4.30) is taken into (4.29), and separate the expectation operation in (4.29) into two sub-functions as (4.27). $F_1(x)$ from (4.31) can be solved as follows.

$$F_1(x)=\frac{\left(\frac{x}{\gamma_{ss}}\right)^{MN}}{\Gamma(M+1)}\frac{e^{\frac{1}{\gamma_{ps}}}}{\gamma_{ps}}\int_0^{\infty}e^{-\frac{1}{\gamma_{ps}}(y+1)}(y+1)^{MN}\times \Gamma\left(1-M(N-1),\frac{x}{\gamma_{ss}}(y+1)\right)dy. \tag{A.9}$$

By defining $\varnothing=(y+1)$, (A. Jeffrey and D. Zwillinger, 2007, Eq. 8.352.5) is employed to change (A.9) into

$$F_1(x)=\frac{\left(\frac{x}{\gamma_{ss}}\right)^{MN}}{\Gamma(M+1)}\frac{e^{\frac{1}{\gamma_{ps}}}}{\gamma_{ps}}\int_1^{\infty}\varnothing^{MN}e^{-\frac{1}{\gamma_{ps}}\varnothing}\frac{(-1)^{M(N-1)+1}}{(M(N-1)-1)!}\times \left[\Gamma\left(0,\frac{x}{\gamma_{ss}}\varnothing\right)-e^{-\frac{x}{\gamma_{ss}}\varnothing}\sum_{k=0}^{M(N-1)-2}\frac{(-1)^k k!}{\varnothing^{k+1}}\left(\frac{x}{\gamma_{ss}}\right)^{-(k+1)}\right]d\varnothing. \tag{A.10}$$

Then, the distributive law is employed. Next, the Ph.D. candidate defines

$A = \frac{\left(\frac{x}{\gamma_{ss}}\right)^{MN}}{\Gamma(M+1)} \frac{e^{\frac{1}{\gamma_{ps}}}}{\gamma_{ps}} \frac{(-1)^{M(N-1)}}{(M(N-1)-1)!}$, and integrates the first part as follows.

$$F_{1.1} = A\int_{1}^{\infty} \varnothing^{MN} e^{-\frac{1}{\gamma_{ps}}\varnothing} \mathrm{Ei}\left(-\frac{x}{\gamma_{ss}}\varnothing\right) d\varnothing. \tag{A.11}$$

The integral by pass method is employed. Hence,

$$\begin{aligned} F_{1.1} = & -A\gamma_{ps}{}^{MN+1}\mathrm{Ei}\left(-\frac{x}{\gamma_{ss}}\varnothing\right)\Gamma\left(MN+1,\frac{\varnothing}{\gamma_{ps}}\right)\Bigg|_{1}^{\infty} + \\ & A\gamma_{ps}{}^{MN+1}\int_{1}^{\infty}\varnothing^{-1}e^{-\frac{x}{\gamma_{ss}}\varnothing}\Gamma\left(MN+1,\frac{\varnothing}{\gamma_{ps}}\right)d\varnothing. \end{aligned} \tag{A.12}$$

(A. Jeffrey and D. Zwillinger, 2007, Eq. 8.352.4) is employed to obtain

$$\begin{aligned} F_{1.1} = & A\gamma_{ps}{}^{MN+1}\Gamma\left(MN+1,\frac{1}{\gamma_{ps}}\right)\mathrm{Ei}\left(-\frac{x}{\gamma_{ss}}\right) + \\ & A\gamma_{ps}{}^{MN+1}\int_{1}^{\infty}\varnothing^{-1}e^{-\frac{x}{\gamma_{ss}}\varnothing}(MN)!\,e^{-\frac{1}{\gamma_{ps}}\varnothing}\sum_{k=1}^{MN}\left(\frac{1}{\gamma_{ps}}\right)^{k}\frac{\varnothing^{k}}{k!}d\varnothing. \end{aligned} \tag{A.13}$$

The integration is completed to obtain

$$\begin{aligned} F_{1.1} = & A\gamma_{ps}{}^{MN+1}\Gamma\left(MN+1,\frac{1}{\gamma_{ps}}\right)\mathrm{Ei}\left(-\frac{x}{\gamma_{ss}}\right) + \\ & A\gamma_{ps}{}^{MN+1}(MN)!\sum_{k=1}^{MN}\frac{\left(\frac{1}{\gamma_{ps}}\right)^{k}}{k!}\left(\frac{1}{\gamma_{ps}}+\frac{x}{\gamma_{ss}}\right)\Gamma\left(k,\left(\frac{1}{\gamma_{ps}}+\frac{x}{\gamma_{ss}}\right)\right). \end{aligned} \tag{A.14}$$

Replacing A back to original form and employing the redundancy law, (A.14) is rearranged to become

$$F_{1.1}=\frac{(-1)^{M(N-1)}\left(\frac{\gamma_{ps}}{\gamma_{ss}}\right)^{MN}e^{\frac{1}{\gamma_{ps}}}}{\Gamma(M+1)(M(N-1)-1)!}\left[\Gamma\left(MN+1,\frac{1}{\gamma_{ps}}\right)x^{MN}\mathrm{Ei}\left(-\frac{x}{\gamma_{ss}}\right)+\right. \tag{A.15}$$
$$\left.(MN)!\sum_{k=1}^{MN}\left(\frac{1}{\gamma_{ps}}\right)^{k}\frac{1}{k!}\left(\frac{1}{\gamma_{ps}}+\frac{x}{\gamma_{ss}}\right)^{-k}x^{MN}\Gamma\left(k,\left(\frac{1}{\gamma_{ps}}+\frac{x}{\gamma_{ss}}\right)\right)\right].$$

Then integrating the next part,

$$F_{1.2}=A\sum_{k=0}^{M(N-1)-2}(-1)^{k}k!\gamma_{ss}{}^{k+1}\int_{1}^{\infty}\varnothing^{MN-k-1}e^{-\left(\frac{1}{\gamma_{ps}}+\frac{x}{\gamma_{ss}}\right)\varnothing}d\varnothing. \tag{A.16}$$

Replacing A back to original form and employing the redundancy law,

$$F_{1.2}=\frac{\left(\frac{x}{\gamma_{ss}}\right)^{MN}}{\Gamma(M+1)}\frac{e^{\frac{1}{\gamma_{ps}}}}{\gamma_{ps}}\frac{(-1)^{M(N-1)}}{(M(N-1)-1)!}\sum_{k=0}^{M(N-1)-2}\frac{(-1)^{k}k!}{x^{k+1}}\gamma_{ss}{}^{k+1}\times \tag{A.17}$$
$$\left(\frac{1}{\gamma_{ps}}+\frac{x}{\gamma_{ss}}\right)^{-MN+k}\Gamma\left(MN-k,\left(\frac{1}{\gamma_{ps}}+\frac{x}{\gamma_{ss}}\right)\right).$$

By composing the new format,

$$F_{1.2}=\frac{(-1)^{M(N-1)}\frac{1}{\gamma_{ps}}e^{\frac{1}{\gamma_{ps}}}\left(\frac{1}{\gamma_{ss}}\right)^{MN}}{\Gamma(M+1)(M(N-1)-1)!}\sum_{k=0}^{M(N-1)-2}(-1)^{k}k!\gamma_{ss}{}^{k+1}x^{MN-k-1}\times \tag{A.18}$$
$$\left(\frac{1}{\gamma_{ps}}+\frac{x}{\gamma_{ss}}\right)^{-MN+k}\Gamma\left(MN-k,\left(\frac{1}{\gamma_{ps}}+\frac{x}{\gamma_{ss}}\right)\right).$$

When combining both parts, (A.18) becomes (4.32). Next, $F_2(x)$ from (4.33) can be solved as follows

$$F_2(x)=\left(\frac{1}{\gamma_{ps}}\right)\frac{e^{\frac{1}{\gamma_{ps}}}}{\Gamma(M+1)}\int_0^{\infty}e^{-\frac{1}{\gamma_{ps}}(y+1)}\gamma\left(M+1,\frac{x}{\gamma_{ss}}(y+1)\right)dy. \quad \text{(A.19)}$$

When defining $\varnothing=(y+1)$,

$$F_2(x)=\left(\frac{1}{\gamma_{ps}}\right)\frac{e^{\frac{1}{\gamma_{ps}}}}{\Gamma(M+1)}\int_0^{\infty}e^{-\frac{1}{\gamma_{ps}}\varnothing}\gamma\left(M+1,\frac{x}{\gamma_{ss}}\varnothing\right)d\varnothing. \quad \text{(A.20)}$$

(A. Jeffrey and D. Zwillinger, 2007, Eq. 3.352.1) is employed to obtain

$$F_2(x)=\frac{\left(\frac{1}{\gamma_{ps}}\right)e^{\frac{1}{\gamma_{ps}}}}{\Gamma(M+1)}\int_0^{\infty}e^{-\frac{1}{\gamma_{ps}}\varnothing}M!\left[1-e^{-\frac{x}{\gamma_{ss}}\varnothing}\sum_{k=0}^{M}\left(\frac{x}{\gamma_{ss}}\right)^k\frac{\varnothing^k}{k!}\right]d\varnothing. \quad \text{(A.21)}$$

By employing the distributive law with the integral operator and performing the integration in (A.21),

$$F_2(x)=\frac{\left(\frac{1}{\gamma_{ps}}\right)e^{\frac{1}{\gamma_{ps}}}}{\Gamma(M+1)}M!\left[\gamma_{ps}e^{-\frac{1}{\gamma_{ps}}}+\sum_{k=0}^{M}\left(\frac{x}{\gamma_{ss}}\right)^k\frac{1}{k!}\left[\left(\frac{1}{\gamma_{ps}}+\frac{x}{\gamma_{ss}}\right)^{-k-1}\times\right.\right.$$
$$\left.\left.\Gamma\left(k+1,\left(\frac{1}{\gamma_{ps}}+\frac{x}{\gamma_{ss}}\right)\varnothing\right)\right]_1^{\infty}\right]. \quad \text{(A.22)}$$

When making the definite integral, (A.22) is completed as (4.34).

A.3 Derivation of equations (4.36), (4.37), (4.38), (4.39) and (4.40)

Eq. (4.32) and (4.34) are combined to obtain

$$F_{\gamma_{int}}(x)=A\Gamma\left(MN+1,\frac{1}{\gamma_{ps}}\right)x^{MN}\mathrm{Ei}\left(-\frac{x}{\gamma_{ss}}\right)+A(MN)!\sum_{k=1}^{MN}\left(\frac{1}{\gamma_{ps}}\right)^{k}\times$$
$$\frac{1}{k!}x^{MN}\left(\frac{1}{\gamma_{ps}}+\frac{x}{\gamma_{ss}}\right)^{-k}\Gamma\left(k,\left(\frac{1}{\gamma_{ps}}+\frac{x}{\gamma_{ss}}\right)\right)+B\left(\frac{x}{\gamma_{ss}}\right)^{MN-k-1}\times$$
$$\left(\frac{1}{\gamma_{ps}}+\frac{x}{\gamma_{ss}}\right)^{k-MN}\Gamma\left(MN-k,\left(\frac{1}{\gamma_{ps}}+\frac{x}{\gamma_{ss}}\right)\right)+ \tag{A.23}$$
$$C\left[1-\left(\frac{1}{\gamma_{ps}}\right)e^{\frac{1}{\gamma_{ps}}}\sum_{k=0}^{M}\left(\frac{x}{\gamma_{ss}}\right)^{k}\left(\frac{1}{\gamma_{ps}}+\frac{x}{\gamma_{ss}}\right)^{-k-1}\frac{1}{k!}\Gamma\left(k+1,\left(\frac{1}{\gamma_{ps}}+\frac{x}{\gamma_{ss}}\right)\right)\right].$$

Meanwhile, the Ph.D. candidate defines $A=\dfrac{(-1)^{M(N-1)}e^{\frac{1}{\gamma_{ps}}}\left(\frac{\gamma_{ps}}{\gamma_{ss}}\right)^{MN}}{\Gamma(M+1)(M(N-1)-1)!}$,

$B=\dfrac{\left(\frac{1}{\gamma_{ps}}\right)}{\Gamma(M+1)}\dfrac{e^{\frac{1}{\gamma_{ps}}}}{(M(N-1)-1)!}\displaystyle\sum_{k=0}^{M(N-1)-2}k!(-1)^{M(N-1)+k}$, and $C=\dfrac{M!}{\Gamma(M+1)}$. Then, (A.23) is taken into (4.35) in which the integration in (4.35) is separated into four parts. Starting with

$$P_1(x)=\frac{a}{2}\sqrt{\frac{b}{2\pi}}A\Gamma\left(MN+1,\frac{1}{\gamma_{ps}}\right)\int_0^{\infty}x^{MN-\frac{1}{2}}e^{-\frac{b}{2}x}\mathrm{Ei}\left(-\frac{x}{\gamma_{ss}}\right)dx. \tag{A.24}$$

When referring to (A. Jeffrey and D. Zwillinger, 2007, Eq. 6.228.2), (A.24) becomes

$$P_1(x)=\frac{a}{2}\sqrt{\frac{b}{2\pi}}\frac{(-1)^{M(N-1)+1}e^{\frac{1}{\gamma_{ps}}}\left(\frac{\gamma_{ps}}{\gamma_{ss}}\right)^{MN}}{\Gamma(M+1)(M(N-1)-1)!}\frac{\Gamma\left(MN+1,\frac{1}{\gamma_{ps}}\right)}{\left(MN+\frac{1}{2}\right)}\times$$
$$\frac{\Gamma\left(MN+\frac{1}{2}\right)}{\left(\frac{1}{\gamma_{ss}}+\frac{b}{2}\right)^{MN+\frac{1}{2}}}{}_2F_1\left(1,MN+\frac{1}{2};MN+\frac{3}{2};\frac{b\gamma_{ss}}{2+b\gamma_{ss}}\right). \tag{A.25}$$

After that, the next part is considered to perform the integration as follows

$$P_2(x)=\frac{a}{2}\sqrt{\frac{b}{2\pi}}A(MN)!\sum_{k=1}^{MN}\left(\frac{1}{\gamma_{ps}}\right)^k\frac{1}{k!}\int_0^\infty x^{MN-\frac{1}{2}}\left(\frac{1}{\gamma_{ps}}+\frac{x}{\gamma_{ss}}\right)^{-k} \times e^{-\frac{b}{2}x}\Gamma\left(k,\left(\frac{1}{\gamma_{ps}}+\frac{x}{\gamma_{ss}}\right)\right)dx. \tag{A.26}$$

By defining $u=\frac{\gamma_{ss}}{\gamma_{ps}}$, $z=u+x$, and $D=\frac{a}{2}\sqrt{\frac{b}{2\pi}}A(MN)!\sum_{k=1}^{MN}\frac{\left(\frac{1}{\gamma_{ps}}\right)^k}{k!}\gamma_{ss}{}^k e^{\frac{b}{2}u}$,

$$P_2(x)=D\int_{u=\frac{\gamma_{ss}}{\gamma_{ps}}}^{\infty}e^{-\frac{b}{2}z}z^{-k}(z-u)^{MN-\frac{1}{2}}(k-1)!e^{-\frac{1}{\gamma_{ss}}z}\sum_{m=0}^{k-1}\frac{\left(\frac{1}{\gamma_{ss}}\right)^m z^m}{m!}dz. \tag{A.27}$$

(A. Jeffrey and D. Zwillinger, 2007, Eq. 3.383.4) is employed to obtain

$$P_2(x)=\frac{a}{2}\sqrt{\frac{b}{2\pi}}\frac{(-1)^{M(N-1)}(MN)!\Gamma\left(MN+\frac{1}{2}\right)}{\Gamma(M+1)(M(N-1)-1)!}e^{\frac{b\gamma_{ss}+2}{4\gamma_{ps}}}\sum_{k=1}^{MN}\frac{(k-1)!}{k!}\times \sum_{m=0}^{k-1}\left(\frac{1}{\gamma_{ss}}\right)^m\frac{1}{m!}\left(\frac{b}{2}+\frac{1}{\gamma_{ss}}\right)^{-\frac{1}{2}\left(MN+m-k+\frac{3}{2}\right)}\left(\frac{\gamma_{ss}}{\gamma_{ps}}\right)^{\frac{1}{4}(2k+2m-2MN-1)}\times W_{\frac{1}{2}\left(m-k-MN-\frac{1}{2}\right),-\frac{1}{2}\left(MN+m-k+\frac{1}{2}\right)}\left(\frac{b\gamma_{ss}+2}{2\gamma_{ps}}\right). \tag{A.28}$$

Then, the next part is

$$P_3(x)=\frac{\frac{a}{2}\sqrt{\frac{b}{2\pi}}B}{\gamma_{ss}{}^{MN-k-1}}\int_0^\infty e^{-\frac{b}{2}x}x^{MN-k-\frac{3}{2}}\left(\frac{1}{\gamma_{ss}}\right)^{k-MN}\left(\frac{\gamma_{ss}}{\gamma_{ps}}+x\right)^{k-MN}\times \Gamma\left(MN-k,\left(\frac{\gamma_{ss}}{\gamma_{ps}}+x\right)\frac{1}{\gamma_{ss}}\right)dx. \tag{A.29}$$

The Ph.D. candidate defines $u=\frac{\gamma_{ss}}{\gamma_{ps}}$, and $z=u+x$. (A. Jeffrey and D. Zwillinger, 2007, Eq. 8.352.4) and (A. Jeffrey and D. Zwillinger, 2007, Eq. 3.383.5) are employed and B is changed back to original form to obtain

$$P_3(x)=\frac{a}{2}\sqrt{\frac{b}{2\pi}}\frac{\left(\frac{1}{\gamma_{ps}}\right)e^{\frac{b\gamma_{ss}+2}{4\gamma_{ps}}}}{\Gamma(M+1)(M(N-1)-1)!}\sum_{k=0}^{M(N-1)-2}k!(-1)^{M(N-1)+k}\times$$
$$\Gamma\left(MN-k-\frac{1}{2}\right)(MN-k-1)!\sum_{m=0}^{MN-k-1}\frac{\gamma_{ss}^{1-m}}{m!}\left(\frac{b}{2}+\frac{1}{\gamma_{ss}}\right)^{-\frac{1}{2}\left(m+\frac{1}{2}\right)}\times \tag{A.30}$$
$$\left(\frac{\gamma_{ps}}{\gamma_{ss}}\right)^{\frac{1}{2}\left(m-\frac{3}{2}\right)}W_{\frac{1}{2}\left(2k-2MN+m+\frac{3}{2}\right),\frac{1}{2}\left(-m+\frac{1}{2}\right)}\left(\frac{b\gamma_{ss}+2}{2\gamma_{ps}}\right).$$

Then, the final part is

$$P_4(x)=\frac{a}{2}\sqrt{\frac{b}{2\pi}}C\left[\int_0^\infty e^{-\frac{b}{2}x}x^{-\frac{1}{2}}dx-\left(\frac{1}{\gamma_{ps}}\right)e^{\frac{1}{\gamma_{ps}}}\sum_{k=0}^{M}\left(\frac{1}{\gamma_{ss}}\right)^k\frac{1}{k!}\times\right.$$
$$\left.\int_0^\infty e^{-\frac{b}{2}x}x^{-\frac{1}{2}}x^k\left(\frac{1}{\gamma_{ps}}+\frac{x}{\gamma_{ss}}\right)^{-k-1}\Gamma\left(k+1,\left(\frac{1}{\gamma_{ps}}+\frac{x}{\gamma_{ss}}\right)\right)dx\right]. \tag{A.31}$$

The integration in (A.31) can be separated into two parts for simplicity. First part is

$$P_{4.1}=\frac{a}{2}\sqrt{\frac{b}{2\pi}}C\int_0^\infty e^{-\frac{b}{2}x}x^{-\frac{1}{2}}dx. \tag{A.32}$$

The integration result in (A.32) is

$$P_{4.1}=\frac{a}{2}\sqrt{\frac{b}{2\pi}}C\sqrt{\frac{2\pi}{b}}\operatorname{erf}\left(\sqrt{\frac{b}{2}x}\right)\Bigg|_0^\infty. \tag{A.33}$$

where $\operatorname{erf}(.)$ is the error function. When making the definite integral, (A.33) is completed as

$$P_{4.1} = \frac{a}{2}\sqrt{\frac{b}{2\pi}}\frac{M!}{\Gamma(M+1)}\sqrt{\frac{2\pi}{b}}. \tag{A.34}$$

Then, the second part is

$$P_{4.2} = -\frac{a}{2}\sqrt{\frac{b}{2\pi}}\frac{M!\left(\frac{1}{\gamma_{ps}}\right)e^{\frac{1}{\gamma_{ps}}}}{\Gamma(M+1)}\sum_{k=0}^{M}\frac{\left(\frac{1}{\gamma_{ss}}\right)^{k}}{k!}\int_{0}^{\infty}e^{-\frac{b}{2}x}x^{k-\frac{1}{2}}\left(\frac{1}{\gamma_{ps}}+\frac{x}{\gamma_{ss}}\right)^{-k-1}\times \tag{A.35}$$
$$\Gamma\left(k+1,\left(\frac{1}{\gamma_{ps}}+\frac{x}{\gamma_{ss}}\right)\right)dx.$$

By defining $E = -\frac{a}{2}\sqrt{\frac{b}{2\pi}}\frac{M!}{\Gamma(M+1)}\left(\frac{1}{\gamma_{ps}}\right)e^{\frac{1}{\gamma_{ps}}}\sum_{k=0}^{M}\frac{\left(\frac{1}{\gamma_{ss}}\right)^{k}}{k!}$,

$$P_{4.2} = E\int_{0}^{\infty}e^{-\frac{b}{2}x}x^{k-\frac{1}{2}}\left(\frac{1}{\gamma_{ss}}\right)^{-k-1}\left(\frac{\gamma_{ss}}{\gamma_{ps}}+x\right)^{-k-1}\Gamma\left(k+1,\frac{1}{\gamma_{ss}}\left(\frac{\gamma_{ss}}{\gamma_{ps}}+x\right)\right)dx. \tag{A.36}$$

When defining $u = \frac{\gamma_{ss}}{\gamma_{ps}}$, and $z = u + x$, (A. Jeffrey and D. Zwillinger, 2007, Eq. 8.352.2) is employed to obtain

$$P_{4.2} = Ee^{\frac{b}{2}u}k!\sum_{m=0}^{k}\frac{\gamma_{ss}^{\,k-m+1}}{m!}\int_{u=\frac{\gamma_{ss}}{\gamma_{ps}}}^{\infty}z^{m-k-1}(z-u)^{k-\frac{1}{2}}e^{-\left(\frac{b}{2}+\frac{1}{\gamma_{ss}}\right)z}dz. \tag{A.37}$$

Finally, (A. Jeffrey and D. Zwillinger, 2007, Eq. 3.383.4) is employed to obtain

$$P_{4.2} = -\frac{a}{2}\sqrt{\frac{b}{2\pi}}\frac{M!}{\Gamma(M+1)}\left(\frac{1}{\gamma_{ps}}\right)e^{\frac{b\gamma_{ss}+2}{4\gamma_{ps}}}\sum_{k=0}^{M}\Gamma\left(k+\frac{1}{2}\right)\sum_{m=0}^{k}\frac{\gamma_{ss}^{\,-m+1}}{m!}\times \tag{A.38}$$
$$\left(\frac{b}{2}+\frac{1}{\gamma_{ss}}\right)^{-\frac{1}{2}\left(m+\frac{1}{2}\right)}\left(\frac{\gamma_{ps}}{\gamma_{ss}}\right)^{\frac{1}{2}\left(m-\frac{3}{2}\right)}W_{\frac{1}{2}\left(m-2k-\frac{1}{2}\right),\frac{1}{2}\left(-m+\frac{1}{2}\right)}\left(\frac{b\gamma_{ss}+2}{2\gamma_{ps}}\right).$$

Then, (A.25), (A.28), (A.30), (A.34) and (A.38) are combined and the combining result is rearranged employing the redundancy law to obtain (4.36).

APPENDIX B

PUBLICATIONS

List of Publications

International Journal Paper

Rattasat Laikanok, Peerapong Uthansakul, and Damar Widjaja (2018). **Position-Based Spectrum Sharing Analysis in Multi-User MIMO Cognitive Radio Systems.** Suranaree Journal of Science & Technology (SJST).

Rattasat Laikanok, Peerapong Uthansakul, and Monthippa Uthansakul (2018). **Self-Evaluation Guideline of Overlapping Spectrum Sharing for Multi-User MIMO Cognitive Radio Systems.** Engineering and Applied Science Research (EASR).

International Conference Paper

Rattasat Laikanok, Peerapong Uthansakul, and Monthippa Uthansakul (2014). **Spectrum Sensing with Integration of Energy Detector and Diversity Techniques for MIMO Systems.** International Conference on Electrical Engineering/Electronics, Computer, Telecommunications and Information Technology (ECTI).

Rattasat Laikanok, Peerapong Uthansakul, and Monthippa Uthansakul (2015). **Integration of Equal Gain Combining and MAJORITY Rule for MIMO Cognitive Radio Systems.** South East Asian Technical University Consortium Symposium (SEATUC).

Rattasat Laikanok, Peerapong Uthansakul, and Monthippa Uthansakul (2016). **Investigation on the Effect of User Position in MIMO Cognitive Radio Systems with Overlapping Spectrum Sharing.** South East Asian Technical University Consortium Symposium (SEATUC).

Position-Based Spectrum Sharing Analysis in Multi-User MIMO Cognitive Radio Systems

Running head : Spectrum Sharing Analysis in Multi-User MIMO CR Systems

Rattasat Laikanok[1], Peerapong Uthansakul[2] and Damar Widjaja[3]

[1,2]School of Telecommunication Engineering, Institute of Engineering, Suranaree University of Technology, Nakhon Ratchasima, 30000, Thailand.

[3]Universitas Sanata Dharma, Yogyakarta, 55002, Indonesia.

[1]Email: pawinee.aum@gmail.com, [2]Email: uthansakul@sut.ac.th and [3]Email: damar@usd.ac.id

Abstract

This paper introduces the performance analysis of multi-user spectrum sharing based the effect of node positions in MIMO cognitive radio (CR) network. The objective is to make a CR technology become reliable and closer to the reality. The authors have developed the performance analysis that supports both of non-overlapping and overlapping spectrum sharing, and also evaluated data in term of node positions inside the coverage area. Which the advantages that enhance the existing works are 1) this paper develops the performance analysis to support multi-user CR systems, 2) it describes the significant effect of each node position and the distance between them, and 3) it combines the decision results on both downlink and uplink operations. The simulation results show the performance of secondary users in terms of the bit error rate inside the coverage area and the comparison result between the non-overlapping and overlapping cases. The outcome of this paper is very useful to enhance CR system. Also, it can be easily implemented in practice at the state

of spectrum sharing. The users can be realized by themselves whether their positions are in the available area or not.

Keywords: Cognitive radio, MIMO, spectrum sharing, multi-user communication, bit error rate

Introduction

After the spectrum sensing process, the CR system can identify whether the considered channel is available or occupied by the primary user (PU). If the channel is available, secondary user (SU) will operate the non-overlapping spectrum sharing, hence the interferences will only appear within the SUs due to themselves. On the other hand, if the channel is occupied, it will operate the overlapping spectrum sharing, which the interference from each SU will affect PU and each SU will cause interference to PU as well. Hence, there are many works in literature to propose the interference reduction methods (Puranachaikeeree S., 2010; Zhang R., et al., 2009). The authors in (Khan F. A., et al., 2014; Tourki K., et al. 2014) have introduced the performance analysis of the transmitting power constraint in spectrum sharing with a transmitting antenna selection technique at the secondary transmitter (ST) and the maximum ratio combining technique at secondary receiver (SR). It can be seen that the interference level is up to the transmitting power of each user in the system, many works have focused on the power control of SU. In (Yang G., et al., 2015; Kim T. K., et al., 2015; Vassaki S., et al., 2016; Khalfi B., et al., 2015), the works have developed power allocation schemes to support multi-user CR systems. However, the existing works have just discussed in the terms of defined power that is not increased or decreased by distances or positions, especially in (Khan F. A., et al., 2014; Tourki K., et al. 2014). They assume the powers of both interferences and users to be constant throughout their equations and experiments. This may be a big problem in practice because only a few limited areas will have such a nature. In fact, PU and SU are roaming in any areas around the base station (BS) and fusion center (FC). So, most of the areas are outage based on the specific conditions of assumed powers. This has happened even the adaptive power allocation can be efficiently employed. However, there are some positions that are not outage for SUs. If SUs can realize the available area to operate the spectrum sharing, it will cause many benefits to the system. So far, there have not been any works to present the performance analysis in multi-user CR systems based on positions.

In this paper, the authors have taken the effect of positions of BS, PU, FC, and SUs into the performance analysis of spectrum sharing for multi-user MIMO CR systems. The simulation results show the signal quality in terms of bit error rate (BER) which can get along with the position information on both downlink and uplink operations. Then, the intersection result from the performance analysis on downlink and uplink can be the good guideline to avoid the terrible damage in multi-user communication.

Materials and Methods

A. System model

The primary link is composed of only one antenna for both primary transmitter (PT) and primary receiver (PR). Whereas, each secondary link is composed of ST and SR, which is equipped with N_u and M_u antennas, respectively, that belong to each SU from overall U number of SUs in a coverage area of FC, when u =1,2,…, U, as seen in Figure 1. It can be seen that the number of antennas of each SU is not necessary to be the same as each other, but it not less than 2 antennas to support the MIMO systems.

For the downlink, BS is defined as PT, FC is defined as ST, PU is defined as PR, and SUs are defined as SRs. The channel between the antennas of FC and the antennas of u^{th} SU has a variance σ_s^2. The channel between the antennas of FC and the antenna of PU has a variance σ_{sp}^2. The channel between an antenna of BS and the antennas of u^{th} SU has a variance σ_{ps}^2.

For the uplink, BS is defined as PR, FC is defined as SR, PU is defined as PT, and SUs are defined as STs. The channel between the antennas of u^{th} SU and the antennas of FC has a variance σ_s^2. The channel between the antennas of u^{th} SU and an antenna of BS has a variance σ_{sp}^2. The channel between an antenna of PU and the antennas of FC has a variance σ_{ps}^2. The channel between the antennas of other SUs in the same coverage area and the antennas of FC has a variance σ_{is}^2.

For more clarity as shown in Figure 2, the received power of primary link for both downlink and uplink, which use the free-space propagation model, are given as

$$P_p = P_{max}\left(\frac{\lambda}{4\pi R_p}\right)^2 G_t G_r, \tag{1}$$

where P_{max} is a maximum primary output power, λ is wavelength, R_p is the distance between PT to PR, G_t and G_r are transmitter gain and receiver gain, respectively.

For both downlink and uplink, the distance from PT to SR is $D_{ps,u}$, and the distance from ST to SR is $D_{ss,u}$. Hence, their received powers from both distances are given as

$$P_{ps,u} = P_{max}\left(\frac{\lambda}{4\pi D_{ps,u}}\right)^2 G_t G_r, \tag{2}$$

$$P_{ss,u} = P_{smax}\left(\frac{\lambda}{4\pi D_{ss,u}}\right)^2 G_t G_r, \tag{3}$$

which P_{smax} is a maximum secondary output power. But only for uplink, it has the interference power vector due to other SUs in the same coverage area, which can be defined as

$$\mathbf{P}'_{ssI\_u} = \mathbf{P}'_{ss\_u} - \begin{bmatrix} 0 & \cdots & P_{ss,u\_u} & 0 & \cdots & 0 \end{bmatrix}, \tag{4}$$

where $P_{ss,u\_u} \in \mathbf{P}_{ss\_u}$. In order to avoid any confusion, we have added subscript $\_u$ into the power variables and power matrices representing for the uplink.

B. Performance analysis

To evaluate BER, the $m-$ QAM modulation is employed, where m is constellation size. Then the received power from ST to PR is given by

$$P_{sp} = \left(\frac{-1.5 P_p G_c}{(m-1)\ln\left(5BER_p\right)} - N_o\right)\frac{1}{\sigma_{sp}^2}, \tag{5}$$

where G_c is the coding gain (Goldsmith A., 2005, Eq. 9.38), and N_o is the power spectral density of the noise assumed to be constant and the same for all states. After that, considering the power from (5), we can find the BER region of primary network due to interference from ST in the same location by using

$$D_{sp} = \frac{\lambda}{4\pi}\left(\frac{P_{smax} G_t G_r}{P_{sp}}\right)^{\frac{1}{2}}. \tag{6}$$

By using PR as a reference point, the distance from ST to PR D_{sp} from (6) will show the possible position of ST that can be available to communicate with FC around PR. Hence, we can predict the positions of ST that affect to PR satisfaction.

The Cumulative Distributed Function (CDF) of σ_s^2 (Tourki K., et al. 2014, Eq. 5) is given by

$$F_{\sigma_s^2}(x)=\frac{1}{\Gamma(M_u+1)}\left[\left(\frac{x}{\sigma_s^2}\right)^{M_uN_u}\Gamma\left(1-M_u(N_u-1),\frac{x}{\sigma_s^2}\right)+\gamma\left(M_u+1,\frac{x}{\sigma_s^2}\right)\right]. \quad (7)$$

where $\Gamma(.)$ is the gamma function, $\Gamma(.\,,.)$ and $\gamma(.\,,.)$ are the upper incomplete gamma function and the lower incomplete gamma function, respectively.

Only in the non-overlapping spectrum sharing case, when interference from PT-SR is ignored ($P_{ps,u}=0$), BER of this case on downlink can be expressed as

$$BER_{s,u}(a,b)=\frac{a}{2}\sqrt{\frac{b}{2\pi}}\int_0^\infty\frac{e^{-\frac{b}{2}x}}{\sqrt{x}}F_{\sigma_s^2}\left(\frac{x}{\frac{P_{ss,u}}{N_0}}\right)dx. \quad (8)$$

where a and b are the modulation-specific constants, such as $(a,b)=(1,2)$ for BPSK, $(a,b)=(1,1)$ for BFSK, and $(a,b)=\left(2(m-1)/m,\ 6\log_2(m)/\left(m^2-1\right)\right)$ for $m-$PAM. Using (Gradshteyn I. S., 2007, Eq. 6.455.1 and Eq. 6.455.2), so the BER in (8) will be the closed form as

$$\begin{aligned}BER_{s,u}(a,b)=&\frac{\Gamma\left(M_u+\frac{3}{2}\right)\frac{a}{2}\sqrt{\frac{b}{2\pi}}\left(\frac{1}{\gamma_{ss,u}}\right)^{1+M_u}}{\Gamma(M_u+1)\left(\frac{1}{\gamma_{ss,u}}+\frac{b}{2}\right)^{M_u+\frac{3}{2}}}\left[\left(\frac{1}{M_uN_u+\frac{1}{2}}\right)\right.\\&\times{}_2F_1\left(1,M_u+\frac{3}{2};M_uN_u+\frac{3}{2};\frac{b\gamma_{ss,u}}{2+b\gamma_{ss,u}}\right)\\&\left.+\left(\frac{1}{1+M_u}\right){}_2F_1\left(1,M_u+\frac{3}{2};M_u+2;\frac{2}{2+b\gamma_{ss,u}}\right)\right],\end{aligned} \quad (9)$$

where ${}_2F_1(.,.;.;.)$ is the hypergeometric function. Then, SNR from ST-SR link for both downlink and uplink are defined as

$$\gamma_{ss,u}=\sigma_s^2\frac{P_{ss,u}}{N_0}. \quad (10)$$

For overlapping spectrum sharing case, when interference from PT- SR is considered ($P_{ps,u} \neq 0$), SNR from PT-SR on downlink is expressed by

$$\gamma_{is,u\_d} = \sigma_{ps}^2 \frac{P_{ps,u\_d}}{N_0}, \tag{11}$$

which the subscription $\_d$ represents the downlink. For the uplink of both spectrum sharing cases, SNR is defined as

$$\gamma_{is,u\_u} = \sigma_{ps}^2 \frac{P_{ps,u\_u}}{N_0} + \sigma_{is}^2 \sum_{u=1}^{U} \frac{P_{ssI,u\_u}}{N_0}. \tag{12}$$

Note that $P_{ps,u} = 0$ in (12) only for uplink of non-overlapping case.

The BER of overlapping cases for downlink and uplink can be expressed in

$$BER_{Int,u}(a,b) = \frac{a}{2}\sqrt{\frac{b}{2\pi}} \int_0^\infty \frac{e^{-\frac{b}{2}x}}{\sqrt{x}} \int_0^\infty \frac{e^{-\frac{y}{\gamma_{is,u}}}}{\gamma_{is,u}} F_{\sigma_s^2}\left(\frac{x(y+1)}{\frac{P_{ss,u}}{N_0}}\right) dy dx. \tag{13}$$

By using (Gradshteyn I. S., 2007, Eq. 8.352.5, Eq. 8.352.4, Eq. 3.352.1, Eq. 6.228.2, Eq. 3.383.5, and Eq. 3.352.2) to get

$$BER_{Int,u}(a,b) = \frac{a}{2}\sqrt{\frac{b}{2\pi}} \frac{1}{\Gamma(M_u+1)} \left[I_{1,u} + I_{2,u} + I_{3,u} + I_{4,u}\right], \tag{14}$$

which is the same as non-overlapping case for uplink, where

$$\begin{aligned} I_{1,u} &= \frac{(-1)^{M_u(N_u-1)+1}}{(M_u(N_u-1)-1)!} e^{\frac{1}{\gamma_{is,u}}} \left(\frac{\gamma_{is,u}}{\gamma_{ss,u}}\right)^{M_u N_u} \frac{\Gamma\left(M_u N_u + 1, \frac{1}{\gamma_{is,u}}\right)}{\left(M_u N_u + \frac{1}{2}\right)} \\ &\times \frac{\Gamma\left(M_u N_u + \frac{1}{2}\right)}{\left(\frac{1}{\gamma_{ss,u}} + \frac{b}{2}\right)^{M_u N_u + \frac{1}{2}}} {}_2F_1\left(1, M_u N_u + \frac{1}{2}; M_u N_u + \frac{3}{2}; \frac{b\gamma_{ss,u}}{2 + b\gamma_{ss,u}}\right), \end{aligned} \tag{15}$$

where ${}_2F_1(.,.;.;.)$ is the hypergeometric function. Next,

$$
\begin{aligned}
I_{2,u} = {} & (-1)^{M_u(N_u-1)}(M_uN_u)!\,\Gamma\left(M_uN_u+\frac{1}{2}\right)e^{\frac{b\gamma_{ss,u}+2}{4\gamma_{is,u}}}\sum_{k=1}^{M_uN_u}\frac{(k-1)!}{k!} \\
& \times\sum_{m=0}^{k-1}\frac{\left(\frac{1}{\gamma_{is,u}}\right)^m}{m!}\left(\frac{1}{\gamma_{ss,u}}+\frac{b}{2}\right)^{-\frac{1}{2}\left(M_uN_u+m-k+\frac{3}{2}\right)}\left(\frac{\gamma_{ss,u}}{\gamma_{is,u}}\right)^{\frac{1}{4}(2k+2m-2M_uN_u-1)} \\
& \times \mathrm{W}_{\frac{1}{2}\left(m-k-M_uN_u-\frac{1}{2}\right),-\frac{1}{2}\left(M_uN_u+m-k+\frac{1}{2}\right)}\left(\frac{b\gamma_{ss,u}+2}{2\gamma_{is,u}}\right),
\end{aligned}
\tag{16}
$$

$$
\begin{aligned}
I_{3,u} = {} & \left(\frac{1}{\gamma_{is,u}}\right)e^{\frac{b\gamma_{ss,u}+2}{4\gamma_{is,u}}}\sum_{k=0}^{M_u(N_u-1)-2}(-1)^{M_u(N_u-1)+k}k!(M_uN_u-k-1)! \\
& \times\Gamma\left(M_uN_u-k-\frac{1}{2}\right)\sum_{m=0}^{M_uN_u-k-1}\frac{\gamma_{ss,u}^{1-m}}{m!}\left(\frac{1}{\gamma_{ss,u}}+\frac{b}{2}\right)^{-\frac{1}{2}\left(m+\frac{1}{2}\right)} \\
& \times\left(\frac{\gamma_{ss,u}}{\gamma_{is,u}}\right)^{\frac{1}{2}\left(m-\frac{3}{2}\right)}\mathrm{W}_{\frac{1}{2}\left(2k-2M_uN_u+m+\frac{3}{2}\right),\frac{1}{2}\left(-m+\frac{1}{2}\right)}\left(\frac{b\gamma_{ss,u}+2}{2\gamma_{is,u}}\right),
\end{aligned}
\tag{17}
$$

and

$$
\begin{aligned}
I_{4,u} = M_u! & \left[\sqrt{\frac{2\pi}{b}}-\left(\frac{1}{\gamma_{is,u}}\right)e^{\frac{b\gamma_{ss,u}+2}{4\gamma_{is,u}}}\sum_{k=0}^{M_u}\Gamma\left(k+\frac{1}{2}\right)\sum_{m=0}^{k}\frac{\gamma_{ss,u}^{-m+1}}{m!}\right. \\
& \left.\times\left(\frac{1}{\gamma_{ss,u}}+\frac{b}{2}\right)^{-\frac{1}{2}\left(m+\frac{1}{2}\right)}\left(\frac{\gamma_{ss,u}}{\gamma_{is,u}}\right)^{\frac{1}{2}\left(m-\frac{3}{2}\right)}\mathrm{W}_{\frac{1}{2}\left(m-2k-\frac{1}{2}\right),\frac{1}{2}\left(-m+\frac{1}{2}\right)}\left(\frac{b\gamma_{ss,u}+2}{2\gamma_{is,u}}\right)\right],
\end{aligned}
\tag{18}
$$

where $W_{\varepsilon,\mu}(\cdot)$ is the Whittaker W-function.

However, there are some limitations that this work support only spectrum sharing for multi-user one-cell CR systems, but it does not support in multi-user multi-cell CR systems. And this work based on the assumption that the primary link is composed of only one antenna for both BS and PU.

Simulation Results and Discussion

The channel model in simulations is based on LTE standard (ETSI T., 2011), which defines the system parameters including: 1920 MHz - 1980 MHz for uplink operating band, 2110 MHz - 2170 MHz for downlink operating band, 23 dBm for maximum transmitted power, -103.535 dBm for minimum received power, the maximum number of MIMO element is 4×4 and the tolerated BER $= 2 \times 10^{-4}$.

In this work, the authors define FC is equipped with 4 antennas, $\sigma_s^2 = 1$ for the considered channels, $\sigma_{sp}^2 = \sigma_{ps}^2 = \sigma_{is}^2 = 0.01$ for the interference channels, $(a,b) = (1,2)$ that we assume only the secondary link communication uses BPSK modulation, $G_t = 0$ dB, $G_r = 6$ dB, and the GPS error around $0-3$ m referred to the current GPS device accuracies. By using MATLAB program for simulations.

The BER of SUs in case of non-overlapping spectrum sharing is presented in Figure 3(a) and Figure 3(b) for downlink and uplink, respectively. This non-overlapping case will be operated only when the system does not sense any power of PU in spectrum sensing process. Therefore, this case does not consider a primary link in calculation due to no any interference to SUs on the downlink.

In turn, each SU makes the interference to each other on uplink. This caused some SUs to have BER more than 2×10^{-4}. Then, the intersection result of available SUs between downlink in Figure 3(a) and uplink in Figure 3(b) is shown in Figure 3(c). It is obvious that only some SUs can be available to make a communication under the case of non-overlapping spectrum sharing.

Next, the case of overlapping spectrum sharing is investigated by assuming $m = 16$ for $m-$QAM modulation used by the primary link communication, $G_c = 6$ dB and 0 dBm for transmitted power of BS. Figure 3(d) and Figure 3(e) show the BER results of SUs for downlink and uplink, respectively. Unlike the previous case, there is PU active in the system then it influenced the secondary link, and the primary link will be taken the effect of secondary link too. For downlink in Figure 3(d), there are the circles around PU to indicate that $BER_p = 2 \times 10^{-4}$, 2×10^{-6}, and 2×10^{-8}. If PU walks into FC too closely, the FC has to access other frequency channels, non-overlapping mode, in order to avoid the undesirable interference to primary link. Also noticed in this figure, there are some SUs having BER more than 2×10^{-4} due to the interferences from BS which are not recommended to establish communication on this spectrum. Apart from these SUs, the others in different positions are available to operate MIMO CR communications. For uplink in Figure 3(e), if SU stays inside the circle that BER= 2×10^{-4}, these SUs cannot operate the spectrum sharing due to the harmful interference to PU. Finally, the intersection result of available SUs between Figure 3(d) and Figure 3(e) is shown in Figure 3(f). It is observed that some SUs can perform overlapping spectrum sharing under successful operation on both downlink and uplink. This is based on each SU position under the condition that BER of PU have to be less than 2×10^{-4}.

The results in Figure 3(c) and Figure 3(f) can reveal that some available SUs in the non-overlapping case will be not available in the overlapping case because of two main causes including the impact of interference from PT which makes the BER of secondary links more than 2×10^{-4} and the bad positions of those SUs which stay inside the prediction line of $BER_p = 2\times10^{-4}$. However, both figures have shown the good guideline for making a decision in multi-user communication.

Conclusions

The position-based performance analysis for both non-overlapping and overlapping spectrum sharing techniques is presented in this paper. The mathematical solution shows the relationship between BER and user positions. The simulation results can describe the interference impact of each user in CR systems related to a thorough performance analysis in terms of BER that supports both downlink and uplink operations. The results are very useful for multi-user MIMO CR implementation to make a decision whether its current position is suitable to establish a communication or not.

Acknowledgments

The authors acknowledge the School of Telecommunication Engineering, Suranaree University of Technology, Thailand, for their full support during the work.

References

Puranachaikeeree, S. (2010). Transmitting and Receiving Beamforming for Interference Cancellation in the Downlink of Cognitive Radio System, [MSc. thesis]. School of Electronics and Telecommunication Engineering, Institute of Engineering, King Mongkut's University of Technology Thonburi. Bangkok, Thailand, 102p.

Zhang, R. (2009). On peak versus average interference power constraints for protecting primary users in cognitive radio networks. IEEE Transactions on Wireless Communications., 8(4): 2112–2120.

Khan, F. A., Tourki, K., Alouini, M. S., and Qaraqe, K. A. (2014). Performance analysis of a power limited spectrum sharing system with TAS/MRC. IEEE Transactions on Signal Processing., 62(4): 954-967.

Tourki, K., Khan, F. A., Qaraqe, K. A., Yang, H. C., and Alouini, M. S. (2014). Exact performance analysis of MIMO cognitive radio systems using transmit antenna selection. IEEE Journal on Selected areas in communications., 32(3): 425-438.

Yang, G., Li, B., Tan, X., and Wang, X. (2015). Adaptive power control algorithm in cognitive radio based on game theory. IET Communications., 9(15): 1807-1811.

Kim, T. K., Kim, H. M., Song, M. G., and Im, G. H. (2015). Improved spectrum-sharing protocol for cognitive radio networks with multiuser cooperation. IEEE Transactions on Communications., 63(4): 1121-1135.

Vassaki, S., Poulakis, M. I., and Panagopoulos, A. D. (2016). State-based potential power allocation game in a cooperative multiuser network. IET Communications., 10(11): 1320-1328.

Khalfi, B., Ghorbel, M. B., Hamdaoui, B., and Guizani, M. (2015). Distributed fair spectrum assignment for large-scale wireless DSA networks. In International Conference on Cognitive Radio Oriented Wireless Networks; Springer, Cham, Chicago, U.S., p. 631-642.

Goldsmith, A. (2005). Wireless communications. Cambridge, Cambridge University Press, 605p.

ETSI T. 136 101 V10. 3.0 (2011-06) LTE. Evolved universal terresterial radio access (E-UTRA).

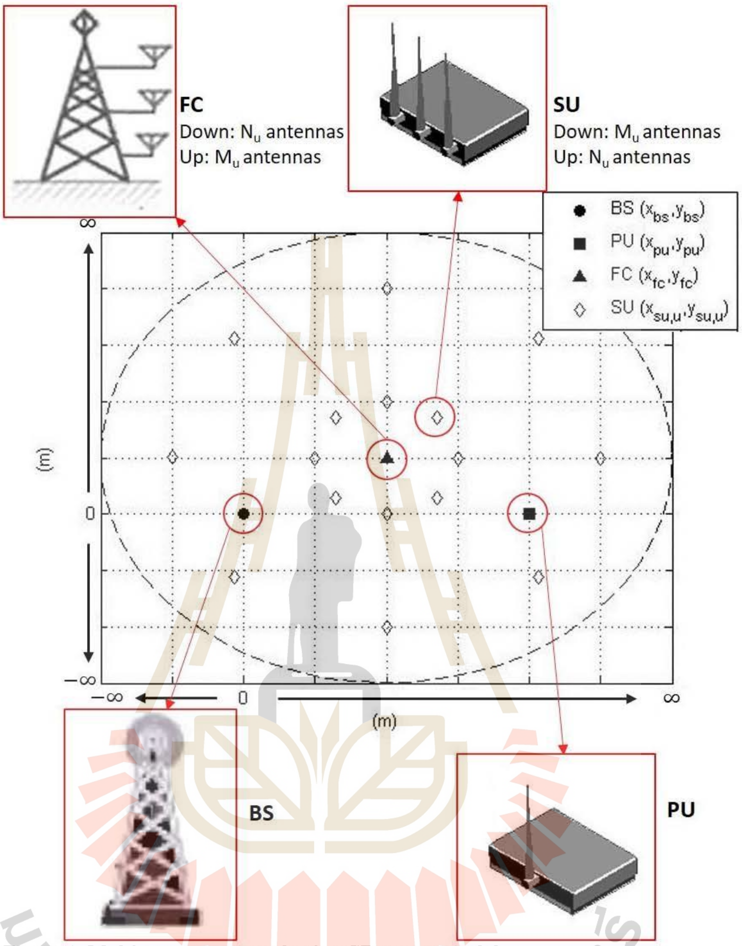

Figure 1. Multi-user spectrum sharing CR system model.

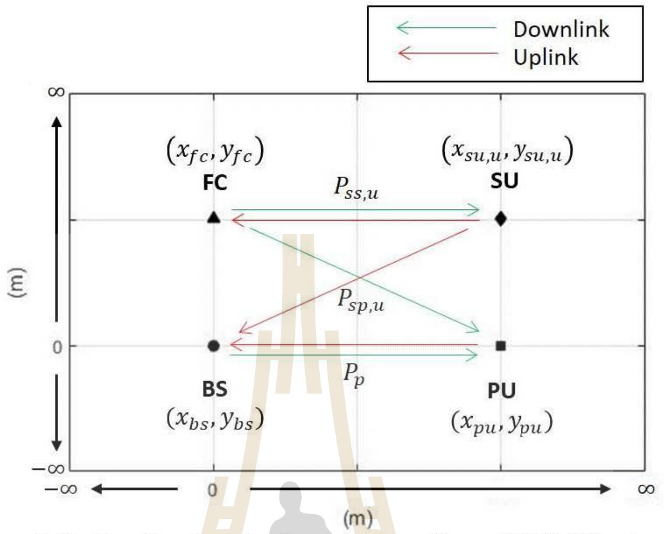

Figure 2. Position allocations of each member in multi-user MIMO CR systems.

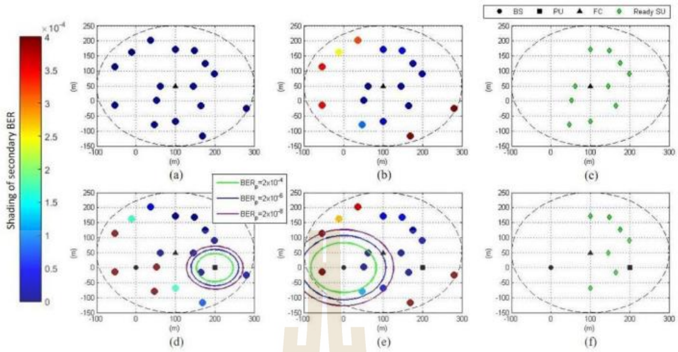

Figure 3. Spectrum sharing for multi-user CR systems for non-overlapping operation, (a) downlink, (b) uplink, and (c) their intersection and for overlapping operation, (d) downlink, (e) uplink, and (f) their intersection.

Research Article

Self-evaluation guideline of overlapping spectrum sharing for multi-user MIMO cognitive radio systems

Rattasat Laikanok*, Peerapong Uthansakul and Monthippa Uthansakul
School of Telecommunication Engineering, Suranaree University of Technology, Nakhon Ratchasima, 30000, Thailand.
*Corresponding author. Tel.: +66-842457259; Email address: D5640034@g.sut.ac.th

---

Abstract

This paper introduces the performance analysis of multi-user spectrum sharing based the effect of node positions in MIMO cognitive radio (CR) network. The objective is to enable the CR technology to be reliable and closer to reality. Hence, The advantages that enhance the existing works are 1) this paper develops the performance analysis to support multi-user CR systems, 2) it describes the significant effect of each node position and the distance between them, 3) it combines the decision results on both downlink and uplink operations, and 4) it presents the spectrum allocation method for all users in CR systems. The simulation results show the performance of secondary users in term of the bit error rate inside their coverage areas together with the effect of GPS error, and finally, the complete self-evaluation guideline of the overlapping spectrum sharing for multi-user CR systems have been presented. The outcome of this paper is very useful to enhance CR system. Also, it can be easily implemented in practice at the state of spectrum sharing. The users can realize by themselves whether their positions are in the available area or not.

Keywords: Cognitive radio, MIMO, Spectrum sharing, Multi-user communication

1. Introduction

After the spectrum sensing process, the CR system can identify whether the considered channel is available or occupied by the primary user (PU). If a channel is available, secondary user (SU) will operate the non-overlapping spectrum sharing, hence the interferences will only appear within the SUs due to themselves. On the other hand, if a channel is occupied, SU will operate the overlapping spectrum sharing, in which the interference from each SU will affect PU and each SU will cause interference to PU as well. Hence, there have been many works of literature that proposes the interference reduction methods [1]-[2]. The works in [3]-[4] have introduced the performance analysis of the transmitted power constraint in spectrum sharing with a transmit antenna selection technique at the secondary transmitter (ST) and the maximum ratio combining technique at the secondary receiver (SR). It shows that the interference level is up to the transmitted power of each user in the system. Many works have focused on the power control of SU. In [5]-[8], the works have developed power allocation schemes to support multi-user CR systems. However, the existing works have only discussed in term of defined power which is not increased or decreased by distances or positions. Especially in [3], [4], the works have assumed the powers of both interferences and users to be constant throughout their equations and experiments. This may be a big problem in practice because only a few limited areas have such nature. In fact, PU and SU operate the roaming in any areas around the base station (BS) and fusion center (FC). So, most areas are outage due to the specific conditions of assumed powers. This can occur even though the effectively adaptive power allocation is employed. However, there are some positions that are not outage for SUs. If SUs can realize the available area to operate the spectrum sharing, it will cause many benefits to the system. So far, there has not been any work that presents the performance analysis in multi-user CR systems based on the position information.

In this paper, the authors have taken the effect of positions of BS, PU, FCs, and SUs into the performance analysis for spectrum sharing and proposed the spectrum allocation scheme for multi-user MIMO CR systems. The simulation results show the signal quality in term of bit error rate (BER) which can get along with the position information on both downlink and uplink operations. Then, the intersection result from the performance analysis on downlink and uplink can avoid the terrible damage in multi-user communication. Finally, the result of spectrum allocation scheme can allocate the proper frequency for each SU in an entire system in order to be the good self-evaluation guideline for the overlapping spectrum sharing in multi-user CR systems.

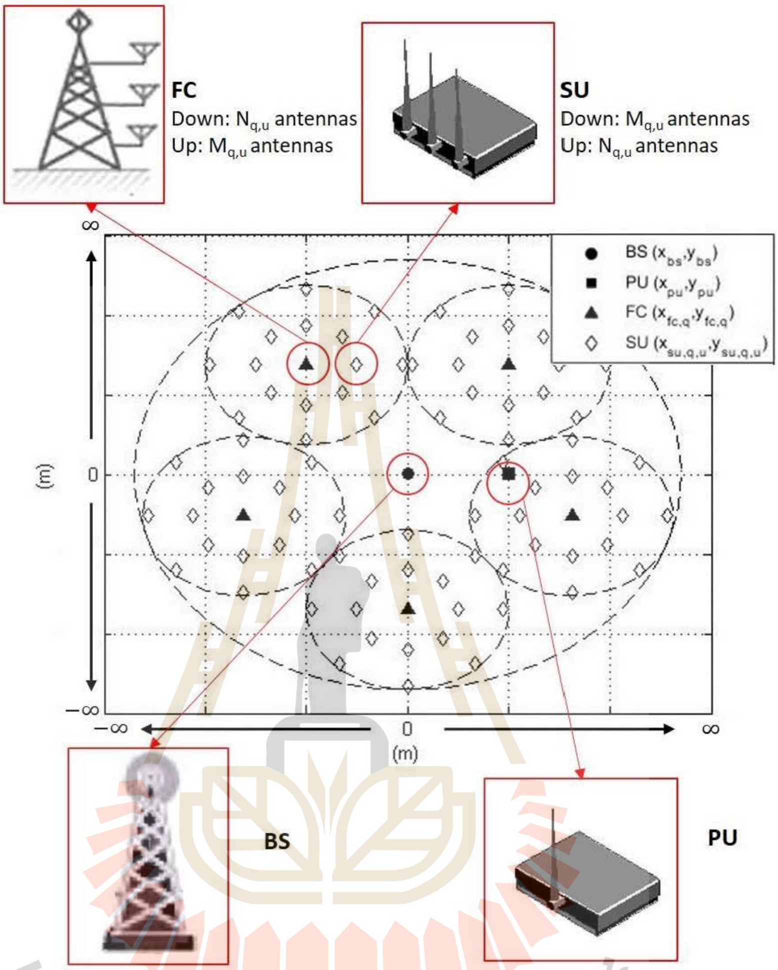

Figure 1 Multi-user spectrum sharing CR system model

2. Materials and methods

2.1 System model

The primary link composes of only one antenna for both primary transmitter (PT) and primary receiver (PR). Whereas, each secondary link composes of ST and SR, which is equipped with $N_{q,u}$ and $M_{q,u}$ antennas, respectively. The number of transmit and receive antennas are according to each SU from the overall U_q number of SUs in each coverage area of q^{th} FC, as seen in Figure 1, in which the channel is modeled as flat fading and Rayleigh distributed. It can be seen that the number of antennas of each SU is not necessary to be the same as each other, but it not less than 2 antennas to support the MIMO systems.

For the downlink, BS is defined as PT, FC is defined as ST, PU is defined as PR, and SUs are defined as SRs. The channel between the antennas of q^{th} FC and the antennas of u^{th} SU in its coverage area has a channel coefficient $h_{ss,q,u}$. The channel between the antennas of q^{th} FC and an antenna of PU has a channel coefficient $h_{sp,q}$. The channel between an antenna of BS and the antennas of u^{th} SU in the coverage area of q^{th} FC has a channel coefficient $h_{ps,q,u}$. And the channel between the antennas of FC in other coverage area and the antennas of u^{th} SU in the coverage area of q^{th} FC has an average channel coefficient $\overline{h}_{is,q,u}$, which is the channel between the interference FC and the considered SU.

For the uplink, BS is defined as PR, FC is defined as SR, PU is defined as PT, and SUs are defined as STs. The channel between the antennas of u^{th} SU and the antennas of its q^{th} FC has a channel coefficient $h_{ss,q,u}$. The channel between the antennas of u^{th} SU in the coverage area of q^{th} FC and an antenna of BS has a channel coefficient $h_{sp,q,u}$. The channel between an antenna of PU and the antennas of q^{th} FC has a channel coefficient $h_{ps,q}$. And the channel between the antennas of other SUs in the system and the antennas of q^{th} FC has an average channel coefficient $\overline{h}_{is,q,u}$.

Focusing on the considered node positions, the distance equations and power equations are created as follows.

The distance between PT to PR is written as

$$R_p = \left(\left(y_{pu} - y_{bs} \right)^2 + \left(x_{pu} - x_{bs} \right)^2 \right)^{\frac{1}{2}}. \quad (1)$$

Hence, the received power of primary link for both downlink and uplink are given by

$$P_p = P_{max}\left(\frac{\lambda}{4\pi R_p}\right)^2 G_t G_r, \tag{2}$$

where P_{max} is maximum primary output power, λ is wavelength, G_t and G_r are transmitter gain and receiver gain, respectively.

For the downlink, the distances from PT to SR and from ST to SR, respectively, are given by

$$D_{ps,q,u\_d} = \left(\left(y_{su,q,u} - y_{bs}\right)^2 + \left(x_{su,q,u} - x_{bs}\right)^2\right)^{\frac{1}{2}}, \tag{3}$$

$$D_{ss,q,u\_d} = \left(\left(y_{su,q,u} - y_{fc,q}\right)^2 + \left(x_{su,q,u} - x_{fc,q}\right)^2\right)^{\frac{1}{2}}, \tag{4}$$

for $q = 1, 2, \cdots, Q$ and Q is the number of FCs. Then, the received power from PT to SR for downlink is expressed as

$$P_{ps,q,u\_d} = P_{max}\left(\frac{\lambda}{4\pi D_{ps,q,u\_d}}\right)^2 G_t G_r, \tag{5}$$

The received power from ST to SR for downlink is expressed as

$$P_{ss,q,u\_d} = P_{smax}\left(\frac{\lambda}{4\pi D_{ss,q,u\_d}}\right)^2 G_t G_r, \tag{6}$$

where P_{smax} is maximum secondary output power. For the downlink, all FCs are the transmitters then they interfere with each other. When we are considering one of them, the interference power matrix due to the nearby FCs can be found from

$$D_{ssI,q,v,u\_d} = \left(\left(y_{su,q,u} - y_{fc,v} \right)^2 + \left(x_{su,q,u} - x_{fc,v} \right)^2 \right)^{\frac{1}{2}}, \tag{7}$$

for $v = 1, 2, \cdots, V$, and $V = Q$ which is defined to be the index for finding the interference power from all FC-SU links. Then we get the downlink interference distance matrix as

$$\mathbf{D}_{ssI,q\_d} = \begin{bmatrix} \left[\mathbf{D}_{ssI,q,1\_d} \right]_{1 \times U_q} \\ \left[\mathbf{D}_{ssI,q,2\_d} \right]_{1 \times U_q} \\ \vdots \\ \left[\mathbf{D}_{ssI,q,q\_d} \right]_{1 \times U_q} = \left[\infty \right]_{1 \times U_q} ;\ \text{at } v = q \\ \vdots \\ \left[\mathbf{D}_{ssI,q,V\_d} \right]_{1 \times U_q} \end{bmatrix}, \tag{8}$$

where $D_{ssI,q,v,u\_d} \in \mathbf{D}_{ssI,q,v\_d}$. When $v = q$ that means we are considering the links between a considered FC and all SUs in its coverage area. At this point, the interference distances can be assumed as too far until almost no any interference power. Hence, the interference power matrix is

$$\mathbf{P}_{ssI,q\_d} = P_{smax} \left(\frac{\lambda}{4\pi \mathbf{D}_{ssI,q\_d}} \right)^2 G_t G_r = \begin{bmatrix} \mathbf{P}_{ssI,q,1\_d} \\ \mathbf{P}_{ssI,q,2\_d} \\ \vdots \\ \left[0 \right]_{1 \times U_q} ;\ \text{at } v = q \\ \vdots \\ \mathbf{P}_{ssI,q,V\_d} \end{bmatrix}, \tag{9}$$

where $P_{ssI,q,v,u\_d} \in \mathbf{P}_{ssI,q,v\_d}$.

For uplink, the distances from PT to SR and from ST to SR, respectively, are given by

$$D_{ps,q\_u} = \left(\left(y_{fc,q} - y_{pu} \right)^2 + \left(x_{fc,q} - x_{pu} \right)^2 \right)^{\frac{1}{2}}, \tag{10}$$

$$D_{ss,q,u\_u} = \left(\left(y_{fc,q} - y_{su,q,u} \right)^2 + \left(x_{fc,q} - x_{su,q,u} \right)^2 \right)^{\frac{1}{2}}. \tag{11}$$

The received power from PT to SR for uplink is expressed as

$$P_{ps,q\_u} = P_{max} \left(\frac{\lambda}{4\pi D_{ps,q\_u}} \right)^2 G_t G_r. \tag{12}$$

And the received power from ST to SR for uplink is expressed as

$$P_{ss,q,u\_u} = P_{smax} \left(\frac{\lambda}{4\pi D_{ss,q,u\_u}} \right)^2 G_t G_r. \tag{13}$$

For the uplink, all SUs are the transmitters then they interfere with each other in both the difference and same coverage areas of picocells. When we are considering one of them, the interference power matrix due to SUs in the coverage area of the other nearby FCs can be found from

$$D_{ssI,q,v,u\_u} = \left(\left(y_{fc,v} - y_{su,q,u} \right)^2 + \left(x_{fc,v} - x_{su,q,u} \right)^2 \right)^{\frac{1}{2}}. \tag{14}$$

So, we get the uplink interference distance matrix as

$$\mathbf{D}_{ssI,q\_u} = \begin{bmatrix} \left[\mathbf{D}_{ssI,q,1\_u} \right]_{1\times U_q} \\ \left[\mathbf{D}_{ssI,q,2\_u} \right]_{1\times U_q} \\ \vdots \\ \left[\mathbf{D}_{ssI,q,q\_u} \right]_{1\times U_q} = \left[\infty \right]_{1\times U_q};\ \text{at } v = q \\ \vdots \\ \left[\mathbf{D}_{ssI,q,V\_u} \right]_{1\times U_q} \end{bmatrix}. \tag{15}$$

When $v = q$, we define the interference distances as infinity to find the interference power only from the other SUs outside the considered coverage area. Hence, the interference power matrix is

$$\mathbf{P}_{ssI,q\_u} = P_{smax}\left(\frac{\lambda}{4\pi \mathbf{D}_{ssI,q\_u}}\right)^2 G_t G_r = \begin{bmatrix} \mathbf{P}_{ssI,q,1\_u} \\ \mathbf{P}_{ssI,q,2\_u} \\ \vdots \\ [0]_{1\times U_q}\text{; at } v = q \\ \vdots \\ \mathbf{P}_{ssI,q,V\_u} \end{bmatrix}, \tag{16}$$

where $P_{ssI,q,v,u\_u} \in \mathbf{P}_{ssI,q,v\_u}$. And the interference power matrix due to other SUs in the same coverage area can be defined as

$$\mathbf{P}'_{ssII,q\_u} = \mathbf{P}'_{ss,q\_u} - \begin{bmatrix} 0 & \cdots & P_{ss,q,u\_u} & 0 & \cdots & 0 \end{bmatrix}, \tag{17}$$

where $P_{ss,q,u\_u} \in \mathbf{P}_{ss,q\_u}$. In order to find the interference power, we have to remove the power value of the considered SU out from the normally received power matrix found from Equation (13). Hence, the rest values in the matrix are the interference due to each ST-SR link in the same coverage area with considered SU.

2.2 Performance analysis

To evaluate BER, the $m-$QAM modulation is employed, where m is constellation size. Then, the received power from ST to PR is given by

$$P_{sp} = \left(\frac{-1.5P_p G_c}{(m-1)\ln(5BER_p)} - N_o\right)\frac{1}{\overline{g}_{sp}}, \tag{18}$$

where G_c is the coding gain [9, Eq. 9.38], N_o is the power spectral density of the noise assumed to be constant and the same for all states, and $\overline{g}_{sp} = avg\left(\left|\mathbf{h}_{sp}\right|^2\right)$ is an average channel gain from ST-PR. After that, considering the power from Equation (18), we can find the BER region of primary network due to interference from ST in the same location by using

$$D_{sp} = \frac{\lambda}{4\pi}\left(\frac{P_{smax}G_t G_r}{P_{sp}}\right)^{\frac{1}{2}}. \tag{19}$$

By using PR as a reference point, the distance from ST to PR D_{sp} from Equation (19) shows the possible position of ST which can be available to communicate with FC around PR. Hence, we can predict the positions of ST that affect PR satisfaction.

Referring to the power equations in section II, the SNR from ST-SR for both downlink and uplink are defined as

$$\gamma_{ss,q,u} = g_{ss,q,u}\frac{P_{ss,q,u}}{N_0}, \tag{20}$$

where $g_{ss,q,u} = \left|h_{ss,q,u}\right|^2$ is the channel gain from ST-SR, in which $P_{ss,q,u}$ is also depend on whether it is downlink from Equation (6) or uplink from Equation (13). In addition, the SNR from whole interferences to the considered SR for the downlink is

$$\gamma_{is,q,u\_d} = g_{ps,q,u}\frac{P_{ps,q,u\_d}}{N_0} + \overline{g}_{is,q,u}\sum_{v=1}^{V}\frac{P_{ssI,q,v,u\_d}}{N_0}, \tag{21}$$

where $g_{ps,q,u} = \left|h_{ps,q,u}\right|^2$ is the channel gain from PT-SR on the downlink, and $\overline{g}_{is,q,u} = \left|\overline{h}_{is,q,u}\right|^2$ is an average channel gain from the interference FC to considered SU. For the uplink, yields

$$\gamma_{is,q,u\_u} = g_{ps,q}\frac{P_{ps,q\_u}}{N_0} + \overline{g}_{is,q,u}\left(\sum_{v=1}^{V}\sum_{u=1}^{U}\frac{P_{ssI,q,v,u\_u}}{N_0} + \sum_{u=1}^{U}\frac{P_{ssII,q,u\_u}}{N_0}\right), \tag{22}$$

where $g_{ps,q} = \left|h_{ps,q}\right|^2$ is the channel gain from PT-SR on the uplink, and $\overline{g}_{is,q,u} = \left|\overline{h}_{is,q,u}\right|^2$ is an average channel gain from other SUs in the system to the considered FC.

The Cumulative Distributed Function (CDF) of the channel gain g_{ss} [4, Eq. 5] is given by

$$F_{g_{ss},q,u}(x) = \frac{1}{\Gamma\left(M_{q,u}+1\right)}\left[\left(\frac{x}{g_{ss,q,u}}\right)^{M_{q,u}N_{q,u}}\Gamma\left(1-M_{q,u}\left(N_{q,u}-1\right),\frac{x}{g_{ss,q,u}}\right) + \gamma\left(M_{q,u}+1,\frac{x}{g_{ss,q,u}}\right)\right], \tag{23}$$

where $\Gamma(.)$ is the gamma function, $\Gamma(.,.)$ and $\gamma(.,.)$ are the upper incomplete gamma function and the lower incomplete gamma function, respectively.

Eventually, the BER of overlapping spectrum sharing for downlink and uplink can be expressed in

$$BER_{Int,q,u}(a,b) = \frac{a}{2}\sqrt{\frac{b}{2\pi}}\int_0^\infty \frac{e^{-\frac{b}{2}x}}{\sqrt{x}}\int_0^\infty \frac{e^{-\frac{y}{\gamma_{is,q,u}}}}{\gamma_{is,q,u}} F_{g_{ss},q,u}\left(\frac{x(y+1)}{\frac{P_{ss,q,u}}{N_0}}\right) dydx, \tag{24}$$

where a and b are the modulation-specific constants, such as $(a,b)=(1,2)$ for BPSK, $(a,b) =(1,1)$ for BFSK, and $(a,b)=\left(2(m-1)/m,\ 6\log_2(m)/\left(m^2-1\right)\right)$ for $m-$PAM. Equation (24) can be proved by starting with

$$F_{g_{ss},q,u}\left(\frac{x(y+1)}{\frac{P_{ss,q,u}}{N_0}}\right)=\frac{1}{\Gamma\left(M_{q,u}+1\right)}\left[\left(\frac{x}{\gamma_{ss,q,u}}\right)^{M_{q,u}N_{q,u}}\Gamma\left(1-M_{q,u}\left(N_{,u}-1\right),\frac{x(y+1)}{\gamma_{ss,q,u}}\right)\right.$$
$$\left.\times(y+1)^{M_{q,u}N_{q,u}}+\gamma\left(M_{q,u}+1,\frac{x(y+1)}{\gamma_{ss,q,u}}\right)\right]. \tag{25}$$

Then,

$$F_{\gamma_{int}}(x)=\int_0^\infty\frac{e^{-\frac{y}{\gamma_{is,q,u}}}}{\gamma_{is,q,u}}F_{g_{ss},q,u}\left(\frac{x(y+1)}{\frac{P_{ss,q,u}}{N_0}}\right)dy. \tag{26}$$

By using [9, Eq. 8.352.5], [9, Eq. 8.352.4], [9, Eq. 3.352.1], then we get

$$F_{\gamma_{int}}(x)=A\Gamma\left(M_{q,u}N_{q,u}+1,\frac{1}{\gamma_{is,q,u}}\right)x^{M_{q,u}N_{q,u}}\mathrm{Ei}\left(-\frac{x}{\gamma_{ss,q,u}}\right)+A\left(M_{q,u}N_{q,u}\right)!$$
$$\times\sum_{k=1}^{M_{q,u}N_{q,u}}\left(\frac{1}{\gamma_{is,q,u}}\right)^k\frac{1}{k!}x^{M_{q,u}N_{q,u}}\left(\frac{1}{\gamma_{is,q,u}}+\frac{x}{\gamma_{ss,q,u}}\right)^{-k}\Gamma\left(k,\left(\frac{1}{\gamma_{is,q,u}}+\frac{x}{\gamma_{ss,q,u}}\right)\right)$$
$$+B\left(\frac{x}{\gamma_{ss,q,u}}\right)^{M_{q,u}N_{q,u}-k-1}\left(\frac{1}{\gamma_{is,q,u}}+\frac{x}{\gamma_{ss,q,u}}\right)^{k-M_{q,u}N_{q,u}}$$
$$\times\Gamma\left(M_{q,u}N_{q,u}-k,\left(\frac{1}{\gamma_{is,q,u}}+\frac{x}{\gamma_{ss,q,u}}\right)\right)$$
$$+C\left[1-\left(\frac{1}{\gamma_{is,q,u}}\right)e^{\frac{1}{\gamma_{is,q,u}}}\sum_{k=0}^{M_{q,u}}\left(\frac{x}{\gamma_{ss,q,u}}\right)^k\left(\frac{1}{\gamma_{is,q,u}}+\frac{x}{\gamma_{ss,q,u}}\right)^{-k-1}\right.$$
$$\left.\times\frac{1}{k!}\Gamma\left(k+1,\left(\frac{1}{\gamma_{is,q,u}}+\frac{x}{\gamma_{ss,q,u}}\right)\right)\right]. \tag{27}$$

Define $A=\dfrac{(-1)^{M_{q,u}(N_{q,u}-1)}e^{\frac{1}{\gamma_{is,q,u}}}\left(\dfrac{\gamma_{is,q,u}}{\gamma_{ss,q,u}}\right)^{M_{q,u}N_{q,u}}}{\Gamma\left(M_{q,u}+1\right)\left(M_{q,u}\left(N_{q,u}-1\right)-1\right)!}$, $B=\dfrac{\left(\dfrac{1}{\gamma_{is,q,u}}\right)}{\Gamma\left(M_{q,u}+1\right)}\dfrac{e^{\frac{1}{\gamma_{is,q,u}}}}{\left(M_{q,u}\left(N_{q,u}-1\right)-1\right)!}$ $\sum_{k=0}^{M_{q,u}(N_{q,u}-1)-2}k!(-1)^{M_{q,u}(N_{,u}-1)+k}$, and $C=\dfrac{M_{q,u}!}{\Gamma\left(M_{q,u}+1\right)}$, then we take (27) into (24). And using [9, Eq. 6.228.2], [9, Eq. 3.383.4], [9, Eq. 3.383.5], and [9, Eq. 3.352.2] to get

$$BER_{Int,q,u}\left(a,b\right)=\frac{a}{2}\sqrt{\frac{b}{2\pi}}\frac{1}{\Gamma\left(M_{q,u}+1\right)}\left[\frac{(-1)^{M_{q,u}(N_{q,u}-1)+1}e^{\frac{1}{\gamma_{is,q,u}}}}{\left(M_{q,u}\left(N_{q,u}-1\right)-1\right)!}\left(\frac{\gamma_{is,q,u}}{\gamma_{ss,q,u}}\right)^{M_{q,u}N_{q,u}}\right.$$

$$\times\frac{\Gamma\left(M_{q,u}N_{q,u}+1,\dfrac{1}{\gamma_{is,q,u}}\right)}{\left(M_{q,u}N_{q,u}+\dfrac{1}{2}\right)}\frac{\Gamma\left(M_{q,u}N_{q,u}+\dfrac{1}{2}\right)}{\left(\dfrac{1}{\gamma_{ss,q,u}}+\dfrac{b}{2}\right)^{M_{q,u}N_{q,u}+\frac{1}{2}}}$$

$$\times{}_2F_1\left(1,M_{q,u}N_{q,u}+\frac{1}{2};M_{q,u}N_{q,u}+\frac{3}{2};\frac{b\gamma_{ss,q,u}}{2+b\gamma_{ss,q,u}}\right)+(-1)^{M_{q,u}(N_{q,u}-1)}$$

$$\times\left(M_{q,u}N_{q,u}\right)!\Gamma\left(M_{q,u}N_{q,u}+\frac{1}{2}\right)e^{\frac{b\gamma_{ss,q,u}+2}{4\gamma_{is,q,u}}}\sum_{k=1}^{M_{q,u}N_{q,u}}\frac{(k-1)!}{k!}\sum_{m=0}^{k-1}\frac{\left(\dfrac{1}{\gamma_{is,q,u}}\right)^{m}}{m!}$$

$$\times\left(\frac{1}{\gamma_{ss,q,u}}+\frac{b}{2}\right)^{-\frac{1}{2}\left(M_{q,u}N_{q,u}+m-k+\frac{3}{2}\right)}\left(\frac{\gamma_{ss,q,u}}{\gamma_{is,q,u}}\right)^{\frac{1}{4}\left(2k+2m-2M_{q,u}N_{q,u}-1\right)}$$

$$\times W_{\frac{1}{2}\left(m-k-M_{q,u}N_{q,u}-\frac{1}{2}\right),-\frac{1}{2}\left(M_{q,u}N_{q,u}+m-k+\frac{1}{2}\right)}\left(\frac{b\gamma_{ss,q,u}+2}{2\gamma_{is,q,u}}\right)+\left(\frac{1}{\gamma_{is,q,u}}\right)$$

$$\times e^{\frac{b\gamma_{ss,q,u}+2}{4\gamma_{is,q,u}}}\sum_{k=0}^{M_{q,u}(N_{q,u}-1)-2}(-1)^{M_{q,u}(N_{q,u}-1)+k}k!\left(M_{q,u}N_{q,u}-k-1\right)!$$

$$\times\Gamma\left(M_{q,u}N_{q,u}-k-\frac{1}{2}\right)\sum_{m=0}^{M_{q,u}N_{q,u}-k-1}\frac{\gamma_{ss,q,u}^{1-m}}{m!}\left(\frac{1}{\gamma_{ss,q,u}}+\frac{b}{2}\right)^{-\frac{1}{2}\left(m+\frac{1}{2}\right)}\left(\frac{\gamma_{ss,q,u}}{\gamma_{is,q,u}}\right)^{\frac{1}{2}\left(m-\frac{3}{2}\right)}$$

$$\times \mathrm{W}_{\frac{1}{2}\left(2k-2M_{q,u}N_{q,u}+m+\frac{3}{2}\right),\frac{1}{2}\left(-m+\frac{1}{2}\right)}\left(\frac{b\gamma_{ss,q,u}+2}{2\gamma_{is,q,u}}\right)+M_{q,u}!$$
$$\times\left[\sqrt{\frac{2\pi}{b}}-\left(\frac{1}{\gamma_{is,q,u}}\right)e^{\frac{b\gamma_{ss,q,u}+2}{4\gamma_{is,q,u}}}\sum_{k=0}^{M_{q,u}}\Gamma\left(k+\frac{1}{2}\right)\sum_{m=0}^{k}\frac{\gamma_{ss,q,u}}{m!}^{-m+1}\left(\frac{1}{\gamma_{ss,q,u}}+\frac{b}{2}\right)^{-\frac{1}{2}\left(m+\frac{1}{2}\right)}\right. \tag{28}$$
$$\left.\left.\times\left(\frac{\gamma_{ss,q,u}}{\gamma_{is,q,u}}\right)^{\frac{1}{2}\left(m-\frac{3}{2}\right)}\mathrm{W}_{\frac{1}{2}\left(m-2k-\frac{1}{2}\right),\frac{1}{2}\left(-m+\frac{1}{2}\right)}\left(\frac{b\gamma_{ss,q,u}+2}{2\gamma_{is,q,u}}\right)\right]\right],$$

where ${}_2F_1(.,.;.;.)$ is the hypergeometric function and $W_{\varepsilon,\mu}(.)$ is the Whittaker W-function.

2.3 GPS error

Although the GPS devices have been developed to make more accuracy in the present, there are still some errors that can't be ignored for the reality overlapping spectrum sharing process. All positions that are inaccurate plainly affecting the SUs' decision. So, we can add the GPS errors into the performance analysis by using Equation (29) and (30) to replace the distance equations of section 2.1.

$$\hat{\mathbf{x}}_{su}=\mathbf{x}_{su}\pm\mathbf{rand}\left[0,error_{GPS}\right]_{U\times Q}\cos\left(\tan^{-1}\left(\frac{\mathbf{y}_{su}}{\mathbf{x}_{su}}\right)\right), \tag{29}$$

$$\hat{\mathbf{y}}_{su}=\mathbf{y}_{su}\pm\mathbf{rand}\left[0,error_{GPS}\right]_{U\times Q}\sin\left(\tan^{-1}\left(\frac{\mathbf{y}_{su}}{\mathbf{x}_{su}}\right)\right), \tag{30}$$

where the GPS errors are random between 0 to $error_{GPS}$, in which $error_{GPS}$ value is up to the accuracy of each GPS device.

2.4 Spectrum allocation scheme

The final process of CR system is the spectrum decision that chooses the proper frequency channel for the need of users. This spectrum allocation scheme arranges the proper frequency for each SU in the entire system. Incidentally, a diagram of this concept is presented in Figure 2 by the following steps.

Step 1: After the spectrum sensing process, spectrum allocation process starts by analyzing the first channel, where the number of considered channels is equal to bandwidth value divided by sub-bandwidth value. Hence, the considered frequency channel $F_{sub} = 1, 2, \ldots, BW / BW_{sub}$, in which BW and BW_{sub} values are defined based on each communication standard, and F_{sub} can be called the sub-band number.

Step 2: The number of all SUs and each position of them are sent into the performance analysis process. The proper SU is SU that passes the BER condition on both downlink and uplink in the considered round. Hence, the result of this process is the number of SUs that are appropriate for communication.

Step 3: In order to know whether the spectrum allocation process has already finished or not, we have to find the rest number of SUs that have not passed yet. The rest number of SUs in the considered round can be calculated from

$$U_{rest} = U_{pre} - U_{pass}, \tag{31}$$

where U_{rest} is the rest number of SUs that do not pass in the round that is being considered, U_{pre} is the number of SUs in the round before the round that is being considered, and U_{pass} is the number of SUs that have already passed the BER condition in the round that is being considered. By the first round, U_{pre} is equal to a number of all SUs.

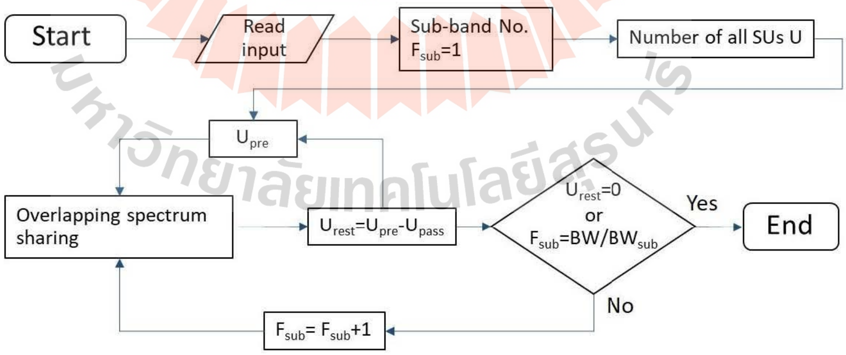

Figure 2 Full-system overlapping spectrum sharing flowchart

Then the step 2 and 3 will be redone until the overall SUs is ready for communication or the process comes to the last round that $F_{sub} = BW / BW_{sub}$. If the process comes to the last round but $U_{rest} \neq 0$, those rest SUs cannot operate at that time.

Step 4: The new term of spectrum sharing has to wait for the next observation time of spectrum sensing.

3. Simulation results and discussions

MATLAB program has been employed for simulations. The channel model in simulations is based on LTE standard [11], which defines the system parameters including 1920 MHz - 1980 MHz for uplink operating band, 2110 MHz - 2170 MHz for downlink operating band, 23 dBm for maximum transmitted power, - 103.535 dBm for minimum received power, and the tolerated $\mathrm{BER} = 2\times10^{-4}$. In this work, the authors have defined $(a,b) = (1,2)$, $G_t = 0$ dB, $G_r = 6$ dB, $G_c = 6$ dB, $m = 16$, 0 dBm for the transmitted power of BS, $N_{q,u}$ and $M_{q,u}$ are random from 2 up to 4 antennas. There is a PU per one frequency channel that randomly appears inside the macrocell. There are 5 FCs (5 picocells) and 16 SUs per one coverage area of FC in which SUs randomly stay inside.

Figure 3 is an ideal case that ignores the GPS error. Figure 3a and Figure 3b show the BER results of SUs for downlink and uplink, respectively. For downlink in Figure 3a, there is a circle around PU that is predicted by defining $BER_p = 2\times10^{-4}$, according to Equation (19). This prediction circle is existed to prevent the normal working of PU from FC that stays inside the circle. Because FCs cannot change the position, when PU appears too close to any FC, that FC has to access other frequency channels. It has to be the non-overlapping mode in order to avoid the undesirable interference to primary link. As noticed in this figure, there are some SUs having BER more than 2×10^{-4} due to the interferences from BS which are not appropriate to perform communication on this spectrum. Apart from these SUs, the others in different positions are available to operate MIMO CR communications. For uplink in Figure 3b, if SUs stay inside the circle that is predicted by defining $BER_p = 2\times10^{-4}$, these SUs cannot operate the spectrum sharing in order to protect the normal working of BS. And there are some SUs having BER more than 2×10^{-4} due to the interferences from PU and the other nearby SUs. Hence, those SUs cannot operate the spectrum sharing in this frequency channel. Finally, the intersection result of available SUs between Figure 3a and Figure 3b is shown in Figure 3c. It is observed that some SUs can perform overlapping spectrum sharing under successful operation on both downlink and uplink. This is based on each SU position under the condition that BER of PU and SU have to be less than 2×10^{-4}.

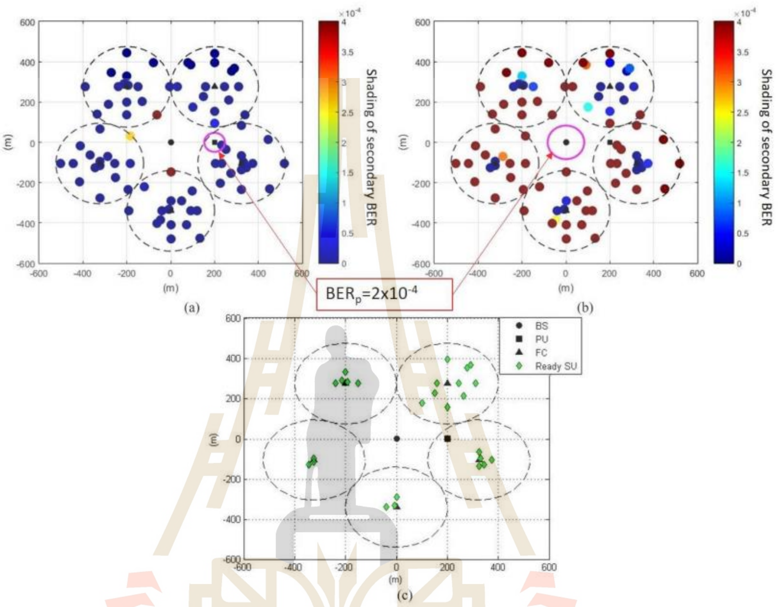

Figure 3 Overlapping spectrum sharing for multi-user multi-cell CR system by ignoring GPS error on (a) downlink and (b) uplink. And (c) the intersection result between downlink and uplink

With the same node positions and the same number of antenna elements of each node member as Figure 3, the authors have enhanced the GPS error around 0-10 m into Figure 4, [12]. Figure 4a and Figure 4b show the BER results of SUs for downlink and uplink respectively. If the GPS error for most of the node positions increases the distance between interference nodes and SR enough, the system may obtain the wrong result. BER of the considered SU has demonstrated that it passes the condition although it shouldn't pass because the calculated BER is less than it should be. It may cause a communication malfunction of other nodes in the system. On the other hand, if the GPS error for most of node positions decreases the distance between interference nodes and SR enough, it may cause the false alarm result because the calculated BER is more than it should be. It may cut the occasion of the considered SU that should pass. From the same operation as Figure 3, the intersection result of available SUs between Figure 4a and Figure 4b is shown in Figure 4c. When compared to Figure 3c, it clearly shows that some SUs that shouldn't pass in Figure 3c appear in this figure. The authors have defined them to be the wrong SUs shown as the red marks. Moreover, some SUs that should pass disappear.

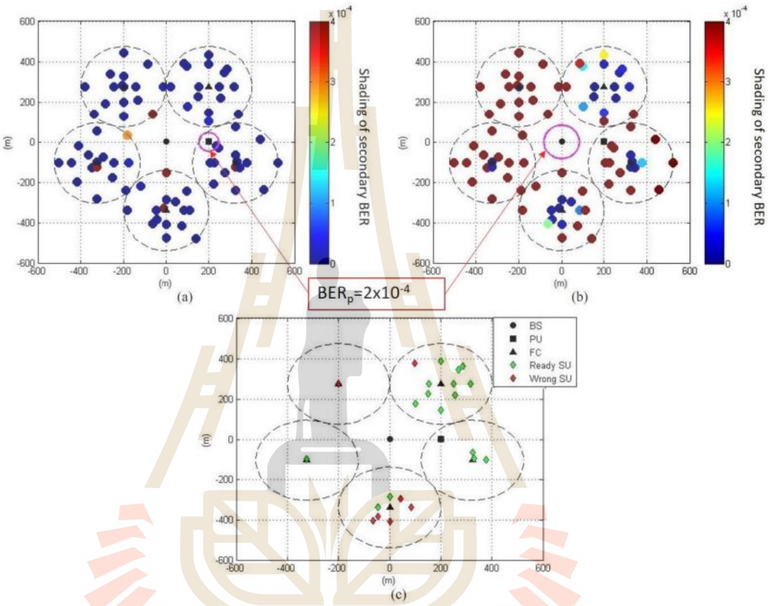

Figure 4 Overlapping spectrum sharing for multi-user multi-cell CR system by adding 10 m GPS error on (a) downlink and (b) uplink. And (c) the intersection result between downlink and uplink

In order to achieve the end of an operation, all of the processes in Figure 2 have to be operated, which the results are shown in Figure 5. The authors have defined each picocell has 16 SUs randomly stayed inside, PUs in all frequency channels have the random positions and $BW_{sub} = 5$ MHz. Hence, the number of sub-bandwidths is 12. Start with the top left figure, it shows the full map of CR system that represents all of node member positions except PU because PU at each frequency channel has a different position. Thus, PU appears in next figure. Like the Figure 4, after the performance analysis process of 1st sub-bandwidth has been performed, the result is shown in the top center figure. The proper SUs have achieved the permission first causing the interference factor is reduced at the next sub-bandwidth. As seen in the bottom center figure, it has only one SU passing the BER condition because it is an influential point affecting other SUs which causes them to do not pass. So, in the next sub-bandwidth many rest SUs achieve the goal. Normally, the operation has to be finished within 12 sub-bandwidths for LTE because $BW = 60$ MHz and $BW_{sub} = 5$ MHz. However this time, all SUs can achieve within 5 sub-bandwidths. Note that, the effect of GPS error of this result is existed but not shown and not focused due to the fact that the system does not know how much impact it has in the reality.

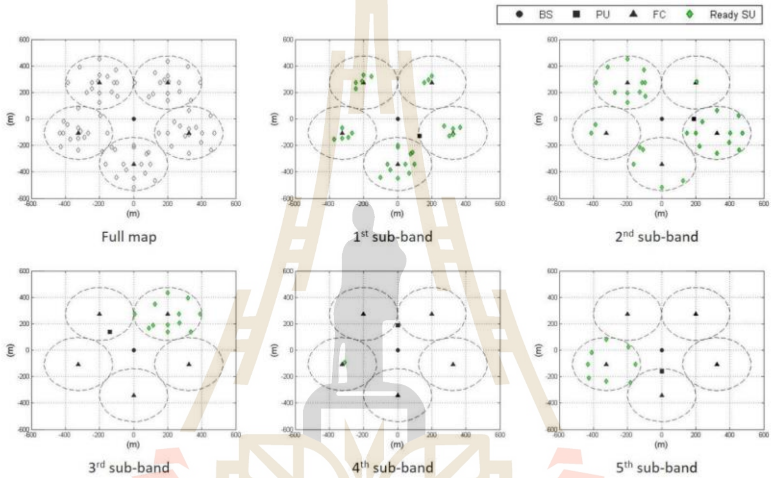

Figure 5 Full-system overlapping spectrum sharing with 16 users per a picocell

4. Conclusions

The position-based performance analysis for the overlapping spectrum sharing techniques has been presented in this paper. The mathematical solution shows the relationship between BER and user positions in which the same frequency users will affect each other, much or less based on their positions. It can be clearly seen in the term of multi-user systems that either distance or direction between transmitter and receiver are different, then the BER result is different definitely. The simulation results can describe the interference impact of each user in CR system related to a thorough performance analysis in terms of BER that supports both downlink and uplink operations. In addition, the system can allocate the frequency channels to all users as thoroughly as possible employing the spectrum allocation scheme. The results are very useful for multi-user MIMO CR implementation to make a decision on whether the current position of SU is suitable for establishing a communication or not.

5. References

[1] Puranachaikeeree S. Transmitting and Receiving Beamforming for Interference Cancellation in the Downlink of Cognitive Radio System [dissertation]. Bangkok: King Mongkut's University of Technology Thonburi; 2010.

[2] Zhang R. On peak versus average interference power constraints for protecting primary users in cognitive radio networks. IEEE Transactions on Wireless Communications. 2009 Apr;8(4): 2112–20.

[3] Khan FA, Tourki K, Alouini MS, Qaraqe KA. Performance analysis of a power limited spectrum sharing system with TAS/MRC. IEEE Transactions on Signal Processing. 2014 Feb 15;62(4):954-67.

[4] Tourki K, Khan FA, Qaraqe KA, Yang HC, Alouini MS. Exact performance analysis of MIMO cognitive radio systems using transmit antenna selection. IEEE Journal on Selected areas in communications. 2014 Mar;32(3):425-38.

[5] Yang G, Li B, Tan X, Wang X. Adaptive power control algorithm in cognitive radio based on game theory. IET Communications. 2015 Sep 3;9(15):1807-11.

[6] Kim TK, Kim HM, Song MG, Im GH. Improved spectrum-sharing protocol for cognitive radio networks with multiuser cooperation. IEEE Transactions on Communications. 2015 Apr;63(4):1121-35.

[7] Vassaki S, Poulakis MI, Panagopoulos AD. State-based potential power allocation game in a cooperative multiuser network. IET Communications. 2016 Jul 21;10(11):1320-8.

[8] Khalfi B, Ghorbel MB, Hamdaoui B, Guizani M. Distributed fair spectrum assignment for large-scale wireless DSA networks. International Conference on Cognitive Radio Oriented Wireless Networks 2015 Apr 21 (pp. 631-642). Springer International Publishing.

[9] Goldsmith A. Wireless communications. Cambridge: Cambridge University Press; 2005.

[10] Gradshteyn IS. and Ryzhik IM. Table of integrals, series, and products. 7th ed. New York: Academic Press; 2007.

[11] ETSI T. 136 101 V10. 3.0 (2011-06) LTE. Evolved universal terrestrial radio access (E-UTRA).

[12] Davari N, Gholami A. An asynchronous adaptive direct Kalman filter algorithm to improve underwater navigation system performance. IEEE Sensors Journal. 2017 Feb 15;17(4):1061-8.

Spectrum Sensing with Integration of Energy Detector and Diversity Techniques for MIMO Systems

Rattasat Laikanok, Peerapong Uthansakul, Monthippa Uthansakul

School of Telecommunication Engineering, Suranaree University of Technology
Muang, Nakhon Ratchasima, Thailand 30000
Email: D5640034@g.sut.ac.th,uthansakul@sut.ac.th and mtp@sut.ac.th

Abstract— **Spectrum sensing is a key enabling cognitive radio networks, which increases the opportunity of spectrum access to cognitive radio users, by avoiding interference with the operation of the primary network (licensed network). In literature many research conducted cognitive radio networks with SISO systems. However, the trend of MIMO users should be taken into account. In fact, the use of spectrum sensing for SISO system can be applied to MIMO system but it is not yet effective enough to limit the interference to the primary users by cognitive radio MIMO users. Thus, in order to improve and use the cognitive radio network for MIMO users, this paper has presented the integration of energy detector and diversity techniques for MIMO systems, which can increase the efficiency of spectrum sensing. The simulation results show that the proposed technique can reduce the probability of false alarms and increase the probability of detection.**

Keywords— **multiple-input-multiple-output (MIMO), cognitive radio (CR), energy detector (ED), maximal-ratio combining, selection combining**

I. Introduction

In present, the services requirement in wireless communication systems is rapidly increased and having modern technologies, to enable communications services anywhere, anytime. When lot communication systems occur, bandwidth is a limited resource. Therefore, spectrum shortage problem is challenging, in the bandwidth utilization for maximum efficiency. Cognitive radio (CR) is the enabling technology for dynamic spectrum access allowing unlicensed secondary users (SUs) to utilize a bandwidth when it is idle from the licensed primary users (PUs) [1], [2], which is referred to as spectrum hole [3], as shown in Fig.1. Spectrum sensing (SS) is one topic in the development of CR by developing signal detection from PU, in order to know that PU signal is present in the channel or not, if not, CR allow SU to access the channel, to avoid interference to the PU.

The main objective of SS is to increase opportunities for SUs to access the spectrum without interference to the primary networks. Several methods have been proposed for single-input-single-output (SISO) case. In [4], the work has focused on finding the optimal transmission and observation time, and introduced a spectrum selection and scheduling algorithm based on the opportunistic capacity concept. In [5], the algorithm of energy detector is proposed, by using receiver operating characteristic (ROC) curves to explore the relationship between the sensitivity and specificity of a sensing method for a variety of different thresholds. In [6], [7], spectrum sensing methods are proposed for multiple-input-multiple-output (MIMO) systems, which show that increasing the number of antennas to optimize the operation of the CR. However, such methods must face with the unknown parameters problem (e.g. channel coefficients), and assumed some assumptions to achieve a theoretical possibility. Cleary it is not the ready solution to implement in practice.

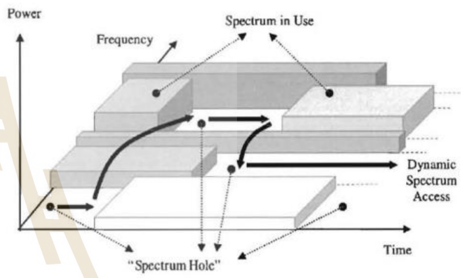

Fig. 1 Spectrum hole concept [3].

In this paper, we have presented two SS techniques, which diversity techniques were applied to the method of energy detector, where observations from multiple SUs are combined to improve detector performance, and no primary signal information is required for these techniques. The first technique is maximal-ratio combining, which focuses on optimizing the detection (probability of detection), by virtue of the increase in signal to noise ratio (SNR) followed the number of antennas. The second technique is selection combining, which focuses on reducing the possibility of error detection (probability of false alarm and probability of miss detection), and this technique can be used with either coherent or differential modulation, that can make it different from the first technique. Both proposed techniques will open the way for cognitive radio technology over MIMO systems and it is possible to easily implement.

II. Spectrum Sensing

The spectrum sensor essentially performs a binary hypothesis test on whether or not there are primary signals in a particular channel. Hence, the hypothesis can be divided into H_0 (idle) and H_1 (busy). Under the idle state, the received signal is only the ambient noise in the radio frequency (RF) environment, and under the busy state, the received signal would consist of the PU signal and the ambient noise, Thus,

$$\begin{aligned} H_0 &: \ y(k) = w(k) \\ H_1 &: \ y(k) = s(k) + w(k) \end{aligned} \tag{1}$$

for $k = 1, \dots, n$, where n is the number of received samples, $w(k)$ represents ambient noise, and $s(k)$ represents the PU signal. It is normal for that the received signal will have more energy when the channel is busy than when it is idle, this is the underlying concept in the energy detector.

Implementation of a performance can be measured by two probabilities: probability of detection P_D and probability of false alarm P_{FA}. P_D is probability of detecting a signal on the considered frequency when it appeared truly. P_D can be written as

$$P_D = 1 - P_{MD}. \tag{2}$$

Probability of miss detection P_{MD} is probability of detecting a signal when busy channel is detected as idle, and P_{FA} is probability of detecting a signal when idle channel is detected as busy, which are defined as

$$P_{MD} = Prob\{Decide\ H_0 | H_1\} \tag{3}$$

$$P_{FA} = Prob\{Decide\ H_1 | H_0\} \tag{4}$$

A. Energy Detector

For the simplified analysis, signal can be modeled as a zero-mean stationary white Gaussian process, independent of the observation noise, which is still modeled as white Gaussian. Therefore, the probabilities P_{FA} and P_{MD} can be calculated as

$$P_{FA} = \Gamma_u(n\tau, n), \tag{5}$$

$$P_{MD} = 1 - \Gamma_u(\tfrac{n\tau}{1+SNR}, n), \tag{6}$$

where $\Gamma_u(.,.)$ is upper incomplete gamma function, τ is detection threshold [8].

In order to demonstrate the model the execution of the upper incomplete gamma function and change happens when we change the number of samples n, as shown in Fig.2, we plot P_{FA} versus τ, and Fig.3, we plot P_D versus τ, Assume that $SNR = -21$ dB for $n = 512$, $n = 1620$, and $n = 10^4$. From both figures, it is clearly seen that the probability of false alarms and the probability of detections depends on the number of samples and the detection threshold. These results are the guideline to design the proper values when sensing the spectrum.

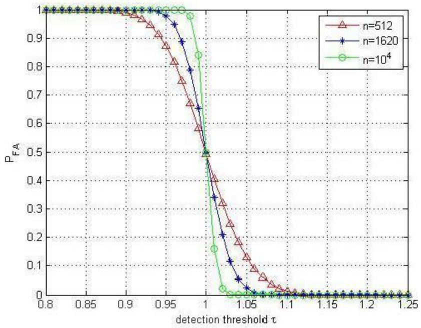

Fig. 2 Comparison of probability of false alarm versus detection threshold, where $n = 512$, $n = 1620$, and $n = 10^4$.

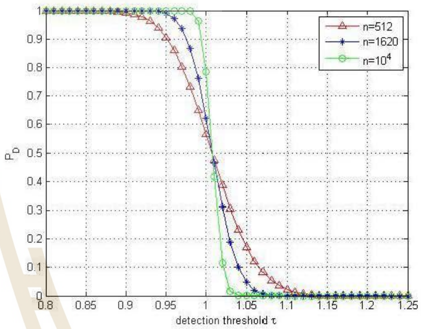

Fig. 3 Comparison of probability of detector versus detection threshold, for $n = 512$, $n = 1620$, and $n = 10^4$, where $SNR = -21$dB.

III. Spectrum Sensing using Energy Detector for MIMO

In this paper, we focus on two different diversity techniques, maximal-ratio combining (MRC) and selection combining (SC) in no fading cases.

A. Maximal-ratio Combining

For M-branch diversity, in no fading case, this can lead to an increase in received SNR. Where original received SNR is expressed in terms of the signal energy per symbol E_s as

$$SNR = \frac{E_s}{N_0 BT_s}. \tag{7}$$

Assume identical noise power spectral density (PSD) $N_0/2$ on each branch and pulse shaping such that $BT_s = 1$. Hence, each branch has the same SNR, $SNR_i = E_s/N_0$. Then the combining received SNR is

$$SNR_{\Sigma} = \frac{\left(\sum_{i=1}^{M}\frac{E_S}{\sqrt{N_0}}\right)^2}{N_0\sum_{i=1}^{M}\frac{E_S}{N_0}} = \frac{ME_S}{N_0} = M.SNR. \quad (8)$$

Where M is the number of branches (antennas), we have applied (8) into probability equations in energy detector then

$$P_{\Sigma FA} = P_{FA}, \quad (9)$$

$$P_{\Sigma MD} = 1 - \Gamma_u\left(\frac{n\tau}{1+M.SNR}, n\right), \quad (10)$$

$$P_{\Sigma D} = \Gamma_u\left(\frac{n\tau}{1+M.SNR}, n\right). \quad (11)$$

B. Selection Combining

In SC, if the noise power is the same on all branches. Only one branch is used at a time, SC only requires one receiver, which is switched into the active antenna branch. Hence, the path output from the combiner, must has maximum SNR among all branches. For M-branch diversity, the probability of the selection combiner for the cutoff SNR (SNR_0) is

$$P_{out}(SNR_0) = \prod_{i=1}^{M} p(SNR_i < SNR_0) = \prod_{i=1}^{M} P_{out,i}\,. \quad (12)$$

Which $P_{out,i}$ in ED are P_{FA} and P_{MD}. Thus, then [9]

$$P_{\Pi FA} = \prod_{i=1}^{M} \Gamma_u(n\tau, n), \quad (13)$$

$$P_{\Pi MD} = \prod_{i=1}^{M}\left[1 - \Gamma_u\left(\frac{n\tau}{1+SNR_i}, n\right)\right], \quad (14)$$

$$P_{\Pi D} = 1 - \prod_{i=1}^{M}\left[1 - \Gamma_u\left(\frac{n\tau}{1+SNR_i}, n\right)\right]. \quad (15)$$

IV. Simulation Results And Discussion

In the foregoing section, we obtained the formulas for ED performance that are suitable for MIMO systems. For M-branch diversity, where SNR is the same on each branch, we can express the performance by simulation results in this section.

Fig.4 shows the comparison of probability of false alarm in MRC technique versus detection threshold, when $M = 1$, $M = 2$, and $M = 4$, where $n = 1620$ samples. It is seen that all the probabilities of false alarm of this technique are equal. This is because the MRC technique deal with the increase of signal power but the factor of detection threshold has already included the signal power to noise power. It means that to increase signal power does not reflect to the threshold.

Fig.5 shows comparison of probability of detection in MRC technique versus detection threshold, when $M = 1$, $M = 2$, and $M = 4$, where $SNR = -18$ dB, $n = 1620$ samples. It is seen that the region with high probability of detection is wider when increasing the number of branches. Thus, the detection performance can be improved by increasing the number of branches and by increasing the SNR.

Fig.6 shows the comparison of probability of false alarm in SC technique versus detection threshold, when $M = 1$, $M = 2$, and $M = 4$, where $n = 1620$ samples. It is seen that the region with high probability is narrower when increasing the number of branches. Thus, the probability of error detection can be reduced by increasing the number of branches

Fig.7 shows the comparison of probability of detection in SC technique versus detection threshold, when $M = 1$, $M = 2$, and $M = 4$, where $SNR = -18$ dB, $n = 1620$ samples. It is seen that the region with high probability of detection is wider when increasing the number of branches. Thus, detection performance can be improved by increasing the number of branches.

Fig.8 shows the ROCs for $M = 2$, $n = 1620$ samples, and $SNR = -18$ dB, for MRC and SC techniques, in order to compared to the ROC for normal ED. As expected, the performance can be improved monotonically with the increase of the number of branches.

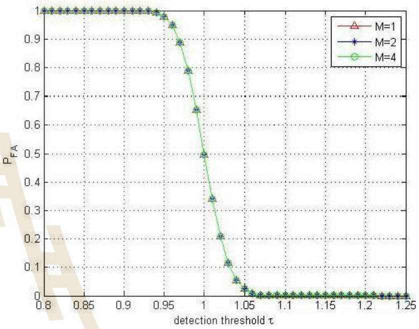

Fig. 4 Comparison of probability of false alarm in MRC versus detection threshold, for $M = 1,2$ and 4, where $n = 1620$.

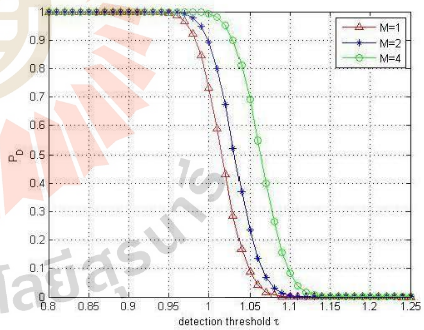

Fig. 5 Comparison of probability of detection in MRC versus detection threshold, for $M = 1,2$ and 4, where $SNR = -18$ dB, $n = 1620$.

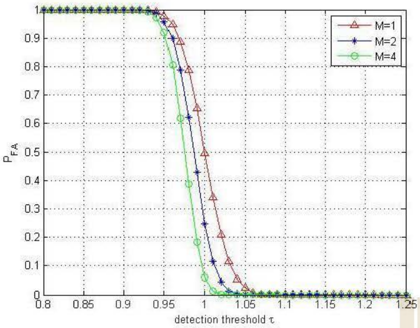

Fig. 6 Comparison of probability of false alarm in SC versus detection threshold, for $M = 1, 2$ and 4, where $n = 1620$.

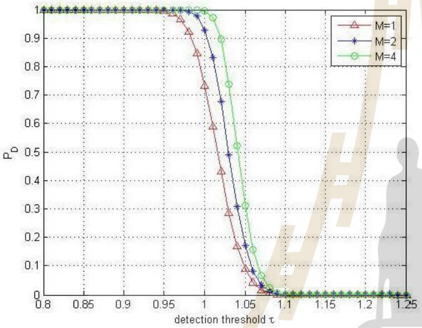

Fig. 7 Comparison of the probability of detection in MRC versus detection threshold, for $M = 1, 2$ and 4, where $SNR = -18$ dB and $n = 1620$.

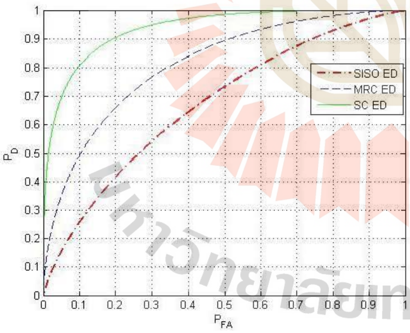

Fig. 8 Comparison of ROC curves for normal SISO ED ($M = 1$), MRC ($M = 2$) and SC ($M = 2$), where $SNR = -18$ dB and $n = 1620$.

Note that for MIMO system MRC technique is suitable for space-time coding scheme and SC technique is suitable for spatial multiplexing scheme. Therefore, the results in Fig.8 show that the better spectrum sensing can be obtained from SC technique which is suited for spatial multiplexing scheme. However, there is a tradeoff on the expense of spatial multiplexing in terms of complexity and bit error rate.

V. Conclusions

In the future, cognitive radios are likely to be widely used, spectrum sensing is important to the development of high quality. In this paper, two energy detector techniques for MIMO systems are introduced, including maximal-ratio combining and selection combining. Maximal-ratio combining will optimize detection by increasing probability of detection with a combination of SNR from all branches. The selection combining will optimize detection by decreasing the probability of false alarm and by decreasing the probability of miss detection. Although both proposed techniques are used to optimize the spectrum detection, but they are suitable for different applications. MRC technique is suitable for space-time coding application while SC technique is suitable for spatial multiplexing application. However, both techniques offer the improved performance of spectrum sensing.

References

[1] J. I. Mitola and J. G. Q. Maquire," Cognitive radio: Making solfware radios more personal," IEEE Pers. Commun., vol. 6, no. 4, pp. 13-18, Aug. 1999.
[2] S. Haykin, "Cognitive radio: Brain-empowered wireless communication," IEEE J. Sel. Areas Commun., vol. 23, no. 2, pp. 201-220, Feb. 2005.
[3] I. F. Akyildiz, W. –Y. Lee and M. C. Vuran, "Next generation/dynamic spectrum access/cognitive radio wireless network: A survey," Science Direct, pp. 2127-2130, 2006.
[4] W. -Y. Lee and I. F. Akyildiz, "Optimal Spectrum Sensing Framework for Cognitive Radio Networks," IEEE Trans Wireless Commun., vol. 7, no. 10, pp. 3845-3857, Oct.2008.
[5] T. Yucek and H. Arslan, "A Survey of Spectrum Sensing Algorithms for Cognitive Radio Applications," IEEE Commun., vol. 11, no. 1, pp. 116-130, Nov. 2007.
[6] W. Lee and D. –H. Cho, "Enhanced Spectrum Sensing Scheme in Cognitive Radio Systems With MIMO Antennae," IEEE Trans Vehicular Tech., vol. 60, no. 3, Mar. 2011.
[7] E. Soltanmohammadi, M. Orooji and M. Naraghi-Pour, "Spectrum Sensing Over MIMO Channels Using Generalized Likelihood Ratio Tests," IEEE Signal Proc. Letters., vol. 20, no. 5, May 2013.
[8] A. M. Wyglinski, M. Nekovee and T. Hou, Cognitive Radio Communications and Networks, ELSEVIER Inc. 2010.
[9] A. Goldsmith, Wireless Communications, Cambridge University Press, 2005.

Integration of Equal Gain Combining and MAJORITY Rule for MIMO Cognitive Radio Systems

Rattasat Laikanok, Peerapong Uthansakul, and Monthippa Uthansakul
School of Telecommunication Engineering, Suranaree University of Technology

ABSTRACT
It is obvious that for cognitive ratio technology the success of using it depends on how accurate of spectrum sensing is. For MIMO systems, there are multiple antennas which can be more utilized for spectrum sensing than only one antenna like conventional systems. However, in literatures, the use of multiple antennas for sensing approach is based on two-state decision; available or occupied spectrums. In this paper, multi-state decision so called soft decision has been proposed to improve the performance of spectrum sensing for MIMO systems. Also this paper proposes the integration of Equal Gain Combining and MAJORITY Rule for sensing the spectrum. The results show that the proposed technique provides the best performance in comparing with other techniques.

1. INTRODUCTION

At present, the frequency resources allocated to primary users in the use of certain frequencies are not occupied all the time and they have a limited area where the communication signals in the frequency band are strong only, which is referred as a spectrum hole [1] as shown in Fig. 1. This causes researchers to find higher efficient technique to utilize resources. A Cognitive Radio (CR) technology has emerged to support the issue mentioned above and many associated techniques have introduced to improve its performance in various aspects. The popularity of CR technology gains the demand of its validation on the compliance with IEEE 802.22 standard as detailed in [2]. Following this standard, the information on the frequency allocation of the TV channels as shown in Tables 1 and 2 will be adopted for simulation in this paper.

The main objective of spectrum sensing is to increase the opportunities for secondary users (SUs) to access the spectrum without interfering to the primary networks. For Multiple Input Multiple Output (MIMO) systems, ther are more than one antenna operating at the same time. Hence, it is possible to utilize the use of multiple anenna for spectrum sensing. The higher accurate sensing results are expected from MIMO systems.

In literatures, the authors have surveyed many spectrum sensing techniques for CR technology that can apply to MIMO systems. One technique among those in literatures is the cooperative sensing concept [3]. In [4], the work described the various techniques of the cooperative sensing and presented the performance comparison of various methods, the advantages-disadvantages of each method. However, the cooperation of many antennas refers to the wasteful use of resources. This is because those methods make a decision based on two-state results either available or occupied spectrum. Hence, the cooperative mechanism can be predicted from two levels fo dicision which the performance can not be improved much for multiple antennas.

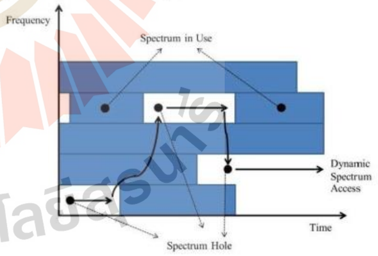

Fig. 1 Spectrum hole concept.

In this paper, the multi-state decision so called soft decision is proposed to the principle of cooperative sensing for array antennas in order to support MIMO systems. Moreover, this paper also presents that the integration of two cooperative sensing techniques, Equal Gain Combining (EGC) and MAJORITY Rule (MJ), provides the best performance among other techniques in literatures.

TABLE 1 FREQUENCY OF TV CHANNELS IN WESTERN EUROPE AND MANY OTHER COUNTRIES IN AFRICA, ASIA, AND THE PACIFIC (BW=7 MHZ)

CH	f_c(MHz)	CH	f_c(MHz)	CH	f_c(MHz)
2	50.5	6	184.5	10	212.5
3	57.5	7	191.5	11	219.5
4	64.5	8	198.5	12	226.5
5	177.5	9	205.5		

TABLE 2 FREQUENCY OF TV CHANNELS IN WESTERN EUROPE AND MANY OTHER COUNTRIES IN AFRICA, ASIA, AND THE PACIFIC (BW=8 MHZ)

CH	f_c (MHz)	CH	f_c (MHz)	CH	f_c (MHz)	CH	f_c (MHz)	CH	f_c (MHz)
21	474	31	554	41	634	51	714	61	794
22	482	32	562	42	642	52	722	62	802
23	490	33	570	43	650	53	730	63	810
24	498	34	578	44	658	54	738	64	818
25	506	35	586	45	666	55	746	65	826
26	514	36	594	46	674	56	754	66	834
27	522	37	602	47	682	57	762	67	842
28	530	38	610	48	690	58	770	68	850
29	538	39	618	49	698	59	778	69	858
30	546	40	626	50	706	60	786		

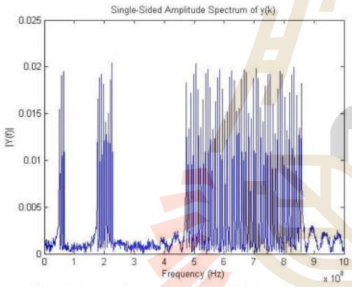

Fig. 2 Received spectrum when all channels are occupied.

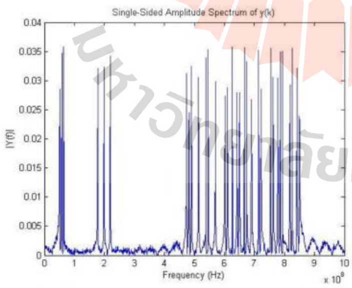

Fig. 3 Received spectrum when some channels are available.

The remainder of this paper is organized as follows. The basis of the energy detector method is given in Section 2. Then, the overview of EGC and cooperative decision rules including MJ are presented in Section 3. In Section 4, the proposed techniques including the integration of various methods and the soft decision are given in details. The simulation results and discussion are presented in Section 5 and then followed by the conclusion in Section 6.

2. ENERGY DETECTION METHOD

The principle of spectrum sensing can be understood easily [5-6] because only the interested spectrum is in just two hypotheses, including H_0 (availabe) and H_1 (occupied). The state is availabe when the primary user (PU) signal is not detected. The received signal is just ambient noise in the radio frequency (RF) environment. For the another, the state is occupied when the received signal would be consisted of the PU signal and the ambient noise, that can be explained by

$$
\begin{aligned}
H_0 &: y(k) = w(k) \\
H_1 &: y(k) = s(k) + w(k) ,
\end{aligned} \tag{1}
$$

when $y(k)$ represents the received signal, $w(k)$ represents the ambient noise, and $s(k)$ represents the PU signal, for $k = 1, \ldots, n$, and n is the number of received samples. In fact, there are many spectrum sensing techniques in literatures such as energy detection, cyclostationary and etc. Among those, the energy detection method is very popular due to its ease for implementation. This paper develops the sensing technique based on the energy detector (ED) because it costs the less for multiple antennas in practice. Also this approach has the advantage that it is easy to distinguish the status of the spectrum energy in a way that is quite straightforward. Hence, it can be implemented as multi-state rather than availabe or occupied.

The simulations are based on the channel from IEEE 802.22 standard. The received spectrum when all channels in Tables 1 and 2 are occupied is presented in Fig. 2. The authors random some channels to be available in order to investigate the performance of sensing techniques. The example of received spectrum when some frequencies are available is illustrated in Fig. 3.

The performance evaluation of spectrum sensing techniques can be significantly viewed from two probabilities: probability of detection P_D and probability of false alarm P_{FA}.

P_D is the probability of detecting a signal on the considered frequency when it truly appears, or can be described in another form which is the probability of remaining apart from the probability of missed detection P_{MD}. This can be written as

$$P_D = 1 - P_{MD}, \tag{2}$$

when P_{MD} is the probability of detecting a signal when the occupied channel is detected as the channel is available. It occurs when the enegy of the received signal is lower than the detection threshold τ. The P_{FA} is the probability of detecting a signal when the available channel is detected as the channel is occupied. it is usually caused by a misunderstanding that interference is too high in the available channel. The P_{MD} and P_{FA} can be defined as

$$P_{MD} = Prob\{Decide\ H_0|H_1\}, \quad (3)$$

$$P_{FA} = Prob\{Decide\ H_1|H_0\}. \quad (4)$$

It can be seen that the P_{FA} is associated with P_D in such a way that P_{FA} is one of the forms of P_D when the total number of signal that is detected. Then, there is a certain amount of noise that is misunderstood.

The probabilities P_{FA} and P_{MD} in the forms of a simple analysis with the signals are modeled as a zero-mean stationary white Gaussian process, independent of the observation white Gaussian noise, which can be calculated as

$$P_{FA} = \Gamma_u(n\tau, n), \quad (5)$$

$$P_{MD} = \Gamma_u(\frac{n\tau}{1+SNR}, n), \quad (6)$$

where $\Gamma_u(.,.)$ is the upper incomplete gamma function [7].

In practice, we can separate the various frequencies of each channel from the received signal in (1) as follows:

$$y(k) = \sum_{ch=1}^{CH} u_{ch}(k), \quad (7)$$

where CH is the number of considered channels.

Then, take the signal being considered in each channel into the one-bit decision equation as:

$$U_{ch} = \begin{cases} 0, avg(|u_{ch}(k)|^2) < \tau \\ 1, avg(|u_{ch}(k)|^2) > \tau \end{cases} \quad (8)$$

To demonstrate the concept of energy detection, the preliminary simulation has been performed. When the available channels are random for 2,000 times, the comparison between closed form solution appeared in (5) and simulated results can be shown in Fig. 4. In this figure, the evaluation of the probabilities P_D and P_{FA} is presented and this figure is well known as the Receiver Operating Characteristic (ROC) curve. The ROC shows the sensitivity in the terms of P_D and the specificity in the terms of P_{FA}. Therefore, the ROC curve that approaches 1 for P_D and 0 for P_{FA} is the ideal case. This figure also shows that the results of the simulation results of the spectrum sensing with energy detector is close to the theoretical analysis, when we refer the channels from Tables 1 and 2.

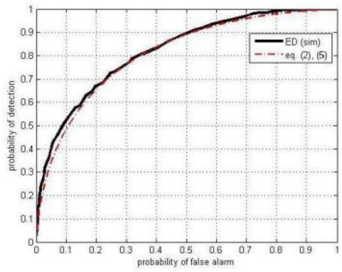

Fig. 4 ROC curves of the normal ED where $SNR = -30$ dB, and $n = 2000$.

3. EGC AND COOPERATIVE DECISION RULE

The difference of normal CR and MIMO CR users is the number of antennas on receiver. Hence, for MIMO CR, the method to utilize the use of multiple antennas is very important. In literatures, there are many techniques that can utilize many antennas for spectrum sensing so called cooperative techniques. Among those, two popular techniques are EGC and cooperative decision rule. This section presents the foundation of developed technique to support the cognitive radio technology in MIMO systems.

3.1 Equal Gain Combining

Equal Gain Combinng (EGC) method fuses all the received signals from each antenna to obtain the following combining result [4]:

$$y_{EGC}(k) = (\frac{1}{M})\sum_{m=1}^{M} y_m(k), \quad (9)$$

where M is the number of antenna elements.

The use of EGC is to take the EGC received signal $y_{EGC}(k)$ in (9) into (7) and (8) instead of $y(k)$.

3.2 Cooperative Decision Rule

The cooperative deicsion rule refers to three different formats including OR rule, AND rule and MAJORITY (MJ) rule. After the signal is received, each signal of each antenna element will be sent to separated detector by (7), and next to (8). Finally, we have the data points $\boldsymbol{U_{ch}}$ of all channels of each antenna, total points of the corresponding channel to perform the final decision according to the following logic rule [4], as follows:

$$U_{total}(k) = \sum_{m=1}^{M} U_m(k) \begin{cases} < \kappa, & H_0 \\ > \kappa, & H_1 \end{cases}, \quad (10)$$

where κ is the decistion factor which the OR rule corresponds to the case of $\kappa = 1$, the AND rule corresponds to the case of $\kappa = M$, and the MAJORITY rule corresponds to the case of $\kappa = M/2$.

4. PROPOSED TECHNIQUES

4.1 MAJORITY++ Rule

From both methods in Section 3, the authors combine them to imrpove the performance of spectrum sensing even better. The authors have named this proposed method as MAJORITY++ (MJ++). The proposed MAJORITY++ rule technique is created by adding the assistant signal:

$$y_{M+1}(k) = (\frac{1}{M})\sum_{m=1}^{M} w_m * y_m(k), \qquad (11)$$

that was taken from the EGC method, and w_m is weighting coefficients. The reason of adding w is is that the received signal of each antenna element has a phase shift from the principle of array antenna [8].

Then we take the signal from (11) and normally received signals to get into the process of normal decision by (7) and (8) respectively. After that, the MJ rule is taken according to (10). The decision factor of this method is given by

$$\kappa_{MJ++} = (\frac{M+1}{2}). \qquad (12)$$

The result in (12) is used for the final decision in (10).

4.2 MAJORITY++ Rule with Soft Decision

Based on a one-bit decision shown in (8), the deficiency is that there are only two-state results. Only either available or occupied channels are the final output. In some cases, the available channel can be the final decision even the signal is slightly below the threshold. This is because the two-state system strictly keep comparing with the threshold level no matter how much the difference between signal and threshold is. In this light, the authors propose the new idea to increase the opportunity for those weak signals being slightly lower than the threshold to give them a greater voice in decision making. By dividing the threshold into mutiple levels L, so called as multi-state threshold, and giving the proper decistion points to them, then we can have the leveled decision, so called as soft decision as shown in (13).

$$U_{L,ch} = \begin{cases} 0, avg(|u_{ch}(k)|^2) < l\tau \\ \downarrow \qquad\qquad\qquad\qquad \downarrow \\ 1, avg(|u_{ch}(k)|^2) \geq L\tau \end{cases}, \qquad (13)$$

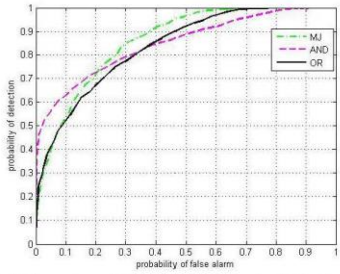

Fig. 5 Comparison of ROC curves for OR rule, AND rule and MJ rule, where $M = 4$, $SNR = -30$ dB, and $n = 2000$.

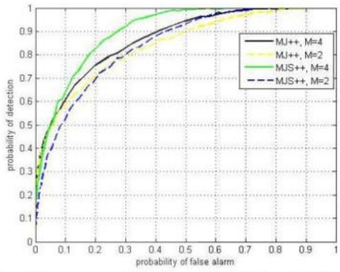

Fig. 6 Comparison of ROC curves for MJ++ and MJS++, where $M = 2$ and 4, $SNR = -30$ dB, and $n = 2000$.

where l is a constant increase in the number of levels up to L. The value of $U_{L,ch}$ is between 0 and 1 as same as U_{ch} in (8). The authors have named this proposed method as MJS++ for a short reference.

5. SIMULATION RESULTS AND DISCUSSION

Based on information in Tables 1 and 2, the simulated signals with the random of available channels is generated. Then, the probability of detection P_D and probability of false alarm P_{FA} are calculated by various spectrum sensing techniques. Fig. 5 shows the ROC comparison of the cooperative decision rules. The results in Fig. 5 reveal that MJ rule is the most effective method among those three cooperative decision rules. Thus, this paper select the MJ rule for the integration of EGC with soft decision as presented in the next results.

Fig. 6 shows the ROC comparison of MAJORITY++ rule (MJ++) and MAJORITY++ rule with solf decision (MJS++), where $SNR = 30$ dB, the number of samples $n = 2000$, the transmitted power of primaly user $P_t = 1$ dBW, and the presence of the signal in each channel has occurred randomly. For the MIMO systems, M is the number of antennas which is limited to 2 and 4 antennas as related to the practical issue.

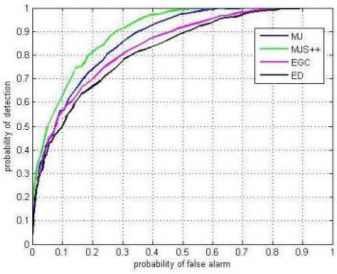

Fig. 7 Comparison of ROC curves for normal ED ($M = 1$), EGC ($M = 4$), MJ rule ($M = 4$) and MJS++ ($M = 4$), where $SNR = -30$ dB and $n = 2000$.

As seen Fig. 6, MJS++ rule offers a better performance than MJ++ rule for both cases of the number of antennas. The results reveal the benefit of soft decision for spectrum sensing. Also in this figure, the more number of antennas, the better performance can be obtained. The results imply the advantage of using the proposed technique for the MIMO CR users.

In Fig. 7, the results show the comparison of the proposed techniques and the existing techniques in literatures, where $SNR = 30$ dB, $n = 2000$, $P_t = 1$ dBW, $M = 4$. For a energy detection technique, the antenna is set to 1 because there is no cooperative help on traditional systems. As expected, the proposed techniques outperform the others. At the 90% probability of detection, the MJS++ technique can reduce the chance of false alarm from 50% of ED technique to 26%. This 24% improvement can indicate the success of proposed technique for practical use.

6. CONCLUSION

This paper has presented the new concept for sensing the spectrum for MIMO CR users. The proposed concept is to divide the decision threshold into multi-state decision so called as soft decision. Also, the soft decision has been applied to the integration of EGC and MAJORITY rule. The performance of proposed techniques has been examined in terms of ROC curve. The results show that the proposed techniques outperform the other existing techniques. Also the better performance can be obtained using the soft decision.

REFERENCES

I. F. Akyildiz, W. -Y. Lee and M. C. Vuran, "Next generation/dynamic spectrum access/cognitive radio wireless network: A survey," Science Direct, pp. 2127-2130, 2006.

802.22-2011 - IEEE Standard for Information technology-- Local and Metropolitan area networks-- Specific requirements-- Part 22: Cognitive Wireless RAN Medium Access Control (MAC) and Physical Layer (PHY) specifications: Policies and procedures for operation in the TV Bands.

T. Yucek and H. Arslan, "A survey of spectrum sensing algorithms for cognitive radio applications," IEEE Commun. Serv. Tutor., vol. 11, no. 1, pp. 116-130, 2009.

C. Hunifang, X. Lei and N. Xiong, "Reputation-based hierarchically cooperative spectrum sensing scheme in cognitive radio networks," Selected papers from IEEE/CIC ICCC2013, pp. 12-25, Jan. 2014.

K. Tourki, K. A. Qaraqe, H-C. Yang and M-S. Alouini, "Exact performance analysis of MIMO cognitive radio systems using transmit antenna selection," IEEE J. Select. Areas Commun., vol. 32, no. 3, Mar. 2014.

F. A. Khan, K. Tourki, M-S. Alouini and K. A. Qaraqe, "Performance analysis of a power limited spectrum sharing system with TAS/MRC," IEEE Tran. Signal Processing, vol. 62, no. 4, Feb. 2014.

A. M. Wyglinski, M. Nekovee and T. Hou, Cognitive Radio Communications and Networks, ELSEVIER Inc. 2010.

J. Foutz, A. Spanias and M. K. Banavar, "Narrowband direction of arrival estimation for antenna arrays," A publication in the Morgan & Claypool publishers series.

INVESTIGATION ON THE EFFECT OF USER POSITION IN MIMO COGNITIVE RADIO SYSTEMS WITH OVERLAPPING SPECTRUM SHARING

Rattasat Laikanok, Peerapong Uthansakul, and Monthippa Uthansakul

School of Telecommunication Engineering, Suranaree University of Technology, Thailand

D5640034@g.sut.ac.th

ABSTRACT

Currently, the wireless communication system is developed and continuously improved due to the need of user services including the development of many new applications. This results in more consumption of frequency resource until it will not be enough to use in the future. One problem is that the spectrum possession of the licensed users is inefficiently utilized. The spectrum sharing in cognitive radio technology can solve the above problems by allowing secondary user to access the same frequency as primary user in the same area, which is divided into two patterns by spectrum sensing. If it detects an idle channel, it will perform a non-overlapping spectrum sharing. In turn, if it detects an occupied channel, it will continue to perform an overlapping spectrum sharing. In this paper, the guidelines for self-evaluation of the cognitive radio network is proposed to judge whether it is in the range of communication or not. The proposed concept must be designed to minimize the effect on the communication of primary network. The simulation results indicate the specific areas for cognitive radio that can be successfully implemented. The proposed work is very helpful for service providers to obtain more benefit from their limited resources.

1. INTRODUCTION

The process of cognitive radio systems is to communicate and adjust the parameters to suit the changed environment. Spectrum sensing is the main key of cognitive radio technology that search for available channels from the use of the Primary User (PU), then allow Secondary Users (SUs) to access those channels. In [1], the work has presented the optimization techniques for spectrum sensing by using cooperation of node clusters, that each node has only one antenna. By the data processing is separated into hierarchies. On the first level, all of the member nodes use the Equal Gain Combining (EGC) technique, then next, on the second level, will bring the data from each group into the processor by statistical decision, MAJORITY rule. But the research of the authors earlier, the work has supported the Multiple-Input-Multiple-Output (MIMO) technology. By applying the above techniques with MIMO technology to make the new technique named as MAJORITY++ Rule with Soft Decision (MJS++), it can operate by just one node to utilize many antennas in order to replace many nodes. In Fig. 2, it can be seen that the spectrum sensing by the new proposed technique outperform the others. At the 90% probability of detection, the MJS++ technique can reduce the chance of false alarm from 50% of ED technique to 26%. This 24% improvement can indicate the success of proposed technique for practical non-overlapping spectrum sharing.

However for spectrum utilization worth more, SU can perform a good communication while being a little interferer to PU on the overlapping scheme. The overlapping spectrum sharing allows SUs to reserve access the same spectrum along with PU but with one strict condition that the received signal of PU must to be under the acceptable level of interference. The work in [2] has presented the interference reduction method in spectrum sharing by the proper designs on transmit and receive beams of MIMO technology. The work in [3] has presented the power constraint techniques of the interference signals to PU in spectrum sharing. By comparing the interference power [4], the performance analysis of the transmit power constraint in spectrum sharing is introduced by a transmit antenna selection at secondary transmitter and the maximum ratio combining at secondary receiver, same as [5] but the performance analysis was in forms of the bit error rate and the channel capacity under two power constraint methods, including the mean value-based power allocation scheme and the channel state information-based power allocation scheme.

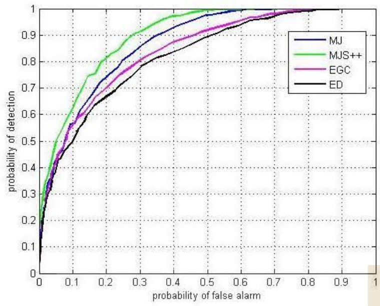

Fig. 1 Comparison of ROC curves for normal ED at $M = 1$, and EGC, MJ, MJS++ at $M = 4$.

So far in literature reviews, there is still no any work that focuses on the self-evaluation guidelines to consider whether the position of SU is suitable to make a good communication as well as interfere to PU under the acceptable limits of overlapping spectrum sharing scheme. The authors realize the need to initiate research on the impact of node positions in cognitive radio systems, and develop self-evaluation technique of secondary network in the system with the above position information in order to enable cognitive radio system for actually operating in practice.

2. PERFORMANCE ANALYSIS

2.1 System Model

This paper considers the overlapping cognitive network that the secondary link is composed of secondary transmitter (ST) and secondary receiver (SR), equipped with N and M antennas, respectively. The primary link is composed of only one antenna for both primary transmitter (PT) and primary receiver (PR). This paper defines that PR is the base station (BS) and SR is the fusion center (FC). The channel coefficient h_{kj} is the channel between k^{th} antenna of ST and j^{th} antenna of SR, the channel coefficient h_{kp} is the channel between k^{th} antenna of ST and PR, the channel coefficient h_{pj} is the channel between PT and j^{th} antenna. All channels are modeled as flat fading and Rayleigh distribution with variances λ_s, λ_p and λ_{ps}, respectively.

Between the transmission slots of ST, one of N antennas will be chosen through the ratio selection criterion, as following

$$s = \arg\max_k \left(\frac{g_{ks}}{g_{kp}}\right), \tag{1}$$

where $g_{ks} = \sum_{j=1}^{M} |h_{kj}|^2$ and $g_{kp} = |h_{kp}|^2$. By obtaining the bit error rate, the analysis will start with CDF of channel gain from ST to SR, $g_{ss} = \sum_{j=1}^{M} |h_{sj}|^2$, when use the ratio selection criterion in (1), are given by

$$F_{g_{ss}}(x) = \frac{1}{\Gamma(M+1)}\left[\left(\frac{x}{\lambda_s}\right)^{MN} \Gamma\left(1 - M(N-1), \frac{x}{\lambda_s}\right) + \gamma\left(M+1, \frac{x}{\lambda_s}\right)\right], \tag{5}$$

where $\Gamma(.)$ is the gamma function. $\Gamma(.,.)$ and $\gamma(.,.)$ is the upper and lower incomplete gamma functions, that is obtained from [6, Eq. 8.350.2] and [6, Eq. 8.350.1], respectively.

On the other hand, for spectrum sharing, it needs to has the statistic values of ST-PR link, when $g_{sp} = |h_{sp}|^2$, will be the PDF of g_{sp}.

$$p_{g_{sp}}(y) = \frac{N\Gamma(MN)}{\Gamma(M)\Gamma(M(N-1))} \sum_{i=0}^{M(N-1)-1} \binom{M(N-1)-1}{i} \times (-1)^i \frac{y^{M+i}}{\lambda_p^{M+i+1}} \Gamma\left(-M - i, \frac{y}{\lambda_p}\right), \tag{6}$$

It also provides the combined signal to noise ratio (SNR), that SR use the power allocation [5, Eq. 12], as given by

$$\gamma_{ss} = \min\left(\frac{I}{\mathbb{E}(g_{sp})}, \bar{\gamma}\right)\lambda_s, \tag{7}$$

where $\bar{\gamma} = \frac{P_m}{N_0}$ at P_m is the maximum transmit power constraint of PT and ST, N_0 is the noise variance, I is the limited level of interference of secondary user, and

$$\mathbb{E}(g_{sp}) = \frac{N\Gamma(MN)\lambda_p}{\Gamma(M)\Gamma(M(N-1))} \sum_{i=0}^{M(N-1)-1} \frac{\binom{M(N-1)-1}{i}(-1)^i}{M+i+2}, \tag{8}$$

that is given from (6), where $\mathbb{E}(.)$ is the expectation operator.

By the way, performance analysis is divided into two cases based on the concentration of interference by distance.

2.2 Performance Analysis without Interference from PT-SR

First case, when interference from PT-SR is ignored, that PT is far from SR, there is very little interference from PT, which the secondary outage probability can be defined as

$$P_{out} = \Pr[\gamma_{ss} < x] = F_{g_{ss}}\left(\frac{x}{\min\left(\frac{I}{\mathbb{E}(g_{sp})}, \bar{\gamma}\right)}\right), \tag{9}$$

where $x = 2^R - 1$ and R is the transmission rate. To yield the typical result for obtaining the end-to-end BER in terms of SNR, the expression is given by

$$P_{s,sys} = -\int_0^\infty \frac{d}{d\gamma} P_e(x) F_\gamma(x) dx, \tag{10}$$

where $F_\gamma(.)$ is the CDF in terms of SNR of any case, and $P_e(.)$ is the condition error probability (CEP) that based on the used modulation scheme, as expressed by

$$P_e(x) = a\mathrm{Q}\left(\sqrt{bx}\right), \tag{11}$$

where a and b are the modulation-specific constants, such as $(a,b) = (1,2)$ for BPSK, $(a,b) = (1,1)$ for BFSK, and $(a,b) = \left(\frac{2(m-1)}{m}, 6\log_2\frac{(m)}{(m^2-1)}\right)$ for m-PAM. And $\mathrm{Q}(.)$ is the Gaussian Q-function.

Consider the CDF of g_{ss} in (9), the BER of this case are as follow

$$P_s(a,b) = \frac{a}{2}\sqrt{\frac{b}{2\pi}}\int_0^\infty \frac{e^{-\frac{b}{2}x}}{\sqrt{x}} F_{g_{ss}}\left(\frac{x}{min\left(\frac{I}{\mathbb{E}(g_{sp})},\bar{\gamma}\right)}\right)dx, \tag{12}$$

so the BER in (12) can be written in the closed form as

$$P_s(a,b) = \frac{\Gamma\left(M+\frac{3}{2}\right)}{\Gamma(M+1)}\frac{\frac{a}{2}\sqrt{\frac{b}{2\pi}}\left(\frac{1}{\gamma_{SS}}\right)^{1+M}}{\left(\frac{1}{\gamma_{SS}}+\frac{b}{2}\right)^{M+\frac{3}{2}}} \times$$
$$\left[\left(\frac{1}{MN+\frac{1}{2}}\right) {}_2F_1\left(1, M+\frac{3}{2}; MN+\frac{3}{2}; \frac{b\gamma_{SS}}{2+b\gamma_{SS}}\right) + \left(\frac{1}{1+M}\right) {}_2F_1\left(1, M+\frac{3}{2}; M+2; \frac{2}{2+b\gamma_{SS}}\right)\right], \tag{13}$$

where ${}_2F_1(.,.:.:.)$ is the hypergeometric function [6, Eq. 9.14.2].

2.4 Performance Analysis with Interference from PT-SR

In the second case, the appearing of interference from primary user. The combined signal to interference plus noise ratio (SINR) at SR when the s^{th} antenna selected at ST are $\gamma_{int} = \frac{\gamma_{SS}}{\bar{\gamma}g_I+1} = \frac{\gamma_{SS}}{\gamma_I+1}$, where $g_I = \frac{\left|\sum_{j=1}^{M} h_{sj}^* h_{pj}\right|^2}{g_{SS}}$ with the PDF $p_{g_I}(y) = \frac{1}{\lambda_{ps}}e^{-\frac{y}{\lambda_{ps}}}$, so the CDF of γ_{int} can be shown as

$$F_{\gamma_{int}}(x) = \Pr[\gamma_{int} < x] = F_1(x) + F_2(x), \tag{14}$$

by $F_1(.)$ and $F_2(.)$ can be defined from the PDF $p_{\gamma_I}(y) = \frac{e^{-\frac{y}{\gamma_{ps}}}}{\gamma_{ps}}$ at $\gamma_{ps} = \lambda_{ps}\bar{\gamma}$. The CDF of γ_{int} can be written as

$$\Pr[\gamma_{int} < x] = \mathbb{E}_{\gamma_I}\left[F_{g_{SS}}\left(\frac{x(y+1)}{\min\left(\frac{I}{\mathbb{E}(g_{sp})},\bar{\gamma}\right)}\right)\middle|\gamma_I = y\right]. \tag{15}$$

then defined $F_1(.)$ as

$$F_1(x) = \int_0^\infty \frac{\left(\frac{x(y+1)}{\gamma_{SS}}\right)^{MN}}{\Gamma(M+1)}\frac{e^{-\frac{y}{\gamma_{ps}}}}{\gamma_{ps}}\Gamma\left(1-M(N-1), \frac{x(y+1)}{\gamma_{SS}}\right)dy \tag{16}$$

so, $F_1(x)$ is as

$$F_1(x) = \frac{(-1)^{M(N-1)}e^{\frac{1}{\gamma_{ps}}}\left(\frac{\gamma_{ps}}{\gamma_{SS}}\right)^{MN}}{\Gamma(M+1)(M(N-1)-1)!}\left[\Gamma\left(MN+1, \frac{1}{\gamma_{ps}}\right)x^{MN} \times \mathrm{Ei}\left(\frac{-x}{\gamma_{SS,MV}}\right) + (MN)!\sum_{k=0}^{MN}\frac{\left(\frac{1}{\gamma_{ps}}\right)^k}{k!}x^{MN}\left(\frac{1}{\gamma_{ps}}+\frac{x}{\gamma_{SS}}\right)^{-k} \times \Gamma\left(k, \frac{1}{\gamma_{ps}}+\frac{x}{\gamma_{SS}}\right)\right] + \frac{\left(\frac{1}{\gamma_{ps}}\right)e^{\frac{1}{\gamma_{ps}}}}{\Gamma(M+1)(M(N-1)-1)!} \times$$
$$\sum_{k=0}^{M(N-1)+k}(-1)^{M(N-1)+k}k!\left(\frac{x}{\gamma_{SS}}\right)^{MN-k-1} \times \left(\frac{1}{\gamma_{ps}}+\frac{x}{\gamma_{SS}}\right)^{k-MN}\Gamma\left(MN-k, \frac{1}{\gamma_{ps}}+\frac{x}{\gamma_{SS}}\right), \tag{17}$$

where $\mathrm{Ei}(.)$ is the exponential integral function. And defined $F_2(.)$ as

$$F_2(x) = \int_0^\infty \frac{\gamma\left(M+1, \frac{x(y+1)}{\gamma_{SS}}\right)}{\Gamma(M+1)}\frac{e^{-\frac{y}{\gamma_{ps}}}}{\gamma_{ps}}dy, \tag{18}$$

so, $F_2(x)$ is as

$$F_2(x) = \frac{\left(\frac{1}{\gamma_{ps}}\right)e^{\frac{1}{\gamma_{ps}}}M!}{\Gamma(M+1)}\left[\gamma_{ps}e^{-\frac{1}{\gamma_{ps}}} - \sum_{k=0}^{M}\frac{\left(\frac{x}{\gamma_{SS}}\right)^k}{k!} \times \left(\frac{1}{\gamma_{ps}}+\frac{x}{\gamma_{SS}}\right)^{-k-1}\Gamma\left(k+1, \frac{1}{\gamma_{ps}}+\frac{x}{\gamma_{SS}}\right)\right]. \tag{19}$$

Finally, the BER obtained by replacing (14) in (12), are as follow

$$P_{Int}(a,b) = \frac{a}{2}\sqrt{\frac{b}{2\pi}}\int_0^\infty \frac{e^{-\frac{b}{2}x}}{\sqrt{x}}F_{\gamma_{int}}(x)\,dx, \tag{20}$$

so, the BER result form is

$$P_{Int}(a,b) = \frac{a}{2}\sqrt{\frac{b}{2\pi}}\frac{1}{\Gamma(M+1)}[I_1 + I_2 + I_3 + I_4], \tag{21}$$

that I_1, I_2, I_3 and I_4 are the sub-function, that have the result forms in (22), (23), (24) and (25), respectively

$$I_1 = \frac{(-1)^{M(N-1)+1}}{(M(N-1)-1)!}e^{\frac{1}{\gamma_{ps}}}\left(\frac{\gamma_{ps}}{\gamma_{SS}}\right)^{MN} \times \frac{\Gamma\left(MN+1, \frac{1}{\gamma_{ps}}\right)\Gamma\left(MN+\frac{1}{2}\right)}{\left(MN+\frac{1}{2}\right)\left(\frac{1}{\gamma_{SS}}+\frac{b}{2}\right)^{MN+\frac{1}{2}}} \times {}_2F_1\left(1, MN+\frac{1}{2}; MN+\frac{3}{2}; \frac{b\gamma_{SS}}{2+b\gamma_{SS}}\right), \tag{22}$$

$$I_2 = (-1)^{M(N-1)}(MN)!\,\Gamma\left(MN+\frac{1}{2}\right)e^{\frac{b\gamma_{SS}+2}{4\gamma_{ps}}}\sum_{k=1}^{MN}\frac{(k-1)!}{k!} \times \sum_{m=0}^{k-1}\frac{\left(\frac{1}{\gamma_{ps}}\right)^m}{m!}\left(\frac{1}{\gamma_{SS}}+\frac{b}{2}\right)^{-\frac{1}{2}\left(MN+m-k+\frac{3}{2}\right)}\left(\frac{\gamma_{SS}}{\gamma_{ps}}\right)^{\frac{1}{4}(2k+2m-2MN-1)}$$
$$\times \mathrm{W}_{\frac{1}{2}\left(m-k-MN-\frac{1}{2}\right), -\frac{1}{2}\left(MN+m-k+\frac{1}{2}\right)}\left(\frac{b\gamma_{SS}+2}{2\gamma_{ps}}\right) \tag{23}$$

where $W_{\lambda,\mu}(.)$ is the Whittaker W-function.

$$I_3 = \left(\frac{1}{\gamma_{ps}}\right) e^{\frac{b\gamma_{ss}+2}{4\gamma_{ps}}} \sum_{k=0}^{M(N-1)-2} (-1)^{M(N-1)+k} k!\,(MN-k-1)!\,\Gamma\left(MN-k-\frac{1}{2}\right) \sum_{m=0}^{MN-k-1} \frac{\gamma_{ss}{}^{1-m}}{m!} \left(\frac{1}{\gamma_{ss}}+\frac{b}{2}\right)^{-\frac{1}{2}\left(m+\frac{1}{2}\right)} \times \left(\frac{\gamma_{ss}}{\gamma_{ps}}\right)^{\frac{1}{2}\left(m-\frac{3}{2}\right)} W_{\frac{1}{2}\left(2k-2MN+m+\frac{3}{2}\right),\frac{1}{2}\left(-m+\frac{1}{2}\right)} \left(\frac{b\gamma_{ss}+2}{2\gamma_{ps}}\right) \quad (24)$$

$$I_4 = M!\left[\sqrt{\frac{2\pi}{b}} - \left(\frac{1}{\gamma_{ps}}\right) e^{\frac{b\gamma_{ss}+2}{4\gamma_{ps}}} \sum_{k=0}^{M} \Gamma\left(k+\frac{1}{2}\right) \sum_{m=0}^{k} \frac{\gamma_{ss}{}^{-m+1}}{m!} \left(\frac{1}{\gamma_{ss}}+\frac{b}{2}\right)^{-\frac{1}{2}\left(m+\frac{1}{2}\right)} \left(\frac{\gamma_{ss}}{\gamma_{ps}}\right)^{\frac{1}{2}\left(m-\frac{3}{2}\right)} W_{\frac{1}{2}\left(m-2k-\frac{1}{2}\right),\frac{1}{2}\left(-m+\frac{1}{2}\right)} \left(\frac{b\gamma_{ss}+2}{2\gamma_{ps}}\right)\right] \quad (25)$$

3. SIMULATION RESULTS AND DISCUSSION

Assuming the primary network use the m-QAM modulation which m is constellation size and G_c is the coding gain, BER of the primary network can be approximately expressed by

$$P_b \approx 0.2e^{-1.5\left(\frac{\bar{\gamma}G_c}{m-1}\right)}, \quad (26)$$

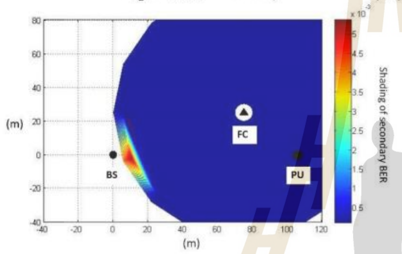

Fig. 2 BER region of secondary network on downlink operation.

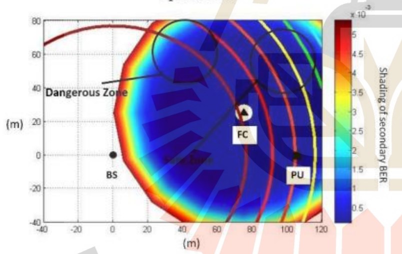

Fig. 3 BER regions of primary network and secondary network on uplink operation.

Fig. 2 shows the BER region of secondary network on downlink operation and Fig.3 shows the BER radius of primary network made obtained by (26) due to the interference from ST nearby interfaced with the BER regions of primary network and secondary network on uplink operation. The considered spectrum has the carrier frequency $f_c = 2.1$ GHz. PU is far from BS with $R_p = 105$ m, $P_m = 23$ dBm, and $G_c = 6$ dB. The dangerous zone is the area that the bit error rates of both primary and secondary networks are more than 10^{-3}. The safe zone is the area that the bit error rates of both primary and secondary networks are less than 10^{-3}. From both figures, the results can be a good guideline to make a decision whether SU can perform the overlapping spectrum sharing or not. If the location of SU is in the safe zone, then the overlapping scheme can be used.

CONCLUSION

The paper has addressed many proposed techniques in the areas of MIMO cognitive radio systems in order to provide a good guideline for researchers to develop the practical use of efficient spectrum sharing. The study goes further on the impact of node position. This is to know whether the secondary user is in the suitable position for communication or not. Also the study can suggest adjusting the transmission power appropriately. Moreover, the results show the impact on position of each node in cognitive radio system. This is very helpful to be the guideline to create self-evaluation method for secondary networks in order to make the right decisions in communication, and to acquire the efficiently spectrum sharing.

REFERENCES

C. Hunifang, X. Lei and N. Xiong, "Reputation-based hierarchically cooperative spectrum sensing scheme in cognitive radio networks," Selected papers from *IEEE/CIC ICCC2013*, pp. 12-25, Jan. 2014.

S. Puranachaikeeree and R. Suleesathira, "Transmitting and Receiving Beamforming for Interference Cancellation in the Downlink of Cognitive Radio System," Thesis 2553.

R. Zhang, "On peak versus average interference power constraints for protecting primary users in cognitive radio networks," *IEEE Trans. Wireles Commun.*, vol. 8, no. 4, pp. 2112–2120, Apr. 2009.

F. A. Khan, K. Tourki, M-S. Alouini and K. A. Qaraqe, "Performance analysis of a power limited spectrum sharing system with TAS/MRC," *IEEE Tran. Signal Processing*, vol. 62, no. 4, Feb. 2014.

K. Tourki, K. A. Qaraqe, H-C. Yang and M-S. Alouini, "Exact performance analysis of MIMO cognitive radio systems using transmit antenna selection," *IEEE J. Select. Areas Commun.*, vol. 32, no. 3, Mar. 2014.

I. S. Gradshteyn and I. M. Ryzhikhev, "Table of Integrals, Series, and Products," 6th ed. San Diego, CA: Academic, 2000.

BIOGRAPHY

Mr. Rattasat Laikanok was born in Suratthani, Thailand, in 1991. He graduated with the Bachelor Degree of Engineering in Telecommunication Engineering in 2012 from Suranaree University of Technology, Nakorn Ratchasima, Thailand. Then he is currently pursuing his Ph.D. program in Telecommunication Engineering, School of Telecommunication Engineering, Suranaree University of Technology. His current research interests concern Wireless Communication, Cognitive Radio Technology, and MIMO Technology.